ISBN 978-82-326-1672-5 (printed version)
ISBN 978-82-326-1673-2 (electronic version)
ISSN 1503-8181

Doctoral theses at NTNU, 2016:167

Mark A. M. Haring

Extremum-seeking control: convergence improvements and asymptotic stability

NTNU
Norwegian University of
Science and Technology
Faculty of Information Technology,
Mathematics and Electrical Engineering
Department of Engineering Cybernetics

NTNU
Norwegian University of
Science and Technology

Doctoral theses at NTNU, 2016:167

NTNU

NTNU
Norwegian University of
Science and Technology

Mark A. M. Haring

Extremum-seeking control: convergence improvements and asymptotic stability

Thesis for the degree of Philosophiae Doctor

Trondheim, June 2016

Norwegian University of Science and Technology
Faculty of Information Technology,
Mathematics and Electrical Engineering
Department of Engineering Cybernetics

NTNU
Norwegian University of
Science and Technology

NTNU
Norwegian University of Science and Technology

Thesis for the degree of Philosophiae Doctor

Faculty of Information Technology,
Mathematics and Electrical Engineering
Department of Engineering Cybernetics

ISBN 978-82-326-1672-5 (printed version)
ISBN 978-82-326-1673-2 (electronic version)
ISSN 1503-8181

ITK-report: 2016-12-W

Doctoral theses at NTNU, 2016:167

Printed by Skipnes Kommunikasjon as

To Masha

Summary

Extremum-seeking control is an adaptive-control methodology that optimizes the steady-state performance of dynamical plants by automated tuning of plant parameters based on measurements. The main advantage of extremum-seeking control compared to many other optimization techniques is that no plant model, or just a relatively simple plant model, is used. This makes extremum-seeking control suitable to optimize the performance of complex systems, for which an accurate model is unavailable, and systems that are subject to unknown disturbances. Due the low requirements about the knowledge of the plant, extremum-seeking control can be applied to many engineering domains. Because the vast majority of the performance-related information about the plant is obtained by measurement, the optimization speed of extremum-seeking control is generally lower than the optimization speed of model-based methods. For model-based methods, the information about the plant's dynamic and steady-state behavior is contained in the plant model and is therefore readily available.

In this work, we study extremum-seeking control methods that do not require a plant model. These methods are often referred to as black-box methods. We mainly focus on extremum-seeking methods that rely on added perturbations to optimize the steady-state performance of a plant. For certain classes of plants, large-amplitude high-frequency perturbations can be applied to speed up the convergence of the optimization process. However, large-amplitude high-frequency perturbations may be undesirable or inadmissible in practice due to actuator limitations, a high control effort, and an increased wear of components. Therefore, we aim to enhance the convergence rate of black-box extremum-seeking methods that use small-amplitude low-frequency perturbations.

Extremum-seeking control aims to find the extremum (that is, the minimum or maximum) of the objective function that represents the steady-state relation between the plant parameters and the plant performance, where the extremum correspond to the optimal steady-state performance. Classical perturbation-based extremum-seeking control methods rely on added perturbations to the plant-parameter values to estimate the gradient of the objective function by correlating the perturbations and the corresponding response in the plant-performance signal. This gradient estimate is subsequently used to steer the plant parameters to the extremum of the objective function using a gradient-descent or gradient-ascent approach. Hence, the obtained convergence rate is dependent on the accuracy of the gradient estimate. As classic methods use the perturbations of the plant-parameter signals to estimate the gradient of the objective function,

an accurate gradient estimate is obtained if the perturbation-related content in the plant-parameter signals is high. We point out in this work that, for small-amplitude low-frequency perturbations, the perturbation-related content in the plant-parameter signals is low and a more accurate gradient estimate and a faster convergence may be achieved by using the entire plant-parameter signals (and not only the perturbation signals) to estimate the gradient of the objective function. This is confirmed by simulation. Moreover, the gradient estimate may be further enhanced by the use of curvature information of the objective function, if available. A continuous-time extremum-seeking controller is presented that uses the entire plant-parameter signals to estimate the gradient of the objective function and allows us to incorporate curvature information of the objective function. In addition, an equivalent discrete-time extremum-seeking controller is presented to optimize the steady-state plant performance in a sampled-data setting.

Perturbations are used to provide sufficient excitation to estimate the gradient (and sometimes higher-order derivatives) of the objective function. One of the drawbacks of added perturbations is that the plant parameters do not converge to their performance-optimizing values. Instead, they converge to a region of the optimum. Perturbations can be omitted for certain classes of plants. Extremum-seeking control methods that rely on the plant-parameter signals to provide sufficient excitation without any form of added excitation are referred to as self driving. Although there exist examples in the literature for which self-driving extremum-seeking control is applied to achieve an optimal steady-state performance, so far, no conditions have been stated under which convergence to the true optimum can be guaranteed. Here, we prove that there exist conditions on the plant and the self-driving extremum-seeking controller under which the plant parameters are certain to converge to their performance-optimizing values.

Self-driving extremum-seeking control has its limitations in terms of applicability. Instead of omitting the perturbations, one may gradually reduce the level of the perturbations to zero as time goes to infinity to arrive at the optimal steady-state performance. Several methods to regulate the amplitude of the added perturbations have been proposed in the literature to obtain asymptotic convergence to the optimum. Commonly local convergence is proved, often for a limited class of plants. In this work, we prove that global asymptotic convergence of the plant parameters to their performance-optimizing values can be guaranteed for general nonlinear plants under certain assumptions. The key to this result is that not only the amplitude but also the frequencies of the perturbations, as well as other tuning parameters of the controller, decay to zero as time goes to infinity. Remarkably, the time-varying tuning parameters can be chosen such that global asymptotic convergence is achieved for all plants that satisfy the assumptions, thereby guaranteeing stability of the resulting closed-loop system of plant and controller regardless of tuning.

In a case study, we show that extremum-seeking control can be applied to

optimize the injection current of an active power filter for system-wide harmonic mitigation in electrical grids. The used extremum-seeking control method can be parallelized under certain design assumptions in order to increase the convergence speed of the method. A case study of a two-bus electrical grid with distributed generators displays an improved performance of the used extremum-seeking control method compared to a local-filtering approach under constant load conditions of the electrical grid, while the performance with respect to a model-based system-wide filtering method is comparable. The case study also shows that the used extremum-seeking control method is slower to respond to changes in load conditions than the local and the model-based system-wide filtering methods. The extremum-seeking control method can be implemented on top of existing approaches to combine the fast transient response of conventional harmonic-mitigation methods with the optimizing capabilities of extremum-seeking control.

Preface

This thesis is submitted in partial fulfillment of the requirements for the degree of Philosophiae Doctor (PhD) at the Norwegian University of Science and Technology (NTNU). The research presented in this thesis has been conducted at the Department of Engineering Cybernetics from September 2011 to March 2016.

Acknowledgments

First, I would like to thank my main supervisor Professor Tor Arne Johansen. I appreciate the help and support he has given me during my PhD studies. I would also like to thank my co-supervisor Associate Professor Kimmo Kansanen for our discussions about useful research directions.

I would also like to thank Dr. Bram Hunnekens, Professor Nathan van de Wouw, Espen Skjong and Professor Marta Molinas for their contributions to the papers on which this thesis is based. Additionally, I am grateful to Atle Rygg Årdal for his help obtaining the preliminary work which has led to the results in Chapter 6.

Funding for the research presented in this thesis has been provided by the Faculty of Information Technology, Mathematics and Electrical Engineering at NTNU and by the Research Council of Norway by the KMB project D2V, project number 210670, and through the Centres of Excellence funding scheme, project number 223254 - NTNU AMOS, for which I am grateful.

Moreover, I would like to thank Professor Martin Guay, Professor Christian Ebenbauer and Professor Bjarne Foss for accepting to be on the dissertation defense committee.

Furthermore, I am thankful to my colleagues and former colleagues at the Department of Engineering Cybernetics for making my time in Trondheim a pleasant one, both during and outside office hours.

In addition, I would like to thank my parents Max and Henriëtte and my sister Janneke for their support and their visits to Norway. Last, I would like to thank Maria, to whom I dedicate this thesis. Thank you for your support, understanding and patience, which means a lot to me.

Contents

Chapter 1

Introduction

1.1 Introduction to extremum-seeking control

Extremum-seeking control is an adaptive control methodology. The aim of extremum-seeking control is to optimize the steady-state performance of a given plant. A cost function is designed to quantify the plant performance as a function of tunable plant parameters and measurable performance indicators such that the steady-state performance of the plant can be expressed as a constant number for each set of constant plant-parameter values. Loosely speaking, any tunable parameter that influences the plant performance is a plant parameter (such as controller setpoints, controller parameters and actuator inputs) and any measurable signal that contains information about the plant performance is a performance indicator. By designing the cost function as such, the relation between constant plant-parameter values and the steady-state plant performance can be represented by a static function, which we refer to as the objective function. The optimal steady-state plant performance corresponds to a global extremum (that is, a minimum or maximum) of the objective function. Similarly, a local extremum of the objective function indicates local optimality of the stead-state performance of the plant.

If the objective function is known explicitly, the global or local extremum of the objective function can be computed with the help of numerical methods; see Boyd and Vandenberghe (2004); Horst and Pardalos (1994); Nocedal and Wright (1999) and many others. Explicit knowledge of the objective function requires that the steady-state relation between the plant parameters and the performance indicators is known. In the context of extremum-seeking, however, the steady-state relation between the plant parameters and the performance indicators is often unknown or only partly known due to insufficient knowledge about the plant. An analytic expression of the objective function is therefore not available, which precludes the use of numerical methods. Extremum-seeking control utilizes measurements of the performance indicators instead of explicit knowledge to find the local or global extremum of the objective function. The measurements may differ from the steady-state values of the performance indicators in two ways. First, the measured values are not equal to the steady-state values due to transients. Second, the measurements are affected by measurement noise.

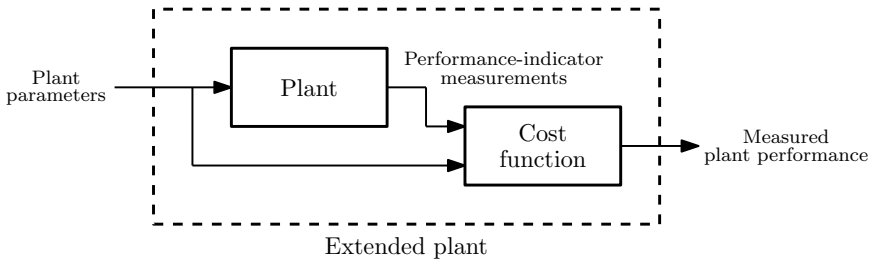

Figure 1.1: Closed-loop system of plant and extremum-seeking controller.

We refer to the output of the cost function as the measured plant performance if the plant parameters and the measurements of the performance indicators are used as input to the cost function. Because the measurements and the steady-state values of the performance indicators deviate, the measured plant performance varies from the objective function value. Hence, the function value of the objective function cannot be evaluated exactly using the measured plant performance. Extremum-seeking control searches for (or seeks) an extremum of the objective function despite the fact that the objective function is unknown, and that its value cannot be evaluated exactly via measurement.

Black-box extremum-seeking methods

A general approach in the field of extremum-seeking control is to consider the plant and the cost function as one extended plant with the plant parameters as input and the measured plant performance as output; see Figure 1.1. Assuming that the measured plant performance remains close to the steady-state performance of the plant, the value of the objective function can be approximated by the measured plant performance. Therefore, derivative-based optimization methods can be applied to search for a local extremum of the objective function if the required derivatives are estimated using the measured plant performance (Ghaffari et al., 2012; Moase et al., 2010; Nešić et al., 2010, 2012; Teel and Popović, 2001). Alternatively, the non-derivative-based optimization methods in Khong et al. (2013a,b); Nešić et al. (2013b) can be applied to obtain an approximation of a global (and not only local) extremum of the objective function. However, these derivative-free methods are more computationally demanding as all measurements need to be stored and processed at each iteration step. The derivative-based and non-derivative-based extremum-seeking methods mentioned above do not require explicit knowledge about the plant. Therefore, they are sometimes referred to as "'black-box" methods (Adetola and Guay, 2011; Dalvi and Guay, 2009; Esmaeilzadeh Azar et al., 2011) or "model-free" methods (Becker et al., 2007; Cochran et al., 2009; Dixon and Frew, 2007).

In order not to excite the dynamics of the plant and to ensure that the measured plant performance remains close to the steady-state performance of the

plant, the plant parameters are required to be slowly time varying with respect to the plant dynamics. This limits the rate of information about the objective function and its derivatives that can be extracted from the measured plant performance. Because all necessary information about the objective function is obtained via the measured plant performance, the converge of black-box methods is generally slow.

Gray-box extremum-seeking methods

A priori knowledge about the plant can be incorporated to increase the convergence rate of the optimization process. In its simplest form, a static model of the extended plant can be obtained from a parametrization of the objective function if the general shape of the objective function is known. By estimating the values of the parameters of the model and computing the derivatives of the model with respect to the plant parameters, derivative-based optimization methods can be applied to search for a local extremum of the objective function (Mohammadi et al., 2014; Nešić et al., 2012). Similarly, simultaneous state estimation and parameter identification can be used to find the performance-optimizing plant-parameter values if a parametrized model of the plant dynamics is available (Nešić et al., 2013a). If the extended plant can be approximated by a Hammerstein model, the parameters of the Hammerstein model can be estimated using a least-squares approach, after which the optimal steady-state plant performance can be computed from the model (Bamberger and Isermann, 1978; Fabri et al., 2015; Golden and Ydstie, 1989). A similar approach is used in (Wittenmark and Evans, 2002) for Wiener-type plants. Extremum-seeking methods that use a parametrized model of the extended plant are referred to as "gray-box" methods (Mohammadi et al., 2014; Nešić et al., 2013a) or "model-based" extremum-seeking methods (Michalowsky and Ebenbauer, 2015; Sharafi et al., 2015; Sternby, 1980).

Other extremum-seeking methods

Although the majority of the proposed extremum-seeking methods can be classified as a black-box method or a gray-box method, there are extremum-seeking methods that do not fall under these categories. These methods often address a different type of extremum-seeking problem where the state of the plant is to be regulated to the unknown extremum of an objective function. In Cougnon et al. (2011); DeHaan and Guay (2005); Guay and Zhang (2003), input-affine plants with unknown parameters are considered. An extremum-seeking-control method is proposed to estimate the plant parameters and to regulate the state of the plant to the extremum of the objective function using the parameter estimates, where the objective function is a function of the state and the unknown parameters of the plant. Zhang and Ordóñez (2007, 2012) consider a class of known nonlinear plants. The objective function is an unknown static function of the

state of the plant. Under the assumption that the plant is feedback linearizable, a controller is designed to regulate the state to any desired value. The extremum of the objective function is identified with the help of non-derivative-based optimization methods, for example the derivative-free trust-region methods in Conn et al. (1997, 2009); Powell (2002).

Cost function design

The objective function is generally considered to be time invariant. However, extremum seeking control can also be applied to track slowly time-varying extrema (Brunton et al., 2010; Krstić, 2000; Zhang et al., 2007b). Nonetheless, it is often essential to define the cost function such that the resulting steady-state performance of the plant is constant for any set of constant plant parameters. If the steady-state response of the performance indicators is constant, the use of a static cost function results in a constant steady-state plant performance, as required. For time-varying steady-state performance-indicator responses, this does not hold, however. If the steady-state response of the performance indicators is periodic with a known period, a cost function that evaluates the performance of the plant over one or multiple periods of the steady-state response of the performance indicators can be employed to obtain a constant steady-state plant performance (Guay et al., 2007; Haring et al., 2013; Höffner et al., 2007; Hunnekens et al., 2015). If the period of the steady-state response is unknown, exponential filters can be utilized to extract the desired characteristic from the steady-state response to quantify the performance of the plant (Antonello et al., 2009; Kim et al., 2009; Wang and Krstić, 2000). The use of exponential filters results in a quasiconstant steady-state plant performance, which deteriorates the optimization accuracy of the extremum-seeking controller, however. For the special case that the state of the plant is resettable, the transient response of the plant can be optimized by defining the cost function such that the performance of the plant is evaluated over a finite time window (Frihauf et al., 2013; Khong et al., 2016; Killingsworth and Krstić, 2006).

Constraints

Extremum-seeking control problems are often formulated as unconstrained optimization problems. Inequality constraints on the plant parameters can be handled by augmenting the cost function with penalty functions; see for example (DeHaan and Guay, 2005; Guay et al., 2015). Alternatively, anti-windup (Ye and Hu, 2013; Tan et al., 2013) or projection (Frihauf et al., 2012; Guay and Zhang, 2003; Mills and Krstić, 2014) can be applied to enforce inequality constraints on the plant parameters. Constraints on the state of the plant and the performance indicators can generally not be imposed because the state is unknown and the influence of the plant parameters on the performance indicators is not known a priori.

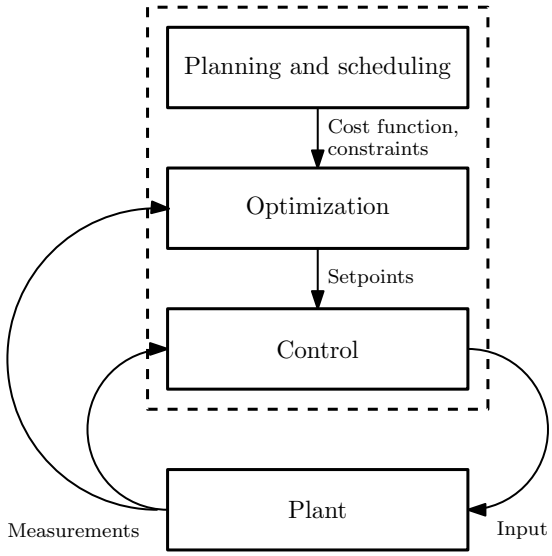

Figure 1.2: Three-layer control structure. Adapted from Jäschke and Skogestad (2011).

Hierarchical control structure

A frequently made assumption in the field of extremum-seeking control is that the plant is inherently stable or stabilized by a low-level controller (Krstić and Wang, 2000; Tan et al., 2006). Extremum-seeking control does not stabilize an unstable plant in general. Exceptions are the vibrational extremum-seeking methods in Moase and Manzie (2012b); Scheinker and Krstić (2013); Zhang et al. (2007b) for example; see Section 1.1.1. A controller with a hierarchical control structure may be employed to stabilize an unstable plant and optimize its performance (Findeisen et al., 1980; Jäschke and Skogestad, 2011; Skogestad, 2004). Jäschke and Skogestad (2011) propose a three-layer control structure for plants in the process industry; see Figure 1.2. The three layers operate on different time scales. Each layer generates an input for the layer below.

- The top layer is the planning and scheduling layer. Its purpose is to quantify the performance of the plant by specifying the cost function and to impose constraints to avoid undesirable or infeasible conditions. The cost function and the constraints may be updated while the plant is under operation to address changing demands. The slowest time scale is assigned to this layer to have sufficient time to reoptimize the plant performance after each update while maintaining stability.

- The optimization layer is below the planning and scheduling layer. Open-loop optimization methods can be applied to find performance-optimal setpoints for the control layer if an accurate model of the plant is available.

If the cost function and the constraints are known in advance, the optimal setpoints can be precomputed offline, which allows for a fast implementation. However, it is often preferable to apply online optimization methods that incorporate plant measurements (including extremum-seeking control) to handle unmodeled disturbances. The implementation of online optimization methods can be complicated and may involve data estimation and reconciliation, steady-state detection, and solving a large-scale nonlinear optimization problem (Jäschke and Skogestad, 2011).

- The bottom layer is the control layer, which consists of PID controllers or other stabilizing feedback controllers. The control layer generates the inputs to the actuators of the plant. The time scale of the control layer is faster than the time scale of the optimization layer to have sufficient time to stabilize the plant at the setpoint values provided by the optimization layer.

In the context of extremum-seeking control, the setpoints for the controllers in the control layer are the plant parameters and the plant measurements are the performance indicators. The planning and scheduling layer can be discarded from the control structure if the cost functions and the constraints do not change. Similarly, it is not always necessary to include a control layer if the plant is inherently stable. Nonetheless, a low-level control layer may be desirable to be able to cope with fast disturbances. Examples of control structures that consist of a high-level extremum-seeking controller and a low-level control layer can be found in Bratcu et al. (2008); Dixon and Frew (2009); van der Meulen et al. (2012). For large-scale plants, it may be necessary to reduce the number of plant parameters that are tuned by extremum-seeking control. Methods based on plant-parameter sensitivity can be applied to determine which (combinations of) plant parameters are most suitable to use, similar to Alstad and Skogestad (2007); Alstad et al. (2009).

1.1.1 Historical overview of extremum-seeking control

Dating back to the work by Leblanc (1922), extremum-seeking control is one of the first forms of adaptive control. Leblanc (1922) applied a perturbation-based extremum-seeking method to maximize the power that is transferred from an overhead electrical transmission line to a tram car. Extremum-seeking control first got considerable attention in the USSR in the 1940s (Kazakevich, 1944). Interest in extremum-seeking control in the Western world stared after the appearance of the survey paper by Draper and Li (1951) on extremum-seeking control for internal combustion engines. Extremum-seeking control went by many different names in the 1950s and the 1960s, such as "optimalizing control" (Draper and Li, 1951; Tsien and Serdengecti, 1955), "hill-climbing regulation" (Roberts, 1965), "extremum control" (Morosanov, 1957; Kazakevich, 1961) and

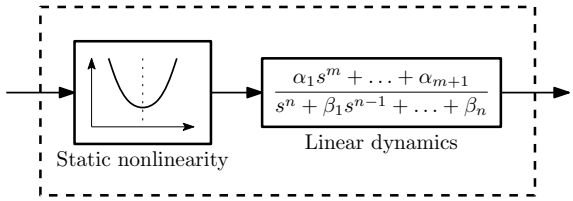

(a) Hammerstein model

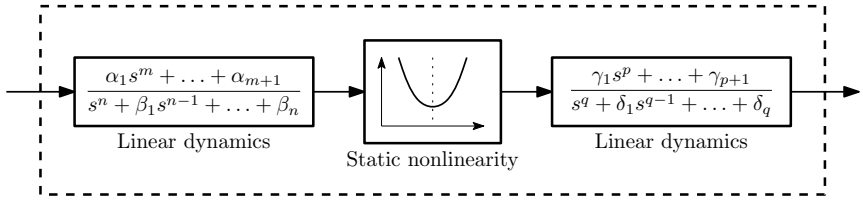

(b) Wiener-Hammerstein model

Figure 1.3: Hammerstein and Wiener-Hammerstein models

"automatic optimization" (Meerkov, 1967a,b, 1968) to name a few. Researchers faced the difficulty of mathematically formulating a model that is general enough to describe a large class of plants, while at the same time detailed enough to allow calculations to be done. Common practice was either to neglect plant dynamics and use a static nonlinear plant model Blackman (1962); Ostrovskii (1957), to mimic the plant dynamics by adding a fixed delay to the static nonlinear model (Frey et al., 1966), or to model the plant as a combination of linear dynamics and a static nonlinearity, resulting in Hammerstein models (a static nonlinearity followed by linear dynamics) (Eveleigh, 1967; Hamza, 1966; Kazakevich, 1961; Jacobs and Shering, 1968) or Wiener-Hammerstein models (linear dynamics followed by a static nonlinearity and again linear dynamics) (Pervozvanskii, 1960; Serdengecti, 1956); see Figure 1.3. Many different extremum-seeking methods were developed. Several authors considered perturbation methods to optimize the steady-state performance of the plant (Eveleigh, 1967; Kisiel and Rippin, 1965; Meerkov, 1967a), similar to Leblanc (1922). By adding perturbations to the plant-parameter signals and correlating the measured plant-performance signal with the same perturbations, an estimate of the gradient of the objective function can be obtained. The gradient estimate can subsequently be used to find the extremum of the objective function. In Blackman (1962); Frait and Eckman (1962), a gradient estimate is obtained by correlating the signals of the measured plant performance and the plant parameter, without adding a perturbation. Other extremum-seeking methods do not rely on an estimate of the gradient of the objective function. Instead, the plant-parameter values are driven in a predefined search direction in a continuous or step-wise manner until no further improvement in the measured plant performance is observed, after

which the search direction is changed (Tsien and Serdengecti, 1955; Jacobs and Wonham, 1961). The methods mentioned here are all black-box methods.

The first gray-box methods were developed in the 1960s and the 1970s. By neglecting plant dynamics and assuming that the objective function is quadratic, the extended plant (that is, the plant plus cost function) can be modeled as a second-order polynomial. By estimating the parameters of the polynomial, an estimate of the extremum of the objective function can be obtained that can be used to optimize the steady-state performance of the plant (Clarke and Godfrey, 1966, 1967; Perelman, 1961). Linear dynamics can also be included in the plant model. Because it is convenient to estimate the model parameters if they appear linearly in the model, the plant model is often restricted to the class of Hammerstein models (Keviczky and Haber, 1974; Roberts, 1965). Least-squares methods are frequently used to estimate the parameters of the Hammerstein model (Bamberger and Isermann, 1978; Kazakevich and Mochalov, 1975; Golden and Ydstie, 1989). Alternative methods to estimate the model parameters are discussed in Kazakevich and Mochalov (1984). The problem of simultaneous estimation and optimization is a dual control problem as defined by Feldbaum (1960a,b, 1961a,b). Optimal solutions for a dual control problem are generally difficult to obtain, even for simple cases (Filatov and Unbehauen, 2000, 2004; Wittenmark, 1995). Suboptimal dual controller are applied in Wittenmark (1993); Wittenmark and Urquhart (1995) to simultaneously estimate the parameters of the Hammerstein model and optimize the steady-state plant performance. In many ways, these approaches are similar to the model-predictive control approaches in Heirung et al. (2015a,b); Marafioti et al. (2014); Shouche et al. (1998, 2002), where simultaneous model identification and optimization is considered.

As research interest shifted to other topics, black-box extremum-seeking methods became less popular after the 1960s. The research activity in black-box methods got reignited by the publication of a paper by Krstić and Wang (2000). Without defining the structure of the plant, Krstić and Wang (2000) proved that a perturbation-based extremum-seeking controller successfully optimizes the plant's performance if the plant satisfies certain properties. Due to this renewed formulation, it became apparent that extremum-seeking control can be applied to a large class of systems. Many applications followed; see for example Ariyur and Krstić (2003); Tan et al. (2010) and references therein. The extremum-seeking method in Krstić and Wang (2000) relies on an estimate of the gradient of the objective function to optimize the steady-state plant performance. The method can be extended to include Hessian information of the objective function so that Newton-like optimization methods can be applied (Ghaffari et al., 2012; Moase et al., 2010; Nešić et al., 2010, 2012). Although many authors consider similar methods as in Krstić and Wang (2000) (see for example Becker et al. (2007); Pastoor et al. (2008); Peterson and Stefanopoulou (2004)), also other extremum-seeking methods have been studied in recent years. Some meth-

ods create a sliding mode outside a region near the extremum of the objective function, such that the plant parameters are steered towards the extremum while in sliding mode (Drakunov et al., 1995; Fu and Özgüner, 2011; Haskara et al., 2000; Pan et al., 2003). Other methods rely on a sampled-data approach where the plant performance is measured and the plant parameters are updated at each time step. By choosing the time between the update of the plant parameters and the measurement of the plant performance to be large, the transient of the plant dynamics has sufficiently died out to apply derivative-based optimization methods in combination with finite-difference methods (Popović et al., 2003; Teel and Popović, 2001) or non-derivative-based optimization methods (Khong et al., 2013a,b; Nešić et al., 2013b) to optimize the steady-state performance of the plant.

Also gray-box methods for general nonlinear plants have been developed in recent years. If plant dynamics are neglected, a parametrization of the objective function can be used as a model for the extended plant (Mohammadi et al., 2014; Nešić et al., 2012). A large selection of parameter estimators and optimizers can be used to estimate the model parameters and regulate the plant parameters to their performance-optimizing values (Nešić et al., 2013a). If a parametrized model of the extended plant (including plant dynamics) is available, a state estimator in addition to the model-parameter estimator can be defined to optimize the steady-state plant performance (Adetola and Guay, 2006; Nešić et al., 2013a).

Recently, a new type of extremum-seeking control has appeared in the literature, which is similar to vibrational control (Bellman et al., 1986; Bullo, 2002; Meerkov, 1980). Instead of slow perturbations (as in Krstić and Wang (2000), for example), these extremum-seeking methods use rapid perturbations to optimize the steady-state plant performance (Moase and Manzie, 2012b; Scheinker and Krstić, 2013). The convergence of these methods is faster than other types of extremum-seeking methods. Even an arbitrarily fast convergence is reported in Moase and Manzie (2012a,b); Zhang et al. (2007b), leading to the term "'fast" extremum-seeking control. Another advantage is that these methods can stabilize unstable plants (Moase and Manzie, 2012b; Scheinker and Krstić, 2013; Zhang et al., 2007b). However, the applications of these methods seems to be restricted to Hammerstein-type or Wiener-Hammerstein-type plants (Moase and Manzie, 2012a,b) or to input-affine plants (Dürr et al., 2013, 2015; Scheinker and Krstić, 2013, 2014). The vast majority of these methods are black-box methods. A gray-box approach for Hammerstein-type plants is presented in Sharafi et al. (2015).

1.1.2 Applications of extremum-seeking control

There are many different methods to optimize the performance of a plant depending on how much information about the plant is available. The available

information about the plant translates to the accuracy of the model of the plant that can be obtained: a perfect model requires exact knowledge of the plant, whereas a simple (or simplified) model only requires approximate knowledge of the plant. If an accurate plant model is available, a large class of numerical optimization methods can be applied to identify the performance-optimal conditions of the plant (Boyd and Vandenberghe, 2004; Horst and Pardalos, 1994; Nocedal and Wright, 1999). However, an accurate plant model is not always available due to insufficient knowledge about the plant. Model uncertainty and unmodeled disturbances result in a loss of performance. Robust optimization methods can be applied to minimize the loss of performance (Bertsimas et al., 2011; Beyer and Sendhoff, 2007). Alternatively, measurements can be used to compensate for the lack of knowledge. Optimization algorithms that use measurements are often referred to as "adaptive" or "real-time" optimization methods (Chachuat et al., 2009). The class of real-time optimization methods includes self-optimizing control (Kariwala et al., 2008; Skogestad, 2000), necessary conditions of optimality tracking (François et al., 2005; Srinivasan et al., 2008), adaptive and real-time model predictive control (Adetola et al., 2009; De Souza et al., 2010; Diehl et al., 2002) and extremum-seeking control (Ariyur and Krstić, 2003; Tan et al., 2010).

Extremum-seeking control is one of the few optimization methods that do not require an accurate model of the plant; black-box extremum-seeking methods do not require a plant model at all, while often a relatively simple plant model with unknown parameters suffices for gray-box extremum-seeking methods. Due to the use of no model or a simple model, incorporating measurement information is relatively easy; the use of a simple update law is often sufficient (Ariyur and Krstić, 2003; Tan et al., 2010). By contrast, real-time model-predictive control commonly requires a recalculation of the performance-optimal conditions after each measurement by solving an optimization problem (De Souza et al., 2010; Diehl et al., 2002). This can be a computationally demanding task, depending on the complexity and scale of the plant model.

Not using an accurate plant model also has its drawbacks. While model information is readily available, the required information to optimize the performance of the plant can generally not be measured instantaneously. Hence, it takes a certain amount of time to gather the necessary information to optimize the plant performance via measurements, which implies that the convergence rate of extremum-seeking control is limited in practice. Because extremum-seeking control is primarily based on measurement information, the convergence of extremum-seeking methods is commonly much slower than the convergence of optimization methods that primarily use model information to optimize the plant performance. Moreover, extremum-seeking control is more sensitive to measurement noise than methods that mainly rely on a plant model. Extremum-seeking methods that utilize multiple identical or similar units of the same plant can be applied to increase the rate of information about the plant that can be obtained (Esmaeilzadeh Azar et al., 2011; Khong et al., 2013b; Srinivasan, 2007). However,

these methods cannot be applied if only one unit of the plant is available. The required amount of information to optimize the plant performance is dependent on the number of plant parameters for black-box extremum-seeking methods, or the number of model parameters for gray-box extremum-seeking methods. Although an arbitrary number of plant parameters or model parameters can be selected in theory, the number of plant parameters or model parameters is in practice limited to a few to ensure that extremum-seeking control does not become impractical to use due to a sluggish convergence.

Due to slow convergence, extremum-seeking control is generally not the most suitable method to optimize the performance of the plant if an accurate model of the plant is available. Therefore, typical applications of extremum-seeking control are applications for which an accurate model is difficult or expensive to obtain. This can have several reasons, for example: the complexity of the plant is high; there are no suitable measurements available to validate the model; the plant is subject to time-varying disturbances that are difficult to model accurately.

Academic applications of extremum-seeking control

In an academic setting, extremum-seeking control has been applied to many engineering domains. Application areas in the automotive industry include internal combustion engines (Hellström et al., 2013; Killingsworth et al., 2009; Larsson and Andersson, 2008), anti-lock braking systems (Dinçmen et al., 2014; Drakunov et al., 1995; Zhang and Ordóñez, 2007) and transmission systems (van der Meulen et al., 2012, 2014). Extremum-seeking control has been used to maximize the generated power of wind turbines (Creaby et al., 2009; Ghaffari et al., 2014; Johnson and Fritsch, 2012) and solar arrays (Brunton et al., 2010; Ghaffari et al., 2015; Leyva et al., 2006). Several applications in process control have been reported (Bastin et al., 2009; Dochain et al., 2011; Guay et al., 2004; Wang et al., 1999). In addition, navigation and source-seeking applications of mobile robots using extremum-seeking control have been investigated (Cochran and Krstić, 2009; Dixon and Frew, 2009; Liu and Krstić, 2010; Matveev et al., 2011; Zhang et al., 2007a). Other application areas include nuclear-fusion reactors (Carnevale et al., 2009; Centioli et al., 2008; Ou et al., 2008), fuel-cell power plants (Bizon, 2010; Dalvi and Guay, 2009; Zhong et al., 2008) and air-flow optimization (Becker et al., 2007; Beaudoin et al., 2006; Pastoor et al., 2008); see also Ariyur and Krstić (2003); Tan et al. (2010); Zhang and Ordóñez (2012) and references therein. Applicability of the proposed extremum-seeking methods are often demonstrated by simulation examples. Nonetheless, there are a significant number of applications for which a proof of concept is given by practical experiments; see for example Ghaffari et al. (2015); Killingsworth et al. (2009); van der Meulen et al. (2012).

Industrial applications of extremum-seeking control

Although many applications of extremum-seeking control have been proposed over the years, only a few industrial applications have been reported where extremum-seeking control is used on a daily basis. Olsen et al. (1976) present an extremum-seeking control method to maximize the output flow of a grinding mill in spite of ore-quality variations by tuning the feed rate of the mill. The influence of the feed rate on the output flow is indirectly obtained from measurements of the power consumption and the oil pressure in the bearings. At the time of publication, the extremum-seeking method had been intermittently tested on a $6\text{m}^{\varnothing} \times 6\text{m}$ grinding mill at Fosdalens Bergverk A/S, Norway, for about a year.

A second industrial application is presented in Borg et al. (1986), where extremum-seeking control is applied to the production of aluminium in alumina reduction cells. Because the alumina concentration in reduction cells cannot be measured directly, the main idea in Borg et al. (1986) is to control the concentration of alumina by adapting the feed rate of alumina such that the electric resistance of the molten liquid inside the cells is minimized. The electric resistance is obtained from current and voltage measurements. The gradient of the electric resistance with respect to the feed rate is estimated using a gray-box approach. The gradient estimate is subsequently used in the control law of the feed rate to keep the electric resistance at a minimum. The proposed control system had been implemented and was in operation on several reduction cells at A/S Årdal og Sunndal Verk, Norway, for almost three years at the time of publication.

There are likely to be several other industrial applications of extremum-seeking control. However, the number of industrial application of extremum-seeking control reported in the open literature is scarce.

1.2 Scope of the thesis

In this work, we consider black-box extremum-seeking control. We mainly focus on extremum-seeking control methods that rely on added perturbations to estimate the required derivatives of the objective function to optimize the steady-state performance of a plant; see for example Ariyur and Krstić (2003); Tan et al. (2010). Because black-box extremum-seeking methods do not require a model of the plant to optimize the steady-state plant performance, they can be applied to many engineering domains. The main drawback of black-box extremum-seeking methods is a slow convergence, as discussed in Section 1.1. Therefore, we aim to improve the convergence rate of these methods. For certain classes of plants, large-amplitude high-frequency perturbations can be used to speed up the convergence of the extremum-seeking scheme (Moase and Manzie, 2012b; Scheinker and Krstić, 2013). However, due to actuator limitations, a high control effort and an increased wear of components, large-amplitude high-frequency perturbations may be undesirable or inadmissible in practice. The first research objective of this thesis is formulated as follows.

> *Develop a black-box extremum-seeking method with an increased convergence rate compared to classical extremum-seeking methods that uses small-amplitude low-frequency perturbations.*

Although to aim of applying extremum-seeking control is to optimize the steady-state performance of a plant, the optimal steady-state performance is commonly not obtained (not even in infinite time). This can be attributed to the use of performance-indicator measurements, often in combination with added perturbations, to find the optimal steady-state plant performance. While the steady-state values of the performance indicators are assumed to be measured, the measurements are different from the steady-state values due to measurement noise and the dynamic response of the plant to changing plant-parameter values. Nonetheless, several extremum-seeking method have been proposed in the literature to obtain asymptotic convergence. These methods are based on regulating the amplitude of the perturbations (Moura and Chang, 2013; Stanković and Stipanović, 2010; Wang et al., 2016) or omitting the perturbations entirely (Blackman, 1962; Frait and Eckman, 1962; Hunnekens et al., 2014). Commonly local convergence to the optimum is proved, often for a limited class of plants. A global asymptotic stability result for general nonlinear plants is missing. This brings us to the second research objective of this thesis.

> *Develop a black-box extremum-seeking method for general nonlinear dynamical plants that ensures global asymptotic stability of the resulting closed-loop system of plant and controller with respect to the optimal steady-state performance of the plant.*

The two research objectives are addressed in the remaining chapters of the thesis.

1.3 Contributions and outline of the thesis

The outline of the thesis is given next. The main contributions of the thesis are highlighted for each chapter.

- **Chapter 2:** In classical extremum-seeking methods, estimates of the required derivatives of the objective function are obtained by correlating the measured plant-performance signal and the perturbation signals. If the perturbation-related content of the plant-parameter signals is low, a more accurate derivative estimate and a faster convergence towards the optimal steady-state plant performance may be obtained by utilizing information of the entire plant-parameter signals. We introduce a least-squares observer that uses the perturbation signals as well as the nominal plant-parameter signals to obtain an accurate estimate of the gradient of the objective function. Moreover, a simulation example illustrates that the accuracy of the gradient estimate and the convergence rate of the extremum-seeking scheme can be further enhanced for sufficiently low perturbation frequencies if curvature information of the objective function is used. In addition, we show that region of attraction of the extremum-seeking scheme can be made global by normalizing the adaptation gain of the extremum-seeking controller.

- **Chapter 3:** The extremum-seeking controller in Chapter 2 assumes that the measurements of the performance indicators and the update of the plant parameters are continuous in time. However, in many practical applications, the measurements of the performance indicators are sampled and the plant parameters are updated in a discrete-time fashion. To optimize the steady-state plant performance in a sampled-data setting, a discrete-time version of the extremum-seeking controller in Chapter 2 is presented. The discrete-time controller is equivalent to the continuous-time controller in Chapter 2 for the limit as the sampling time approaches zero. A simulation example displays that the response of the discrete-time controller is similar to the response of the continuous-time controller in Chapter 2 for sufficiently high sampling rates.

- **Chapter 4:** Perturbations may not be necessary to optimize the steady-state performance of the plant; the plant-parameter signals may be sufficiently rich without any added excitation to accurately estimate the required derivatives of the objective function. A self-driving extremum-seeking controller can be applied to optimize the steady-state performance of a certain class of dynamical plants. It is proved that the performance of the plant exponentially converges to the optimal steady-state plant performance. To the best of the authors' knowledge, this is the first time a rigorous stability proof of a self-driving extremum-seeking scheme for dynamical plants is presented.

- **Chapter 5:** The self-driving extremum-seeking scheme in Chapter 4 only convergences to the optimal steady-state plant performance for a certain class of dynamical plants. We present an perturbation-based extremum-seeking controller to optimize the steady-state performance of general nonlinear plants. A stability analysis proves that the closed-loop system of plant and controller is globally asymptotically stable with respect to the optimal steady-state plant performance under given assumptions and suitable tuning conditions. The key to this result is that the amplitude and the frequencies of the perturbations, as well as other tuning parameters of the controller, are time varying and asymptotically decay to zero as time goes to infinity. Global asymptotic stability can even be obtained if the plant is subject to a time-varying disturbance under the assumption that the perturbations and the zero-mean component of the disturbance are uncorrelated. In addition, the time-varying tuning parameters can be chosen such that global asymptotic stability is guaranteed for any plant that satisfies the given assumptions.

- **Chapter 6:** The mitigation of harmonic distortion in electrical grids using active power filters is discussed. An extremum-seeking control method is proposed to tune the current injection of an active power filter to the grid. We show that the extremum-seeking control method can be parallellized under certain design assumptions to significantly increase its optimization speed. Moreover, the extremum-seeking control method can be implemented on top of existing approaches to combine the fast transient response of conventional harmonic-mitigation methods with the optimizing capabilities of extremum-seeking control. A case study a two-bus electrical grid with distributed generators is presented. The extremum-seeking method is compared with two benchmark methods. The differences in performance for various load conditions, measurement noise and model mismatch are discussed.

- **Chapter 7:** The main conclusions in this thesis are summarized and some recommendations for future work are provided.

1.3.1 List of publications

The following list of publications forms the basis of the thesis:

- M. Haring and T. A. Johansen. Extremum-seeking control for nonlinear plants by least-squares gradient estimation. *Automatica*, 2015. Manuscript submitted for publication.

- M. Haring and T. A. Johansen. Asymptotic stability of perturbation-based extremum-seeking control for nonlinear plants. *IEEE Transactions on Automatic Control*, 2016. Manuscript submitted for publication.

- M. Haring, B. Hunnekens, T. A. Johansen, and N. van de Wouw. Self-driving extremum-seeking control for nonlinear dynamic plants. *Automatica*, 2016a. Manuscript submitted for publication.

- M. Haring, E. Skjong, T. A. Johansen, and M. Molinas. An extremum-seeking control approach to harmonic mitigation in electrical grids. *IEEE Transactions on Control Systems Technology*, 2016b. Manuscript submitted for publication.

Chapters 2, 4, 5 and 6 are based on Haring and Johansen (2015), Haring et al. (2016a), Haring and Johansen (2016) and Haring et al. (2016b), respectively.

Additional publications

The following conference paper is not part of the thesis, but serves as a background work:

- B. G. B. Hunnekens, M. A. M. Haring, N. van de Wouw, and H. Nijmeijer. A dither-free extremum-seeking control approach using 1st-order least-squares fits for gradient estimation. In *Proceedings of the 53rd IEEE Conference on Decision and Control*, pages 2679–2684, Los Angeles, California, December 15-17, 2014.

The missing stability proof for dynamical plants in the above mentioned paper is the main motivation for the results in Chapter 4. The following publications were written in the period of the doctoral study, but are not included in the thesis:

- B. G. B. Hunnekens, M. A. M. Haring, N. van de Wouw, and H. Nijmeijer. Steady-state performance optimization for variable-gain motion control using extremum seeking. In *Proceedings of the 51st IEEE Conference on Decision and Control*, pages 3796–3801, Maui, Hawaii, USA, December 10-13, 2012.

- N. van de Wouw, M. Haring, and D. Nešić. Extremum-seeking control for periodic steady-state response optimization. In *Proceedings of the 51st IEEE Conference on Decision and Control*, pages 1603–1608, Maui, Hawaii, USA, December 10-13, 2012.

- M. Haring, N. van de Wouw, and D. Nešić. Extremum-seeking control for nonlinear systems with periodic steady-state outputs. *Automatica*, 49(6): 1883–1891, 2013.

1.4 Notations

The set of real numbers is denoted by $\mathbb{R}$. The set of natural numbers (nonnegative integers) is denoted by $\mathbb{N}$. The sets of positive real numbers and nonnegative real numbers are denoted by $\mathbb{R}_{>0}$ and $\mathbb{R}_{\geq 0}$, respectively. Similarly, the set of positive integers is denoted by $\mathbb{N}_{>0}$. Vectors, matrices as well as functions with multidimensional outputs are printed in a bold font, whereas scalars and functions with scalar outputs are printed in a normal (nonbold) font. Note that multidimensional variables are printed in a normal font if their dimensions are set to one for illustrative purposes. By $\mathbf{I}$ and $\mathbf{0}$, we denote the identity matrix and the zero matrix, respectively. The Euclidean norm is denoted by $\|\cdot\|$.

Chapter 2

Extremum-seeking control for nonlinear plants by least-squares gradient estimation

In this chapter, we present a perturbation-based extremum-seeking controller to optimize the performance of a general nonlinear plant with an arbitrary number of tunable plant parameters in the presence of an unknown bounded disturbance. The gradient of the objective function that relates the plant-parameter values to the steady-state performance of the plant is accurately estimated using a least-squares observer. We show that the region of attraction for the closed-loop system of plant and controller can be made global by normalizing the adaptation gain of the extremum-seeking controller. The convergence rates of our controller and three controllers in the literature are compared for a variety of simulation examples. Our controller compares favorably for five of the eight tested examples. Results of an additional in-depth example indicate that a faster convergence can be obtained with an observer-based controller than with a classical controller if small-amplitude perturbations are applied. Furthermore, the simulation results show that incorporating curvature information of the objective function, if available, significantly improves the convergence of the presented controller if the frequency of the perturbations is low.

2.1 Introduction

In this chaper, we focus on extremum-seeking methods that rely on added perturbations to optimize the steady-state performance of a plant. Although already popular in the 1950s and 1960s (Draper and Li, 1951; Eveleigh, 1967; Jacobs and Shering, 1968), perturbation-based methods have become the most popular class of extremum-seeking control methods in recent years. Much of this success can be attributed to the paper (Krstić and Wang, 2000). Until its publication, it was common practice to assume that the plant is static (Blackman, 1962; Ostrovskii, 1957) or can be described by a combination of a static nonlinearity and linear dynamics (Eveleigh, 1967; Jacobs and Shering, 1968; Pervozvanskii, 1960).

Without defining the structure of the plant, Krstić and Wang (2000) proved that the a plant's performance can successfully be optimized with a perturbation-based extremum-seeking method if the plant satisfies certain properties. Due to this renewed formulation, it became apparent that extremum-seeking control can be applied to a large class of systems. Many applications followed, often using a similar extremum-seeking controller as in Krstić and Wang (2000); see for example Bizon (2010); Ou et al. (2008); Pastoor et al. (2008); Peterson and Stefanopoulou (2004); Zhong et al. (2008).

Tuning largely determines the optimization performance of extremum-seeking controllers. Tan et al. (2006) showed that, for fixed tuning conditions, there exists a trade-off between the convergence rate and the size of the region of the optimum to which the plant parameters ultimately converge (that is, a high convergence rate implies a large ultimate bound). For plants of the Hammerstein or Wiener-Hammerstein type, Moase and Manzie (2012a,b) found that an arbitrarily high convergence rate and an arbitrarily small ultimate bound can be achieved simultaneously by selecting a sufficiently high perturbation frequency and a sufficiently low perturbation amplitude, respectively. However, as the extremum-seeking methods in Moase and Manzie (2012a,b) are more sensitive to measurement noise for higher perturbations frequencies and lower perturbation amplitudes, the presence of measurement noise may require that the perturbation frequency is lowered or the perturbation amplitude is raised. Large-amplitude high-frequency perturbations can be undesirable or inadmissible in practice due to actuator limitations, a high control effort and an increased wear of components. We will therefore restrict ourselves to perturbations with small amplitudes and low frequencies for which the tuning trade-off in Tan et al. (2006) holds.

The classical extremum-seeking methods in Krstić and Wang (2000); Tan et al. (2006) rely on an estimate of the gradient of the objective function that represents the steady-state relation between the plant parameters and the plant performance to optimize the steady-state plant performance. Therefore, the convergence rate of the extremum-seeking scheme is dependent on the accuracy of the gradient estimate. A more accurate gradient estimate may lead to a faster optimization process, as reported in Gelbert et al. (2012). In Krstić and Wang (2000); Tan et al. (2006), an estimate of the gradient of the objective function is obtained by adding perturbations to the plant-parameter signals and correlating the response in the plant-performance signal with the perturbation signals. This results in an accurate gradient estimate if the perturbation-related content in the plant-parameter signals is high. However, for small-amplitude low-frequency perturbations, the perturbation-related content is small, in which case a more accurate gradient estimate and a faster convergence may be achieved if the entire plant-parameter signals (and not only the perturbation signals) are used.

The contributions of this chapter are summarized as follows. First, we introduce an extremum-seeking controller that uses a least-squares observer to

accurately estimate the gradient of the objective function. The observer uses the perturbation signals as well as the nominal part of the plant-parameter signals to compute a gradient estimate. Moreover, curvature information of the objective function can be incorporated to further enhance the accuracy of the gradient estimate. Second, we prove that the region of attraction for the closed-loop system of plant an controller can be made global under the assumptions in this chapter by normalizing the adaptation gain of the extremum-seeking controller. Third, simulations for a variety of examples taken from the extremum-seeking literature are conducted to compare the convergence rates of the presented extremum-seeking controller and of three extremum-seeking controllers in the literature: the multivariable extension of the classical extremum-seeking controller in Krstić and Wang (2000) given in Ghaffari et al. (2012), the phasor extremum-seeking controller in Atta et al. (2015) and the observer-based controller in Guay and Dochain (2015). The fastest convergence is achieved with the presented controller for five of the eight tested examples. Simulation results of an additional in-depth example indicate that a faster convergence can be obtained with the two observer-based controllers than with the classical controller and the phasor controller if perturbations with small amplitudes are used. Moreover, the simulation results show that incorporating curvature information can significantly improve the convergence of the presented controller if the frequency of the perturbations is sufficiently low.

The remaining part of the chapter is organized as follows. After the extremum-seeking problem is stated in Section 2.2, we present our extremum-seeking controller with least-squares observer in Section 2.3. A stability analysis of the presented scheme is provided in Section 2.4, on the basis of which tuning guidelines are derived. The comparison of the presented controller and the three controllers in the literature is given in Section 2.5. The conclusion of this chapter is presented in Section 2.6.

2.2 Formulation of the extremum-seeking problem

Consider the following multi-input-multi-output nonlinear plant:

$$\begin{aligned} \dot{\mathbf{x}}(t) &= \mathbf{f}(\mathbf{x}(t), \mathbf{u}(t)) \\ \mathbf{e}(t) &= \mathbf{g}(\mathbf{x}(t), \mathbf{u}(t)) + \mathbf{n}(t), \end{aligned} \tag{2.1}$$

where $\mathbf{x} \in \mathbb{R}^{n_\mathbf{x}}$ is the state, $\mathbf{u} \in \mathbb{R}^{n_\mathbf{u}}$ is the input, $\mathbf{e} \in \mathbb{R}^{n_\mathbf{e}}$ is the output of the plant, $\mathbf{n} \in \mathbb{R}^{n_\mathbf{e}}$ is an output disturbance and $t \in \mathbb{R}_{\geq 0}$ is the time. The dimensions of the state, the input and the output are given by $n_\mathbf{x}, n_\mathbf{u}, n_\mathbf{e} \in \mathbb{N}_{>0}$, respectively. In the context of extremum-seeking control, the input $\mathbf{u}$ is a vector of tunable plant parameters, the output $\mathbf{e}$ is a vector of measured performance indicators and the disturbance $\mathbf{n}$ is measurement noise. The state $\mathbf{x}$, the measurement

noise $\mathbf{n}$ and the functions $\mathbf{f}$ and $\mathbf{g}$ are unknown. Therefore, the relation between the plant parameters and the performance indicators is unknown. It is the task of the designer to define a cost function, denoted by Z, that quantifies the performance of the plant. The corresponding measured plant performance is given by

$$y(t) = Z(\mathbf{e}(t), \mathbf{u}(t)). \tag{2.2}$$

To simplify notations, we write the plant (2.1) and the cost function (2.2) as one extended plant

$$\begin{aligned} \dot{\mathbf{x}}(t) &= \mathbf{f}(\mathbf{x}(t), \mathbf{u}(t)) \\ y(t) &= h(\mathbf{x}(t), \mathbf{u}(t)) + d(t), \end{aligned} \tag{2.3}$$

with output function $h(\mathbf{x}, \mathbf{u}) = Z(\mathbf{g}(\mathbf{x}, \mathbf{u}), \mathbf{u})$ and disturbance $d = Z(\mathbf{g}(\mathbf{x}, \mathbf{u}) + \mathbf{n}, \mathbf{u}) - Z(\mathbf{g}(\mathbf{x}, \mathbf{u}), \mathbf{u})$. Note that h and d are unknown because the function $\mathbf{g}$ and the disturbance $\mathbf{n}$ are unknown. Although we do not know the functions $\mathbf{f}$ and h, for analytical purposes, we assume that the following holds.

Assumption 2.1. *The functions $\mathbf{f} : \mathbb{R}^{n_\mathbf{x}} \times \mathbb{R}^{n_\mathbf{u}} \to \mathbb{R}^{n_\mathbf{x}}$ and $h : \mathbb{R}^{n_\mathbf{x}} \times \mathbb{R}^{n_\mathbf{u}} \to \mathbb{R}$ in (2.3) are twice continuously differentiable. Moreover, there exist constants $L_\mathbf{fx}, L_\mathbf{fu}, L_{h\mathbf{x}}, L_{h\mathbf{u}} \in \mathbb{R}_{>0}$ such that*

$$\left\| \frac{\partial \mathbf{f}}{\partial \mathbf{x}}(\mathbf{x}, \mathbf{u}) \right\| \leq L_\mathbf{fx}, \qquad \left\| \frac{\partial \mathbf{f}}{\partial \mathbf{u}}(\mathbf{x}, \mathbf{u}) \right\| \leq L_\mathbf{fu} \tag{2.4}$$

and

$$\left\| \frac{\partial^2 h}{\partial \mathbf{x} \partial \mathbf{x}^T}(\mathbf{x}, \mathbf{u}) \right\| \leq L_{h\mathbf{x}}, \qquad \left\| \frac{\partial^2 h}{\partial \mathbf{x} \partial \mathbf{u}^T}(\mathbf{x}, \mathbf{u}) \right\| \leq L_{h\mathbf{u}} \tag{2.5}$$

for all $\mathbf{x} \in \mathbb{R}^{n_\mathbf{x}}$ and all $\mathbf{u} \in \mathbb{R}^{n_\mathbf{u}}$.

We assume that the steady-state solutions of the plant are constant. The existence of a constant steady-state solution of the plant is formulated in the following assumption.

Assumption 2.2. *There exists a twice continuously differentiable map $\mathbf{X} : \mathbb{R}^{n_\mathbf{u}} \to \mathbb{R}^{n_\mathbf{x}}$ and a constant $L_\mathbf{X} \in \mathbb{R}_{>0}$, such that*

$$\mathbf{0} = \mathbf{f}(\mathbf{X}(\mathbf{u}), \mathbf{u}) \tag{2.6}$$

and

$$\left\| \frac{d\mathbf{X}}{d\mathbf{u}}(\mathbf{u}) \right\| \leq L_\mathbf{X} \tag{2.7}$$

for all $\mathbf{u} \in \mathbb{R}^{n_\mathbf{u}}$.

The solution $\mathbf{x} = \mathbf{X}(\mathbf{u})$ satisfies (2.6) and is therefore a constant steady-state solution of the plant dynamics in (2.3) for each constant vector of plant parameters $\mathbf{u}$ in $\mathbb{R}^{n_\mathbf{u}}$. From Assumption 2.2, it does not follow that the stead-state solution $\mathbf{X}(\mathbf{u})$ is unique. Neither ensures Assumption 2.2 that other solutions of the plant dynamics will converge to the steady-state solution $\mathbf{X}(\mathbf{u})$. The following assumption is formulated to ensure the uniqueness and the stability of the steady-state solution $\mathbf{X}(\mathbf{u})$.

Assumption 2.3. *There exist constants $\mu_{\mathbf{x}}, \nu_{\mathbf{x}} \in \mathbb{R}_{>0}$, such that for each constant $\mathbf{u} \in \mathbb{R}^{n_{\mathbf{u}}}$, the solutions of the dynamics in (2.3) satisfy*

$$\|\tilde{\mathbf{x}}(t)\| \leq \mu_{\mathbf{x}} \|\tilde{\mathbf{x}}(t_0)\| e^{-\nu_{\mathbf{x}}(t-t_0)}, \tag{2.8}$$

with

$$\tilde{\mathbf{x}}(t) = \mathbf{x}(t) - \mathbf{X}(\mathbf{u}), \tag{2.9}$$

for all $\mathbf{x}(t_0) \in \mathbb{R}^{n_{\mathbf{x}}}$ and all $t \geq t_0 \geq 0$.

From Assumption 2.3, it follows that the solutions of the plant are globally exponentially stable with respect to the steady-state solution $\mathbf{X}(\mathbf{u})$ for any constant vector of plant parameters $\mathbf{u}$. The disturbance-free steady-state relation between constant plant parameters and the plant performance can now be obtained by the static input-to-output map

$$F(\mathbf{u}) = h(\mathbf{X}(\mathbf{u}), \mathbf{u}) = Z(\mathbf{g}(\mathbf{X}(\mathbf{u}), \mathbf{u}), \mathbf{u}). \tag{2.10}$$

We refer to the map F as the objective function. We assume that the cost function Q is designed such that there exists a unique minimum of the objective function F on the domain $\mathbb{R}^{n_{\mathbf{u}}}$, where the minimum of the map F corresponds to the optimal plant performance. This is formulated as follows.

Assumption 2.4. *The objective function $F : \mathbb{R}^{n_{\mathbf{u}}} \to \mathbb{R}$ is twice continuously differentiable and exhibits a unique minimum on the domain $\mathbb{R}^{n_{\mathbf{u}}}$. Let the corresponding minimizer be denoted by*

$$\mathbf{u}^* = \underset{\mathbf{u} \in \mathbb{R}^{n_{\mathbf{u}}}}{\arg\min} F(\mathbf{u}). \tag{2.11}$$

There exist constants $L_{F1}, L_{F2} \in \mathbb{R}_{>0}$ such that

$$\frac{dF}{d\mathbf{u}}(\mathbf{u})(\mathbf{u} - \mathbf{u}^*) \geq L_{F1} \|\mathbf{u} - \mathbf{u}^*\|^2 \tag{2.12}$$

and

$$\left\| \frac{d^2F}{d\mathbf{u} d\mathbf{u}^T}(\mathbf{u}) \right\| \leq L_{F2} \tag{2.13}$$

for all $\mathbf{u} \in \mathbb{R}^{n_{\mathbf{u}}}$.

In addition to the previous assumptions, we assume that the disturbance d satisfies the following bound.

Assumption 2.5. *There exist constants $\delta_{\mathbf{n}}, \delta_{\mathbf{x}}, \delta_{\mathbf{u}} \in \mathbb{R}_{\geq 0}$, such that*

$$|d(t)| \leq \delta_{\mathbf{n}} + \delta_{\mathbf{x}} \|\mathbf{x}(t) - \mathbf{X}(\mathbf{u}(t))\| + \delta_{\mathbf{u}} \|\mathbf{u}(t) - \mathbf{u}^*\| \tag{2.14}$$

for all $\mathbf{x} \in \mathbb{R}^{n_{\mathbf{x}}}$, all $\mathbf{u} \in \mathbb{R}^{n_{\mathbf{u}}}$ and all $t \in \mathbb{R}_{\geq 0}$.

Remark 2.6. *Measurement noise is often neglected in the analysis of extremum-seeking schemes. To show that the extremum-seeking controller optimizes the steady-state plant performance in spite of measurement noise, it is assumed that the noise signal and the perturbation signals are uncorrelated in Ariyur and Krstić (2003); Tan et al. (2010). Alternatively, it is assumed that the measurement noise satisfies certain stochastic properties in Stanković and Stipanović (2010). In this chapter, we only assume that the measurement noise is bounded (see Assumption 2.5). Although measurement noise may impair the obtainable performance, we prove that the closed-loop system of plant and extremum-seeking controller is stable under this less restrictive assumption.*

Remark 2.7. *To simplify the calculations in this chapter, we optimize the steady-state plant performance for any initial conditions* $\mathbf{x}(0) \in \mathbb{R}^{n_\mathbf{x}}$ *and* $\mathbf{u}(0) \in \mathbb{R}^{n_\mathbf{u}}$. *For this reason, we require that Assumptions 2.1-2.5 are satisfied for all* $\mathbf{x} \in \mathbb{R}^{n_\mathbf{x}}$ *and all* $\mathbf{u} \in \mathbb{R}^{n_\mathbf{u}}$. *For a local result, it is sufficient to assume that Assumptions 2.1-2.5 hold for compact sets of* $\mathbf{x}$ *and* $\mathbf{u}$, *where the steady-state solution* $\mathbf{X}(\mathbf{u})$ *is in the interior of the compact set of* $\mathbf{x}$ *and the minimizer* $\mathbf{u}^*$ *is in the interior of the compact set of* $\mathbf{u}$. *We note that Assumption 2.1 holds for any compact sets of* $\mathbf{x}$ *and* $\mathbf{u}$ *if the functions* $\mathbf{f}$ *and* h *are twice continuously differentiable.*

We note that the map $\mathbf{X}$, the objective function F and its minimizer $\mathbf{u}^*$ are unknown because the functions $\mathbf{f}$ and h are unknown. Nonetheless, we aim to design an extremum-seeking controller that regulates the plant parameters $\mathbf{u}$ towards their performance-optimizing values $\mathbf{u}^*$.

2.3 Controller design

From Assumption 2.4, it follows that the plant parameters $\mathbf{u}$ will converge to the minimizer $\mathbf{u}^*$ as time goes to infinity for any initial value $\mathbf{u}(0) \in \mathbb{R}^{n_\mathbf{u}}$ if we design a controller that drives the plant parameters in the direction opposite to the gradient of the objective function in (2.10). However, such a gradient-descent controller cannot be implemented because the gradient of the objective function is unknown. To estimate the gradient of the objective function and use this estimated gradient to drive $\mathbf{u}$ towards $\mathbf{u}^*$, we define

$$\mathbf{u}(t) = \hat{\mathbf{u}}(t) + \alpha_{\boldsymbol{\omega}} \boldsymbol{\omega}(t), \tag{2.15}$$

where $\alpha_{\boldsymbol{\omega}} \boldsymbol{\omega}$ is a vector of perturbation signals with amplitude $\alpha_{\boldsymbol{\omega}} \in \mathbb{R}_{>0}$. The vector $\boldsymbol{\omega}$ is defined by $\boldsymbol{\omega}(t) = [\omega_1(t), \omega_2(t), \ldots, \omega_{n_\mathbf{u}}(t)]^T$, with

$$\omega_i(t) = \begin{cases} \sin\left(\dfrac{i+1}{2}\eta_{\boldsymbol{\omega}} t\right), & \text{if } i \text{ is odd,} \\ \cos\left(\dfrac{i}{2}\eta_{\boldsymbol{\omega}} t\right), & \text{if } i \text{ is even,} \end{cases} \tag{2.16}$$

for $i = \{1, 2, \ldots, n_{\mathbf{u}}\}$, where $\eta_{\boldsymbol{\omega}} \in \mathbb{R}_{>0}$ is a tuning parameter. The purpose of the perturbation signals is to provide sufficient excitation to accurately estimate the gradient of the objective function. The nominal plant parameters $\hat{\mathbf{u}}$ can be regarded as an estimate of the minimizer $\mathbf{u}^*$.

We model the input-to-output behavior of the plant (2.3) in a general form. Let the state of the model be given by

$$\mathbf{m}(t) = \begin{bmatrix} F(\hat{\mathbf{u}}(t)) \\ \alpha_{\boldsymbol{\omega}} \frac{dF}{d\mathbf{u}^T}(\hat{\mathbf{u}}(t)) \end{bmatrix}. \tag{2.17}$$

From the output equation in (2.3) and the expression of the objective function in (2.10), it follows that the measured plant performance y can be written as

$$y(t) = h(\mathbf{x}(t), \mathbf{u}(t)) - h(\mathbf{X}(\mathbf{u}(t)), \mathbf{u}(t)) + F(\mathbf{u}(t)) + d(t). \tag{2.18}$$

From Taylor's theorem and (2.15), we obtain

$$\begin{aligned} F(\mathbf{u}(t)) &= F(\hat{\mathbf{u}}(t) + \alpha_{\boldsymbol{\omega}}\boldsymbol{\omega}(t)) \\ &= F(\hat{\mathbf{u}}(t)) + \alpha_{\boldsymbol{\omega}} \frac{dF}{d\mathbf{u}}(\hat{\mathbf{u}}(t))\boldsymbol{\omega}(t) \\ &\quad + \alpha_{\boldsymbol{\omega}}^2 \boldsymbol{\omega}^T(t) \int_0^1 (1-s) \frac{d^2F}{d\mathbf{u}d\mathbf{u}^T}(\hat{\mathbf{u}}(t) + s\alpha_{\boldsymbol{\omega}}\boldsymbol{\omega}(t)) ds \boldsymbol{\omega}(t). \end{aligned} \tag{2.19}$$

Using (2.3) and (2.17)-(2.19), the input-to-output behavior of the plant can be modeled as follows:

$$\begin{aligned} \dot{\mathbf{m}}(t) &= \mathbf{A}(t)\mathbf{m}(t) + \alpha_{\boldsymbol{\omega}}^2 \mathbf{B}\mathbf{w}(t) \\ y(t) &= \mathbf{C}(t)\mathbf{m}(t) + \alpha_{\boldsymbol{\omega}}^2 v(t) + z(t) + d(t), \end{aligned} \tag{2.20}$$

with matrices

$$\mathbf{A}(t) = \begin{bmatrix} 0 & \frac{\dot{\hat{\mathbf{u}}}^T(t)}{\alpha_{\boldsymbol{\omega}}} \\ \mathbf{0} & \mathbf{0} \end{bmatrix}, \qquad \mathbf{B} = \begin{bmatrix} \mathbf{0} \\ \mathbf{I} \end{bmatrix}, \qquad \mathbf{C}(t) = \begin{bmatrix} 1 & \boldsymbol{\omega}^T(t) \end{bmatrix}, \tag{2.21}$$

where the disturbances $\mathbf{w}$, v and z are given by

$$\begin{aligned} \mathbf{w}(t) &= \frac{d^2F}{d\mathbf{u}d\mathbf{u}^T}(\hat{\mathbf{u}}(t)) \frac{\dot{\hat{\mathbf{u}}}(t)}{\alpha_{\boldsymbol{\omega}}}, \\ v(t) &= \boldsymbol{\omega}^T(t) \int_0^1 (1-s) \frac{d^2F}{d\mathbf{u}d\mathbf{u}^T}(\hat{\mathbf{u}}(t) + s\alpha_{\boldsymbol{\omega}}\boldsymbol{\omega}(t)) ds \boldsymbol{\omega}(t), \\ z(t) &= h(\mathbf{x}(t), \mathbf{u}(t)) - h(\mathbf{X}(\mathbf{u}(t)), \mathbf{u}(t)). \end{aligned} \tag{2.22}$$

The reason for modeling the input-to-output behavior of the plant (2.3) in this way is that the state vector $\mathbf{m}$ in (2.17) contains a scaled version of the gradient

of the objective function, which implies that an estimate of the gradient of the objective function can directly be obtained from an estimate of the state vector $\mathbf{m}$.

We will design an observer to estimate the state vector $\mathbf{m}$. The disturbances $\mathbf{w}$ and v in (2.22) depend on the Hessian of the unknown objective function F and are therefore unknown. The disturbance z in (2.22) is unknown because it depends on the state $\mathbf{x}$, the map $\mathbf{X}$ and the function h, which are unknown. For the design of the observer, we assume that $z = d = 0$ and that the disturbances $\mathbf{w}$ and v can be approximated by the estimates $\hat{\mathbf{w}}$ and $\hat{v}$, which are given by

$$\begin{aligned} \hat{\mathbf{w}}(t) &= \mathbf{H}(\hat{\mathbf{u}}(t))\frac{\dot{\hat{\mathbf{u}}}(t)}{\alpha_{\boldsymbol{\omega}}}, \\ \hat{v}(t) &= \frac{1}{2}\boldsymbol{\omega}^T(t)\mathbf{H}(\hat{\mathbf{u}}(t))\boldsymbol{\omega}(t), \end{aligned} \tag{2.23}$$

where the function $\mathbf{H} : \mathbb{R}^{n_\mathbf{u}} \to \mathbb{R}^{n_\mathbf{u} \times n_\mathbf{u}}$ is chosen by the designer and satisfies

$$\|\mathbf{H}(\hat{\mathbf{u}})\| \leq L_\mathbf{H} \tag{2.24}$$

for all $\hat{\mathbf{u}} \in \mathbb{R}^{n_\mathbf{u}}$ and some constant $L_\mathbf{H} \in \mathbb{R}_{>0}$. An overall good choice for the function $\mathbf{H}$ is given by $\mathbf{H}(\hat{\mathbf{u}}) = \mathbf{0}$, in which case $\hat{\mathbf{w}} = \mathbf{0}$ and $\hat{v} = 0$. However, if a reasonably accurate approximation of Hessian of the objective function is available, a more accurate gradient estimate and a faster convergence towards the optimum may be obtained for small values of $\eta_{\boldsymbol{\omega}}$ by selecting $\mathbf{H}(\hat{\mathbf{u}}) \approx \frac{d^2F}{d\mathbf{u}d\mathbf{u}^T}(\hat{\mathbf{u}})$; see Section 2.5.

We introduce a least-squares observer that minimizes a quadratic cost function with respect to an exponentially weighted time window of the estimation error, similar to Hammouri and de Leon Morales (1990):

$$\begin{aligned} (t, \hat{\mathbf{m}}(t)) = \underset{\mathbf{p}(t) \in \mathbb{R}^{n_\mathbf{u}+1}}{\arg\min}\ & J(t, \mathbf{p}(t)), \\ \text{subject to:}\quad \dot{\mathbf{p}}(\tau) &= \mathbf{A}(\tau)\mathbf{p}(\tau) + \alpha_{\boldsymbol{\omega}}^2\mathbf{B}\hat{\mathbf{w}}(\tau) \\ \hat{y}(\tau) &= \mathbf{C}(\tau)\mathbf{p}(\tau) + \alpha_{\boldsymbol{\omega}}^2\hat{v}(\tau), \qquad \forall \tau \in [0, t], \end{aligned} \tag{2.25}$$

where the cost function J is given by

$$\begin{aligned} J(t, \mathbf{p}(t)) = \eta_\mathbf{m} \int_0^t e^{-\eta_\mathbf{m}(t-\tau)} \left(|y(\tau) - \hat{y}(\tau)|^2 + \sigma_r |\mathbf{D}\mathbf{p}(\tau)|^2 \right) d\tau \\ + e^{-\eta_\mathbf{m} t} (\hat{\mathbf{m}}_0 - \mathbf{p}(0))^T \mathbf{Q}_0^{-1} (\hat{\mathbf{m}}_0 - \mathbf{p}(0)), \end{aligned} \tag{2.26}$$

with

$$\mathbf{D} = \begin{bmatrix} \mathbf{0} & \mathbf{I} \end{bmatrix} \tag{2.27}$$

and $\hat{\mathbf{m}}_0 \in \mathbb{R}^{n_\mathbf{u}+1}$, where $\mathbf{Q}_0 \in \mathbb{R}^{n_\mathbf{u}+1 \times n_\mathbf{u}+1}$ is a symmetric positive-definite matrix. The tuning parameter $\eta_\mathbf{m} \in \mathbb{R}_{>0}$ is often referred to as the forgetting factor; see for instance Ioannou and Sun (1996, Section 4.3.6). The tuning parameter $\sigma_r \in \mathbb{R}_{\geq 0}$ is a regularization constant, similar to Guay and Dochain (2015). The state estimate $\hat{\mathbf{m}}$ in (2.25) can be written explicitly as

$$\hat{\mathbf{m}}(t) = \mathbf{Q}(t)\mathbf{\Psi}(t) \tag{2.28}$$

for all $t \in \mathbb{R}_{\geq 0}$, with

$$\begin{aligned}\mathbf{Q}(t) = \Bigg(&\eta_\mathbf{m} \int_0^t e^{-\eta_\mathbf{m}(t-\tau)} \mathbf{\Phi}^T(\tau, t) \left(\mathbf{C}^T(\tau)\mathbf{C}(\tau) + \sigma_r \mathbf{D}^T\mathbf{D} \right) \mathbf{\Phi}(\tau, t) d\tau \\ &+ e^{-\eta_\mathbf{m} t} \mathbf{\Phi}^T(0, t) \mathbf{Q}_0^{-1} \mathbf{\Phi}(0, t) \Bigg)^{-1}\end{aligned} \tag{2.29}$$

and

$$\begin{aligned}\mathbf{\Psi}(t) = \eta_\mathbf{m} \int_0^t e^{-\eta_\mathbf{m}(t-\tau)} \mathbf{\Phi}^T(\tau, t) \Bigg(&\mathbf{C}^T(\tau) \left(y(\tau) - \alpha_{\boldsymbol{\omega}}^2 \hat{v}(\tau) \right) \\ &+ \alpha_{\boldsymbol{\omega}}^2 \left(\mathbf{C}^T(\tau)\mathbf{C}(\tau) + \sigma_r \mathbf{D}^T\mathbf{D} \right) \int_\tau^t \mathbf{\Phi}(\tau, \sigma) \mathbf{B}\hat{\mathbf{w}}(\sigma) d\sigma \Bigg) d\tau \\ &+ e^{-\eta_\mathbf{m} t} \mathbf{\Phi}^T(0, t) \mathbf{Q}_0^{-1} \left(\hat{\mathbf{m}}_0 + \alpha_{\boldsymbol{\omega}}^2 \int_0^t \mathbf{\Phi}(0, \sigma) \mathbf{B}\hat{\mathbf{w}}(\sigma) d\sigma \right),\end{aligned} \tag{2.30}$$

where $\mathbf{\Phi}$ is the state-transition matrix given by

$$\mathbf{\Phi}(\tau, t) = \begin{bmatrix} 1 & \dfrac{\hat{\mathbf{u}}^T(\tau) - \hat{\mathbf{u}}^T(t)}{\alpha_{\boldsymbol{\omega}}} \\ \mathbf{0} & \mathbf{I} \end{bmatrix}. \tag{2.31}$$

By differentiating the expressions in (2.28)-(2.29) with respect to time, we obtain the following differential equations for the least-squares observer:

$$\begin{aligned}\dot{\hat{\mathbf{m}}}(t) = &\left(\mathbf{A}(t) - \eta_\mathbf{m} \sigma_r \mathbf{Q}(t) \mathbf{D}^T\mathbf{D} \right) \hat{\mathbf{m}}(t) + \alpha_{\boldsymbol{\omega}}^2 \mathbf{B}\hat{\mathbf{w}}(t) \\ &+ \eta_\mathbf{m} \mathbf{Q}(t) \mathbf{C}^T(t) (y(t) - \mathbf{C}(t)\hat{\mathbf{m}}(t) - \alpha_{\boldsymbol{\omega}}^2 \hat{v}(t))\end{aligned} \tag{2.32}$$

and

$$\begin{aligned}\dot{\mathbf{Q}}(t) = &\eta_\mathbf{m} \mathbf{Q}(t) + \mathbf{A}(t)\mathbf{Q}(t) + \mathbf{Q}(t)\mathbf{A}^T(t) \\ &- \eta_\mathbf{m} \mathbf{Q}(t) (\mathbf{C}^T(t)\mathbf{C}(t) + \sigma_r \mathbf{D}^T\mathbf{D}) \mathbf{Q}(t),\end{aligned} \tag{2.33}$$

with initial conditions $\hat{\mathbf{m}}(0) = \hat{\mathbf{m}}_0$ and $\mathbf{Q}(0) = \mathbf{Q}_0$. Similar to Hammouri and de Leon Morales (1990), it can be shown that the matrix $\mathbf{Q}$ remains positive definite and bounded over time if the plant parameters $\mathbf{u}$ are uniformly persistently exciting. The regularization term related to σ_r prevents the matrix $\mathbf{Q}$ from becoming excessively large if the level of excitation is low. As regularization

deteriorates the accuracy the state estimate, the value of σ_r is chosen to be small.

Because $\hat{\mathbf{m}}$ is an estimate of the state $\mathbf{m}$, we note that $\mathbf{D}\hat{\mathbf{m}}$ is a scaled estimate of the gradient of the objective function. We define the following gradient descent optimizer:

$$\dot{\hat{\mathbf{u}}}(t) = -\lambda_{\mathbf{u}} \frac{\eta_{\mathbf{u}} \mathbf{D}\hat{\mathbf{m}}(t)}{\eta_{\mathbf{u}} + \lambda_{\mathbf{u}} \|\mathbf{D}\hat{\mathbf{m}}(t)\|}, \tag{2.34}$$

where $\lambda_{\mathbf{u}}, \eta_{\mathbf{u}} \in \mathbb{R}_{>0}$ are tuning parameters. By normalizing the adaptation gain in (2.34), we prevent the solutions of the closed-loop system of plant and extremum-seeking controller from having a finite escape time if the state estimate $\hat{\mathbf{m}}$ is inaccurate. Loosely speaking, it gives the observer sufficient time to produce an accurate state estimate for arbitrary initial conditions of the closed-loop system. This is essential for the global stability result in Section 2.4.

By combining the plant (2.3) and the extremum-seeking controller in (2.15), (2.32)-(2.34), we obtain the closed-loop system in Figure 2.1, where the perturbation vector $\boldsymbol{\omega}$ and the disturbance estimates $\hat{\mathbf{w}}$ and $\hat{v}$ are defined in (2.23) and (2.16), respectively, where d is an unknown disturbance, and where $\alpha_{\boldsymbol{\omega}}$, $\eta_{\boldsymbol{\omega}}$, $\eta_{\mathbf{m}}$, $\lambda_{\mathbf{u}}$, $\eta_{\mathbf{u}}$ and σ_r are tuning parameters. For an arbitrary unknown initial state $\mathbf{x}(0)$, it is the task of the designer to choose the initial conditions $\hat{\mathbf{m}}(0)$, $\mathbf{Q}(0)$, $\hat{\mathbf{u}}(0)$ and the values of the tuning parameters $\alpha_{\boldsymbol{\omega}}$, $\eta_{\boldsymbol{\omega}}$, $\eta_{\mathbf{m}}$, $\lambda_{\mathbf{u}}$, $\eta_{\mathbf{u}}$ and σ_r such that the optimizer state $\hat{\mathbf{u}}$ converges towards the performance-optimal value $\mathbf{u}^*$. We investigate the stability of the presented extremum-seeking scheme in the next section to identify suitable initial conditions and tuning conditions.

2.4 Stability analysis

Due to the perturbation and the disturbance, the optimizer state $\hat{\mathbf{u}}$ will generally converge to a region of the performance-optimal value $\mathbf{u}^*$ rather than to its exact value. We state our main result which states the initial conditions and tuning-parameter values under which the extremum-seeking scheme is globally uniformly ultimately bounded. The proof is presented in Section 2.4.1.

Theorem 2.8. *Under Assumptions 2.1-2.5, there exist (sufficiently small) constants $\varepsilon_1, \varepsilon_2, \ldots, \varepsilon_6 \in \mathbb{R}_{>0}$ such that the solutions of the closed-loop system of the plant (2.3) and the extremum-seeking controller in (2.15), (2.32)-(2.34) are uniformly bounded for all $\mathbf{x}(0) \in \mathbb{R}^{n_{\mathbf{x}}}$, all $\hat{\mathbf{m}}(0) \in \mathbb{R}^{n_{\mathbf{u}}+1}$, all symmetric positive-definite $\mathbf{Q}(0) \in \mathbb{R}^{n_{\mathbf{u}}+1 \times n_{\mathbf{u}}+1}$, all $\hat{\mathbf{u}}(0) \in \mathbb{R}^{n_{\mathbf{u}}}$, all $\alpha_{\boldsymbol{\omega}}, \eta_{\mathbf{u}}, \eta_{\mathbf{m}}, \eta_{\boldsymbol{\omega}} \in \mathbb{R}_{>0}$ and all $\sigma_r \in \mathbb{R}_{\geq 0}$ that satisfy $\alpha_{\boldsymbol{\omega}}\varepsilon_1 \geq \delta_{\mathbf{u}}$, $\eta_{\boldsymbol{\omega}} \leq \varepsilon_2$, $\eta_{\mathbf{m}} \leq \eta_{\boldsymbol{\omega}}\varepsilon_3$, $\alpha_{\boldsymbol{\omega}}\lambda_{\mathbf{u}} \leq \eta_{\mathbf{m}}\varepsilon_4$, $\eta_{\mathbf{u}} \leq \alpha_{\boldsymbol{\omega}}\eta_{\mathbf{m}}\varepsilon_5$ and $\sigma_r \leq \varepsilon_6$. Moreover, the solutions of $\hat{\mathbf{u}}$ satisfy*

$$\limsup_{t\to\infty} \|\hat{\mathbf{u}}(t) - \mathbf{u}^*\| \leq \max\left\{\alpha_{\boldsymbol{\omega}}c_1, \eta_{\boldsymbol{\omega}}c_2, \frac{\delta_{\mathbf{n}}}{\alpha_{\boldsymbol{\omega}}}c_3, \delta_{\mathbf{u}}c_4, \eta_{\boldsymbol{\omega}}\delta_{\mathbf{x}}c_5\right\} \tag{2.35}$$

for some constants $c_1, c_2, \ldots, c_5 \in \mathbb{R}_{>0}$.

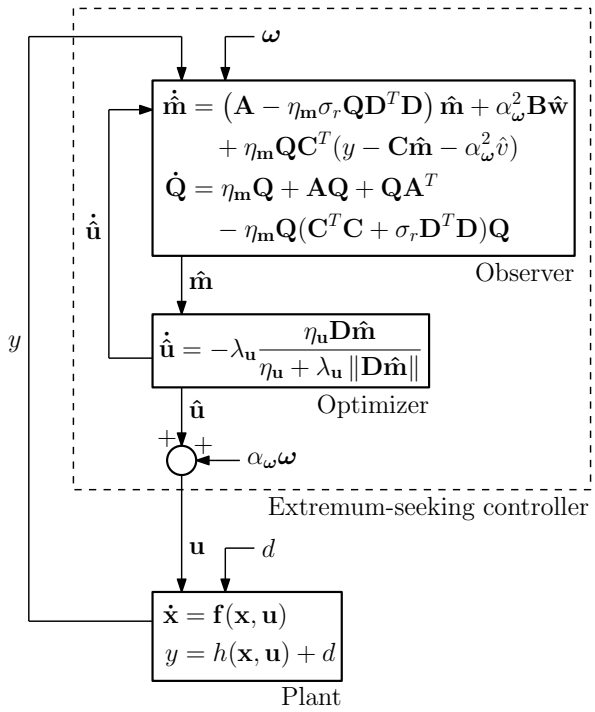

Figure 2.1: Closed-loop system of plant and extremum-seeking controller.

Under the conditions of the theorem, it follows that the optimizer state $\hat{\mathbf{u}}$ converges to an arbitrarily small region of the performance-optimal value $\mathbf{u}^*$ for sufficiently small $\alpha_{\boldsymbol{\omega}}$ and $\eta_{\boldsymbol{\omega}}$ in the absence of the disturbance d (that is, $\delta_{\mathbf{n}} = \delta_{\mathbf{u}} = \delta_{\mathbf{x}} = 0$). In the presence of the disturbance d, the perturbation amplitude $\alpha_{\boldsymbol{\omega}}$ should be chosen sufficiently large to dominate the disturbance in order to keep the extremum-seeking scheme stable; the region to which $\hat{\mathbf{u}}$ converges generally cannot be made arbitrarily small in this case.

Under the given tuning conditions, the extremum-seeking scheme is ultimately bounded for any initial condition as long as $\mathbf{Q}(0)$ is symmetric and positive definite. For a fast convergence of the extremum-seeking scheme, the initial conditions $\hat{\mathbf{u}}(0)$ and $\hat{\mathbf{m}}(0)$ should ideally be chosen such that $\hat{\mathbf{u}}(0) \approx \mathbf{u}^*$ and $\hat{\mathbf{m}}(0) \approx \mathbf{m}(0)$. However, this requires detailed knowledge of the objective function and might therefore not be feasible. From the proof of Theorem 2.8 in Section 2.4.1, it follows that a good initial condition for $\mathbf{Q}$ is given by

$$\boldsymbol{\Xi} = \begin{bmatrix} 1 & \mathbf{0} \\ \mathbf{0} & \frac{2}{1+2\sigma_r}\mathbf{I} \end{bmatrix}. \tag{2.36}$$

Remark 2.9. *With $\alpha_{\boldsymbol{\omega}}$ and $\eta_{\boldsymbol{\omega}}$ associated with the perturbation vector, $\eta_{\mathbf{m}}$ associated with the observer, and $\eta_{\mathbf{u}}$ associated with the optimizer, the tuning conditions in Theorem 2.8 imply that, for small values of ε_2, ε_3, ε_4 and ε_5, the plant is faster than the perturbation vector, that the perturbation vector is faster than the observer, and that the observer is faster than the optimizer. These differences in time scale between the various components of the extremum-seeking scheme can be exploited using singular-perturbation methods to prove local or semiglobal stability properties of the extremum-seeking scheme, similarly to Krstić and Wang (2000); Tan et al. (2006). We note, however, that Theorem 2.8 proves a stronger global stability property.*

2.4.1 Proof of Theorem 2.8

For notational convenience, we introduce the following coordinate transformation:

$$\begin{aligned}\tilde{\mathbf{x}}(t) &= \mathbf{x}(t) - \mathbf{X}(\mathbf{u}(t)),\\ \tilde{\mathbf{m}}(t) &= \hat{\mathbf{m}}(t) - \mathbf{m}(t),\\ \tilde{\mathbf{Q}}(t) &= \mathbf{Q}^{-1}(t) - \boldsymbol{\Xi}^{-1} - \frac{\eta_{\mathbf{m}}}{\eta_{\boldsymbol{\omega}}}\mathbf{l}(t),\\ \tilde{\mathbf{u}}(t) &= \hat{\mathbf{u}}(t) - \mathbf{u}^*,\end{aligned} \tag{2.37}$$

with

$$\mathbf{l}(t) = \int_0^t \eta_{\boldsymbol{\omega}} \begin{bmatrix} 0 & \boldsymbol{\omega}^T(\tau) \\ \boldsymbol{\omega}(\tau) & \boldsymbol{\omega}(\tau)\boldsymbol{\omega}^T(\tau) - \frac{1}{2}\mathbf{I} \end{bmatrix} d\tau. \tag{2.38}$$

We note that $\mathbf{l}$ is uniformly bounded, which follows from the definition of $\boldsymbol{\omega}$ in (2.16). Loosely speaking, the solutions of the state variables in (2.37) converge in two stages:

- for $0 \leq t < t_1$, the solutions of $\tilde{\mathbf{x}}$ and $\tilde{\mathbf{Q}}$ converge to a region of the origin and remain there, while the solutions of $\tilde{\mathbf{m}}$ and $\tilde{\mathbf{u}}$ may drift;
- for $t \geq t_1$, the solutions of $\tilde{\mathbf{m}}$ and $\tilde{\mathbf{u}}$ converge to a region of the origin.

To prove Theorem 2.8, we first derive bounds on each of the variables in (2.37) in coherence with the two stages. A bound on the solutions of $\tilde{\mathbf{x}}$ is presented in Lemma 2.10.

Lemma 2.10. *Under the conditions of Theorem 2.8, there exist constants $c_{\mathbf{x}1}, c_{\mathbf{x}2}, \beta_{\mathbf{x}} \in \mathbb{R}_{>0}$ such that the solutions of $\tilde{\mathbf{x}}$ satisfy*

$$\|\tilde{\mathbf{x}}(t)\| \leq \max\left\{c_{\mathbf{x}1}\|\tilde{\mathbf{x}}(0)\|e^{-\beta_{\mathbf{x}}t}, \alpha_{\boldsymbol{\omega}}\eta_{\boldsymbol{\omega}}c_{\mathbf{x}2}\right\} \tag{2.39}$$

for all $t \geq 0$ and all $\tilde{\mathbf{x}}(0) \in \mathbb{R}^{n_{\mathbf{x}}}$.

Proof. See Section 2.7.1. □

Next, we derive bounds on the solutions of $\tilde{\mathbf{Q}}$ in Lemma 2.11.

Lemma 2.11. *Under the conditions of Theorem 2.8, there exist constants $c_{\mathbf{Q}}, \beta_{\mathbf{Q}} \in \mathbb{R}_{>0}$ such that the solutions of $\tilde{\mathbf{Q}}$ satisfy*

$$\|\tilde{\mathbf{Q}}(t)\| \leq \max\left\{c_{\mathbf{Q}}\|\tilde{\mathbf{Q}}(0)\|e^{-\eta_{\mathbf{m}}\beta_{\mathbf{Q}}t}, \frac{1}{8}\right\} \tag{2.40}$$

for all $t \geq 0$ and all $\tilde{\mathbf{Q}}(0) \in \mathbb{R}^{n_{\mathbf{u}}+1 \times n_{\mathbf{u}}+1}$ for which $\mathbf{Q}(0)$ is symmetric and positive definite.

Proof. See Section 2.7.2. □

From Lemmas 2.10-2.11, we obtain that there exists a finite time $t_1 \geq 0$ such that $\|\tilde{\mathbf{x}}(t)\| \leq \alpha_{\boldsymbol{\omega}}\eta_{\boldsymbol{\omega}}c_{\mathbf{x}2}$ and $\|\tilde{\mathbf{Q}}(t)\| \leq \frac{1}{8}$ for all $t \geq t_1$. We utilize these bounds on $\tilde{\mathbf{x}}$ and $\tilde{\mathbf{Q}}$ to obtain the following bounds on the solutions of $\tilde{\mathbf{u}}$ and $\tilde{\mathbf{m}}$ in Lemmas 2.12 and 2.13, respectively.

Lemma 2.12. *Under the conditions of Theorem 2.8, for any finite time $t_1 \geq 0$, the solutions of $\tilde{\mathbf{u}}$ are bounded for all $0 \leq t \leq t_1$ and all $\tilde{\mathbf{u}}(0) \in \mathbb{R}^{n_{\mathbf{u}}}$. In addition, there exist constants $c_{\mathbf{u}1}, c_{\mathbf{u}2} \in \mathbb{R}_{>0}$ such that the solutions of $\tilde{\mathbf{u}}$ satisfy*

$$\sup_{t\geq t_1}\|\tilde{\mathbf{u}}(t)\| \leq \max\left\{c_{\mathbf{u}1}\|\tilde{\mathbf{u}}(t_1)\|, \frac{1}{\alpha_{\boldsymbol{\omega}}}c_{\mathbf{u}2}\sup_{t\geq t_1}\|\tilde{\mathbf{m}}(t)\|\right\} \tag{2.41}$$

and

$$\limsup_{t\to\infty}\|\tilde{\mathbf{u}}(t)\| \leq \frac{1}{\alpha_{\boldsymbol{\omega}}}c_{\mathbf{u}2}\limsup_{t\to\infty}\|\tilde{\mathbf{m}}(t)\|. \tag{2.42}$$

Proof. See Section 2.7.3. □

Lemma 2.13. *Under the conditions of Theorem 2.8, there exists a finite time $t_1 \geq 0$ such that the solutions of $\tilde{\mathbf{m}}$ are bounded for all $0 \leq t \leq t_1$ and all $\tilde{\mathbf{m}}(0) \in \mathbb{R}^{n_{\mathbf{u}}+1}$. In addition, there exist constants $c_{\mathbf{m}1}, c_{\mathbf{m}2}, \ldots, c_{\mathbf{m}10} \in \mathbb{R}_{>0}$ such that the solutions of $\tilde{\mathbf{u}}$ satisfy*

$$\begin{aligned}\sup_{t\geq t_1}\|\tilde{\mathbf{m}}(t)\| \leq \sup_{t\geq t_1}\max\Big\{&c_{\mathbf{m}1}\|\tilde{\mathbf{m}}(t_1)\|, \alpha_{\boldsymbol{\omega}}^2c_{\mathbf{m}2}, \alpha_{\boldsymbol{\omega}}\eta_{\boldsymbol{\omega}}c_{\mathbf{m}3}, \alpha_{\boldsymbol{\omega}}\eta_{\boldsymbol{\omega}}c_{\mathbf{m}4}\|\tilde{\mathbf{u}}(t)\|,\\ &\frac{\alpha_{\boldsymbol{\omega}}^2\lambda_{\mathbf{u}}}{\eta_{\mathbf{m}}}c_{\mathbf{m}5}\|\tilde{\mathbf{u}}(t)\|, \alpha_{\boldsymbol{\omega}}\sqrt{\sigma_r}c_{\mathbf{m}6}\|\tilde{\mathbf{u}}(t)\|, \delta_{\mathbf{n}}c_{\mathbf{m}7},\\ &\alpha_{\boldsymbol{\omega}}\eta_{\boldsymbol{\omega}}\delta_{\mathbf{x}}c_{\mathbf{m}8}, \alpha_{\boldsymbol{\omega}}\delta_{\mathbf{u}}c_{\mathbf{m}9}, \delta_{\mathbf{u}}c_{\mathbf{m}10}\|\tilde{\mathbf{u}}(t)\|\Big\}\end{aligned} \tag{2.43}$$

and

$$\begin{aligned}\limsup_{t\to\infty}\|\tilde{\mathbf{m}}(t)\| \leq \limsup_{t\to\infty}\max\Big\{&\alpha_{\boldsymbol{\omega}}^2c_{\mathbf{m}2}, \alpha_{\boldsymbol{\omega}}\eta_{\boldsymbol{\omega}}c_{\mathbf{m}3}, \alpha_{\boldsymbol{\omega}}\eta_{\boldsymbol{\omega}}c_{\mathbf{m}4}\|\tilde{\mathbf{u}}(t)\|,\\ &\frac{\alpha_{\boldsymbol{\omega}}^2\lambda_{\mathbf{u}}}{\eta_{\mathbf{m}}}c_{\mathbf{m}5}\|\tilde{\mathbf{u}}(t)\|, \alpha_{\boldsymbol{\omega}}\sqrt{\sigma_r}c_{\mathbf{m}6}\|\tilde{\mathbf{u}}(t)\|, \delta_{\mathbf{n}}c_{\mathbf{m}7},\\ &\alpha_{\boldsymbol{\omega}}\eta_{\boldsymbol{\omega}}\delta_{\mathbf{x}}c_{\mathbf{m}8}, \alpha_{\boldsymbol{\omega}}\delta_{\mathbf{u}}c_{\mathbf{m}9}, \delta_{\mathbf{u}}c_{\mathbf{m}10}\|\tilde{\mathbf{u}}(t)\|\Big\}.\end{aligned} \tag{2.44}$$

Proof. See Section 2.7.4. □

The $\tilde{\mathbf{u}}$-dynamics and the $\tilde{\mathbf{m}}$-dynamics can be regarded as interconnected subsystems for which the solutions satisfy the bounds in Lemmas 2.12 and 2.13, respectively. For sufficiently small constants ε_1, ε_2, ε_4 and ε_6, the cycle-small-gain condition in Dashkovskiy et al. (2007); Liu et al. (2011) is satisfied for all $\alpha_{\boldsymbol{\omega}}\varepsilon_1 \geq \delta_{\mathbf{u}}$, all $\eta_{\boldsymbol{\omega}} \leq \varepsilon_2$, all $\alpha_{\boldsymbol{\omega}}\lambda_{\mathbf{u}} \leq \eta_{\mathbf{m}}\varepsilon_4$ and all $\sigma_r \leq \varepsilon_6$. Therefore, from (2.41) and (2.43), we obtain that

$$\begin{aligned}\sup_{t\geq t_1}\|\tilde{\mathbf{u}}(t)\| \leq \max\Big\{ & c_{\mathbf{u}1}\|\tilde{\mathbf{u}}(t_1)\|, \frac{1}{\alpha_{\boldsymbol{\omega}}}c_{\mathbf{u}2}c_{\mathbf{m}1}\|\tilde{\mathbf{m}}(t_1)\|, \alpha_{\boldsymbol{\omega}}c_{\mathbf{u}2}c_{\mathbf{m}2}, \\ & \eta_{\boldsymbol{\omega}}c_{\mathbf{u}2}c_{\mathbf{m}3}, \frac{\delta_{\mathbf{n}}}{\alpha_{\boldsymbol{\omega}}}c_{\mathbf{u}2}c_{\mathbf{m}7}, \eta_{\boldsymbol{\omega}}\delta_{\mathbf{x}}c_{\mathbf{u}2}c_{\mathbf{m}8}, \delta_{\mathbf{u}}c_{\mathbf{u}2}c_{\mathbf{m}9}\Big\}\end{aligned} \tag{2.45}$$

and

$$\begin{aligned}\sup_{t\geq t_1}\|\tilde{\mathbf{m}}(t)\| \leq \max\Big\{ & c_{\mathbf{m}1}\|\tilde{\mathbf{m}}(t_1)\|, \alpha_{\boldsymbol{\omega}}\eta_{\boldsymbol{\omega}}c_{\mathbf{m}4}c_{\mathbf{u}1}\|\tilde{\mathbf{u}}(t_1)\|, \frac{\alpha_{\boldsymbol{\omega}}^2\lambda_{\mathbf{u}}}{\eta_{\mathbf{m}}}c_{\mathbf{m}5}c_{\mathbf{u}1}\|\tilde{\mathbf{u}}(t_1)\|, \\ & \alpha_{\boldsymbol{\omega}}\sqrt{\sigma_r}c_{\mathbf{m}6}c_{\mathbf{u}1}\|\tilde{\mathbf{u}}(t_1)\|, \alpha_{\boldsymbol{\omega}}^2c_{\mathbf{m}2}, \alpha_{\boldsymbol{\omega}}\eta_{\boldsymbol{\omega}}c_{\mathbf{m}3}, \delta_{\mathbf{u}}c_{\mathbf{m}10}c_{\mathbf{u}1}\|\tilde{\mathbf{u}}(t_1)\|, \\ & \delta_{\mathbf{n}}c_{\mathbf{m}7}, \alpha_{\boldsymbol{\omega}}\eta_{\boldsymbol{\omega}}\delta_{\mathbf{x}}c_{\mathbf{m}8}, \alpha_{\boldsymbol{\omega}}\delta_{\mathbf{u}}c_{\mathbf{m}9}\Big\}.\end{aligned} \tag{2.46}$$

Similarly, from (2.42) and (2.44), it follows that

$$\limsup_{t\to\infty}\|\tilde{\mathbf{u}}(t)\| \leq \max\Big\{\alpha_{\boldsymbol{\omega}}c_{\mathbf{u}2}c_{\mathbf{m}2}, \eta_{\boldsymbol{\omega}}c_{\mathbf{u}2}c_{\mathbf{m}3}, \frac{\delta_{\mathbf{n}}}{\alpha_{\boldsymbol{\omega}}}c_{\mathbf{u}2}c_{\mathbf{m}7}, \eta_{\boldsymbol{\omega}}\delta_{\mathbf{x}}c_{\mathbf{u}2}c_{\mathbf{m}8}, \delta_{\mathbf{u}}c_{\mathbf{u}2}c_{\mathbf{m}9}\Big\} \tag{2.47}$$

and

$$\limsup_{t\to\infty}\|\tilde{\mathbf{m}}(t)\| \leq \max\Big\{\alpha_{\boldsymbol{\omega}}^2c_{\mathbf{m}2}, \alpha_{\boldsymbol{\omega}}\eta_{\boldsymbol{\omega}}c_{\mathbf{m}3}, \delta_{\mathbf{n}}c_{\mathbf{m}7}, \alpha_{\boldsymbol{\omega}}\eta_{\boldsymbol{\omega}}\delta_{\mathbf{x}}c_{\mathbf{m}8}, \alpha_{\boldsymbol{\omega}}\delta_{\mathbf{u}}c_{\mathbf{m}9}\Big\}. \tag{2.48}$$

The boundedness of the solutions of the closed-loop system in Theorem 2.8 follows from Lemmas 2.10-2.13, (2.45), (2.46) and the coordinate transformation in (2.37). The bound in (2.35) of Theorem 2.8 follows from (2.47) and the coordinate transformation in (2.37).

2.5 Simulation comparison

2.5.1 Comparison of convergence rate for examples in the literature

To demonstrate the effectiveness of the extremum-seeking controller in this chapter, we compare its convergence rate against the convergence rate of three other extremum-seeking controllers in the literature: the multivariable extension

of the classical extremum-seeking controller in Krstić and Wang (2000) given in Ghaffari et al. (2012) (that is, the gradient-based controller, not the Newton-based controller), the phasor extremum-seeking controller in Atta et al. (2015) and the observer-based controller in Guay and Dochain (2015). The convergence rates of the extremum-seeking controllers are tested for eight different examples taken from the extremum-seeking literature. For each of the eight examples, one hundred initial conditions for the nominal plant parameters $\hat{\mathbf{u}}$ are randomly selected from a predefined set. As a measure for the convergence rate, we define the convergence time as the average of the times it takes for the nominal plant parameters to converge from their one hundred initial conditions to a predefined region of their optimal values $\mathbf{u}^*$. For all three controllers, the same perturbation signals are applied as in the works the examples are taken from. The remaining initial conditions of the plant and controllers are chosen such that the extremum-seeking scheme is at steady state if the adaptation of the optimizer is turned off (that is, if $\dot{\hat{\mathbf{u}}} = \mathbf{0}$). We let $\sigma_r = 10^{-4}$ and $\mathbf{H}(\hat{\mathbf{u}}) = \mathbf{0}$ for each of the examples. The regularization constant σ of the controller in Guay and Dochain (2015) is set to $\sigma = 10^{-6}$.

The references and corresponding perturbations of the eight examples are listed in Table 2.1. The predefined set of initial conditions and the ultimate bound to which the solutions of $\hat{\mathbf{u}}$ are required to convergence are given in Table 2.2. A random-search algorithm is employed to find the tuning parameters of the controller for which the convergence time is minimal. The obtained minimal convergence times for each example and each controller are presented in Table 2.3. The corresponding tuning parameters of the controllers are given in Tables 2.4-2.7. To verify that the obtained convergence times in Table 2.3 are (at least close to) minimal the convergence times for one thousand randomly chosen parameter sets have been computed for each example and each controller, where the values of the parameters ranged from one fifth to five times the values in Tables 2.4-2.7.

From Table 2.3, it follows that the fastest convergence to the ultimate bound is obtained with the presented extremum-seeking controller for five of the eight examples. This indicates that the controller presented in this chapter can be a valid alternative to present-day extremum-seeking controllers for a variety of applications. Moreover, we obtain from Table 2.3 that the obtained minimal convergence times of the controller in Guay and Dochain (2015) and the presented controller are comparable for about half of the examples. Similar to the controller presented in this chapter, the extremum-seeking controller in Guay and Dochain (2015) relies on an observer that uses the perturbation signals as well as the nominal part of the plant-parameter signals to compute a gradient estimate of the objective function. This in contrary to the extremum-seeking controllers in Atta et al. (2015) and Ghaffari et al. (2012) that do not utilize the nominal part of the plant-parameter signal for their gradient estimation. We note that the extremum-seeking controller in Atta et al. (2015) requires a distinct perturbation

Table 2.1: References and perturbations of the examples used in the comparison.

Example	Reference	Perturbations
1	(Tan et al., 2006, Section 6)	$0.3\sin(0.5t)$
2	(Ariyur and Krstić, 2003, Section 8.5)	$0.03\sin(0.08t)$
3	(Tan et al., 2010, Section 5, page 20)	$0.1\sin(t)$
4	(Moase and Manzie, 2012b, Section V.B)	$0.05\sin(2t)$
5	(Bastin et al., 2009, page 685)	$0.02\sin(0.1t)$
6	(Ariyur and Krstić, 2003, Section 1.3)	$0.05\sin(5t)$
7	(Ghaffari et al., 2012, Section 8)	$0.1\sin(7t)$
		$0.1\sin(5t)$
8	(Ariyur and Krstić, 2003, Section 2.3.1)	$0.05\sin(5.48t)$
		$0.05\cos(5.48t)$
		$0.05\sin(6.32t)$
		$0.05\cos(6.32t)$

Table 2.2: Sets of initial conditions and ultimate bounds.

Example	Set of initial conditions	Ultimate bound
1	$\lvert\hat{u}(0)-u^*\rvert \leq 5$	$\lvert\hat{u}-u^*\rvert \leq 0.01$
2	$u^*-0.4 \leq \hat{u}(0) \leq u^*$	$\lvert\hat{u}-u^*\rvert \leq 0.01$
3	$\lvert\hat{u}(0)-u^*\rvert \leq 1$	$\lvert\hat{u}-u^*\rvert \leq 0.1$
4	$\lvert\hat{u}(0)-u^*\rvert \leq 4$	$\lvert\hat{u}-u^*\rvert \leq 0.01$
5	$u^* \leq \hat{u}(0) \leq u^*+1$	$\lvert\hat{u}-u^*\rvert \leq 0.01$
6	$\lvert\hat{u}(0)-u^*\rvert \leq 5$	$\lvert\hat{u}-u^*\rvert \leq 0.01$
7	$\lVert\hat{\mathbf{u}}(0)-\mathbf{u}^*\rVert \leq 5$	$\lVert\hat{\mathbf{u}}-\mathbf{u}^*\rVert \leq 0.01$
8	$\lVert\hat{\mathbf{u}}(0)-\mathbf{u}^*\rVert \leq 5$	$\lVert\hat{\mathbf{u}}-\mathbf{u}^*\rVert \leq 0.01$

Table 2.3: Minimal convergence times of the extremum-seeking controllers.

Example	Atta et al.	Ghaffari et al.	Guay and Dochain	Presented
1	1.04×10^4	217	94.1	**61.5**
2	217	126	19.4	**5.3**
3	23.2	**18.6**	26.4	26.9
4	229	78.0	24.6	**24.4**
5	733	750	534	**423**
6	136	90.0	168	**42.6**
7	55.5	48.8	**25.9**	34.0
8	–	**52.6**	196	205

Table 2.4: Tuning parameters of the controller in Atta et al. (2015).

Example	k	$\frac{q}{r}$
1	4.92×10^{-3}	0.0215
2	0.0416	48.4
3	0.339	0.558
4	47.4	0.0251
5	0.240	278
6	29.9	0.0167
7	0.0728	0.129
8	–	–

Table 2.5: Tuning parameters of the gradient-based controller in Ghaffari et al. (2012), with $\mathbf{K} = k\mathbf{I}$.

Example	k	ω_h	ω_l
1	0.248	0.686	∞
2	1.74×10^{-3}	0.0373	∞
3	0.0856	1.45	0.412
4	18.4	13.3	0.250
5	5.69×10^{-3}	0.0314	0.0159
6	2.27	0.630	0.129
7	7.21×10^{-3}	0.410	0.231
8	1.31	15.7	0.290

Table 2.6: Tuning parameters of the controller in Guay and Dochain (2015).

Example	k	k_T	$k_{\eta 1}$	$k_{\eta 2}$
1	0.172	6.17	0.255	0.443
2	0.0700	9.93	18.3	27.1
3	0.0316	0.474	0.677	1.66
4	16.5	659	14.7	181
5	7.08×10^{-3}	0.0679	0.765	4.91
6	1.27	0.899	14.6	5.14
7	0.0230	1.12	7.61	3.18
8	0.864	2.98	4.52	0.841

Table 2.7: Tuning parameters of the presented controller.

Example	$\eta_{\mathbf{m}}$	$\eta_{\mathbf{u}}$	$\lambda_{\mathbf{u}}$
1	0.822	0.0866	0.773
2	113	0.0854	7.77
3	0.497	0.185	0.368
4	34.0	1.57	365
5	0.468	3.44×10^{-3}	0.556
6	3.67	0.121	178
7	0.933	0.547	0.239
8	3.85	2.16	17.8

frequency for each plant parameter. Therefore, it cannot be applied to Example 8 using the perturbations in Table 2.1.

2.5.2 In-depth example

For the comparison in Section 2.5.1, we used the same perturbations as in the works the examples were taken from. In this section, we present an in-depth example to investigate the influence of the perturbation amplitude and the perturbation frequency on the minimal convergence time. Moreover, we explore the effect of using curvature information of the objective function on the minimal convergence time. Consider the following plant:

$$\begin{aligned} \dot{x}_1(t) &= -x_1(t) + u(t) \\ \dot{x}_2(t) &= -x_2(t) + 0.5x_1^2(t) \\ y(t) &= x_2(t). \end{aligned} \tag{2.49}$$

The four extremum-seeking controllers in Section 2.5.1 are applied to minimizes the steady-state value of y. The perturbation used by the four controllers is given by $a_\omega \sin(\eta_\omega t)$, as defined in (2.16). We apply the same procedure to obtain the minimal convergence times of the four controllers as in Section 2.5.1. Let the set of initial conditions and the ultimate bound be given by $|\hat{u}(0) - u^*| \leq 5$ and $|\hat{u} - u^*| \leq 0.01$, respectively. The values of the regularization constants are given by $\sigma_r = 1 \times 10^{-4}$ and $\sigma = 1 \times 10^{-6}$. In Figures 2.2-2.4, the obtained minimal convergence times of the four controllers are plotted as a function of the angular perturbation frequency η_ω. The obtained minimal convergence times for the presented controller are displayed for both $H(\hat{u}) = 0$ and $H(\hat{u}) = \frac{d^2F}{du^2}(\hat{u}) = 1$. The perturbation amplitude in Figures 2.2-2.4 is given by $a_\omega = 0.05$, $a_\omega = 0.1$ and $a_\omega = 0.5$, respectively.

Figures 2.2-2.4 display that the obtained minimal convergence times for the extremum-seeking controller in Guay and Dochain (2015) and the presented controller for $H(\hat{u}) = 0$ similar overall. Only for the smallest perturbation amplitude in Figure 2.2, a significantly faster convergence is obtained with the presented controller than with the controller in Guay and Dochain (2015) for certain perturbation frequencies. The controller in Atta et al. (2015), the controller in Guay and Dochain (2015) and the presented controller are generally not stable in closed loop with the plant for high perturbation frequencies due to the large phase delay induced by the plant dynamics. The controller in Ghaffari et al. (2012) is able to compensate for the phase delay to some extent by creating a phase lead with the high-pass filter of the controller for high values of the cutoff frequency of the filter. Therefore, the nominal plant parameter $\hat{u}$ is able to converge to the ultimate bound for high perturbation frequencies if the controller in Ghaffari et al. (2012) in used. The main difference in the obtained minimal convergence times of the controllers in Atta et al. (2015) and in Ghaffari et al. (2012) and the observer-based controllers in Ghaffari et al. (2012)

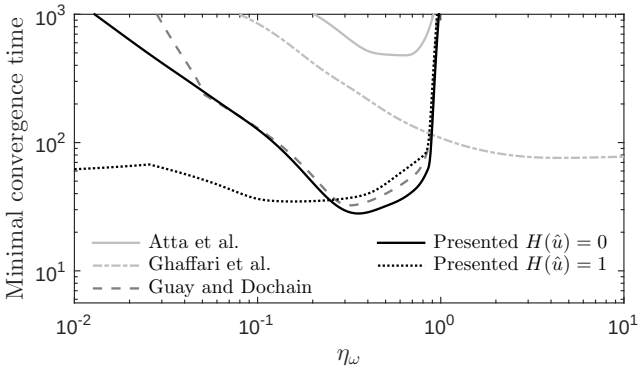

Figure 2.2: Minimal convergence time as a function of η_ω for $a_\omega = 0.05$.

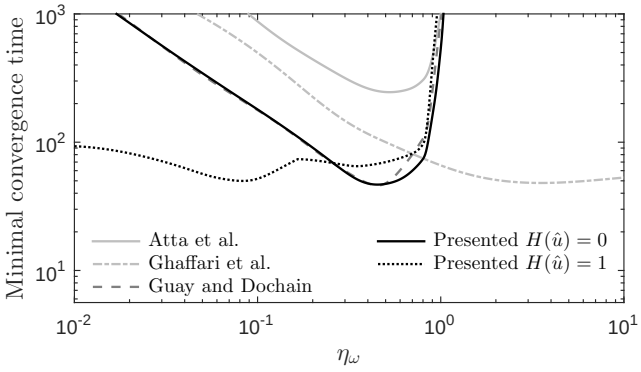

Figure 2.3: Minimal convergence time as a function of η_ω for $a_\omega = 0.1$.

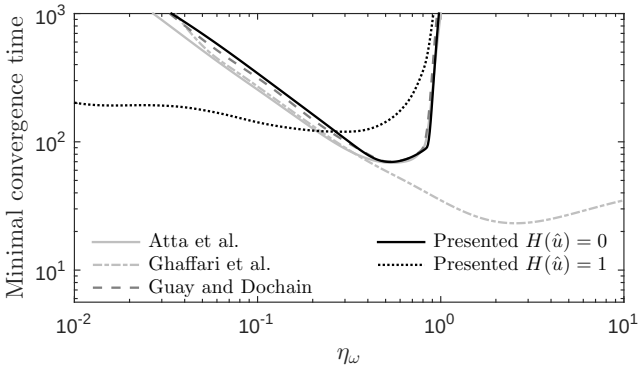

Figure 2.4: Minimal convergence time as a function of η_ω for $a_\omega = 0.5$.

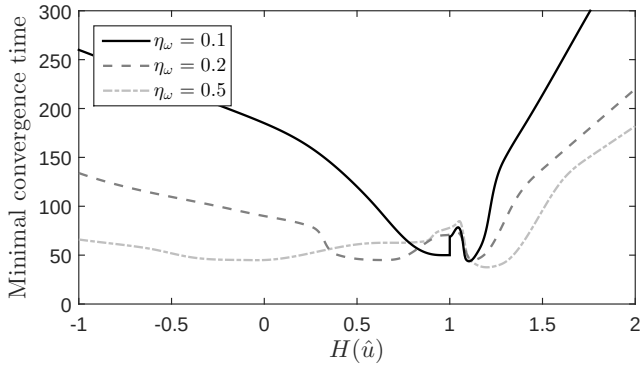

Figure 2.5: Minimal convergence time as a function of $H(\hat{u})$ for $a_\omega = 0.1$.

and in this chapter is that the fastest convergence with the phasor controller in Atta et al. (2015) and with the classical controller in Ghaffari et al. (2012) is obtained for the largest perturbation amplitude, while the fastest convergence with the two observer-based controllers is obtained for the smallest perturbation amplitude. Therefore, the possible benefit of using the nominal part of the plant-parameter signal in addition to the perturbation signal to estimate the gradient of the objective function (as for the observer-based controllers) may depend on the perturbation amplitude.

We observe in Figures 2.2-2.4 that a smaller minimal convergence time of the presented controller is obtained for $H(\hat{u}) = \frac{d^2F}{du^2}(\hat{u}) = 1$ than for $H(\hat{u}) = 0$ if the perturbation frequency is sufficiently low. Choosing $H(\hat{u}) = \frac{d^2F}{du^2}(\hat{u})$ requires explicit knowledge of the objective function. Because the objective function is unknown, it is not reasonable to assume that the Hessian of the objective function is known exactly. In Figure 2.5, the minimal convergence time is plotted as a function of constant values of $H(\hat{u})$ for the angular perturbation frequencies $\eta_\omega = 0.1$, $\eta_\omega = 0.2$ and $\eta_\omega = 0.5$. We obtain from Figure 2.5 that, for sufficiently low perturbation frequencies, a significantly faster convergence can be obtained compared to $H(\hat{u}) = 0$ if H is a moderately good approximation of the Hessian of the objective function. On the other hand, $H(\hat{u}) = 0$ is the more suitable choice for high perturbation frequencies. The tuning-parameter values that correspond to the obtained minimal convergence time make a jump at $H(\hat{u}) = 1$, which explains the bump in the curves near $H(\hat{u}) = 1$ in Figure 2.5.

Remark 2.14. *We note that the plant (2.49) is of the Wiener-Hammerstein type. It was found in Moase and Manzie (2012b) that an arbitrarily fast convergence to an arbitrarily small ultimate bound can be obtained for Wiener-Hammerstein plants by selecting a sufficiently large perturbation frequency and an sufficiently small perturbation amplitude if the delay due to the plant dynamics is compensated for. We note that, with a similar delay compensation, the convergences*

times in this section can be further reduced, especially for high perturbation frequencies for which the phase delay is large.

2.6 Conclusion

In this chapter, we have presented an extremum-seeking controller that optimizes the performance of a general nonlinear plant with an arbitrary number of plant parameters in the presence of an unknown bounded disturbance. The extremum-seeking controller uses a least-squares observer to accurately compute an estimate of the gradient of the objective function. The observer utilizes both the perturbation signals and the nominal part of the plant-parameter signals to obtain a gradient estimate. Moreover, curvature information of the objective function can be used to improve the accuracy of the estimate. The convergence region of the closed-loop system of plant an controller can be made global by normalizing the adaptation gain of the controller. A simulation comparison of the presented controller and three other controllers in the literature shows that a competitive convergence rate can be obtained with the presented controller for a variety of examples. Simulation results of an additional in-depth example indicate that utilizing the nominal part of the plant-parameter signals in addition to the perturbation signals to compute an estimate of the gradient of the objective function may result in a faster convergence for small perturbation amplitudes. In addition, the simulation results display that using the Hessian of the objective function to enhance the gradient estimate may have a positive effect on the convergence rate if the frequency of perturbations is low, even for a moderately good approximation of the Hessian. Further research is required to generalize the last two statements.

2.7 Appendix

2.7.1 Proof of Lemma 2.10

From (2.3) and (2.37), it follows that the state equation for $\tilde{\mathbf{x}}$ is given by

$$\dot{\tilde{\mathbf{x}}} = \mathbf{f}\left(\tilde{\mathbf{x}} + \mathbf{X}(\mathbf{u}), \mathbf{u}\right) - \frac{d\mathbf{X}}{d\mathbf{u}}(\mathbf{u})\dot{\mathbf{u}}. \tag{2.50}$$

From Assumptions 2.1-2.3, it follows that there exists a Lyapunov function for the $\tilde{\mathbf{x}}$-dynamics in (2.50) for constant values of $\mathbf{u}$, as formulated in the following converse lemma.

Lemma 2.15. *Under Assumptions 2.1-2.3, there exists a function* $V_{\mathbf{x}} : \mathbb{R}^{n_{\mathbf{x}}} \times \mathbb{R}^{n_{\mathbf{u}}} \to \mathbb{R}$*, and constants* $\gamma_{\mathbf{x}1}, \gamma_{\mathbf{x}2}, \ldots, \gamma_{\mathbf{x}5} \in \mathbb{R}_{>0}$*, such that the inequalities*

$$\gamma_{\mathbf{x}1}\|\tilde{\mathbf{x}}\|^2 \leq V_{\mathbf{x}}(\tilde{\mathbf{x}}, \mathbf{u}) \leq \gamma_{\mathbf{x}2}\|\tilde{\mathbf{x}}\|^2, \tag{2.51}$$

$$\frac{\partial V_{\mathbf{x}}}{\partial \tilde{\mathbf{x}}}(\tilde{\mathbf{x}}, \mathbf{u}) \mathbf{f}(\tilde{\mathbf{x}} + \mathbf{X}(\mathbf{u}), \mathbf{u}) \leq -\gamma_{\mathbf{x}3} \|\tilde{\mathbf{x}}\|^2 \tag{2.52}$$

and

$$\left\| \frac{\partial V_{\mathbf{x}}}{\partial \tilde{\mathbf{x}}}(\tilde{\mathbf{x}}, \mathbf{u}) \right\| \leq \gamma_{\mathbf{x}4} \|\tilde{\mathbf{x}}\|, \qquad \left\| \frac{\partial V_{\mathbf{x}}}{\partial \mathbf{u}}(\tilde{\mathbf{x}}, \mathbf{u}) \right\| \leq \gamma_{\mathbf{x}5} \|\tilde{\mathbf{x}}\|, \tag{2.53}$$

are satisfied for all $\tilde{\mathbf{x}} \in \mathbb{R}^{n_{\mathbf{x}}}$ *and all* $\mathbf{u} \in \mathbb{R}^{n_{\mathbf{u}}}$.

Proof. The proof follows similar steps as the proof of Khalil (2002, Lemma 9.8). Let $\boldsymbol{\phi}(t; \tilde{\mathbf{x}}, \mathbf{u})$ be the solution of (2.50) for constant $\mathbf{u}$ that starts at $\tilde{\mathbf{x}}$ for $t = 0$, that is $\boldsymbol{\phi}(0; \tilde{\mathbf{x}}, \mathbf{u}) = \tilde{\mathbf{x}}$. For any $\tilde{\mathbf{x}} \in \mathbb{R}^{n_{\mathbf{x}}}$ and any $\mathbf{u} \in \mathbb{R}^{n_{\mathbf{u}}}$, (2.50) can be written as

$$\frac{\partial \boldsymbol{\phi}}{\partial t}(t; \tilde{\mathbf{x}}, \mathbf{u}) = \mathbf{f}\left(\boldsymbol{\phi}(t; \tilde{\mathbf{x}}, \mathbf{u}) + \mathbf{X}(\mathbf{u}), \mathbf{u}\right). \tag{2.54}$$

We define the function

$$V_{\mathbf{x}}(\tilde{\mathbf{x}}, \mathbf{u}) = \int_0^{T_{\mathbf{x}}} \|\boldsymbol{\phi}(t; \tilde{\mathbf{x}}, \mathbf{u})\|^2 dt, \tag{2.55}$$

with constant $T_{\mathbf{x}} > \frac{\ln(\mu_{\mathbf{x}})}{\nu_{\mathbf{x}}} \geq 0$, where $\mu_{\mathbf{x}}, \nu_{\mathbf{x}} \in \mathbb{R}_{>0}$ are defined in Assumption 2.3. We note that, without loss of generality, this implies that $\mu_{\mathbf{x}} \geq 1$. Due to the bound on the trajectories in (2.8), we have

$$V_{\mathbf{x}}(\tilde{\mathbf{x}}, \mathbf{u}) \leq \int_0^{T_{\mathbf{x}}} \mu_{\mathbf{x}}^2 e^{-2\nu_{\mathbf{x}} t} \|\tilde{\mathbf{x}}\|^2 dt = \frac{\mu_{\mathbf{x}}^2 \left(1 - e^{-2\nu_{\mathbf{x}} T_{\mathbf{x}}}\right)}{2\nu_{\mathbf{x}}} \|\tilde{\mathbf{x}}\|^2. \tag{2.56}$$

From (2.4) of Assumption 2.1 and from (2.6) of Assumption 2.2, we have

$$\|\mathbf{f}(\tilde{\mathbf{x}} + \mathbf{X}(\mathbf{u}), \mathbf{u})\| = \left\| \int_0^1 \frac{\partial \mathbf{f}}{\partial \mathbf{x}}(\sigma \tilde{\mathbf{x}} + \mathbf{X}(\mathbf{u}), \mathbf{u}) d\sigma \tilde{\mathbf{x}} \right\| \leq L_{\mathbf{fx}} \|\tilde{\mathbf{x}}\| \tag{2.57}$$

for all $\tilde{\mathbf{x}} \in \mathbb{R}^{n_{\mathbf{x}}}$ and all $\mathbf{u} \in \mathbb{R}^{n_{\mathbf{u}}}$. From (2.54) and (2.57), we obtain

$$\frac{\partial}{\partial t}\left(\|\boldsymbol{\phi}(t; \tilde{\mathbf{x}}, \mathbf{u})\|^2\right) \geq -2L_{\mathbf{fx}} \|\boldsymbol{\phi}(t; \tilde{\mathbf{x}}, \mathbf{u})\|^2 \tag{2.58}$$

for all $t \geq 0$. We use this inequality to obtain

$$\frac{\partial}{\partial t}\left(\|\boldsymbol{\phi}(t; \tilde{\mathbf{x}}, \mathbf{u})\|^2 e^{2L_{\mathbf{fx}} t}\right) \geq 0. \tag{2.59}$$

By integrating both sides of (2.59) with respect to time over the domain $[0, t]$, it follows that

$$\|\boldsymbol{\phi}(t; \tilde{\mathbf{x}}, \mathbf{u})\|^2 e^{2L_{\mathbf{fx}} t} - \|\tilde{\mathbf{x}}\|^2 \geq 0. \tag{2.60}$$

Therefore, the following bound is obtained:

$$V_{\mathbf{x}}(\tilde{\mathbf{x}}, \mathbf{u}) \geq \int_0^{T_{\mathbf{x}}} e^{-2L_{\mathbf{fx}} t} \|\tilde{\mathbf{x}}\|^2 dt = \frac{1 - e^{-2L_{\mathbf{fx}} T_{\mathbf{x}}}}{2L_{\mathbf{fx}}} \|\tilde{\mathbf{x}}\|^2. \tag{2.61}$$

The bounds on $V_{\mathbf{x}}$ in (2.56) and (2.61) imply that (2.51) is satisfied with $\gamma_{\mathbf{x}1} = \frac{1-e^{-2L_{\mathbf{fx}}T_{\mathbf{x}}}}{2L_{\mathbf{fx}}}$ and $\gamma_{\mathbf{x}2} = \frac{\mu_{\mathbf{x}}^2\left(1-e^{-2\nu_{\mathbf{x}}T_{\mathbf{x}}}\right)}{2\nu_{\mathbf{x}}}$. Because $L_{\mathbf{fx}}$, $\nu_{\mathbf{x}}$ and $T_{\mathbf{x}}$ are positive constants, we have $\gamma_{\mathbf{x}1} > 0$ and $\gamma_{\mathbf{x}2} > 0$.

By integrating both sides of (2.54) with respect to time, we have

$$\boldsymbol{\phi}(t;\tilde{\mathbf{x}},\mathbf{u}) = \tilde{\mathbf{x}} + \int_0^t \mathbf{f}(\boldsymbol{\phi}(\tau;\tilde{\mathbf{x}},\mathbf{u}) + \mathbf{X}(\mathbf{u}),\mathbf{u})d\tau. \tag{2.62}$$

From straightforward computation, we obtain

$$\frac{\partial\boldsymbol{\phi}}{\partial\tilde{\mathbf{x}}}(t;\tilde{\mathbf{x}},\mathbf{u}) = \mathbf{I} + \int_0^t \frac{\partial\mathbf{f}}{\partial\mathbf{x}}(\boldsymbol{\phi}(\tau;\tilde{\mathbf{x}},\mathbf{u}) + \mathbf{X}(\mathbf{u}),\mathbf{u})\frac{\partial\boldsymbol{\phi}}{\partial\tilde{\mathbf{x}}}(\tau;\tilde{\mathbf{x}},\mathbf{u})d\tau. \tag{2.63}$$

The differential equation in (2.54) can be written as

$$\frac{\partial\boldsymbol{\phi}}{\partial t}(t;\tilde{\mathbf{x}},\mathbf{u}) = \mathbf{f}(\tilde{\mathbf{x}} + \mathbf{X}(\mathbf{u}),\mathbf{u}) + \int_0^t \frac{\partial\mathbf{f}}{\partial\mathbf{x}}(\boldsymbol{\phi}(\tau;\tilde{\mathbf{x}},\mathbf{u}) + \mathbf{X}(\mathbf{u}),\mathbf{u})\frac{\partial\boldsymbol{\phi}}{\partial t}(\tau;\tilde{\mathbf{x}},\mathbf{u})d\tau. \tag{2.64}$$

We define the variable

$$\boldsymbol{\xi}(t;\tilde{\mathbf{x}},\mathbf{u}) = \frac{\partial\boldsymbol{\phi}}{\partial t}(t;\tilde{\mathbf{x}},\mathbf{u}) - \frac{\partial\boldsymbol{\phi}}{\partial\tilde{\mathbf{x}}}(t;\tilde{\mathbf{x}},\mathbf{u})\mathbf{f}(\tilde{\mathbf{x}} + \mathbf{X}(\mathbf{u}),\mathbf{u}). \tag{2.65}$$

From (2.63) and (2.64), it follows that

$$\frac{\partial\boldsymbol{\xi}}{\partial t}(t;\tilde{\mathbf{x}},\mathbf{u}) = \frac{\partial\mathbf{f}}{\partial\mathbf{x}}(\boldsymbol{\phi}(t;\tilde{\mathbf{x}},\mathbf{u}) + \mathbf{X}(\mathbf{u}),\mathbf{u})\boldsymbol{\xi}(t;\tilde{\mathbf{x}},\mathbf{u}), \tag{2.66}$$

with initial condition $\boldsymbol{\xi}(0;\tilde{\mathbf{x}},\mathbf{u}) = \mathbf{0}$, which implies that $\boldsymbol{\xi}(t;\tilde{\mathbf{x}},\mathbf{u}) = \mathbf{0}$ for all $t \geq 0$. Therefore, from (2.65), we obtain that

$$\frac{\partial\boldsymbol{\phi}}{\partial t}(t;\tilde{\mathbf{x}},\mathbf{u}) = \frac{\partial\boldsymbol{\phi}}{\partial\tilde{\mathbf{x}}}(t;\tilde{\mathbf{x}},\mathbf{u})\mathbf{f}(\tilde{\mathbf{x}} + \mathbf{X}(\mathbf{u}),\mathbf{u}), \tag{2.67}$$

for all $t \geq 0$. We use this equation and the bound on the trajectories in (2.8) of Assumption 2.3 to obtain

$$\begin{aligned}\frac{\partial V_{\mathbf{x}}}{\partial\tilde{\mathbf{x}}}(\tilde{\mathbf{x}},\mathbf{u})\mathbf{f}(\tilde{\mathbf{x}} + \mathbf{X}(\mathbf{u}),\mathbf{u}) &= \int_0^{T_{\mathbf{x}}} 2\boldsymbol{\phi}(t;\tilde{\mathbf{x}},\mathbf{u})\frac{\partial\boldsymbol{\phi}}{\partial t}(t;\tilde{\mathbf{x}},\mathbf{u})dt \\ &= \|\boldsymbol{\phi}(T_{\mathbf{x}};\tilde{\mathbf{x}},\mathbf{u})\|^2 - \|\tilde{\mathbf{x}}\|^2 \\ &\leq -\left(1 - \mu_{\mathbf{x}}^2 e^{-2\nu_{\mathbf{x}}T_{\mathbf{x}}}\right)\|\tilde{\mathbf{x}}\|^2.\end{aligned} \tag{2.68}$$

This implies that the bound in (2.52) is satisfied with $\gamma_{\mathbf{x}3} = 1 - \mu_{\mathbf{x}}^2 e^{-2\nu_{\mathbf{x}}T_{\mathbf{x}}}$. Because $T_{\mathbf{x}} > \frac{\ln(\mu_{\mathbf{x}})}{\nu_{\mathbf{x}}}$, we have $\gamma_{\mathbf{x}3} > 0$.

From (2.63) and (2.4) of Assumption 2.1, we obtain

$$\frac{\partial}{\partial t}\left\|\frac{\partial\boldsymbol{\phi}}{\partial\tilde{\mathbf{x}}}(t;\tilde{\mathbf{x}},\mathbf{u})\right\| \leq L_{\mathbf{fx}}\left\|\frac{\partial\boldsymbol{\phi}}{\partial\tilde{\mathbf{x}}}(t;\tilde{\mathbf{x}},\mathbf{u})\right\|, \tag{2.69}$$

from which it follows that

$$\frac{\partial}{\partial t}\left(\left\|\frac{\partial \boldsymbol{\phi}}{\partial \tilde{\mathbf{x}}}(t;\tilde{\mathbf{x}},\mathbf{u})\right\| e^{-L_{\mathbf{fx}}t}\right) \leq 0. \tag{2.70}$$

Similar to (2.60), by integrating both sides of (2.70) with respect to time over the domain $[0,t]$, we obtain

$$\left\|\frac{\partial \boldsymbol{\phi}}{\partial \tilde{\mathbf{x}}}(t;\tilde{\mathbf{x}},\mathbf{u})\right\| e^{-L_{\mathbf{fx}}t} - 1 \leq 0. \tag{2.71}$$

This inequality is used to obtain the bound

$$\begin{aligned}\left\|\frac{\partial V_{\mathbf{x}}}{\partial \tilde{\mathbf{x}}}(\tilde{\mathbf{x}},\mathbf{u})\right\| &\leq \int_0^{T_{\mathbf{x}}} 2\|\boldsymbol{\phi}(t;\tilde{\mathbf{x}},\mathbf{u})\| \left\|\frac{\partial \boldsymbol{\phi}}{\partial \tilde{\mathbf{x}}}(t;\tilde{\mathbf{x}},\mathbf{u})\right\| dt \\ &\leq \int_0^{T_{\mathbf{x}}} 2\mu_{\mathbf{x}} e^{-\nu_{\mathbf{x}}t}\|\tilde{\mathbf{x}}\| e^{L_{\mathbf{fx}}t} dt \\ &= \frac{2\mu_{\mathbf{x}}\left(e^{(L_{\mathbf{fx}}-\nu_{\mathbf{x}})T_{\mathbf{x}}}-1\right)}{L_{\mathbf{fx}}-\nu_{\mathbf{x}}}\|\tilde{\mathbf{x}}\|.\end{aligned} \tag{2.72}$$

By taking the derivative with respect to $\mathbf{u}$ of both sides of the equation (2.62), we obtain

$$\begin{aligned}\frac{\partial \boldsymbol{\phi}}{\partial \mathbf{u}}(t;\tilde{\mathbf{x}},\mathbf{u}) = \int_0^t \Bigg(&\frac{\partial \mathbf{f}}{\partial \mathbf{x}}(\boldsymbol{\phi}(\tau;\tilde{\mathbf{x}},\mathbf{u})+\mathbf{X}(\mathbf{u}),\mathbf{u})\left(\frac{\partial \boldsymbol{\phi}}{\partial \mathbf{u}}(\tau;\tilde{\mathbf{x}},\mathbf{u})+\frac{d\mathbf{X}}{d\mathbf{u}}(\mathbf{u})\right) \\ &+ \frac{\partial \mathbf{f}}{\partial \mathbf{u}}(\boldsymbol{\phi}(\tau;\tilde{\mathbf{x}},\mathbf{u})+\mathbf{X}(\mathbf{u}),\mathbf{u})\Bigg) d\tau.\end{aligned} \tag{2.73}$$

By using the bounds in Assumptions 2.1-2.2, it follows that

$$\left\|\frac{\partial \boldsymbol{\phi}}{\partial \mathbf{u}}(t;\tilde{\mathbf{x}},\mathbf{u})\right\| \leq \int_0^t L_{\mathbf{fx}}\left\|\frac{\partial \boldsymbol{\phi}}{\partial \mathbf{u}}(\tau;\tilde{\mathbf{x}},\mathbf{u})\right\| d\tau + (L_{\mathbf{fx}}L_{\mathbf{X}} + L_{\mathbf{fu}})t. \tag{2.74}$$

Subsequently, use of the Gronwall-Bellman inequality yields

$$\left\|\frac{\partial \boldsymbol{\phi}}{\partial \mathbf{u}}(t;\tilde{\mathbf{x}},\mathbf{u})\right\| \leq (L_{\mathbf{fx}}L_{\mathbf{X}} + L_{\mathbf{fu}})te^{L_{\mathbf{fx}}t}. \tag{2.75}$$

Therefore, from this inequality and the bound on the trajectories in (2.8) of Assumption 2.3, we obtain

$$\begin{aligned}\left\|\frac{\partial V_{\mathbf{x}}}{\partial \mathbf{u}}(\tilde{\mathbf{x}},\mathbf{u})\right\| &\leq \int_0^{T_{\mathbf{x}}} 2\|\boldsymbol{\phi}(t;\tilde{\mathbf{x}},\mathbf{u})\| \left\|\frac{\partial \boldsymbol{\phi}}{\partial \mathbf{u}}(t;\tilde{\mathbf{x}},\mathbf{u})\right\| dt \\ &\leq \int_0^{T_{\mathbf{x}}} 2\mu_{\mathbf{x}} e^{-\nu_{\mathbf{x}}t}\|\tilde{\mathbf{x}}\|(L_{\mathbf{fx}}L_{\mathbf{X}}+L_{\mathbf{fu}})te^{L_{\mathbf{fx}}t} dt \\ &= \frac{2\mu_{\mathbf{x}}(L_{\mathbf{fx}}L_{\mathbf{X}}+L_{\mathbf{fu}})}{(L_{\mathbf{fx}}-\nu_{\mathbf{x}})^2}\Bigg(1 - e^{(L_{\mathbf{fx}}-\nu_{\mathbf{x}})T_{\mathbf{x}}} \\ &\quad + (L_{\mathbf{fx}}-\nu_{\mathbf{x}})T_{\mathbf{x}}e^{(L_{\mathbf{fx}}-\nu_{\mathbf{x}})T_{\mathbf{x}}}\Bigg)\|\tilde{\mathbf{x}}\|,\end{aligned} \tag{2.76}$$

The bounds in (2.53) follows from (2.72) and (2.76), with $\gamma_{\mathbf{x}4} = \frac{2\mu_{\mathbf{x}}\left(e^{(L_{\mathbf{fx}}-\nu_{\mathbf{x}})T_{\mathbf{x}}}-1\right)}{L_{\mathbf{fx}}-\nu_{\mathbf{x}}}$ and $\gamma_{\mathbf{x}5} = \frac{2\mu_{\mathbf{x}}(L_{\mathbf{fx}}L_{\mathbf{X}}+L_{\mathbf{fu}})}{(L_{\mathbf{fx}}-\nu_{\mathbf{x}})^2}\left(1+((L_{\mathbf{fx}}-\nu_{\mathbf{x}})T_{\mathbf{x}}-1)e^{(L_{\mathbf{fx}}-\nu_{\mathbf{x}})T_{\mathbf{x}}}\right)$. Without loss of generality, we assume that $L_{\mathbf{fx}} > \nu_{\mathbf{x}}$ such that $\gamma_{\mathbf{x}4} > 2\mu_{\mathbf{x}}T_{\mathbf{x}} > 0$ and $\gamma_{\mathbf{x}5} > \mu_{\mathbf{x}}(L_{\mathbf{fx}}L_{\mathbf{X}} + L_{\mathbf{fu}})T_{\mathbf{x}}^2 > 0$. □

By using the function $V_{\mathbf{x}}$ in Lemma 2.15 as a Lyapunov function candidate for the $\tilde{\mathbf{x}}$-dynamics in (2.50) for time-varying $\mathbf{u}$, we obtain

$$\begin{aligned}\dot{V}_{\mathbf{x}}(\tilde{\mathbf{x}},\mathbf{u}) = &\frac{\partial V_{\mathbf{x}}}{\partial \tilde{\mathbf{x}}}(\tilde{\mathbf{x}},\mathbf{u})\mathbf{f}(\tilde{\mathbf{x}}+\mathbf{X}(\mathbf{u}),\mathbf{u})\\ &+\left(\frac{\partial V_{\mathbf{x}}}{\partial \mathbf{u}}(\tilde{\mathbf{x}},\mathbf{u})-\frac{\partial V_{\mathbf{x}}}{\partial \tilde{\mathbf{x}}}(\tilde{\mathbf{x}},\mathbf{u})\frac{d\mathbf{X}}{d\mathbf{u}}(\mathbf{u})\right)\dot{\mathbf{u}}.\end{aligned} \tag{2.77}$$

for all $\tilde{\mathbf{x}} \in \mathbb{R}^{n_{\mathbf{x}}}$ and all $\mathbf{u} \in \mathbb{R}^{n_{\mathbf{u}}}$. Use of the bounds in Assumption 2.2 and Lemma 2.15 yields

$$\dot{V}_{\mathbf{x}}(\tilde{\mathbf{x}},\mathbf{u}) \leq -\gamma_{\mathbf{x}3}\|\mathbf{x}\|^2 + (\gamma_{\mathbf{x}5}+\gamma_{\mathbf{x}4}L_{\mathbf{X}})\|\mathbf{x}\|\|\dot{\mathbf{u}}\|. \tag{2.78}$$

Subsequently, from Lemma 2.15 and Young's inequality, we obtain

$$\dot{V}_{\mathbf{x}}(\tilde{\mathbf{x}},\mathbf{u}) \leq -\frac{\gamma_{\mathbf{x}3}}{2\gamma_{\mathbf{x}2}}V_{\mathbf{x}}(\tilde{\mathbf{x}},\mathbf{u}) + \frac{(\gamma_{\mathbf{x}5}+\gamma_{\mathbf{x}4}L_{\mathbf{X}})^2}{2\gamma_{\mathbf{x}3}}\|\dot{\mathbf{u}}\|^2. \tag{2.79}$$

To find an upper bound for $\|\dot{\mathbf{u}}\|$, we note that it follows from (2.15) that

$$\dot{\mathbf{u}} = \dot{\hat{\mathbf{u}}} + \alpha_{\boldsymbol{\omega}}\dot{\boldsymbol{\omega}}. \tag{2.80}$$

From the definition of $\boldsymbol{\omega}$ in (2.16), we have that there exists a constant $L_{\boldsymbol{\omega}2} \in \mathbb{R}_{>0}$ such that

$$\|\dot{\boldsymbol{\omega}}\| \leq \eta_{\boldsymbol{\omega}}L_{\omega 2}. \tag{2.81}$$

Moreover, from (2.34), we have that $\|\dot{\hat{\mathbf{u}}}\| \leq \eta_{\mathbf{u}}$. Therefore, from (2.80)-(2.81) and $\|\dot{\hat{\mathbf{u}}}\| \leq \eta_{\mathbf{u}}$, we obtain

$$\|\dot{\mathbf{u}}\| \leq \eta_{\mathbf{u}} + \alpha_{\boldsymbol{\omega}}\eta_{\boldsymbol{\omega}}L_{\omega 2}, \tag{2.82}$$

which implies that

$$\|\dot{\mathbf{u}}\| \leq \alpha_{\boldsymbol{\omega}}\eta_{\boldsymbol{\omega}}\left(\varepsilon_3\varepsilon_5 + L_{\boldsymbol{\omega}2}\right). \tag{2.83}$$

for all $\eta_{\mathbf{m}} \leq \eta_{\boldsymbol{\omega}}\varepsilon_3$ and all $\eta_{\mathbf{u}} \leq \alpha_{\boldsymbol{\omega}}\eta_{\mathbf{m}}\varepsilon_5$. Substituting this in (2.79) gives

$$\dot{V}_{\mathbf{x}}(\tilde{\mathbf{x}},\mathbf{u}) \leq -\frac{\gamma_{\mathbf{x}3}}{2\gamma_{\mathbf{x}2}}V_{\mathbf{x}}(\tilde{\mathbf{x}},\mathbf{u}) + \alpha_{\boldsymbol{\omega}}^2\eta_{\boldsymbol{\omega}}^2\frac{(\gamma_{\mathbf{x}5}+\gamma_{\mathbf{x}4}L_{\mathbf{X}})^2}{2\gamma_{\mathbf{x}3}}\left(\varepsilon_3\varepsilon_5+L_{\boldsymbol{\omega}2}\right)^2. \tag{2.84}$$

Then, from the comparison lemma Khalil (2002, Lemma 3.4), it follows that

$$\begin{aligned}V_{\mathbf{x}}(\tilde{\mathbf{x}}(t),\mathbf{u}(t)) \leq &\, V_{\mathbf{x}}(\tilde{\mathbf{x}}(0),\mathbf{u}(0))e^{-\frac{\gamma_{\mathbf{x}3}}{2\gamma_{\mathbf{x}2}}t}\\ &+\alpha_{\boldsymbol{\omega}}^2\eta_{\boldsymbol{\omega}}^2\frac{\gamma_{\mathbf{x}2}}{\gamma_{\mathbf{x}3}^2}(\gamma_{\mathbf{x}5}+\gamma_{\mathbf{x}4}L_{\mathbf{X}})^2(\varepsilon_3\varepsilon_5+L_{\boldsymbol{\omega}2})^2\end{aligned} \tag{2.85}$$

for all $t \geq 0$ and all $\tilde{\mathbf{x}}(0) \in \mathbb{R}^{n_{\mathbf{x}}}$. From (2.85) and Lemma 2.15, it follows that

$$\|\tilde{\mathbf{x}}(t)\| \leq \max\left\{\sqrt{\frac{2\gamma_{\mathbf{x}2}}{\gamma_{\mathbf{x}1}}}\|\tilde{\mathbf{x}}(0)\|e^{-\frac{\gamma_{\mathbf{x}3}}{4\gamma_{\mathbf{x}2}}t}, \alpha_{\boldsymbol{\omega}}\eta_{\boldsymbol{\omega}}\sqrt{\frac{2\gamma_{\mathbf{x}2}}{\gamma_{\mathbf{x}1}}}\frac{\gamma_{\mathbf{x}\bar{5}}+\gamma_{\mathbf{x}4}L_{\mathbf{X}}}{\gamma_{\mathbf{x}3}}\left(\varepsilon_3\varepsilon_{\bar{5}}+L_{\boldsymbol{\omega}2}\right)\right\}. \tag{2.86}$$

The proof of the lemma follows from (2.86).

2.7.2 Proof of Lemma 2.11

First, we note that $\tilde{\mathbf{Q}}$ in (2.37) is well defined if $\mathbf{Q}^{-1}$ exists. From (2.29), we have that

$$\begin{aligned}\mathbf{Q}^{-1}(t) = \eta_{\mathbf{m}}\int_0^t e^{-\eta_{\mathbf{m}}(t-\tau)}\boldsymbol{\Phi}^T(\tau,t)\left(\mathbf{C}^T(\tau)\mathbf{C}(\tau)+\sigma_r\mathbf{D}^T\mathbf{D}\right)\boldsymbol{\Phi}(\tau,t)d\tau \\ + e^{-\eta_{\mathbf{m}}t}\boldsymbol{\Phi}^T(0,t)\mathbf{Q}(0)^{-1}\boldsymbol{\Phi}(0,t),\end{aligned} \tag{2.87}$$

where we substituted $\mathbf{Q}(0) = \mathbf{Q}_0$. From (2.34), it follows that $\|\dot{\hat{\mathbf{u}}}\| \leq \eta_{\mathbf{u}}$. Therefore, we have

$$\|\tilde{\mathbf{u}}(t) - \tilde{\mathbf{u}}(\tau)\| = \left\|\int_\tau^t \dot{\tilde{\mathbf{u}}}(\tau)d\tau\right\| \leq \eta_{\mathbf{u}}(t-\tau) \tag{2.88}$$

for all $t \geq \tau \geq 0$, which implies that state-transition matrix $\boldsymbol{\Phi}(\tau,t)$ in (2.31) is bounded for any $t \geq \tau \geq 0$. Moreover, the matrix $\mathbf{C}$ in (2.21) is uniformly bounded because the perturbation vector $\boldsymbol{\omega}$ in (2.16) is uniformly bounded. Because each time-varying matrix in the right-hand side of (2.87) is bounded for any $t \geq 0$, the matrix $\mathbf{Q}^{-1}(t)$ in (2.87) is bounded for any $t \geq 0$. In addition, the matrix $\mathbf{Q}^{-1}(t)$ is positive definite for any $t \geq 0$ and any symmetric positive-definite $\mathbf{Q}(0) \in \mathbb{R}^{n_{\mathbf{u}}+1 \times n_{\mathbf{u}}+1}$ because the first term in the right-hand side of (2.87) is positive semidefinite and the second term in the right-hand side of (2.87) is positive definite if $\mathbf{Q}(0)$ is positive definite. Hence, $\mathbf{Q}^{-1}(t)$ exists for any $t \geq 0$, which implies that $\tilde{\mathbf{Q}}(t)$ is well defined for any $t \geq 0$.

Now, from (2.33) and (2.36)-(2.38), we obtain that the state equation for $\tilde{\mathbf{Q}}$ is given by

$$\dot{\tilde{\mathbf{Q}}} = -\eta_{\mathbf{m}}\tilde{\mathbf{Q}} - \tilde{\mathbf{Q}}\mathbf{A} - \mathbf{A}^T\tilde{\mathbf{Q}} - \left(\boldsymbol{\Xi}^{-1} + \frac{\eta_{\mathbf{m}}}{\eta_{\boldsymbol{\omega}}}\mathbf{l}\right)\mathbf{A} - \mathbf{A}^T\left(\boldsymbol{\Xi}^{-1} + \frac{\eta_{\mathbf{m}}}{\eta_{\boldsymbol{\omega}}}\mathbf{l}\right) - \eta_{\mathbf{m}}\frac{\eta_{\mathbf{m}}}{\eta_{\boldsymbol{\omega}}}\mathbf{l}. \tag{2.89}$$

We note that $\tilde{\mathbf{Q}}$ is symmetric because $\mathbf{Q}$, $\boldsymbol{\Xi}$ and $\mathbf{l}$ are symmetric. We define the following Lyapunov-function candidate for the $\tilde{\mathbf{Q}}$-dynamics:

$$V_{\mathbf{Q}}(\tilde{\mathbf{Q}}) = \operatorname{tr}\left(\tilde{\mathbf{Q}}^2\right). \tag{2.90}$$

From (2.89), we have that the time derivative of $V_{\mathbf{Q}}$ can be written as

$$\begin{aligned}\dot{V}_{\mathbf{Q}}(\tilde{\mathbf{Q}}) = -2\eta_{\mathbf{m}}\operatorname{tr}\left(\tilde{\mathbf{Q}}^2\right) - 4\operatorname{tr}\left(\tilde{\mathbf{Q}}^2\mathbf{A}\right) \\ - 4\operatorname{tr}\left(\tilde{\mathbf{Q}}\left(\boldsymbol{\Xi}^{-1} + \frac{\eta_{\mathbf{m}}}{\eta_{\boldsymbol{\omega}}}\mathbf{l}\right)\mathbf{A}\right) - 2\eta_{\mathbf{m}}\frac{\eta_{\mathbf{m}}}{\eta_{\boldsymbol{\omega}}}\operatorname{tr}\left(\tilde{\mathbf{Q}}\mathbf{l}\right).\end{aligned} \tag{2.91}$$

From Young's inequality, (2.90) and (2.91), we get

$$\begin{aligned}\dot{V}_{\mathbf{Q}}(\tilde{\mathbf{Q}}) \leq -\eta_{\mathbf{m}} V_{\mathbf{Q}}(\tilde{\mathbf{Q}}) - 4\,\mathrm{tr}\left(\tilde{\mathbf{Q}}^2\mathbf{A}\right) \\ + \frac{8}{\eta_{\mathbf{m}}}\,\mathrm{tr}\left(\mathbf{A}^T\left(\Xi^{-1} + \frac{\eta_{\mathbf{m}}}{\eta_{\boldsymbol{\omega}}}\mathbf{l}\right)^2\mathbf{A}\right) + 2\eta_{\mathbf{m}}\left(\frac{\eta_{\mathbf{m}}}{\eta_{\boldsymbol{\omega}}}\right)^2\mathrm{tr}\left(\mathbf{l}^2\right).\end{aligned} \tag{2.92}$$

From (2.90), it follows that

$$\|\tilde{\mathbf{Q}}\|^2 \leq V_{\mathbf{Q}}(\tilde{\mathbf{Q}}) \leq n_{\mathbf{u}}\|\tilde{\mathbf{Q}}\|^2. \tag{2.93}$$

We note that

$$\mathrm{tr}\left(\tilde{\mathbf{Q}}^2\mathbf{A}\right) \leq n_{\mathbf{u}}\|\tilde{\mathbf{Q}}\|^2\|\mathbf{A}\| \tag{2.94}$$

and

$$\mathrm{tr}\left(\mathbf{A}^T\left(\Xi^{-1} + \frac{\eta_{\mathbf{m}}}{\eta_{\boldsymbol{\omega}}}\mathbf{l}\right)^2\mathbf{A}\right) \leq n_{\mathbf{u}}\left\|\Xi^{-1} + \frac{\eta_{\mathbf{m}}}{\eta_{\boldsymbol{\omega}}}\mathbf{l}\right\|^2\|\mathbf{A}\|^2. \tag{2.95}$$

From the definition of $\mathbf{l}$ in (2.38), it follows that there exists a constant $L_{\mathbf{l}} \in \mathbb{R}_{>0}$ such that

$$\|\mathbf{l}\| \leq L_{\mathbf{l}}, \tag{2.96}$$

which implies that $\mathrm{tr}\left(\mathbf{l}^2\right) \leq n_{\mathbf{u}}L_{\mathbf{l}}^2$. Moreover, from the definition of $\mathbf{A}$ in (2.21) and from $\|\dot{\hat{\mathbf{u}}}\| \leq \eta_{\mathbf{u}}$, we have that

$$\|\mathbf{A}\| \leq \frac{\eta_{\mathbf{u}}}{\alpha_{\boldsymbol{\omega}}}. \tag{2.97}$$

Without loss of generality, we assume that ε_3 and ε_6 in Theorem 2.8 are sufficiently small such that it follows from (2.36) and (2.96) that

$$\left\|\Xi^{-1} + \frac{\eta_{\mathbf{m}}}{\eta_{\boldsymbol{\omega}}}\mathbf{l}\right\| \leq 2 \tag{2.98}$$

for all $\eta_{\mathbf{m}} \leq \eta_{\boldsymbol{\omega}}\varepsilon_3$ and all $\sigma_r \leq \varepsilon_6$. By combining the bounds in (2.91)-(2.98), we obtain

$$\dot{V}_{\mathbf{Q}}(\tilde{\mathbf{Q}}) \leq -\eta_{\mathbf{m}}V_{\mathbf{Q}}(\tilde{\mathbf{Q}}) + 4\frac{\eta_{\mathbf{u}}}{\alpha_{\boldsymbol{\omega}}}n_{\mathbf{u}}V_{\mathbf{Q}}(\tilde{\mathbf{Q}}) + \frac{32}{\eta_{\mathbf{m}}}\left(\frac{\eta_{\mathbf{u}}}{\alpha_{\boldsymbol{\omega}}}\right)^2 n_{\mathbf{u}} + 2\eta_{\mathbf{m}}\left(\frac{\eta_{\mathbf{m}}}{\eta_{\boldsymbol{\omega}}}\right)^2 n_{\mathbf{u}}L_{\mathbf{l}}^2. \tag{2.99}$$

Now, without loss of generality, we assume that ε_3 and ε_5 in Theorem 2.8 are sufficiently small such that

$$\dot{V}_{\mathbf{Q}}(\tilde{\mathbf{Q}}) \leq -\frac{\eta_{\mathbf{m}}}{2}V_{\mathbf{Q}}(\tilde{\mathbf{Q}}) + \frac{\eta_{\mathbf{m}}}{256}. \tag{2.100}$$

for all $\eta_{\mathbf{m}} \leq \eta_{\boldsymbol{\omega}}\varepsilon_3$ and all $\eta_{\mathbf{u}} \leq \alpha_{\boldsymbol{\omega}}\eta_{\mathbf{m}}$. Use of the comparison lemma Khalil (2002, Lemma 3.4) yields

$$V_{\mathbf{Q}}(\tilde{\mathbf{Q}}(t)) \leq V_{\mathbf{Q}}(\tilde{\mathbf{Q}}(0))e^{-\frac{\eta_{\mathbf{m}}}{2}t} + \frac{1}{128} \tag{2.101}$$

for all $t \geq 0$. From (2.93) and (2.101), we obtain

$$\|\tilde{\mathbf{Q}}(t)\| \leq \max\left\{\sqrt{2n_{\mathbf{u}}}\|\tilde{\mathbf{Q}}(0)\|e^{-\frac{\eta_{\mathbf{m}}}{4}t}, \frac{1}{8}\right\}, \tag{2.102}$$

which completes the proof of Lemma 2.11.

2.7.3 Proof of Lemma 2.12

From (2.17), (2.34) and (2.37), we obtain that the state equation for $\tilde{\mathbf{u}}$ is given by

$$\dot{\tilde{\mathbf{u}}} = -\lambda_{\mathbf{u}}\frac{\eta_{\mathbf{u}}\left(\alpha_{\boldsymbol{\omega}}\frac{dF}{d\mathbf{u}^T}(\hat{\mathbf{u}}) + \mathbf{D}\tilde{\mathbf{m}}\right)}{\eta_{\mathbf{u}} + \lambda_{\mathbf{u}}\left\|\alpha_{\boldsymbol{\omega}}\frac{dF}{d\mathbf{u}^T}(\hat{\mathbf{u}}) + \mathbf{D}\tilde{\mathbf{m}}\right\|}. \tag{2.103}$$

From (2.103), it follows that $\|\dot{\tilde{\mathbf{u}}}\| \leq \eta_{\mathbf{u}}$, from which we obtain that

$$\|\tilde{\mathbf{u}}(t)\| \leq \|\tilde{\mathbf{u}}(0)\| + \eta_{\mathbf{u}}t \tag{2.104}$$

for all $t \geq 0$. We define the following Lyapunov-function candidate for the $\tilde{\mathbf{u}}$-dynamics:

$$V_{\mathbf{u}}(\tilde{\mathbf{u}}) = \|\tilde{\mathbf{u}}\|^2. \tag{2.105}$$

From (2.103) and (2.105), we obtain that the time derivative of $V_{\mathbf{u}}$ is given by

$$\dot{V}_{\mathbf{u}}(\tilde{\mathbf{u}}) = -2\lambda_{\mathbf{u}}\frac{\eta_{\mathbf{u}}\left(\alpha_{\boldsymbol{\omega}}\frac{dF}{d\mathbf{u}}(\hat{\mathbf{u}})\tilde{\mathbf{u}} + \tilde{\mathbf{u}}^T\mathbf{D}\tilde{\mathbf{m}}\right)}{\eta_{\mathbf{u}} + \lambda_{\mathbf{u}}\left\|\alpha_{\boldsymbol{\omega}}\frac{dF}{d\mathbf{u}^T}(\hat{\mathbf{u}}) + \mathbf{D}\tilde{\mathbf{m}}\right\|}. \tag{2.106}$$

From Assumption 2.4, it subsequently follows that

$$\dot{V}_{\mathbf{u}}(\tilde{\mathbf{u}}) \leq -\frac{2\alpha_{\boldsymbol{\omega}}\lambda_{\mathbf{u}}\eta_{\mathbf{u}}L_{F1}\|\tilde{\mathbf{u}}\|^2}{\eta_{\mathbf{u}} + \lambda_{\mathbf{u}}\left\|\alpha_{\boldsymbol{\omega}}\frac{dF}{d\mathbf{u}^T}(\hat{\mathbf{u}}) + \mathbf{D}\tilde{\mathbf{m}}\right\|} + \frac{2\lambda_{\mathbf{u}}\eta_{\mathbf{u}}\|\tilde{\mathbf{u}}\|\|\mathbf{D}\|\|\tilde{\mathbf{m}}\|}{\eta_{\mathbf{u}} + \lambda_{\mathbf{u}}\left\|\alpha_{\boldsymbol{\omega}}\frac{dF}{d\mathbf{u}^T}(\hat{\mathbf{u}}) + \mathbf{D}\tilde{\mathbf{m}}\right\|}. \tag{2.107}$$

By applying Young's inequality and substituting $\|\mathbf{D}\| = 1$, we obtain

$$\dot{V}_{\mathbf{u}}(\tilde{\mathbf{u}}) \leq -\frac{\alpha_{\boldsymbol{\omega}}\lambda_{\mathbf{u}}\eta_{\mathbf{u}}L_{F1}\|\tilde{\mathbf{u}}\|^2}{\eta_{\mathbf{u}} + \lambda_{\mathbf{u}}\left\|\alpha_{\boldsymbol{\omega}}\frac{dF}{d\mathbf{u}^T}(\hat{\mathbf{u}}) + \mathbf{D}\tilde{\mathbf{m}}\right\|} + \frac{\lambda_{\mathbf{u}}\eta_{\mathbf{u}}\|\tilde{\mathbf{m}}\|^2}{\alpha_{\boldsymbol{\omega}}L_{F1}\left(\eta_{\mathbf{u}} + \lambda_{\mathbf{u}}\left\|\alpha_{\boldsymbol{\omega}}\frac{dF}{d\mathbf{u}^T}(\hat{\mathbf{u}}) + \mathbf{D}\tilde{\mathbf{m}}\right\|\right)}. \tag{2.108}$$

From (2.105) and (2.108), it follows that

$$\dot{V}_{\mathbf{u}}(\tilde{\mathbf{u}}) \leq -\frac{\alpha_{\boldsymbol{\omega}}\lambda_{\mathbf{u}}\eta_{\mathbf{u}}L_{F1}V_{\mathbf{u}}(\tilde{\mathbf{u}})}{2\left(\eta_{\mathbf{u}} + \lambda_{\mathbf{u}}\left\|\alpha_{\boldsymbol{\omega}}\frac{dF}{d\mathbf{u}^T}(\hat{\mathbf{u}}) + \mathbf{D}\tilde{\mathbf{m}}\right\|\right)} \tag{2.109}$$

if $V_{\mathbf{u}}(\tilde{\mathbf{u}}) \geq \frac{2}{\alpha_{\boldsymbol{\omega}}^2 L_{F1}^2}\|\tilde{\mathbf{m}}\|^2$. From Assumption 2.4, (2.105) and (2.109), we obtain that

$$\dot{V}_{\mathbf{u}}(\tilde{\mathbf{u}}) \leq -\frac{\alpha_{\boldsymbol{\omega}}\lambda_{\mathbf{u}}\eta_{\mathbf{u}}L_{F1}V_{\mathbf{u}}(\tilde{\mathbf{u}})}{2\left(\eta_{\mathbf{u}} + \alpha_{\boldsymbol{\omega}}\lambda_{\mathbf{u}}\left(L_{F2} + \frac{L_{F1}}{\sqrt{2}}\right)\sqrt{V_{\mathbf{u}}(\tilde{\mathbf{u}})}\right)} \tag{2.110}$$

if $V_{\mathbf{u}}(\tilde{\mathbf{u}}) \geq \frac{2}{\alpha_{\boldsymbol{\omega}}^2 L_{F1}^2}\|\tilde{\mathbf{m}}\|^2$. By using similar arguments as in the proof of Khalil (2002, Theorem 4.18), we obtain from (2.110) that

$$\sup_{t\geq t_1} V_{\mathbf{u}}(\tilde{\mathbf{u}}(t)) \leq \max\left\{V_{\mathbf{u}}(\tilde{\mathbf{u}}(t_1)), \frac{2}{\alpha_{\boldsymbol{\omega}}^2 L_{F1}^2}\sup_{t\geq t_1}\|\tilde{\mathbf{m}}(t)\|^2\right\} \tag{2.111}$$

and

$$\limsup_{t\to\infty} V_{\mathbf{u}}(\tilde{\mathbf{u}}(t)) \leq \frac{2}{\alpha_{\boldsymbol{\omega}}^2 L_{F1}^2}\limsup_{t\to\infty}\|\tilde{\mathbf{m}}(t)\|^2 \tag{2.112}$$

for any $t_1 \geq 0$, where we applied (Sontag and Wang, 1996, Lemma II.1) to obtain the limit superior in the right-hand side of (2.112). From (2.105) and (2.111), it follows that

$$\sup_{t\geq t_1}\|\tilde{\mathbf{u}}(t)\| \leq \max\left\{\|\tilde{\mathbf{u}}(t_1)\|, \frac{\sqrt{2}}{\alpha_{\boldsymbol{\omega}} L_{F1}}\sup_{t\geq t_1}\|\tilde{\mathbf{m}}(t)\|\right\}. \tag{2.113}$$

Similarly, from (2.105) and (2.112), we obtain that

$$\limsup_{t\to\infty}\|\tilde{\mathbf{u}}(t)\| \leq \frac{\sqrt{2}}{\alpha_{\boldsymbol{\omega}} L_{F1}}\limsup_{t\to\infty}\|\tilde{\mathbf{m}}(t)\|. \tag{2.114}$$

The boundedness of the solutions of $\tilde{\mathbf{u}}$ for $0 \leq t \leq t_1$ follows from (2.104) for any finite time $t_1 \geq 0$. The bounds in (2.41) and (2.42) of Lemma 2.12 follow from (2.113) and (2.114), respectively. This completes the proof of the lemma.

2.7.4 Proof of Lemma 2.13

From (2.17), (2.20), (2.32) and (2.37), we obtain that the state equation for $\tilde{\mathbf{m}}$ is given by

$$\begin{aligned}\dot{\tilde{\mathbf{m}}} = &\left(\mathbf{A} - \eta_{\mathbf{m}}\mathbf{Q}\left(\mathbf{C}^T\mathbf{C} + \sigma\mathbf{D}^T\mathbf{D}\right)\right)\tilde{\mathbf{m}} + \alpha_{\boldsymbol{\omega}}^2\mathbf{B}\left(\hat{\mathbf{w}} - \mathbf{w}\right)\\ &- \eta_{\mathbf{m}}\mathbf{Q}\mathbf{C}^T\left(\alpha_{\boldsymbol{\omega}}^2\left(\hat{v} - v\right) - z - d\right) - \alpha_{\boldsymbol{\omega}}\eta_{\mathbf{m}}\sigma_r\mathbf{Q}\mathbf{D}^T\frac{dF}{d\mathbf{u}^T}(\hat{\mathbf{u}}).\end{aligned} \tag{2.115}$$

We define the following Lyapunov-function candidate for the $\tilde{\mathbf{m}}$-dynamics:

$$V_{\mathbf{m}}(\tilde{\mathbf{m}}, \mathbf{Q}) = \tilde{\mathbf{m}}^T\mathbf{Q}^{-1}\tilde{\mathbf{m}}. \tag{2.116}$$

We note that

$$\lambda_{\min}(\mathbf{Q}^{-1})\|\tilde{\mathbf{m}}\|^2 \leq V_{\mathbf{m}}(\tilde{\mathbf{m}}, \mathbf{Q}) \leq \lambda_{\max}(\mathbf{Q}^{-1})\|\tilde{\mathbf{m}}\|^2, \tag{2.117}$$

where $\lambda_{\min}(\mathbf{Q}^{-1})$ and $\lambda_{\max}(\mathbf{Q}^{-1})$ are the smallest and largest eigenvalue of $\mathbf{Q}^{-1}$, respectively. From (2.115) and (2.33), it follows that the time derivative of $V_{\mathbf{m}}$

is given by

$$\begin{aligned}\dot{V}_{\mathbf{m}}(\tilde{\mathbf{m}},\mathbf{Q}) = &-\eta_{\mathbf{m}}\tilde{\mathbf{m}}^T\mathbf{Q}^{-1}\tilde{\mathbf{m}} - \eta_{\mathbf{m}}\tilde{\mathbf{m}}^T\left(\mathbf{C}^T\mathbf{C} + \sigma_r\mathbf{D}^T\mathbf{D}\right)\tilde{\mathbf{m}} \\ &+ 2\alpha_{\boldsymbol{\omega}}^2\tilde{\mathbf{m}}^T\mathbf{Q}^{-1}\mathbf{B}(\hat{\mathbf{w}} - \mathbf{w}) - 2\eta_{\mathbf{m}}\tilde{\mathbf{m}}^T\mathbf{C}^T(\alpha_{\boldsymbol{\omega}}^2(\hat{v} - v) - z - d) \\ &- 2\alpha_{\boldsymbol{\omega}}\eta_{\mathbf{m}}\sigma_r\tilde{\mathbf{m}}^T\mathbf{D}^T\frac{dF}{d\mathbf{u}^T}(\hat{\mathbf{u}}).\end{aligned} \tag{2.118}$$

From (2.116), (2.118) and Young's inequality, we obtain

$$\begin{aligned}\dot{V}_{\mathbf{m}}(\tilde{\mathbf{m}},\mathbf{Q}) \leq &-\frac{\eta_{\mathbf{m}}}{2}V_{\mathbf{m}}(\tilde{\mathbf{m}},\mathbf{Q}) + \frac{2\alpha_{\boldsymbol{\omega}}^4}{\eta_{\mathbf{m}}}\|\mathbf{Q}^{-1}\|\|\mathbf{B}\|^2\|\hat{\mathbf{w}} - \mathbf{w}\|^2 \\ &+ 3\alpha_{\boldsymbol{\omega}}^4\eta_{\mathbf{m}}|\hat{v} - v|^2 + 3\eta_{\mathbf{m}}|z|^2 + 3\eta_{\mathbf{m}}|d|^2 + \alpha_{\boldsymbol{\omega}}^2\eta_{\mathbf{m}}\sigma_r\left\|\frac{dF}{d\mathbf{u}}(\hat{\mathbf{u}})\right\|^2.\end{aligned} \tag{2.119}$$

From Assumption 2.4 and (2.22)-(2.24), we have

$$\|\hat{\mathbf{w}} - \mathbf{w}\| \leq \frac{1}{\alpha_{\boldsymbol{\omega}}}\left(L_{\mathbf{H}} + L_{F2}\right)\|\dot{\hat{\mathbf{u}}}\|. \tag{2.120}$$

From the definition of $\boldsymbol{\omega}$ in (2.16), it follows that there exists a constant $L_{\boldsymbol{\omega}1} \in \mathbb{R}_{>0}$ such that

$$\|\boldsymbol{\omega}\| \leq L_{\boldsymbol{\omega}1}. \tag{2.121}$$

From Assumption 2.4, (2.22)-(2.24 and (2.121), we obtain

$$|\hat{v} - v| \leq \frac{1}{2}\left(L_{\mathbf{H}} + L_{F2}\right)L_{\boldsymbol{\omega}1}^2. \tag{2.122}$$

Furthermore, to obtain a bound on $|z|$, from (2.22), we have

$$\begin{aligned}|z| \leq &\left|\int_0^1\left(\frac{\partial h}{\partial \mathbf{x}}(\sigma\tilde{\mathbf{x}} + \mathbf{X}(\mathbf{u}),\mathbf{u}) - \frac{\partial h}{\partial \mathbf{x}}(\mathbf{X}(\mathbf{u}),\mathbf{u})\right)d\sigma\tilde{\mathbf{x}}\right| \\ &+ \left|\left(\frac{\partial h}{\partial \mathbf{x}}(\mathbf{X}(\mathbf{u}),\mathbf{u}) - \frac{\partial h}{\partial \mathbf{x}}(\mathbf{X}(\mathbf{u}^*),\mathbf{u}^*)\right)\tilde{\mathbf{x}}\right| + \left|\frac{\partial h}{\partial \mathbf{x}}(\mathbf{X}(\mathbf{u}^*),\mathbf{u}^*)\tilde{\mathbf{x}}\right|\end{aligned} \tag{2.123}$$

From Assumption 2.1, it follows that

$$\left\|\frac{\partial h}{\partial \mathbf{x}}(\mathbf{x}_1,\mathbf{u}_1) - \frac{\partial h}{\partial \mathbf{x}}(\mathbf{x}_2,\mathbf{u}_2)\right\| \leq L_{h\mathbf{x}}\|\mathbf{x}_1 - \mathbf{x}_2\| + L_{h\mathbf{u}}\|\mathbf{u}_1 - \mathbf{u}_2\| \tag{2.124}$$

for all $\mathbf{x}_1, \mathbf{x}_2 \in \mathbb{R}^{n_{\mathbf{x}}}$ and all $\mathbf{u}_1, \mathbf{u}_2 \in \mathbb{R}^{n_{\mathbf{u}}}$. By applying the bound in (2.124) to (2.123), we obtain

$$|z| \leq \frac{L_{h\mathbf{x}}}{2}\|\tilde{\mathbf{x}}\|^2 + L_{h\mathbf{x}}\|\mathbf{X}(\mathbf{u}) - \mathbf{X}(\mathbf{u}^*)\|\|\tilde{\mathbf{x}}\| + L_{h\mathbf{u}}\|\mathbf{u} - \mathbf{u}^*\|\|\tilde{\mathbf{x}}\| + L_{h*}\|\tilde{\mathbf{x}}\|, \tag{2.125}$$

with $L_{h*} = \|\frac{\partial h}{\partial \mathbf{x}}(\mathbf{X}(\mathbf{u}^*),\mathbf{u}^*)\|$. Subsequently, from Assumption 2.2, it follows that

$$|z| \leq \frac{L_{h\mathbf{x}}}{2}\|\tilde{\mathbf{x}}\|^2 + (L_{h\mathbf{x}}L_{\mathbf{X}} + L_{h\mathbf{u}})\|\mathbf{u} - \mathbf{u}^*\|\|\tilde{\mathbf{x}}\| + L_{h*}\|\tilde{\mathbf{x}}\|. \tag{2.126}$$

From (2.15), (2.37) and (2.121), we have

$$\|\mathbf{u}-\mathbf{u}^*\| \leq \|\tilde{\mathbf{u}}\| + \alpha_{\boldsymbol{\omega}} L_{\boldsymbol{\omega}1}. \tag{2.127}$$

By substituting (2.127) in (2.126), we obtain the following bound on $|z|$:

$$\begin{aligned} |z| \leq \frac{L_{h\mathbf{x}}}{2}\|\tilde{\mathbf{x}}\|^2 + (L_{h\mathbf{x}}L_{\mathbf{X}} + L_{h\mathbf{u}})\|\tilde{\mathbf{u}}\|\|\tilde{\mathbf{x}}\| \\ + \alpha_{\boldsymbol{\omega}}(L_{h\mathbf{x}}L_{\mathbf{X}} + L_{h\mathbf{u}})L_{\boldsymbol{\omega}1}\|\tilde{\mathbf{x}}\| + L_{h*}\|\tilde{\mathbf{x}}\|. \end{aligned} \tag{2.128}$$

From Assumption 2.4, it follows that

$$\left\| \frac{dF}{d\mathbf{u}}(\hat{\mathbf{u}}) \right\| \leq L_{F2}\|\tilde{\mathbf{u}}\|. \tag{2.129}$$

Moreover, from Assumption 2.5, (2.15), (2.37), (2.121) and (2.37), we have

$$|d| \leq \delta_{\mathbf{n}} + \delta_{\mathbf{x}}\|\tilde{\mathbf{x}}\| + \delta_{\mathbf{u}}\|\tilde{\mathbf{u}}\| + \alpha_{\boldsymbol{\omega}}\delta_{\mathbf{u}}L_{\boldsymbol{\omega}1} \tag{2.130}$$

By combining (2.119), (2.120), (2.122), (2.128)-(2.130) and $\|\mathbf{B}\| = 1$, we obtain

$$\begin{aligned} \dot{V}_{\mathbf{m}}(\tilde{\mathbf{m}},\mathbf{Q}) \leq -\frac{\eta_{\mathbf{m}}}{2}V_{\mathbf{m}}(\tilde{\mathbf{m}},\mathbf{Q}) + \frac{2\alpha_{\boldsymbol{\omega}}^2}{\eta_{\mathbf{m}}}\|\mathbf{Q}^{-1}\|\left(L_{\mathbf{H}}+L_{F2}\right)^2\|\dot{\hat{\mathbf{u}}}\|^2 \\ + \frac{3}{4}\alpha_{\boldsymbol{\omega}}^4\eta_{\mathbf{m}}\left(L_{\mathbf{H}}+L_{F2}\right)^2 L_{\boldsymbol{\omega}1}^4 + 3\eta_{\mathbf{m}}(\delta_{\mathbf{n}} + \delta_{\mathbf{x}}\|\tilde{\mathbf{x}}\| + \delta_{\mathbf{u}}\|\tilde{\mathbf{u}}\| \\ + \alpha_{\boldsymbol{\omega}}\delta_{\mathbf{u}}L_{\boldsymbol{\omega}1})^2 + 3\eta_{\mathbf{m}}\bigg(\frac{L_{h\mathbf{x}}}{2}\|\tilde{\mathbf{x}}\|^2 + (L_{h\mathbf{x}}L_{\mathbf{X}} + L_{h\mathbf{u}})\|\tilde{\mathbf{u}}\|\|\tilde{\mathbf{x}}\| \\ + \alpha_{\boldsymbol{\omega}}(L_{h\mathbf{x}}L_{\mathbf{X}} + L_{h\mathbf{u}})L_{\boldsymbol{\omega}1}\|\tilde{\mathbf{x}}\| + L_{h*}\|\tilde{\mathbf{x}}\|\bigg)^2 + \alpha_{\boldsymbol{\omega}}^2\eta_{\mathbf{m}}\sigma_r L_{F2}^2\|\tilde{\mathbf{u}}\|^2. \end{aligned} \tag{2.131}$$

From Lemmas 2.10 and 2.12, it follows that, for any finite time $t_1 \geq 0$, the solutions of $\tilde{\mathbf{x}}$ and $\tilde{\mathbf{u}}$ are bounded for all $0 \leq t \leq t_1$. Moreover, from the proof of Lemma 2.11 in Section 2.7.2, we have that $\mathbf{Q}^{-1}(t)$ is positive definite and bounded for all $0 \leq t \leq t_1$. From this and $\|\dot{\mathbf{u}}\| \leq \eta_{\mathbf{u}}$ (see (2.34)), we obtain that the right-hand side of (2.131) is bounded for all $0 \leq t \leq t_1$. Therefore, by applying the comparison lemma Khalil (2002, Lemma 3.4), we obtain that $V_{\mathbf{m}}(\tilde{\mathbf{m}}(\mathbf{t}),\mathbf{Q}(t))$ is bounded for all $0 \leq t \leq t_1$. Subsequently, because $V_{\mathbf{m}}(\tilde{\mathbf{m}}(t),\mathbf{Q}(t))$ is bounded for $0 \leq t \leq t_1$ and $\mathbf{Q}^{-1}(t)$ is positive definite and bounded for all $0 \leq t \leq t_1$, it follows from (2.117) that the solutions of $\tilde{\mathbf{m}}$ are bounded for all $0 \leq t \leq t_1$. Further details regarding the boundedness of $\tilde{\mathbf{m}}(t)$ for $0 \leq t \leq t_1$ are left to the reader.

Let us define $t_1 \geq 0$ such that

$$\|\tilde{\mathbf{x}}(t)\| \alpha_{\boldsymbol{\omega}}\eta_{\boldsymbol{\omega}}c_{\mathbf{x}2}, \qquad \|\tilde{\mathbf{Q}}(t)\| \leq \frac{1}{8} \tag{2.132}$$

for all $t \geq t_1$. The existence of a finite time $t_1 \geq 0$ such that (2.132) holds follows from Lemmas 2.10 and 2.11. Now, from (2.37) and the bound on $\mathbf{l}$ in (2.96) in the proof of Lemma 2.11, it follows that

$$\left\|\mathbf{Q}^{-1} - \boldsymbol{\Xi}^{-1}\right\| \leq \|\tilde{\mathbf{Q}}(t)\| + \frac{\eta_{\mathbf{m}}}{\eta_{\boldsymbol{\omega}}} L_{\mathbf{l}}. \tag{2.133}$$

Without loss of generality, we assume that ε_3 and ε_6 in Theorem 2.8 are sufficiently small such that we obtain from (2.36), Lemma 2.11 and (2.133) that

$$\frac{1}{4}\mathbf{I} \preceq \mathbf{Q}^{-1} \preceq \frac{5}{4}\mathbf{I} \tag{2.134}$$

for all $t \geq t_1$, all $\eta_{\mathbf{m}} \leq \eta_{\boldsymbol{\omega}}\varepsilon_3$ and all $\sigma_r \leq \varepsilon_6$. From (2.117) and (2.134), it follows that

$$\frac{1}{4}\|\tilde{\mathbf{m}}\|^2 \leq V_{\mathbf{m}}(\tilde{\mathbf{m}}, \mathbf{Q}) \leq \frac{5}{4}\|\tilde{\mathbf{m}}\|^2 \tag{2.135}$$

for all $t \geq t_1$. Moreover, from (2.134), we have

$$\|\mathbf{Q}^{-1}\| \leq \frac{5}{4} \tag{2.136}$$

for all $t \geq t_1$. From (2.17), (2.34), (2.37) and $\|\mathbf{D}\| = 1$, it follows that

$$\|\dot{\hat{\mathbf{u}}}\| \leq \lambda_{\mathbf{u}}\|\mathbf{D}\hat{\mathbf{m}}\| \leq \lambda_{\mathbf{u}}\left(\alpha_{\boldsymbol{\omega}}\left\|\frac{dF}{d\mathbf{u}}(\hat{\mathbf{u}})\right\| + \|\tilde{\mathbf{m}}\|\right). \tag{2.137}$$

Subsequently, from (2.137) and Assumption 2.4, we obtain

$$\|\dot{\hat{\mathbf{u}}}\| \leq \lambda_{\mathbf{u}}\left(\alpha_{\boldsymbol{\omega}} L_{F2}\|\tilde{\mathbf{u}}\| + \|\tilde{\mathbf{m}}\|\right). \tag{2.138}$$

From (2.135) and (2.138), it follows that

$$\|\dot{\hat{\mathbf{u}}}\|^2 \leq 8\lambda_{\mathbf{u}}^2 V_{\mathbf{m}}(\tilde{\mathbf{m}}, \mathbf{Q}) + 2\alpha_{\boldsymbol{\omega}}^2\lambda_{\mathbf{u}}^2 L_{F2}^2\|\tilde{\mathbf{u}}\|^2 \tag{2.139}$$

for all $t_1 \geq 0$. Without loss of generality, we assume that ε_2 and ε_4 in Theorem 2.8 are sufficiently small such that we obtain from (2.131), (2.132), (2.136) and (2.139) that

$$\begin{aligned}
\dot{V}_{\mathbf{m}}(\tilde{\mathbf{m}}, \mathbf{Q}) \leq\ & -\frac{\eta_{\mathbf{m}}}{4} V_{\mathbf{m}}(\tilde{\mathbf{m}}, \mathbf{Q}) + 5\frac{\alpha_{\boldsymbol{\omega}}^4\lambda_{\mathbf{u}}^2}{\eta_{\mathbf{m}}}\left(L_{\mathbf{H}} + L_{F2}\right)^2 L_{F2}^2\|\tilde{\mathbf{u}}\|^2 \\
& + \frac{3}{2}\alpha_{\boldsymbol{\omega}}^4\eta_{\mathbf{m}}\left(L_{\mathbf{H}} + L_{F2}\right)^2 L_{\boldsymbol{\omega}1}^4 + 12\eta_{\mathbf{m}}\delta_{\mathbf{n}}^2 + 12\alpha_{\boldsymbol{\omega}}^2\eta_{\boldsymbol{\omega}}^2\eta_{\mathbf{m}}\delta_{\mathbf{x}}^2 c_{\mathbf{x}2}^2 \\
& + 12\alpha_{\boldsymbol{\omega}}^2\eta_{\mathbf{m}}\delta_{\mathbf{u}}^2 L_{\boldsymbol{\omega}1}^2 + 12\alpha_{\boldsymbol{\omega}}^2\eta_{\boldsymbol{\omega}}^2\eta_{\mathbf{m}}(L_{h\mathbf{x}}L_{\mathbf{X}} + L_{h\mathbf{u}})^2 c_{\mathbf{x}2}^2\|\tilde{\mathbf{u}}\|^2 \\
& + 12\eta_{\mathbf{m}}\delta_{\mathbf{u}}^2\|\tilde{\mathbf{u}}\|^2 + 12\alpha_{\boldsymbol{\omega}}^2\eta_{\boldsymbol{\omega}}^2\eta_{\mathbf{m}}L_{h*}^2 c_{\mathbf{x}2}^2 + \alpha_{\boldsymbol{\omega}}^2\eta_{\mathbf{m}}\sigma_r L_{F2}^2\|\tilde{\mathbf{u}}\|^2.
\end{aligned} \tag{2.140}$$

for all $t \geq t_1$, all $\eta_{\boldsymbol{\omega}} \leq \varepsilon_2$ and all $\alpha_{\boldsymbol{\omega}}\lambda_{\mathbf{u}} \leq \eta_{\mathbf{m}}\varepsilon_4$. From the comparison lemma (Khalil, 2002, Lemma 3.4) and (2.140), we obtain

$$\begin{aligned}\sup_{t\geq t_1} V_{\mathbf{m}}(\tilde{\mathbf{m}}(t), \mathbf{Q}(t)) \leq 10 \sup_{t\geq t_1} \max\Big\{ & V_{\mathbf{m}}(\tilde{\mathbf{m}}(t_1), \mathbf{Q}(t_1)), 6\alpha_{\boldsymbol{\omega}}^4 \left(L_{\mathbf{H}} + L_{F2}\right)^2 L_{\boldsymbol{\omega}1}^4, \\ & 48\alpha_{\boldsymbol{\omega}}^2\eta_{\boldsymbol{\omega}}^2 L_{h*}^2 c_{\mathbf{x}2}^2, 48\alpha_{\boldsymbol{\omega}}^2\eta_{\boldsymbol{\omega}}^2 (L_{h\mathbf{x}}L_{\mathbf{X}} + L_{h\mathbf{u}})^2 c_{\mathbf{x}2}^2 \|\tilde{\mathbf{u}}(t)\|^2, \\ & 20\frac{\alpha_{\boldsymbol{\omega}}^4\lambda_{\mathbf{u}}^2}{\eta_{\mathbf{m}}^2} \left(L_{\mathbf{H}} + L_{F2}\right)^2 L_{F2}^2 \|\tilde{\mathbf{u}}(t)\|^2, 4\alpha_{\boldsymbol{\omega}}^2\sigma_r L_{F2}^2 \|\tilde{\mathbf{u}}(t)\|^2, \\ & 48\delta_{\mathbf{n}}^2, 48\alpha_{\boldsymbol{\omega}}^2\eta_{\boldsymbol{\omega}}^2\delta_{\mathbf{x}}^2 c_{\mathbf{x}2}^2, 48\alpha_{\boldsymbol{\omega}}^2\delta_{\mathbf{u}}^2 L_{\boldsymbol{\omega}1}^2, 48\delta_{\mathbf{u}}^2 \|\tilde{\mathbf{u}}(t)\|^2 \Big\}\end{aligned} \tag{2.141}$$

and

$$\begin{aligned}\limsup_{t\to\infty} V_{\mathbf{m}}(\tilde{\mathbf{m}}(t), \mathbf{Q}(t)) \leq 10 \limsup_{t\to\infty} \max\Big\{ & 6\alpha_{\boldsymbol{\omega}}^4 \left(L_{\mathbf{H}} + L_{F2}\right)^2 L_{\boldsymbol{\omega}1}^4, \\ & 48\alpha_{\boldsymbol{\omega}}^2\eta_{\boldsymbol{\omega}}^2 L_{h*}^2 c_{\mathbf{x}2}^2, 48\alpha_{\boldsymbol{\omega}}^2\eta_{\boldsymbol{\omega}}^2 (L_{h\mathbf{x}}L_{\mathbf{X}} + L_{h\mathbf{u}})^2 c_{\mathbf{x}2}^2 \|\tilde{\mathbf{u}}(t)\|^2, \\ & 20\frac{\alpha_{\boldsymbol{\omega}}^4\lambda_{\mathbf{u}}^2}{\eta_{\mathbf{m}}^2} \left(L_{\mathbf{H}} + L_{F2}\right)^2 L_{F2}^2 \|\tilde{\mathbf{u}}(t)\|^2, 4\alpha_{\boldsymbol{\omega}}^2\sigma_r L_{F2}^2 \|\tilde{\mathbf{u}}(t)\|^2, \\ & 48\delta_{\mathbf{n}}^2, 48\alpha_{\boldsymbol{\omega}}^2\eta_{\boldsymbol{\omega}}^2\delta_{\mathbf{x}}^2 c_{\mathbf{x}2}^2, 48\alpha_{\boldsymbol{\omega}}^2\delta_{\mathbf{u}}^2 L_{\boldsymbol{\omega}1}^2, 48\delta_{\mathbf{u}}^2 \|\tilde{\mathbf{u}}(t)\|^2 \Big\},\end{aligned} \tag{2.142}$$

where we applied Sontag and Wang (1996, Lemma II.1) to obtain the limit superior in the right-hand side of (2.142). From (2.135) and (2.141), it follows that

$$\begin{aligned}\sup_{t\geq t_1} \|\tilde{\mathbf{m}}(t)\| \leq 2\sqrt{10} \sup_{t\geq t_1} \max\Big\{ & \frac{\sqrt{5}}{2}\|\tilde{\mathbf{m}}(t_1)\|, \sqrt{6}\alpha_{\boldsymbol{\omega}}^2 \left(L_{\mathbf{H}} + L_{F2}\right) L_{\boldsymbol{\omega}1}^2, \\ & 4\sqrt{3}\alpha_{\boldsymbol{\omega}}\eta_{\boldsymbol{\omega}} L_{h*} c_{\mathbf{x}2}, 4\sqrt{3}\alpha_{\boldsymbol{\omega}}\eta_{\boldsymbol{\omega}} (L_{h\mathbf{x}}L_{\mathbf{X}} + L_{h\mathbf{u}}) c_{\mathbf{x}2} \|\tilde{\mathbf{u}}(t)\|, \\ & 2\sqrt{5}\frac{\alpha_{\boldsymbol{\omega}}^2\lambda_{\mathbf{u}}}{\eta_{\mathbf{m}}} \left(L_{\mathbf{H}} + L_{F2}\right) L_{F2} \|\tilde{\mathbf{u}}(t)\|, 2\alpha_{\boldsymbol{\omega}}\sqrt{\sigma_r} L_{F2} \|\tilde{\mathbf{u}}(t)\|, \\ & 4\sqrt{3}\delta_{\mathbf{n}}, 4\sqrt{3}\alpha_{\boldsymbol{\omega}}\eta_{\boldsymbol{\omega}}\delta_{\mathbf{x}} c_{\mathbf{x}2}, 4\sqrt{3}\alpha_{\boldsymbol{\omega}}\delta_{\mathbf{u}} L_{\boldsymbol{\omega}1}, 4\sqrt{3}\delta_{\mathbf{u}} \|\tilde{\mathbf{u}}(t)\| \Big\}.\end{aligned} \tag{2.143}$$

Similarly, from (2.135) and (2.141), we obtain

$$\begin{aligned}\limsup_{t\to\infty} \|\tilde{\mathbf{m}}(t)\| \leq 2\sqrt{10} \limsup_{t\to\infty} \max\Big\{ & \sqrt{6}\alpha_{\boldsymbol{\omega}}^2 \left(L_{\mathbf{H}} + L_{F2}\right) L_{\boldsymbol{\omega}1}^2, \\ & 4\sqrt{3}\alpha_{\boldsymbol{\omega}}\eta_{\boldsymbol{\omega}} L_{h*} c_{\mathbf{x}2}, 4\sqrt{3}\alpha_{\boldsymbol{\omega}}\eta_{\boldsymbol{\omega}} (L_{h\mathbf{x}}L_{\mathbf{X}} + L_{h\mathbf{u}}) c_{\mathbf{x}2} \|\tilde{\mathbf{u}}(t)\|, \\ & 2\sqrt{5}\frac{\alpha_{\boldsymbol{\omega}}^2\lambda_{\mathbf{u}}}{\eta_{\mathbf{m}}} \left(L_{\mathbf{H}} + L_{F2}\right) L_{F2} \|\tilde{\mathbf{u}}(t)\|, 2\alpha_{\boldsymbol{\omega}}\sqrt{\sigma_r} L_{F2} \|\tilde{\mathbf{u}}(t)\|, \\ & 4\sqrt{3}\delta_{\mathbf{n}}, 4\sqrt{3}\alpha_{\boldsymbol{\omega}}\eta_{\boldsymbol{\omega}}\delta_{\mathbf{x}} c_{\mathbf{x}2}, 4\sqrt{3}\alpha_{\boldsymbol{\omega}}\delta_{\mathbf{u}} L_{\boldsymbol{\omega}1}, 4\sqrt{3}\delta_{\mathbf{u}} \|\tilde{\mathbf{u}}(t)\| \Big\}.\end{aligned} \tag{2.144}$$

The bounds in (2.43) and (2.44) of Lemma 2.13 follow from (2.143) and (2.144), respectively. This completes the proof of the lemma.

Chapter 3

A sampled-data extremum-seeking control approach using a least-squares observer

Although many extremum-seeking control methods assume that the measurements of the performance indicators and the update of the plant parameters are continuous in time, the performance-indicator measurements are often sampled and the plant parameters are updated in a discrete-time fashion in many practical applications. A discrete-time version of the extremum-seeking controller in Chapter 2 is presented to optimize the steady-state plant performance in a sampled-data setting. We show that the discrete-time controller is equivalent to the continuous-time controller in Chapter 2 for the limit as the sampling time approaches zero. A simulation example displays that the response of the discrete-time controller resembles the response of the continuous-time controller in Chapter 2 for sufficiently high sampling rates.

3.1 Introduction

The majority of extremum-seeking control methods are designed to operate in continuous time: the measurements of the performance indicators are assumed to be available for any given time, while the plant-parameter values are continuously updated; see for example Krstić and Wang (2000); Nešić et al. (2013a); Pan et al. (2003); Tsien and Serdengecti (1955). In practice, however, the performance-indicator measurements are commonly sampled and the plant-parameter values are updated at a finite rate. Although a combination of continuous-time extremum-seeking control methods and numerical integration methods (for example, Euler or Runge-Kutta methods) can be used to optimize the steady-state plant performance in a sampled-data setting (Mohammadi et al., 2014), it is often computationally more efficient to apply discrete-time extremum-seeking control methods.

We make the distinction between three types of discrete-time extremum-seeking control methods. The first type of discrete-time extremum-seeking control methods are methods for which the sampling time is generally large.

By choosing a sufficiently large sampling time and keeping the plant-parameter values constant between samples, the transient response of the plant dynamics has almost died out at the time a new sample is taken so that the measured performance of the plant is approximately equal to its constant steady-state value. Hence, the relation between the plant parameters and the measured plant performance can be treated as a quasistatic function which can be optimized by a variety of derivative-free numerical methods (Khong et al., 2013b; Popović et al., 2003; Teel and Popović, 2001; Zhang and Ordóñez, 2012).

The second type of discrete-time extremum-seeking control methods are gray-box methods that use autoregressive models to identify the plant and subsequently optimize its steady-state performance (Bamberger and Isermann, 1978; Fabri et al., 2015; Golden and Ydstie, 1989).

The third type of discrete-time extremum-seeking control methods use a discrete-time update law to compute a new plant-parameter value at each sampling instance (Choi et al., 2002; Guay, 2014; Ryan and Speyer, 2010; Stanković and Stipanović, 2010). Discrete-time extremum-seeking control methods of this type are most similar to continuous-time extremum-seeking control methods. Many of these methods can be regarded as discrete-time versions of their continuous-time counterparts; see for example Choi et al. (2002)/Krstić (2000) and Guay (2014)/Guay and Dochain (2015).

In this chapter, we present a discrete-time extremum-seeking controller of the third type. The controller is a discrete-time equivalent of the continuous-time extremum-seeking controller in Chapter 2. The discrete-time extremum-seeking controller in this chapter optimizes the performance of a general nonlinear plant with an arbitrary number of plant parameters in a sampled-data setting. The discrete-time controller is equivalent to the continuous-time controller in Chapter 2 for the limit as the sampling time approaches zero. A simulation example displays that the responses of the continuous-time controller in Chapter 2 and the discrete-time controller in this chapter are comparable for sufficiently high sampling rates.

The sampled-data extremum-seeking control problem is formulated in in Section 3.2. We present our discrete-time extremum-seeking controller in Section 3.3. In Section 3.4, we investigate the relation between the discrete-time controller and the continuous-time controller in Chapter 2. The simulation example is given Sections 3.5. This chapter is concluded in Section 3.6.

3.2 Extremum-seeking problem formulation

Consider the following multi-input-multi-output nonlinear plant:

$$\begin{aligned} \dot{\mathbf{x}}(t) &= \mathbf{f}(\mathbf{x}(t), \mathbf{u}(t)) \\ \mathbf{e}(t) &= \mathbf{g}(\mathbf{x}(t), \mathbf{u}(t)) + \mathbf{n}(t), \end{aligned} \tag{3.1}$$

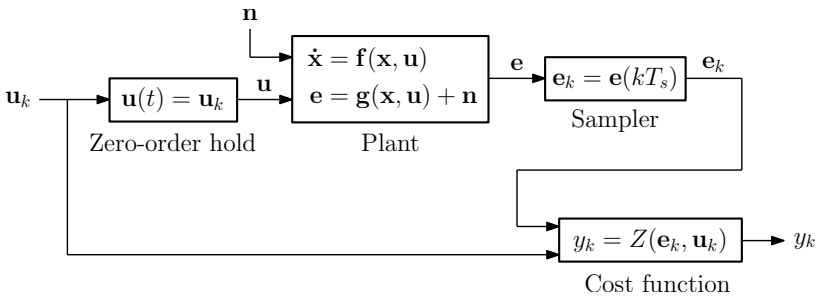

Figure 3.1: Sampled-data plant and cost function.

with state $\mathbf{x} \in \mathbb{R}^{n_\mathbf{x}}$, input $\mathbf{u} \in \mathbb{R}^{n_\mathbf{u}}$, output $\mathbf{e} \in \mathbb{R}^{n_\mathbf{e}}$ and disturbance $\mathbf{n} \in \mathbb{R}^{n_\mathbf{e}}$, where $n_\mathbf{x}, n_\mathbf{u}, n_\mathbf{e} \in \mathbb{N}_{>0}$ are the corresponding dimensions and $t \in \mathbb{R}_{\geq 0}$ is the time. The input $\mathbf{u}$ is a vector of tunable plant parameters and the output $\mathbf{e}$ is a vector of performance indicators. The state $\mathbf{x}$, the disturbance $\mathbf{n}$ and the functions $\mathbf{f}$ and $\mathbf{g}$ are unknown, which implies that the relation between the input and the output of the plant is unknown. The output $\mathbf{e}$ is sampled with a fixed sampling time $T_s \in \mathbb{R}_{>0}$. The kth sample is denoted by $\mathbf{e}_k = \mathbf{e}(kT_s)$ for $k \in \mathbb{N}$. The output sample $\mathbf{e}_k$ is used to compute a new input $\mathbf{u}_{k+1}$. The input $\mathbf{u}_{k+1}$ is subsequently fed to the plant using a zero-order hold such that $\mathbf{u}(t) = \mathbf{u}_{k+1}$ for all $t \in (kT_s, (k+1)T_s]$. For simplicity, we assume that the computation time of $\mathbf{u}_{k+1}$ is negligibly short compared to the sampling time. Note that $t = (k+1)T_s$ is the last (and not the first) time instance that $\mathbf{u}(t)$ is equal to $\mathbf{u}_{k+1}$.

A cost function Z is designed that quantifies the performance of the plant given any plant parameters $\mathbf{u}_k$ and any performance-indicator measurements $\mathbf{e}_k$. The corresponding measured plant performance $y(t)$ at time $t = kT_s$ is denoted by

$$y_k = Z(\mathbf{e}_k, \mathbf{u}_k). \tag{3.2}$$

The sampled-data plant and the cost function are illustrated in Figure 3.1. With some abuse of notation, we write the sampled-data plant and the cost function as one extended plant

$$\begin{aligned} \dot{\mathbf{x}}(t) &= \mathbf{f}(\mathbf{x}(t), \mathbf{u}(t)) \\ y_k &= h(\mathbf{x}_k, \mathbf{u}_k) + d_k, \end{aligned} \tag{3.3}$$

with $\mathbf{x}_k = \mathbf{x}(kT_s)$, $h(\mathbf{x}_k, \mathbf{u}_k) = Z(\mathbf{g}(\mathbf{x}_k, \mathbf{u}_k), \mathbf{u}_k)$, $d_k = Z(\mathbf{g}(\mathbf{x}_k, \mathbf{u}_k) + \mathbf{n}_k, \mathbf{u}_k) - Z(\mathbf{g}(\mathbf{x}_k, \mathbf{u}_k), \mathbf{u}_k)$ and $\mathbf{n}_k = \mathbf{n}(kT_s)$. We note that the function h and the disturbance d are unknown because $\mathbf{g}$, $\mathbf{x}$ and $\mathbf{n}$ are unknown. We assume the following.

Assumption 3.1. *The functions $\mathbf{f} : \mathbb{R}^{n_\mathbf{x}} \times \mathbb{R}^{n_\mathbf{u}} \to \mathbb{R}^{n_\mathbf{x}}$ and $h : \mathbb{R}^{n_\mathbf{x}} \times \mathbb{R}^{n_\mathbf{u}} \to \mathbb{R}$ in (3.3) are twice continuously differentiable. Moreover, there exist constants $L_{\mathbf{fx}}, L_{\mathbf{fu}}, L_{h\mathbf{x}}, L_{h\mathbf{u}} \in \mathbb{R}_{>0}$ such that*

$$\left\| \frac{\partial \mathbf{f}}{\partial \mathbf{x}}(\mathbf{x}, \mathbf{u}) \right\| \leq L_{\mathbf{fx}}, \qquad \left\| \frac{\partial \mathbf{f}}{\partial \mathbf{u}}(\mathbf{x}, \mathbf{u}) \right\| \leq L_{\mathbf{fu}}, \tag{3.4}$$

$$\left\| \frac{\partial^2 h}{\partial \mathbf{x} \partial \mathbf{x}^T}(\mathbf{x}, \mathbf{u}) \right\| \leq L_{h\mathbf{x}}, \qquad \left\| \frac{\partial^2 h}{\partial \mathbf{x} \partial \mathbf{u}^T}(\mathbf{x}, \mathbf{u}) \right\| \leq L_{h\mathbf{u}} \tag{3.5}$$

for all $\mathbf{x} \in \mathbb{R}^{n_\mathbf{x}}$ *and all* $\mathbf{u} \in \mathbb{R}^{n_\mathbf{u}}$.

Moreover, we assume that there exists a constant steady-state solution of the state $\mathbf{x}$ of the plant dynamics, denoted by $\mathbf{X}(\mathbf{u})$, for each constant vector of plant parameters $\mathbf{u} \in \mathbb{R}^{n_\mathbf{u}}$.

Assumption 3.2. *There exists a twice continuously differentiable map* $\mathbf{X} : \mathbb{R}^{n_\mathbf{u}} \to \mathbb{R}^{n_\mathbf{x}}$ *and a constant* $L_\mathbf{X} \in \mathbb{R}_{>0}$*, such that*

$$\mathbf{0} = \mathbf{f}(\mathbf{X}(\mathbf{u}), \mathbf{u}), \qquad \left\| \frac{d\mathbf{X}}{d\mathbf{u}}(\mathbf{u}) \right\| \leq L_\mathbf{X} \tag{3.6}$$

for all $\mathbf{u} \in \mathbb{R}^{n_\mathbf{u}}$.

In addition, we assume that the steady-state solution $\mathbf{X}(\mathbf{u})$ is globally exponentially stable for each constant vector of plant parameters $\mathbf{u} \in \mathbb{R}^{n_\mathbf{u}}$.

Assumption 3.3. *There exist constants* $\mu_\mathbf{x}, \nu_\mathbf{x} \in \mathbb{R}_{>0}$*, such that for each constant* $\mathbf{u} \in \mathbb{R}^{n_\mathbf{u}}$*, the solutions of the dynamics in (3.3) satisfy*

$$\|\tilde{\mathbf{x}}(t)\| \leq \mu_\mathbf{x} \|\tilde{\mathbf{x}}(t_0)\| e^{-\nu_\mathbf{x}(t-t_0)}, \tag{3.7}$$

for all $\mathbf{x}(t_0) \in \mathbb{R}^{n_\mathbf{x}}$ *and all* $t \geq t_0 \geq 0$*, with* $\tilde{\mathbf{x}}(t) = \mathbf{x}(t) - \mathbf{X}(\mathbf{u})$.

The disturbance-free steady-state relation between constant plant parameters $\mathbf{u}$ and the plant-performance is given by

$$F(\mathbf{u}) = h(\mathbf{X}(\mathbf{u}), \mathbf{u}) = Z(\mathbf{g}(\mathbf{X}(\mathbf{u}), \mathbf{u}), \mathbf{u}). \tag{3.8}$$

We refer to F as the objective function. We assume that the cost function is designed such that the objective function exhibits a unique minimum on the domain $\mathbb{R}^{n_\mathbf{u}}$, where the minimum of the objective function relates to the optimal steady-state plant performance.

Assumption 3.4. *The objective function* $F : \mathbb{R}^{n_\mathbf{u}} \to \mathbb{R}$ *is twice continuously differentiable and exhibits a unique minimum on the domain* $\mathbb{R}^{n_\mathbf{u}}$*. Let the corresponding minimizer be denoted by* $\mathbf{u}^* = \arg\min_{\mathbf{u} \in \mathbb{R}^{n_\mathbf{u}}} F(\mathbf{u})$*. There exist constants* $L_{F1}, L_{F2} \in \mathbb{R}_{>0}$ *such that*

$$\frac{dF}{d\mathbf{u}}(\mathbf{u})(\mathbf{u} - \mathbf{u}^*) \geq L_{F1} \|\mathbf{u} - \mathbf{u}^*\|^2, \qquad \left\| \frac{d^2 F}{d\mathbf{u} d\mathbf{u}^T}(\mathbf{u}) \right\| \leq L_{F2} \tag{3.9}$$

for all $\mathbf{u} \in \mathbb{R}^{n_\mathbf{u}}$.

In addition, we assume that the disturbance d_k satisfies the following bound.

Assumption 3.5. *There exist constants* $\delta_{\mathbf{n}}, \delta_{\mathbf{x}}, \delta_{\mathbf{u}} \in \mathbb{R}_{\geq 0}$ *such that*

$$|d_k| \leq \delta_{\mathbf{n}} + \delta_{\mathbf{x}} \|\mathbf{x}_k - \mathbf{X}(\mathbf{u}_k)\| + \delta_{\mathbf{u}} \|\mathbf{u}_k - \mathbf{u}^*\| \tag{3.10}$$

for all $\mathbf{x}_k \in \mathbb{R}^{n_{\mathbf{x}}}$*, all* $\mathbf{u}_k \in \mathbb{R}^{n_{\mathbf{u}}}$ *and all* $k \in \mathbb{N}$*.*

Remark 3.6. *The assumptions for the sampled-date setting in this chapter are equivalent to the assumptions for the continuous-time setting in Chapter 2.*

We note that the map $\mathbf{X}$, the map F and its minimizer $\mathbf{u}^*$ are unknown because the functions $\mathbf{f}$ and h are unknown. In the next section, we present a discrete-time extremum-seeking controller to regulate the plant parameters $\mathbf{u}_k$ to their performance-optimizing values $\mathbf{u}^*$.

3.3 Discrete-time controller

Similar to Chapter 2, we present an extremum-seeking controller that estimates the gradient of the objective function and subsequently uses this gradient estimate to steer the plant parameters $\mathbf{u}_k$ to the minimizer $\mathbf{u}^*$. We define

$$\mathbf{u}_k = \hat{\mathbf{u}}_k + \alpha_{\boldsymbol{\omega}} \boldsymbol{\omega}_k, \tag{3.11}$$

where $\hat{\mathbf{u}}_k$ is a vector of nominal plant-parameter values, which can be thought of as an estimate of the minimizer $\mathbf{u}^*$, and where $\alpha_{\boldsymbol{\omega}} \boldsymbol{\omega}_k$ is a vector of perturbation signals with amplitude $\alpha_{\boldsymbol{\omega}} \in \mathbb{R}_{>0}$. The vector $\boldsymbol{\omega}_k$ is defined by $\boldsymbol{\omega}_k = [\omega_{1,k}, \omega_{2,k}, \ldots, \omega_{n_{\mathbf{u}},k}]^T$, with

$$\omega_{i,k} = \begin{cases} \sin\left(\dfrac{(i+1)\pi k}{N_{\boldsymbol{\omega}} C_{lcm}}\right), & \text{if } i \text{ is odd,} \\ \cos\left(\dfrac{i\pi k}{N_{\boldsymbol{\omega}} C_{lcm}}\right), & \text{if } i \text{ is even,} \end{cases} \tag{3.12}$$

for $i = 1, 2, \ldots, n_{\mathbf{u}}$, where C_{lcm} is the least common multiple of $1, 2, \ldots, \left\lceil \frac{n_{\mathbf{u}}}{2} \right\rceil$, and where $a_{\boldsymbol{\omega}} \in \mathbb{R}_{>0}$ and $N_{\boldsymbol{\omega}} \in \mathbb{N}_{>0}$ are tuning parameters, with $N_{\boldsymbol{\omega}} C_{lcm} > 2 \left\lceil \frac{n_{\mathbf{u}}}{2} \right\rceil$.

To estimate the gradient of the objective function, we model the input-to-output behavior of the extended plant in the following general form with the help of Taylor's theorem:

$$\begin{aligned} \mathbf{m}_{k+1} &= \mathbf{A}_k \mathbf{m}_k + \alpha_{\boldsymbol{\omega}}^2 \left(\mathbf{B}_{1,k} \mathbf{w}_{1,k} + \mathbf{B}_{2,k} \mathbf{w}_{2,k}\right) \\ y_k &= \mathbf{C}_k \mathbf{m}_k + \alpha_{\boldsymbol{\omega}}^2 v_k + z_k + d_k, \end{aligned} \tag{3.13}$$

with state

$$\mathbf{m}_k = \begin{bmatrix} F(\hat{\mathbf{u}}_k) \\ \alpha_{\boldsymbol{\omega}} \frac{dF}{d\mathbf{u}^T}(\hat{\mathbf{u}}_k) \end{bmatrix}, \tag{3.14}$$

where the matrices $\mathbf{A}_k$, $\mathbf{B}_{1,k}$, $\mathbf{B}_{2,k}$ and $\mathbf{C}_k$ are defined as

$$\mathbf{A}_k = \begin{bmatrix} 1 & \frac{\Delta \hat{\mathbf{u}}_k^T}{\alpha_{\boldsymbol{\omega}}} \\ \mathbf{0} & \mathbf{I} \end{bmatrix}, \quad \mathbf{B}_{1,k} = \begin{bmatrix} \mathbf{0} \\ \mathbf{I} \end{bmatrix}, \quad \mathbf{B}_{2,k} = \begin{bmatrix} \frac{\Delta \hat{\mathbf{u}}_k^T}{2\alpha_{\boldsymbol{\omega}}} \\ \mathbf{0} \end{bmatrix}, \quad \mathbf{C}_k = \begin{bmatrix} 1 & \boldsymbol{\omega}_k^T \end{bmatrix}, \tag{3.15}$$

with

$$\Delta \hat{\mathbf{u}}_k = \hat{\mathbf{u}}_{k+1} - \hat{\mathbf{u}}_k, \tag{3.16}$$

and where the disturbances $\mathbf{w}_{1,k}$, $\mathbf{w}_{2,k}$, v_k and z_k are given by

$$\begin{aligned} \mathbf{w}_{1,k} &= \int_0^1 \frac{d^2F}{d\mathbf{u}d\mathbf{u}^T}(\hat{\mathbf{u}}_k + s\Delta\hat{\mathbf{u}}_k)ds\frac{\Delta\hat{\mathbf{u}}_k}{\alpha_{\boldsymbol{\omega}}}, \\ \mathbf{w}_{2,k} &= 2\int_0^1 (1-s)\frac{d^2F}{d\mathbf{u}d\mathbf{u}^T}(\hat{\mathbf{u}}_k + s\Delta\hat{\mathbf{u}}_k)ds\frac{\Delta\hat{\mathbf{u}}_k}{\alpha_{\boldsymbol{\omega}}}, \\ v_k &= \boldsymbol{\omega}_k^T \int_0^1 (1-s)\frac{d^2F}{d\mathbf{u}d\mathbf{u}^T}(\hat{\mathbf{u}}_k + s\alpha_{\boldsymbol{\omega}}\boldsymbol{\omega}_k)ds\boldsymbol{\omega}_k, \\ z_k &= h(\mathbf{x}_k, \mathbf{u}_k) - h(\mathbf{X}(\mathbf{u}_k), \mathbf{u}_k). \end{aligned} \tag{3.17}$$

We note that the state $\mathbf{m}_k$ contains a scaled version of the gradient of the objective function. To obtain an estimate for the gradient of the objective function, we design an observer to estimate the state $\mathbf{m}_k$. The disturbances $\mathbf{w}_{1,k}$, $\mathbf{w}_{2,k}$ and v_k are unknown because they depend on the Hessian of the objective function. Similarly, the disturbance z_k is unknown because the state $\mathbf{x}_k$, the map $\mathbf{X}$ and the function h are unknown. For the design of the observer, we assume that $z_k = d_k = 0$. We approximate the disturbances $\mathbf{w}_1$, $\mathbf{w}_2$ and v by

$$\begin{aligned} \hat{\mathbf{w}}_k &= \hat{\mathbf{w}}_{1,k} = \hat{\mathbf{w}}_{2,k} = \mathbf{H}(\hat{\mathbf{u}}_k)\frac{\Delta\hat{\mathbf{u}}_k}{\alpha_{\boldsymbol{\omega}}}, \\ \hat{v}_k &= \frac{1}{2}\boldsymbol{\omega}_k^T\mathbf{H}(\hat{\mathbf{u}}_k)\boldsymbol{\omega}_k, \end{aligned} \tag{3.18}$$

where the function $\mathbf{H} : \mathbb{R}^{n_{\mathbf{u}}} \to \mathbb{R}^{n_{\mathbf{u}} \times n_{\mathbf{u}}}$ satisfies

$$\|\mathbf{H}(\hat{\mathbf{u}})\| \leq L_{\mathbf{H}} \tag{3.19}$$

for all $\hat{\mathbf{u}} \in \mathbb{R}^{n_{\mathbf{u}}}$ and some constant $L_{\mathbf{H}} \in \mathbb{R}_{>0}$. An overall good choice of $\mathbf{H}$ is $\mathbf{H}(\hat{\mathbf{u}}) = \mathbf{0}$. However, $\mathbf{H}(\hat{\mathbf{u}}) \approx \frac{d^2F}{d\mathbf{u}d\mathbf{u}^T}(\hat{\mathbf{u}})$ is more suitable under certain tuning conditions, assuming that a reasonably accurate approximation of the Hessian of the objective function is available; see Section 2.5.

We introduce a recursive three-step observer to estimate the state $\mathbf{m}_k$. Let the estimate of the state $\mathbf{m}_k$ be denoted by $\hat{\mathbf{m}}_{k|3}$. Moreover, let $\hat{\mathbf{m}}_{k|1}$ and $\hat{\mathbf{m}}_{k|2}$ be intermediate variables. The intermediate variables $\hat{\mathbf{m}}_{k|1}$ and $\hat{\mathbf{m}}_{k|2}$ and the state estimate $\hat{\mathbf{m}}_{k|3}$ are each obtained by minimizing a quadratic cost function

with respect to an exponentially weighted time window of the estimation error:

$$\begin{aligned}(k, \hat{\mathbf{m}}_{k|i}) = \underset{\mathbf{p}_k \in \mathbb{R}^{n_\mathbf{u}+1}}{\arg\min}\ J_i(k, \mathbf{p}_k),\\ \text{subject to:}\quad \mathbf{p}_{j+1} = \mathbf{A}_j \mathbf{p}_j + \alpha_{\boldsymbol{\omega}}^2 \mathbf{B}_j \hat{\mathbf{w}}_j\\ \hat{y}_j = \mathbf{C}_j \mathbf{p}_j + \alpha_{\boldsymbol{\omega}}^2 \hat{v}_j, \qquad \forall j \in \{0, 1, \ldots, k\},\end{aligned} \tag{3.20}$$

for $i = \{1, 2, 3\}$, with

$$\mathbf{B}_k = \mathbf{B}_{1,k} + \mathbf{B}_{2,k}, \qquad \forall k \in \mathbb{N}. \tag{3.21}$$

The corresponding cost functions J_1, J_2 and J_3 are given by

$$\begin{aligned}J_1(k, \mathbf{p}_k) &= (1-\lambda_\mathbf{m}) \sum_{q=0}^{k-1} \lambda_\mathbf{m}^{k-q} \|\mathbf{y}_q - \hat{\mathbf{y}}_q\|^2 + \sigma_r (1-\lambda_\mathbf{m}) \sum_{j=0}^{k-1} \lambda_\mathbf{m}^{k-j} \|\mathbf{D}\mathbf{p}_j\|^2\\ &\quad + \lambda_\mathbf{m}^k (\hat{\mathbf{m}}_0 - \mathbf{p}_0)^T \mathbf{Q}_0^{-1} (\hat{\mathbf{m}}_0 - \mathbf{p}_0),\\ J_2(k, \mathbf{p}_k) &= (1-\lambda_\mathbf{m}) \sum_{q=0}^{k} \lambda_\mathbf{m}^{k-q} \|\mathbf{y}_q - \hat{\mathbf{y}}_q\|^2 + \sigma_r (1-\lambda_\mathbf{m}) \sum_{j=0}^{k-1} \lambda_\mathbf{m}^{k-j} \|\mathbf{D}\mathbf{p}_j\|^2\\ &\quad + \lambda_\mathbf{m}^k (\hat{\mathbf{m}}_0 - \mathbf{p}_0)^T \mathbf{Q}_0^{-1} (\hat{\mathbf{m}}_0 - \mathbf{p}_0),\\ J_3(k, \mathbf{p}_k) &= (1-\lambda_\mathbf{m}) \sum_{q=0}^{k} \lambda_\mathbf{m}^{k-q} \|\mathbf{y}_q - \hat{\mathbf{y}}_q\|^2 + \sigma_r (1-\lambda_\mathbf{m}) \sum_{j=0}^{k} \lambda_\mathbf{m}^{k-j} \|\mathbf{D}\mathbf{p}_j\|^2\\ &\quad + \lambda_\mathbf{m}^k (\hat{\mathbf{m}}_0 - \mathbf{p}_0)^T \mathbf{Q}_0^{-1} (\hat{\mathbf{m}}_0 - \mathbf{p}_0),\end{aligned} \tag{3.22}$$

with

$$\mathbf{D} = \begin{bmatrix}\mathbf{0} & \mathbf{I}\end{bmatrix} \tag{3.23}$$

and $\hat{\mathbf{m}}_0 \in \mathbb{R}^{n_\mathbf{u}+1}$, where $\lambda_\mathbf{m} \in (0, 1)$ is a tuning parameter and $\mathbf{Q}_0 \in \mathbb{R}^{n_\mathbf{u}+1 \times n_\mathbf{u}+1}$ is a symmetric positive-definite matrix. The tuning parameter $\sigma_r \in \mathbb{R}_{\geq 0}$ is a regularization constant. We note that $J_2(k, \mathbf{p}_k) = J_1(k, \mathbf{p}_k) + (1-\lambda_\mathbf{m})\|\mathbf{y}_k - \hat{\mathbf{y}}_k\|^2$ and $J_3(k, \mathbf{p}_k) = J_2(k, \mathbf{p}_k) + \sigma_r(1-\lambda_\mathbf{m})\|\mathbf{D}\mathbf{p}_k\|^2$. To recursively compute $\hat{\mathbf{m}}_{k|3}$, we derive the update steps $\hat{\mathbf{m}}_{k|1} \to \hat{\mathbf{m}}_{k|2}$, $\hat{\mathbf{m}}_{k|2} \to \hat{\mathbf{m}}_{k|3}$ and $\hat{\mathbf{m}}_{k|3} \to \hat{\mathbf{m}}_{k+1|1}$. We note that an explicit expression for $\hat{\mathbf{m}}_{k|i}$ is given by

$$\hat{\mathbf{m}}_{k|i} = \mathbf{Q}_{k|i} \boldsymbol{\Psi}_{k|i} \tag{3.24}$$

for all $i = \{1, 2, 3\}$ and all $k \in \mathbb{N}$, with

$$\begin{aligned}
\mathbf{Q}_{k|1} &= \Bigg((1-\lambda_{\mathbf{m}}) \sum_{q=0}^{k-1} \lambda_{\mathbf{m}}^{k-q} \mathbf{\Phi}_{q,k}^T \mathbf{C}_q^T \mathbf{C}_q \mathbf{\Phi}_{q,k} + \sigma_r (1-\lambda_{\mathbf{m}}) \sum_{j=0}^{k-1} \lambda_{\mathbf{m}}^{k-j} \mathbf{\Phi}_{j,k}^T \mathbf{D}^T \mathbf{D} \mathbf{\Phi}_{j,k} \\
&\quad + \lambda_{\mathbf{m}}^k \mathbf{\Phi}_{0,k}^T \mathbf{Q}_0^{-1} \mathbf{\Phi}_{0,k} \Bigg)^{-1}, \\
\mathbf{Q}_{k|2} &= \Bigg((1-\lambda_{\mathbf{m}}) \sum_{q=0}^{k} \lambda_{\mathbf{m}}^{k-q} \mathbf{\Phi}_{q,k}^T \mathbf{C}_q^T \mathbf{C}_q \mathbf{\Phi}_{q,k} + \sigma_r (1-\lambda_{\mathbf{m}}) \sum_{j=0}^{k-1} \lambda_{\mathbf{m}}^{k-j} \mathbf{\Phi}_{j,k}^T \mathbf{D}^T \mathbf{D} \mathbf{\Phi}_{j,k} \\
&\quad + \lambda_{\mathbf{m}}^k \mathbf{\Phi}_{0,k}^T \mathbf{Q}_0^{-1} \mathbf{\Phi}_{0,k} \Bigg)^{-1}, \\
\mathbf{Q}_{k|3} &= \Bigg((1-\lambda_{\mathbf{m}}) \sum_{q=0}^{k} \lambda_{\mathbf{m}}^{k-q} \mathbf{\Phi}_{q,k}^T \mathbf{C}_q^T \mathbf{C}_q \mathbf{\Phi}_{q,k} + \sigma_r (1-\lambda_{\mathbf{m}}) \sum_{j=0}^{k} \lambda_{\mathbf{m}}^{k-j} \mathbf{\Phi}_{j,k}^T \mathbf{D}^T \mathbf{D} \mathbf{\Phi}_{j,k} \\
&\quad + \lambda_{\mathbf{m}}^k \mathbf{\Phi}_{0,k}^T \mathbf{Q}_0^{-1} \mathbf{\Phi}_{0,k} \Bigg)^{-1}
\end{aligned} \tag{3.25}$$

and

$$\begin{aligned}
\mathbf{\Psi}_{k|1} &= (1-\lambda_{\mathbf{m}}) \sum_{q=0}^{k-1} \lambda_{\mathbf{m}}^{k-q} \mathbf{\Phi}_{q,k}^T \mathbf{C}_q^T \left(\mathbf{y}_q + \alpha_{\boldsymbol{\omega}}^2 \mathbf{C}_q \sum_{s=q}^{k-1} \mathbf{\Phi}_{q,s+1} \mathbf{B}_s \hat{\mathbf{w}}_s - \alpha_{\boldsymbol{\omega}}^2 \hat{\mathbf{v}}_q \right) \\
&\quad + \alpha_{\boldsymbol{\omega}}^2 \sigma_r (1-\lambda_{\mathbf{m}}) \sum_{j=0}^{k-1} \lambda_{\mathbf{m}}^{k-j} \mathbf{\Phi}_{j,k}^T \mathbf{D}^T \mathbf{D} \sum_{l=j}^{k-1} \mathbf{\Phi}_{j,l+1} \mathbf{B}_l \hat{\mathbf{w}}_l \\
&\quad + \lambda_{\mathbf{m}}^k \mathbf{\Phi}_{0,k}^T \mathbf{Q}_0^{-1} \left(\hat{\mathbf{m}}_0 + \alpha_{\boldsymbol{\omega}}^2 \sum_{p=0}^{k-1} \mathbf{\Phi}_{0,p+1} \mathbf{B}_p \hat{\mathbf{w}}_p \right), \\
\mathbf{\Psi}_{k|2} &= (1-\lambda_{\mathbf{m}}) \sum_{q=0}^{k} \lambda_{\mathbf{m}}^{k-q} \mathbf{\Phi}_{q,k}^T \mathbf{C}_q^T \left(\mathbf{y}_q + \alpha_{\boldsymbol{\omega}}^2 \mathbf{C}_q \sum_{s=q}^{k-1} \mathbf{\Phi}_{q,s+1} \mathbf{B}_s \hat{\mathbf{w}}_s - \alpha_{\boldsymbol{\omega}}^2 \hat{\mathbf{v}}_q \right) \\
&\quad + \alpha_{\boldsymbol{\omega}}^2 \sigma_r (1-\lambda_{\mathbf{m}}) \sum_{j=0}^{k-1} \lambda_{\mathbf{m}}^{k-j} \mathbf{\Phi}_{j,k}^T \mathbf{D}^T \mathbf{D} \sum_{l=j}^{k-1} \mathbf{\Phi}_{j,l+1} \mathbf{B}_l \hat{\mathbf{w}}_l \\
&\quad + \lambda_{\mathbf{m}}^k \mathbf{\Phi}_{0,k}^T \mathbf{Q}_0^{-1} \left(\hat{\mathbf{m}}_0 + \alpha_{\boldsymbol{\omega}}^2 \sum_{p=0}^{k-1} \mathbf{\Phi}_{0,p+1} \mathbf{B}_p \hat{\mathbf{w}}_p \right),
\end{aligned} \tag{3.26}$$

$$\begin{aligned}\boldsymbol{\Psi}_{k|3} = (1-\lambda_{\mathbf{m}})\sum_{q=0}^{k}\lambda_{\mathbf{m}}^{k-q}\boldsymbol{\Phi}_{q,k}^{T}\mathbf{C}_{q}^{T}\left(\mathbf{y}_{q}+\alpha_{\boldsymbol{\omega}}^{2}\mathbf{C}_{q}\sum_{s=q}^{k-1}\boldsymbol{\Phi}_{q,s+1}\mathbf{B}_{s}\hat{\mathbf{w}}_{s}-\alpha_{\boldsymbol{\omega}}^{2}\hat{\mathbf{v}}_{q}\right)\\ +\alpha_{\boldsymbol{\omega}}^{2}\sigma_{r}(1-\lambda_{\mathbf{m}})\sum_{j=0}^{k}\lambda_{\mathbf{m}}^{k-j}\boldsymbol{\Phi}_{j,k}^{T}\mathbf{D}^{T}\mathbf{D}\sum_{l=j}^{k-1}\boldsymbol{\Phi}_{j,l+1}\mathbf{B}_{l}\hat{\mathbf{w}}_{l}\\ +\lambda_{\mathbf{m}}^{k}\boldsymbol{\Phi}_{0,k}^{T}\mathbf{Q}_{0}^{-1}\left(\hat{\mathbf{m}}_{0}+\alpha_{\boldsymbol{\omega}}^{2}\sum_{p=0}^{k-1}\boldsymbol{\Phi}_{0,p+1}\mathbf{B}_{p}\hat{\mathbf{w}}_{p}\right),\end{aligned} \tag{3.27}$$

where the state-transition matrix $\boldsymbol{\Phi}$ is given by

$$\boldsymbol{\Phi}_{j,k} = \begin{bmatrix} 1 & \dfrac{\hat{\mathbf{u}}_{j}^{T}-\hat{\mathbf{u}}_{k}^{T}}{\alpha_{\boldsymbol{\omega}}} \\ \mathbf{0} & \mathbf{I}\end{bmatrix} \tag{3.28}$$

for all $j,k\in\mathbb{N}$. From (3.24), we obtain the following update equations of the observer:

Step $1\to 2$ (correction step):

$$\begin{aligned}\hat{\mathbf{m}}_{k|2} &= \hat{\mathbf{m}}_{k|1}+\mathbf{L}_{k|1}\left(y_{k}-\mathbf{C}_{k}\hat{\mathbf{m}}_{k|1}-\alpha_{\boldsymbol{\omega}}^{2}\hat{v}_{k}\right),\\ \mathbf{Q}_{k|2} &= \left(\mathbf{I}-\mathbf{L}_{k|1}\mathbf{C}_{k}\right)\mathbf{Q}_{k|1}\left(\mathbf{I}-\mathbf{L}_{k|1}\mathbf{C}_{k}\right)^{T}+\frac{1}{1-\lambda_{\mathbf{m}}}\mathbf{L}_{k|1}\mathbf{L}_{k|1}^{T},\end{aligned} \tag{3.29}$$

Step $2\to 3$ (regularization step):

$$\begin{aligned}\hat{\mathbf{m}}_{k|3} &= \begin{cases}\hat{\mathbf{m}}_{k|2}-\mathbf{L}_{k|2}\mathbf{D}\hat{\mathbf{m}}_{k|2}, & \text{if } \sigma_{r}>0,\\ \hat{\mathbf{m}}_{k|2}, & \text{if } \sigma_{r}=0,\end{cases}\\ \mathbf{Q}_{k|3} &= \begin{cases}\left(\mathbf{I}-\mathbf{L}_{k|2}\mathbf{D}\right)\mathbf{Q}_{k|2}\left(\mathbf{I}-\mathbf{L}_{k|2}\mathbf{D}\right)^{T}+\dfrac{1}{\sigma_{r}(1-\lambda_{\mathbf{m}})}\mathbf{L}_{k|2}\mathbf{L}_{k|2}^{T}, & \\ & \text{if } \sigma_{r}>0,\\ \mathbf{Q}_{k|2}, & \text{if } \sigma_{r}=0,\end{cases}\end{aligned} \tag{3.30}$$

Step $3\to 1$ (prediction step):

$$\begin{aligned}\hat{\mathbf{m}}_{k+1|1} &= \mathbf{A}_{k}\hat{\mathbf{m}}_{k|3}+\alpha_{\boldsymbol{\omega}}^{2}\mathbf{B}_{k}\hat{\mathbf{w}}_{k},\\ \mathbf{Q}_{k+1|1} &= \frac{1}{\lambda_{\mathbf{m}}}\mathbf{A}_{k}\mathbf{Q}_{k|3}\mathbf{A}_{k}^{T},\end{aligned} \tag{3.31}$$

with

$$\begin{aligned}\mathbf{L}_{k|1} &= \mathbf{Q}_{k|1}\mathbf{C}_k^T\left(\frac{1}{1-\lambda_{\mathbf{m}}}+\mathbf{C}_k\mathbf{Q}_{k|1}\mathbf{C}_k^T\right)^{-1},\\ \mathbf{L}_{k|2} &= \mathbf{Q}_{k|2}\mathbf{D}^T\left(\frac{1}{\sigma_r(1-\lambda_{\mathbf{m}})}\mathbf{I}+\mathbf{D}\mathbf{Q}_{k|2}\mathbf{D}^T\right)^{-1}\end{aligned} \tag{3.32}$$

and initial conditions $\hat{\mathbf{m}}_{0|1} = \hat{\mathbf{m}}_0$ and $\mathbf{Q}_{0|1} = \mathbf{Q}_0$. The regularization step in (3.30) prevents the matrix $\mathbf{Q}_{k|3}$ from becoming excessively large if the level of excitation of the plant parameters $\mathbf{u}_k$ is low for $\sigma_r > 0$. Regularization deteriorates the accuracy of the state estimate. Therefore, the regularization constant σ_r is commonly chosen to be small. No regularization is applied if $\sigma_r = 0$.

Because $\hat{\mathbf{m}}_{k|3}$ is an estimate of the state $\mathbf{m}_k$, we have that $\mathbf{D}\hat{\mathbf{m}}_{k|3}$ is an estimate of the gradient of the objective function scaled by $\alpha_{\boldsymbol{\omega}}$. We define the following gradient-descent optimizer to drive $\hat{\mathbf{u}}_k$ towards $\mathbf{u}^*$:

$$\hat{\mathbf{u}}_{k+1} = \hat{\mathbf{u}}_k - \lambda_{\mathbf{u}}\frac{\eta_{\mathbf{u}}\mathbf{D}\hat{\mathbf{m}}_{k|3}}{\eta_{\mathbf{u}}+\lambda_{\mathbf{u}}\|\mathbf{D}\hat{\mathbf{m}}_{k|3}\|}, \tag{3.33}$$

where $\lambda_{\mathbf{u}}, \eta_{\mathbf{u}} \in \mathbb{R}_{>0}$ are tuning parameters. The adaptation gain in (3.33) is normalized to prevent the solutions of the closed-loop system of plant and extremum-seeking controller from having a finite escape time; see also Section 2.3.

An illustration of the extremum-seeking controller in (3.29)-(3.31), (3.33) is given in Figure 3.2. The resulting optimization scheme is obtained by closing the loop between the sampled-data plant and cost function in Section 3.2 and the extremum-seeking controller presented in this section; see also Figures 3.1 and 3.2.

3.4 Relation to the continuous-time controller

To relate the discrete-time controller in Section 3.3 to the continuous-time controller in Section 2.3, we introduce the following lemma.

Lemma 3.7. *Let the tuning parameters of the continuous-time controller in Section 2.3 be denoted by $\alpha'_{\boldsymbol{\omega}}$, $\eta'_{\boldsymbol{\omega}}$, $\eta'_{\mathbf{m}}$, $\lambda'_{\mathbf{u}}$, $\eta'_{\mathbf{u}}$ and σ'_r. Let the tuning parameters of the discrete-time controller in Section 3.3 be given by*

$$\begin{aligned}\alpha_{\boldsymbol{\omega}} &= \alpha'_{\boldsymbol{\omega}}, & N_{\boldsymbol{\omega}} &= \frac{2\pi}{\eta'_{\boldsymbol{\omega}}T_s C_{lcm}}, & \lambda_{\mathbf{m}} &= e^{-\eta'_{\mathbf{m}}T_s},\\ \lambda_{\mathbf{u}} &= \lambda'_{\mathbf{u}}T_s, & \eta_{\mathbf{u}} &= \eta'_{\mathbf{u}}T_s, & \sigma_r &= \sigma'_r.\end{aligned} \tag{3.34}$$

Under these tuning conditions, the discrete-time controller in Section 3.3 is equivalent to the continuous-time controller in Section 2.3 for the limit as the sampling time T_s approaches zero.

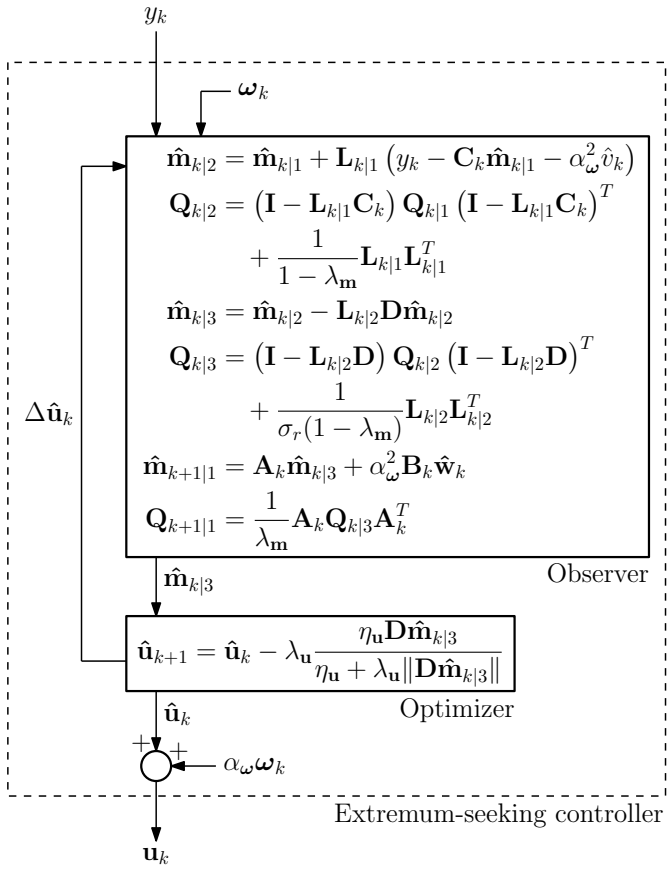

Figure 3.2: Discrete-time extremum-seeking controller for $\sigma_r > 0$.

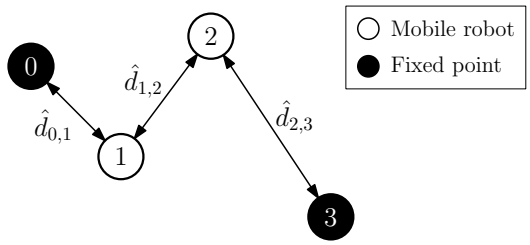

Figure 3.3: Chain of two mobile robots and two fixed points.

Proof. See Section 3.7.1. □

We conclude from Lemma 3.7 that the solutions of the closed-loop system of the sampled-data plant in Section 3.2 and the discrete-time controller in Section 3.3 are similar to the solutions of the closed-loop system of the continuous-time plant in Section 2.2 and the continuous-time controller in Section 2.3 if the tuning conditions in (3.34) are satisfied and the sampling time is sufficiently small.

Remark 3.8. *The influence of the sampling is relatively small if the discrete-time extremum-seeeking controller is slow with respect to the sampling time. We note that we can make the extremum-seeking controller arbitrarily slow under appropriate tuning conditions. Hence, for any finite sampling time, we can make the extremum-seeking controller sufficiently slow such that the sampling has little effect on the solutions of the closed-loop system of plant and controller.*

3.5 Simulation example

To demonstrate the influence of the sampling time on the solutions of the closed-loop system of plant and controller, we introduce the following example. Consider two mobile robots, numbered one and two. Although the position in the XY-plane of the two robots is unknown, our aim is to manoeuvre the robots such that they are equally spaced on a straight line between two fixed points in the XY-plane. The two fixed points in the XY-plane are numbered zero and three, such that a chain of four links (numbered zero to three) is obtained consisting of the first fixed point, the two robots and the second fixed point; see Figure 3.3.

The position of link i in the XY-plane is denoted by $\mathbf{p}_i(t) = [p_{x,i}(t), p_{y,i}(t)]^T$ for $i = \{0, 1, 2, 3\}$, which implies that the distance between link i and link $i+1$ is given by

$$\hat{d}_{i,i+1}(t) = \sqrt{(p_{x,i+1}(t) - p_{x,i}(t))^2 + (p_{y,i+1}(t) - p_{y,i}(t))^2} \tag{3.35}$$

for $i = \{0, 1, 2\}$; see Figure 3.3. The dynamics of the two robots is given by

$$\mathbf{M}_i\ddot{\mathbf{p}}_i(t) + \mathbf{g}_i(\dot{\mathbf{p}}_i(t)) = \boldsymbol{\tau}_i(t) \tag{3.36}$$

for $i = \{1, 2\}$, where the positive-definite matrix $\mathbf{M}_i$ and the function $\mathbf{g}_i$ are uncertain. Although the position $\mathbf{p}_i(t)$ is unknown, the difference $\Delta\mathbf{p}_{i,k} = \mathbf{p}_{i,k+1} - \mathbf{p}_{i,k}$ is obtained by sampled measurements, where $\mathbf{p}_{i,k}$ is defined such that $\mathbf{p}_{i,k} = \mathbf{p}_i(kT_s)$. We define $\Delta\mathbf{r}_{i,k} = \mathbf{r}_{i,k+1} - \mathbf{r}_{i,k}$ for $i \in \{1, 2\}$, where $\mathbf{r}_{i,k} = [r_{x,i,k}, r_{y,i,k}]^T$ is a reference for the position $\mathbf{p}_{i,k}$. The control input $\boldsymbol{\tau}_i(t)$ in (3.36) is given by $\boldsymbol{\tau}_i(t) = 0$ for all $t \in [0, T_s]$ and $\boldsymbol{\tau}_i(t) = \boldsymbol{\tau}_{i,k+1}$ for all $t \in (kT_s, (k+1)T_s]$ and all $k \in \mathbb{N}_{>0}$, with

$$\begin{aligned}\boldsymbol{\tau}_{i,k+1} = \hat{\mathbf{M}}_i \frac{\Delta\mathbf{r}_{i,k} - \Delta\mathbf{r}_{i,k-1}}{T_s^2} + \hat{\mathbf{g}}_i(\frac{\Delta\mathbf{p}_{i,k-1}}{T_s}) \\ + \mathbf{K}_{1,i}\frac{\Delta\mathbf{r}_{i,k-1} - \Delta\mathbf{p}_{i,k-1}}{T_s} + \mathbf{K}_{2,i}\sum_{j=0}^{k-1} \Delta\mathbf{r}_{i,j} - \Delta\mathbf{p}_{i,j},\end{aligned} \tag{3.37}$$

where $\mathbf{K}_{1,i}$ and $\mathbf{K}_{2,i}$ are positive-definite matrices, and where the positive-definite matrix $\hat{\mathbf{M}}_i$ and the function $\hat{\mathbf{g}}_i$ are approximations of $\mathbf{M}_i$ and $\mathbf{g}_i$.

We assume that sampled measurements of the distances $\hat{d}_{i,i+1}(t)$ are available. The sampled measurement of $\hat{d}_{i,i+1}(t)$ for $t = kT_s$ is denoted by $\hat{d}_{i,i+1,k}$. We define the plant-parameter vector $\mathbf{u}_k = [\mathbf{r}_{1,k}^T, \mathbf{r}_{2,k}^T]^T$ and the cost function

$$Z(\mathbf{e}_k) = \sum_{i=0}^{2} d_{i,i+1,k}^2, \tag{3.38}$$

with $\mathbf{e}_k = [d_{0,1,k}, d_{1,2,k}, d_{2,3,k}]^T$. Note that $\mathbf{e}_k$ indirectly depend on the plant parameters $\mathbf{u}_k$, and that output of the cost function is minimal if the two robots are equally spaced on a straight line between the two fixed points.

Let $\mathbf{J}_i = \mathbf{I}$, $\mathbf{g}_i = 0.5\mathbf{id}$, $\hat{\mathbf{J}}_i = 0.9\mathbf{I}$, $\hat{\mathbf{g}}_i = 0.4\mathbf{id}$, $\mathbf{K}_{1,i} = 5\mathbf{I}$ and $\mathbf{K}_{2,i} = 10\mathbf{I}$ for $i = \{1, 2\}$, where $\mathbf{id}$ is the identify function. Moreover, let the positions of the two fixed points be given by $\mathbf{p}_0 = [1, 0]^T$ and $\mathbf{p}_3 = [7, 6]^T$. We use the discrete-time extremum-seeking controller in Section 3.3 to minimize the output of the cost function in (3.38). The tuning parameters of the controller are chosen such that they satisfy (3.34), with $\alpha'_{\boldsymbol{\omega}} = 0.2$, $\eta'_{\boldsymbol{\omega}} = \pi$, $\eta'_{\mathbf{m}} = 1$, $\lambda'_{\mathbf{u}} = 2$, $\eta'_{\mathbf{u}} = 0.5$ and $\sigma'_r = 1 \times 10^{-3}$. The function $\mathbf{H}$ is given by

$$\mathbf{H}(\hat{\mathbf{u}}) = \begin{bmatrix} 4 & 0 & -2 & 0 \\ 0 & 4 & 0 & -2 \\ -2 & 0 & 4 & 0 \\ 0 & -2 & 0 & 4 \end{bmatrix} \tag{3.39}$$

for all $\hat{\mathbf{u}} \in \mathbb{R}^{n_{\mathbf{u}}}$. We note that $\mathbf{H}(\hat{\mathbf{u}}) = \frac{d^2F}{d\mathbf{u}d\mathbf{u}^T}(\hat{\mathbf{u}})$ for this choice of $\mathbf{H}$, where the objective function is obtained from (3.35) and (3.38) assuming that $\mathbf{p}_{i,k} = \mathbf{r}_{i,k}$

for $i = \{1, 2\}$. Although the objective function is dependent on the unknown positions of the fixed points, computation of the Hessian of the objective function does not require that the positions of the fixed points are known.

Simulation results for the discrete-time extremum-seeking controller for $T_s = 0.02$ and $T_s = 0.1$ are presented in Figures 3.4-3.9. For comparison's sake, simulation results for the continuous-time extremum-seeking controller in Section 2.3 are also presented in Figures 3.4-3.9. The control input and the cost function for the continuous-time extremum-seeking controller are obtained by taking the limit for $T_s \to 0$, which leads to

$$\boldsymbol{\tau}_i(t) = \hat{\mathbf{M}}_i \ddot{\mathbf{r}}_i(t) + \hat{\mathbf{g}}_i(\dot{\mathbf{p}}_i(t)) + \mathbf{K}_{1,i}(\dot{\mathbf{r}}_i(t) - \dot{\mathbf{p}}_i(t)) + \mathbf{K}_{2,i} \int_0^t (\dot{\mathbf{r}}_i(\tau) - \dot{\mathbf{p}}_i(\tau)) d\tau \tag{3.40}$$

and

$$Z(\mathbf{e}(t)) = \sum_{i=0}^{2} d_{i,i+1}^2(t). \tag{3.41}$$

The discrete-time control input $\boldsymbol{\tau}_{i,k+1}$ in (3.37) only depends on the difference $\Delta\mathbf{r}_{i,k} = \mathbf{r}_{i,k+1} - \mathbf{r}_{i,k}$ and not on $\mathbf{r}_{i,k}$ itself. Therefore, an identical control input is obtained for different initial conditions $\mathbf{r}_{i,0}$ as long as the difference $\Delta\mathbf{r}_{i,k}$ is the same. For convenience, we have set $\mathbf{r}_{i,0} = \mathbf{p}_{i,0}$ in Figures 3.4-3.9.

Figures 3.4 and 3.5 illustrate successful implementations of the extremum-seeking controllers as $\mathbf{u}_k = [\mathbf{r}_{1,k}^T, \mathbf{r}_{2,k}^T]^T$ converges to a small region of their performance-optimizing values $\mathbf{u}^* = [3, 2, 5, 4]^T$. There are substantial differences between the plant-parameter signals of the continuous-time extremum-seeking and the discrete-time extremum-seeking controller for $T_s = 0.1$. For $T_s = 0.02$, however, the plant-parameter signals of the continuous-time extremum-seeking and the discrete-time extremum-seeking controller are alike. Additional simulation results (not presented here) confirm that the plant-parameter signals of the discrete-time controller converge to those of the continuous-time controller as the sampling time approaches zero, as stated in Section 3.4.

The paths of the mobile robots in the XY-plane are displayed in Figure 3.6. We observe in Figure 3.6 that the mobile robots travel from their initial positions to a region of the points $[3, 2]^T$ and $[5, 4]^T$, respectively. These points are equally spaced on a straight line between the fixed points $\mathbf{p}_0 = [1, 0]^T$ and $\mathbf{p}_3 = [7, 6]^T$, which satisfies our aim. Similar to Figures 3.4 and 3.5, the paths of the mobile robots are comparable for the continuous-time controller and the discrete-time controller if $T_s = 0.02$ is used, while large deviations are observed if $T_s = 0.1$ is applied.

From Figures 3.7 and 3.8, we obtain that the mobile robots have more difficulty tracking the position reference if the sampling time is large, especially mobile robot two, which is required to move faster than mobile robot one due to a higher-frequency perturbation in the corresponding reference signal for the position

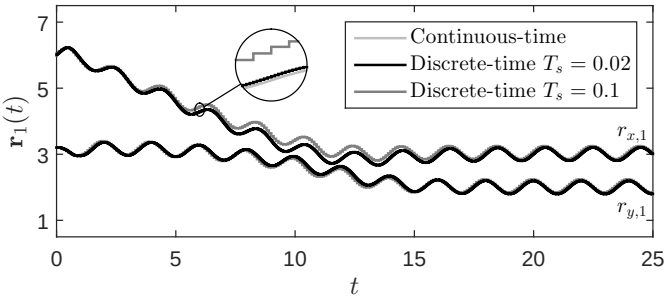

Figure 3.4: Position reference for mobile robot one as a function of time.

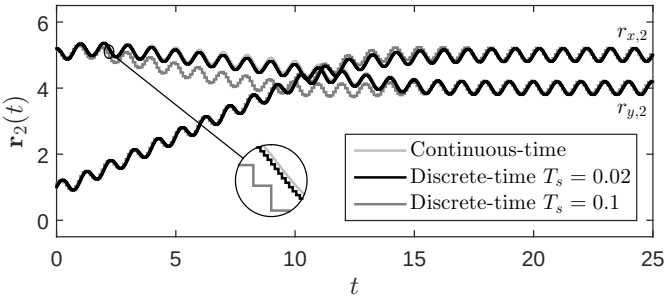

Figure 3.5: Position reference for mobile robot two as a function of time.

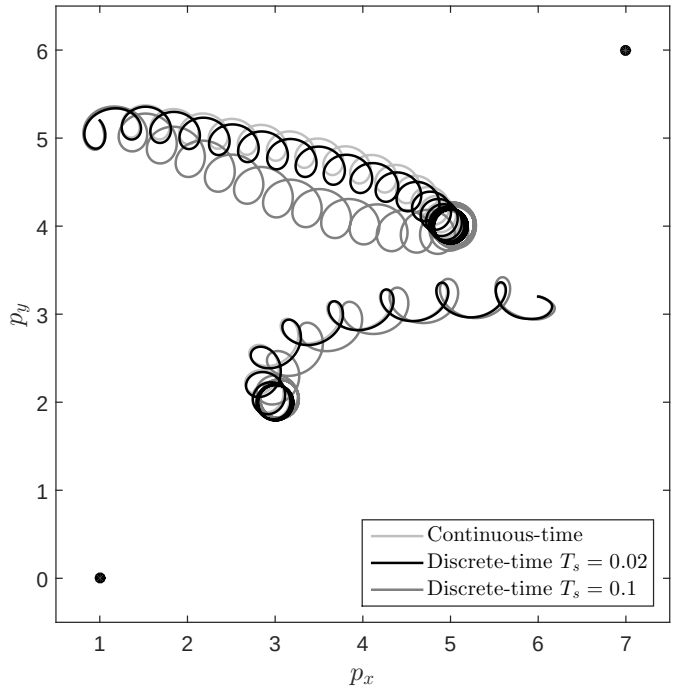

Figure 3.6: Paths of the mobile robots in the XY-plane.

of the robot. Any tracking error influences the estimate of the gradient of the objective function. Figure 3.9 reveals that the estimate of the gradient of the objective function is less accurate for the the discrete-time controller with sampling time $T_s = 0.1$ than continuous-time controller or the discrete-time controller with sampling time $T_s = 0.02$. By noting that the gradient estimate of the objective function drives the nominal values of the position references of the mobile robots, the differences in the paths of the mobile robots in Figure 3.6 can be explained by the differences in the estimate of the gradient of the objective function and the tracking error of the positions of the robots.

3.6 Conclusion

In this chapter, we have presented a discrete-time extremum-seeking controller that optimizes the performance of a nonlinear plant with an arbitrary number of plant parameters in a sampled-data setting. The controller is a discrete-time counterpart of the continuous-time extremum-seeking controller in Chapter 2. We have proved that the discrete-time controller is equivalent to the continuous-time controller in Chapter 2 for the limit as the sampling time approaches zero. A simulation example displays that comparable results are obtained with the discrete-time controller and the continuous-time controller in Chapter 2 if the sampling rate is sufficiently high.

3.7 Appendix

3.7.1 Proof of Lemma 3.7

Analogously to Section 3.2, we define the continuous-time signals $\boldsymbol{\omega}(t)$, $\hat{\mathbf{m}}(t)$, $\mathbf{Q}(t)$ and $\hat{\mathbf{u}}(t)$ such that $\boldsymbol{\omega}(0) = \boldsymbol{\omega}_0$, $\hat{\mathbf{m}}(0) = \hat{\mathbf{m}}_{0|3}$, $\mathbf{Q}(0) = \mathbf{Q}_{0|3}$, $\hat{\mathbf{u}}(0) = \hat{\mathbf{u}}_0$ and $\boldsymbol{\omega}(t) = \boldsymbol{\omega}_{k+1}$, $\hat{\mathbf{m}}(t) = \hat{\mathbf{m}}_{k+1|3}$, $\mathbf{Q}(t) = \mathbf{Q}_{k+1|3}$, $\hat{\mathbf{u}}(t) = \hat{\mathbf{u}}_{k+1}$ for all $t \in (kT_s, (k+1)T_s]$ and all $k \in \mathbb{N}$. From (3.12) and (3.34), we have that $\boldsymbol{\omega}_k = [\omega_{1,k}, \omega_{2,k}, \ldots, \omega_{n_{\mathbf{u}},k}]^T$, with

$$\omega_{i,k} = \begin{cases} \sin\left(\dfrac{i+1}{2}\eta'_{\boldsymbol{\omega}} k T_s\right), & \text{if } i \text{ is odd,} \\ \cos\left(\dfrac{i}{2}\eta'_{\boldsymbol{\omega}} k T_s\right), & \text{if } i \text{ is even,} \end{cases} \tag{3.42}$$

for $i = \{1, 2, \ldots, n_{\mathbf{u}}\}$. For $T_s \to 0$, we obtain from (3.42) that $\boldsymbol{\omega}(t) = [\omega_1(t), \omega_2(t), \ldots, \omega_{n_{\mathbf{u}}}(t)]^T$, with

$$\omega_i(t) = \begin{cases} \sin\left(\dfrac{i+1}{2}\eta'_{\boldsymbol{\omega}} t\right), & \text{if } i \text{ is odd,} \\ \cos\left(\dfrac{i}{2}\eta'_{\boldsymbol{\omega}} t\right), & \text{if } i \text{ is even} \end{cases} \tag{3.43}$$

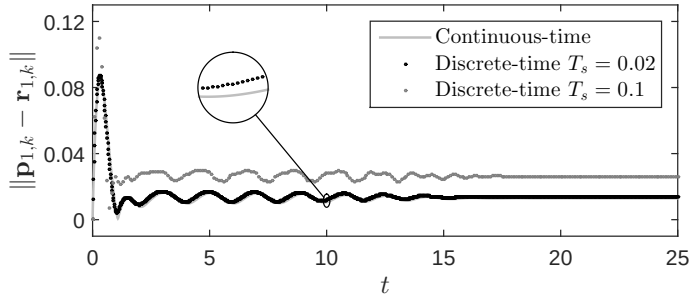

Figure 3.7: Euclidean norm of the tracking error at sampling instances for mobile robot one.

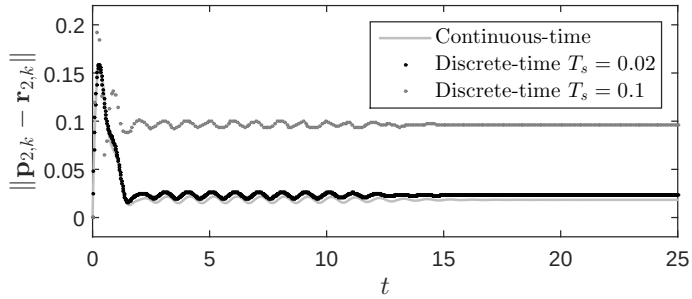

Figure 3.8: Euclidean norm of the tracking error at sampling instances for mobile robot two.

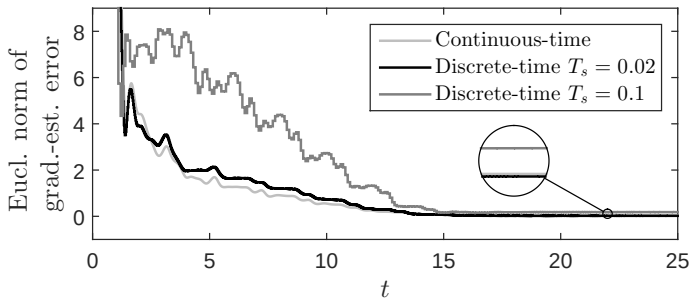

Figure 3.9: Euclidean norm of the gradient-estimation error as a function of time.

for all $t \in \mathbb{R}_{\geq 0}$. Similarly, from (3.33) and (3.34), we have that

$$\frac{\hat{\mathbf{u}}_{k+1} - \hat{\mathbf{u}}_k}{T_s} = -\lambda'_{\mathbf{u}} \frac{\eta'_{\mathbf{u}} \mathbf{D}\hat{\mathbf{m}}_{k|3}}{\eta'_{\mathbf{u}} + \lambda'_{\mathbf{u}} \|\mathbf{D}\hat{\mathbf{m}}_{k|3}\|}, \tag{3.44}$$

which implies that

$$\dot{\hat{\mathbf{u}}}(t) = -\lambda'_{\mathbf{u}} \frac{\eta'_{\mathbf{u}} \mathbf{D}\hat{\mathbf{m}}(t)}{\eta'_{\mathbf{u}} + \lambda'_{\mathbf{u}} \|\mathbf{D}\hat{\mathbf{m}}(t)\|} \tag{3.45}$$

for $T_s \to 0$. From (3.25) (or alternatively from (3.29)-(3.32)), it follows that

$$\mathbf{Q}^{-1}_{k+1|3} = \lambda_{\mathbf{m}} \mathbf{A}_k^{-T} \mathbf{Q}^{-1}_{k|3} \mathbf{A}_k^{-1} + (1 - \lambda_{\mathbf{m}}) \left(\mathbf{C}_k^T \mathbf{C}_k + \sigma_r \mathbf{D}^T \mathbf{D} \right). \tag{3.46}$$

We define the matrix

$$\bar{\mathbf{A}}_k = \frac{1}{T_s} \left(\mathbf{I} - \mathbf{A}_k^{-1} \right). \tag{3.47}$$

From (3.46) and (3.47), we obtain

$$\begin{aligned} \mathbf{Q}^{-1}_{k+1|3} = \lambda_{\mathbf{m}} \mathbf{Q}^{-1}_{k|3} - \lambda_{\mathbf{m}} \bar{\mathbf{A}}_k^T \mathbf{Q}^{-1}_{k|3} T_s - \lambda_{\mathbf{m}} \mathbf{Q}^{-1}_{k|3} \bar{\mathbf{A}}_k T_s \\ + \lambda_{\mathbf{m}} \bar{\mathbf{A}}_k^T \mathbf{Q}^{-1}_{k|3} \bar{\mathbf{A}}_k T_s^2 + (1 - \lambda_{\mathbf{m}}) \left(\mathbf{C}_k^T \mathbf{C}_k + \sigma_r \mathbf{D}^T \mathbf{D} \right). \end{aligned} \tag{3.48}$$

Combining (3.34) and (3.48) yields

$$\begin{aligned} \frac{\mathbf{Q}^{-1}_{k+1|3} - \mathbf{Q}^{-1}_{k|3}}{T_s} = -\frac{1 - e^{-\eta'_{\mathbf{m}} T_s}}{T_s} \mathbf{Q}^{-1}_{k|3} - e^{-\eta'_{\mathbf{m}} T_s} \bar{\mathbf{A}}_k^T \mathbf{Q}^{-1}_{k|3} - e^{-\eta'_{\mathbf{m}} T_s} \mathbf{Q}^{-1}_{k|3} \bar{\mathbf{A}}_k \\ + e^{-\eta'_{\mathbf{m}} T_s} \bar{\mathbf{A}}_k^T \mathbf{Q}^{-1}_{k|3} \bar{\mathbf{A}}_k T_s + \frac{1 - e^{-\eta'_{\mathbf{m}} T_s}}{T_s} \left(\mathbf{C}_k^T \mathbf{C}_k + \sigma'_r \mathbf{D}^T \mathbf{D} \right). \end{aligned} \tag{3.49}$$

By letting $T_s \to 0$, it follows from (3.49) that

$$\begin{aligned} \frac{d}{dt} \left(\mathbf{Q}^{-1}(t) \right) = -\eta'_{\mathbf{m}} \mathbf{Q}^{-1}(t) - \mathbf{A}'^T(t) \mathbf{Q}^{-1}(t) - \mathbf{Q}^{-1}(t) \mathbf{A}'(t) \\ + \eta'_{\mathbf{m}} \left(\mathbf{C}'^T(t) \mathbf{C}'(t) + \sigma'_r \mathbf{D}^T \mathbf{D} \right), \end{aligned} \tag{3.50}$$

with

$$\mathbf{A}'(t) = \lim_{T_s \to 0} \bar{\mathbf{A}}_k = \begin{bmatrix} 0 & \dot{\hat{\mathbf{u}}}^T(t) \\ \mathbf{0} & \alpha_{\boldsymbol{\omega}} \\ & \mathbf{0} \end{bmatrix}, \qquad \mathbf{C}'(t) = \lim_{T_s \to 0} \mathbf{C}_k = \begin{bmatrix} 1 & \boldsymbol{\omega}^T(t) \end{bmatrix}. \tag{3.51}$$

From (3.50), it directly follows that

$$\begin{aligned} \dot{\mathbf{Q}}(t) = \eta'_{\mathbf{m}} \mathbf{Q}(t) + \mathbf{Q}(t) \mathbf{A}'^T(t) + \mathbf{A}'(t) \mathbf{Q}(t) \\ - \eta'_{\mathbf{m}} \mathbf{Q}(t) \left(\mathbf{C}'^T(t) \mathbf{C}'(t) + \sigma'_r \mathbf{D}^T \mathbf{D} \right) \mathbf{Q}(t). \end{aligned} \tag{3.52}$$

Now, from (3.24) and (3.27), we have that

$$\begin{aligned}\mathbf{Q}_{k+1|3}^{-1}\hat{\mathbf{m}}_{k+1|3} = \lambda_{\mathbf{m}}\mathbf{A}_k^{-T}\mathbf{Q}_{k|3}^{-1}\hat{\mathbf{m}}_{k|3} + \alpha_{\boldsymbol{\omega}}^2\lambda_{\mathbf{m}}\mathbf{A}_k^{-T}\mathbf{Q}_{k|3}^{-1}\mathbf{A}_k^{-1}\mathbf{B}_k\hat{\mathbf{w}}_k \\ + (1-\lambda_{\mathbf{m}})\mathbf{C}_k^T(y_k - \alpha_{\boldsymbol{\omega}}^2\hat{v}_k).\end{aligned} \tag{3.53}$$

Using (3.47), we obtain that (3.53) can be written as

$$\begin{aligned}\mathbf{Q}_{k+1|3}^{-1}\hat{\mathbf{m}}_{k+1|3} = \lambda_{\mathbf{m}}\mathbf{Q}_{k|3}^{-1}\hat{\mathbf{m}}_{k|3} - \lambda_{\mathbf{m}}\bar{\mathbf{A}}_k^T\mathbf{Q}_{k|3}^{-1}\hat{\mathbf{m}}_{k|3}T_s + \alpha_{\boldsymbol{\omega}}^2\lambda_{\mathbf{m}}\mathbf{Q}_{k|3}^{-1}\mathbf{B}_k\bar{\mathbf{w}}_kT_s \\ - \alpha_{\boldsymbol{\omega}}^2\lambda_{\mathbf{m}}\bar{\mathbf{A}}_k^T\mathbf{Q}_{k|3}^{-1}\mathbf{B}_k\bar{\mathbf{w}}_kT_s^2 - \alpha_{\boldsymbol{\omega}}^2\lambda_{\mathbf{m}}\mathbf{Q}_{k|3}^{-1}\bar{\mathbf{A}}_k\mathbf{B}_k\bar{\mathbf{w}}_kT_s^2 \\ + \alpha_{\boldsymbol{\omega}}^2\lambda_{\mathbf{m}}\bar{\mathbf{A}}_k^T\mathbf{Q}_{k|3}^{-1}\bar{\mathbf{A}}_k\mathbf{B}_k\bar{\mathbf{w}}_kT_s^3 + (1-\lambda_{\mathbf{m}})\mathbf{C}_k^T(y_k - \alpha_{\boldsymbol{\omega}}^2\hat{v}_k).\end{aligned} \tag{3.54}$$

with

$$\bar{\mathbf{w}}_k = \frac{\hat{\mathbf{w}}_k}{T_s}. \tag{3.55}$$

From (3.34) and (3.54), it follows that

$$\begin{aligned}\frac{\mathbf{Q}_{k+1|3}^{-1}\hat{\mathbf{m}}_{k+1|3} - \mathbf{Q}_{k|3}^{-1}\hat{\mathbf{m}}_{k|3}}{T_s} = -\frac{1-e^{-\eta'_{\mathbf{m}}T_s}}{T_s}\mathbf{Q}_{k|3}^{-1}\hat{\mathbf{m}}_{k|3} - e^{-\eta'_{\mathbf{m}}T_s}\bar{\mathbf{A}}_k^T\mathbf{Q}_{k|3}^{-1}\hat{\mathbf{m}}_{k|3} \\ + \alpha_{\boldsymbol{\omega}}^2e^{-\eta'_{\mathbf{m}}T_s}\mathbf{Q}_{k|3}^{-1}\mathbf{B}_k\bar{\mathbf{w}}_k - \alpha_{\boldsymbol{\omega}}^2e^{-\eta'_{\mathbf{m}}T_s}\bar{\mathbf{A}}_k^T\mathbf{Q}_{k|3}^{-1}\mathbf{B}_k\bar{\mathbf{w}}_kT_s \\ - \alpha_{\boldsymbol{\omega}}^2e^{-\eta'_{\mathbf{m}}T_s}\mathbf{Q}_{k|3}^{-1}\bar{\mathbf{A}}_k\mathbf{B}_k\bar{\mathbf{w}}_kT_s + \alpha_{\boldsymbol{\omega}}^2e^{-\eta'_{\mathbf{m}}T_s}\bar{\mathbf{A}}_k^T\mathbf{Q}_{k|3}^{-1}\bar{\mathbf{A}}_k\mathbf{B}_k\bar{\mathbf{w}}_kT_s^2 \\ + \frac{1-e^{-\eta'_{\mathbf{m}}T_s}}{T_s}\mathbf{C}_k^T(y_k - \alpha_{\boldsymbol{\omega}}^2\hat{v}_k).\end{aligned} \tag{3.56}$$

For $T_s \to 0$, we obtain from (3.56) that

$$\begin{aligned}\frac{d}{dt}\left(\mathbf{Q}^{-1}(t)\hat{\mathbf{m}}(t)\right) = -\eta'_{\mathbf{m}}\mathbf{Q}^{-1}(t)\hat{\mathbf{m}}(t) - \mathbf{A}'^T\mathbf{Q}^{-1}(t)\hat{\mathbf{m}}(t) \\ + \alpha_{\boldsymbol{\omega}}^2\mathbf{Q}^{-1}(t)\mathbf{B}'\hat{\mathbf{w}}'(t) + \eta'_{\mathbf{m}}\mathbf{C}'^T(t)(y(t) - \alpha_{\boldsymbol{\omega}}^2\hat{v}'(t)),\end{aligned} \tag{3.57}$$

with

$$\mathbf{B}' = \lim_{T_s\to 0}\mathbf{B}_k = \lim_{T_s\to 0}\begin{bmatrix}\frac{1}{2\alpha_{\boldsymbol{\omega}}}\left(\frac{\hat{\mathbf{u}}_{k+1}-\hat{\mathbf{u}}_k}{T_s}\right)^T T_s \\ \mathbf{I}\end{bmatrix} = \begin{bmatrix}\mathbf{0} \\ \mathbf{I}\end{bmatrix} \tag{3.58}$$

and

$$\hat{\mathbf{w}}'(t) = \lim_{T_s\to 0}\bar{\mathbf{w}}_k = \mathbf{H}(\hat{\mathbf{u}}(t))\frac{\dot{\hat{\mathbf{u}}}(t)}{\alpha_{\boldsymbol{\omega}}}, \qquad \hat{v}'(t) = \lim_{T_s\to 0}\hat{v}_k = \frac{1}{2}\boldsymbol{\omega}^T(t)\mathbf{H}(\hat{\mathbf{u}}(t))\boldsymbol{\omega}(t), \tag{3.59}$$

where we used (3.15), (3.16) and (3.21) to obtain (3.58). Subsequently, from (3.50) and (3.57), it follows that

$$\begin{aligned}\dot{\hat{\mathbf{m}}}(t) = \left(\mathbf{A}' - \eta'_{\mathbf{m}}\sigma'_r\mathbf{Q}(t)\mathbf{D}^T\mathbf{D}\right)\hat{\mathbf{m}}(t) + \alpha_{\boldsymbol{\omega}}^2\mathbf{B}'\hat{\mathbf{w}}'(t) \\ + \eta'_{\mathbf{m}}\mathbf{Q}(t)\mathbf{C}'^T(t)(y(t) - \mathbf{C}'(t)\hat{\mathbf{m}}(t) - \alpha_{\boldsymbol{\omega}}^2\hat{v}'(t)).\end{aligned} \tag{3.60}$$

We note that (3.43), (3.45), (3.52) and (3.60) are equivalent to (2.16), (2.34), (2.33) and (2.32) in Section 2.3, respectively. Hence, under the tuning conditions in (3.34), the equations of the discrete-time controller in Section 3.3 and the equations of the continuous-time controller in Section 2.3 are equivalent for the limit as $T_s \to 0$.

Chapter 4

Self-driving extremum-seeking control for nonlinear dynamical plant

The vast majority of extremum-seeking methods rely on added perturbations to optimize the steady-state performance of a plant. Contrary to these perturbation-based methods, self-driving extremum-seeking methods do not require perturbations to obtain the optimal plant performance. One of the main advantages of such self-driving extremum seeking schemes is that asymptotic convergence to the true optimum can be achieved, instead of convergence to a neighborhood of the optimum. Moreover, the absence of perturbations eliminates one of the time scales present in classical extremum-seeking schemes, which potentially allows for a faster convergence. In this chapter, we present a novel easy-to-tune self-driving extremum-seeking controller. The stability analysis in this chapter shows that exponential convergence to the performance-optimal conditions is achieved for dynamical plants under the given assumptions. A simulation example illustrates the effectiveness of the presented approach.

4.1 Introduction

In the early heydays of extremum-seeking control in the 1950s and 1960s, many different types of extremum-seeking controllers were developed. In his survey, Sternby (1980) mentions four different types of extremum-seeking methods: perturbation methods, switching methods, self-driving systems and model-oriented methods. Since the introduction of the first extremum-seeking schemes, perturbation methods have been the most popular type of extremum-seeking methods; see Ariyur and Krstić (2003); Sternby (1980); Tan et al. (2010) and references therein. Although switching methods (Flärdh et al., 2005), self-driving systems (Hunnekens et al., 2014) and model-oriented methods (Fabri et al., 2015) have recently reappeared in the literature, they have received considerably less attention than perturbation methods.

In this chapter, we will focus on self-driving systems. Self-driving systems have two main advantages compared to the vast majority of perturbation methods.

First, asymptotic convergence to the optimal plant performance can be achieved instead of practical convergence, even in the presence of plant dynamics. Second, because no perturbations are used, a faster convergence towards the optimum may be achieved because there is no time scale associated with the perturbations, contrary to the perturbation methods in for example Krstić and Wang (2000); Tan et al. (2006).

A simple self-driving system for static plants is presented in the survey by Blackman (1962). Blackman (1962) proposes to divide the time derivative of the output of the plant by the time derivative of the input of the plant to obtain the gradient of the plant's input-to-output map. This gradient is subsequently used to drive the input to its the performance-optimal value. Frait and Eckman (1962) extended this idea to dynamical plants. To compensate for the effect of the plant dynamics, the use of a compensating filter is proposed, which mimics the effective delay due to the plant dynamics. The self-driving systems in Blackman (1962); Frait and Eckman (1962) are difficult to implement in practice due to use of a divider and differentiators, which are highly sensitive to noise. Moreover, the design of a suitable compensating filter requires explicit knowledge about the plant, which is generally not available. Recently, a new type of self-driving extremum-seeking controller was introduced in Hunnekens et al. (2014). Instead of using a divider and differentiators, Hunnekens et al. (2014) propose to use a least-squares estimator to extract the gradient of the plant's input-to-output map. The authors prove that the plant parameter converges to the extremum of the map under mild assumptions on the initial conditions if the plant is static. In addition, simulation results of a Hammerstein-type plant in Hunnekens et al. (2014) display that the proposed self-driving system can also be used to optimize dynamical plants. A similar observation was made in Guay and Dochain (2015), where a simulation example of a Wiener-type plant illustrates an asymptotic convergence of the plant parameter if the perturbation signal of the perturbation-based extremum-seeking controller in Guay and Dochain (2015) is omitted. However, neither Hunnekens et al. (2014) nor Guay and Dochain (2015) specify under which conditions these self-driving methods can successfully be applied to dynamical systems. Moreover, a formal stability proof of these self-driving methods is lacking because the stability proof in Hunnekens et al. (2014) does not consider dynamical systems and the plant-parameter signal without perturbations does not satisfy the uniform persistence-of-excitation assumption in Guay and Dochain (2015).

The main contributions of this chapter are summarized as follows. First, we we present a novel self-driving extremum-seeking controller. The controller is described by ordinary differential equations, which implies that no data buffers are required to store the input and output signals as in Hunnekens et al. (2014). The presented extremum-seeking scheme has only two tuning parameters, which makes it easy to tune. Second, a stability analysis is presented, which shows that exponential convergence of the plant parameter to its performance-optimal value

can be obtained for suitable initial conditions and tuning-parameter values. To the best of our knowledge, this is the first rigorous stability proof of self-driving systems for dynamical plants. In addition, a simulation example of a nonlinear dynamical plant is provided to illustrate the effectiveness of the presented self-driving extremum-seeking scheme.

This chapter is organized as follows. The extremum-seeking problem is formulated in Section 4.2. The self-driving extremum-seeking controller is presented in Section 4.3. The stability analysis of the resulting closed-loop scheme is presented in Section 4.4. An illustrative example of the proposed self-driving extremum-seeking method is given in Section 4.5. The findings in this chapter are summarized in Section 4.6.

4.2 Problem formulation

Consider a single-input-single-output nonlinear plant given by the following general state-space model:

$$\begin{aligned} \dot{\mathbf{x}}(t) &= \mathbf{f}(\mathbf{x}(t), u(t)) \\ y(t) &= h(\mathbf{x}(t), u(t)), \end{aligned} \tag{4.1}$$

with state $\mathbf{x} \in \mathbb{R}^{n_{\mathbf{x}}}$, state dimension $n_{\mathbf{x}} \in \mathbb{N}_{>0}$, input $u \in \mathbb{R}$, output $y \in \mathbb{R}$ and time $t \in \mathbb{R}_{\geq 0}$. The input u can be regarded as a tunable plant parameter. The state $\mathbf{x}$ and the functions $\mathbf{f}$ and h are unknown. The output y is a measure for the performance of the plant and is obtained by measurement. Although the relation between the input u and the output y is unknown, we consider the plant to be a cascade of three subsystems: a dynamical system, a static nonlinearity and a second dynamical system; see Figure 4.1. Let the dynamical subsystems (numbered one and two as in Figure 4.1) be given by the state-space models

$$\begin{aligned} \dot{\mathbf{x}}_i(t) &= \mathbf{f}_i(\mathbf{x}_i(t), u_i(t)) \\ y_i(t) &= h_i(\mathbf{x}_i(t), u_i(t)), \end{aligned} \tag{4.2}$$

for $i = 1, 2$, with states $\mathbf{x}_i \in \mathbb{R}^{n_{\mathbf{x}i}}$, inputs $u_i \in \mathbb{R}$ and outputs $y_i \in \mathbb{R}$, where the state dimensions $n_{\mathbf{x}i} \in \mathbb{N}_{>0}$ are such that $n_{\mathbf{x}} = n_{\mathbf{x}1} + n_{\mathbf{x}2}$. The input of the plant is the input of the first subsystem, that is $u = u_1$. The output of the plant is the output of the second subsystem, that is $y = y_2$. Moreover, let the static nonlinearity be denoted by G, such that

$$u_2(t) = G(y_1(t)). \tag{4.3}$$

If the dynamical subsystems of the plant are linear, then the plant is of the Wiener-Hammerstein type. Wiener-Hammerstein systems have proven to be useful in modelling real-life systems such as biological systems, diesel engines and

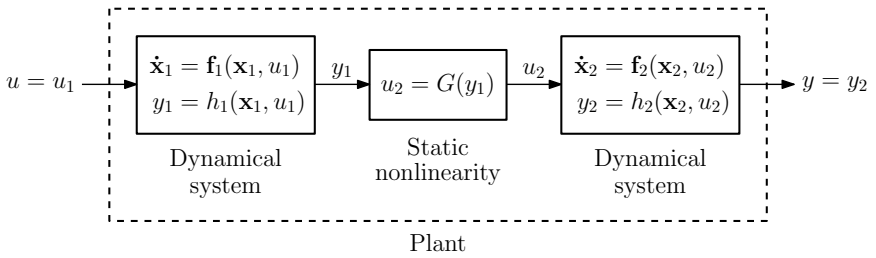

Figure 4.1: Plant consisting of two dynamical subsystems and a static nonlinearity.

systems in the process industry; see Moase and Manzie (2012b); Sternby (1980) and references therein. Extremum-seeking control for Wiener-Hammerstein-type plants is studied in several publications; see for example Ariyur and Krstić (2003); Moase and Manzie (2012b); Shekhar et al. (2014) and also Pervozvanskii (1960); Serdengecti (1956). Although not every nonlinear dynamical plant exhibits the above structure, we note that the class of plants that we consider in this chapter includes and exceeds the class of Wiener-Hammerstein systems, due to the fact that the dynamical plants are allowed to be nonlinear.

In line with our knowledge of the plant, the states $\mathbf{x}_1$ and $\mathbf{x}_2$ and the functions $\mathbf{f}_1$, h_1, $\mathbf{f}_2$, h_2 and G are considered to be unknown. For later computational ease, we make the following assumption regarding the smoothness of the functions $\mathbf{f}_1$, h_1, $\mathbf{f}_2$ and h_2.

Assumption 4.1. *For $i = 1, 2$, the functions $\mathbf{f}_i : \mathbb{R}^{n_{\mathbf{x}i}} \times \mathbb{R} \to \mathbb{R}^{n_{\mathbf{x}i}}$ and $h_i : \mathbb{R}^{n_{\mathbf{x}i}} \times \mathbb{R} \to \mathbb{R}$ are twice continuously differentiable. Moreover, there exist constants $L_{\mathbf{f}\mathbf{x}i}, L_{\mathbf{f}ui}, L_{h\mathbf{x}i}, L_{hui} \in \mathbb{R}_{>0}$ such that*

$$\left\| \frac{\partial \mathbf{f}_i}{\partial \mathbf{x}_i}(\mathbf{x}_i, u_i) \right\| \leq L_{\mathbf{f}\mathbf{x}i}, \qquad \left\| \frac{\partial \mathbf{f}_i}{\partial u_i}(\mathbf{x}_i, u_i) \right\| \leq L_{\mathbf{f}ui} \tag{4.4}$$

and

$$\left\| \frac{\partial h_i}{\partial \mathbf{x}_i}(\mathbf{x}_i, u_i) \right\| \leq L_{h\mathbf{x}i}, \qquad \left\| \frac{\partial h_i}{\partial u_i}(\mathbf{x}_i, u_i) \right\| \leq L_{hui} \tag{4.5}$$

for all $\mathbf{x}_i \in \mathbb{R}^{n_{\mathbf{x}i}}$ and all $u_i \in \mathbb{R}$.

We assume that for each constant input, the dynamical subsystems exhibit a constant steady-state response, which is formulated as follows.

Assumption 4.2. *For $i = 1, 2$, there exists a twice continuously differentiable map $\mathbf{X}_i : \mathbb{R} \to \mathbb{R}^{n_{\mathbf{x}i}}$ such that*

$$\mathbf{0} = \mathbf{f}_i(\mathbf{X}_i(u_i), u_i) \tag{4.6}$$

for all $u_i \in \mathbb{R}$. Moreover, there exists a constant $L_{\mathbf{X}i} \in \mathbb{R}_{>0}$ such that

$$\left\| \frac{\partial \mathbf{X}_i}{\partial u_i}(u_i) \right\| \leq L_{\mathbf{X}i} \tag{4.7}$$

for all $u_i \in \mathbb{R}$ and $i \in \{1, 2\}$.

Here, we note that the map $\mathbf{X}_i$ is the explicit solution of the implicit equation (4.6). Moreover, for each of the dynamical subsystems, we assume that the constant steady-state solution $\mathbf{x}_i = \mathbf{X}_i(u_i)$ is unique and globally exponentially stable, as formalized below.

Assumption 4.3. *For $i = 1, 2$, there exist constants $\mu_{\mathbf{x}i}, k_{\mathbf{x}i} \in \mathbb{R}_{>0}$ such that*

$$\|\tilde{\mathbf{x}}_i(t)\| \leq k_{\mathbf{x}i}\|\tilde{\mathbf{x}}_i(t_0)\|e^{-\mu_{\mathbf{x}i}(t-t_0)}, \tag{4.8}$$

with $\tilde{\mathbf{x}}_i(t) = \mathbf{x}_i(t) - \mathbf{X}_i(u_i)$, for all $\mathbf{x}_i(t_0) \in \mathbb{R}^{n_{\mathbf{x}i}}$, all $t \geq t_0 \geq 0$ and all constant $u_i \in \mathbb{R}$.

From this assumption, it follows that, for each constant input u_i, the dynamical subsystems have a unique constant steady-state output given by

$$y_i = F_i(u_i) = h_i(\mathbf{X}_i(u_i), u_i),\ i = 1, 2. \tag{4.9}$$

As a consequence, for each fixed input u, the plant has a unique constant steady-state output given by

$$y = F(u) = F_2(G(F_1(u))). \tag{4.10}$$

Recall that y is a measure of the plant performance. In this chapter, we assume that the lowest[1] steady-state value of y corresponds to the best plant performance. We refer to F as the objective function. We assume below that there exists a unique minimum of the objective function for which the steady-state plant performance is optimal as formulated in the following assumption.

Assumption 4.4. *The objective function $F : \mathbb{R} \to \mathbb{R}$ is twice continuously differentiable and exhibits a unique minimum on the domain $\mathbb{R}$ denoted by*

$$u^* = \arg\min_{u \in \mathbb{R}} F(u). \tag{4.11}$$

Moreover, the minimizer u^* corresponds to an extremum of the twice continuously differentiable map $G : \mathbb{R} \to \mathbb{R}$ such that

$$\frac{dG}{dy_1}(F_1(u^*)) = 0. \tag{4.12}$$

Furthermore, there exist constants $L_{F_1}, L_{F_2}, L_G \in \mathbb{R}_{>0}$ such that

$$\frac{dF}{du}(u)(u - u^*) \geq L_{F1}|u - u^*|^2 \tag{4.13}$$

and

$$\left|\frac{d^2F}{du^2}(u)\right| \leq L_{F2}, \qquad \left|\frac{d^2G}{dy_1^2}(y_1)\right| \leq L_G \tag{4.14}$$

for all $u, y_1 \in \mathbb{R}$.

[1] If the highest value of y corresponds to the best plant performance, the plant output can be defined as $-y$.

Because the functions $\mathbf{f}_1$, h_1, $\mathbf{f}_2$, h_2 and G are unknown, the maps $\mathbf{X}_1$, $\mathbf{X}_2$, F_1, F_2 and F are also unknown. Hence, the performance-optimizing plant-parameter value $u = u^*$ is unknown. In this chapter, we aim to drive the input u towards u^* by means of an extremum-seeking controller.

Remark 4.5. *Assumptions 4.1-4.4 can be relaxed by assuming that the given bounds hold only locally (that is, the bounds hold for all $\mathbf{x}_i$ in a neighborhood of $\mathbf{X}_i$, for all u in a neighborhood of u^* and for all y_1 in a neigborhood of $F_1(u^*)$) if a local extremum-seeking result is required. We emphasize that the presented structure of the plant is essential for the results in this chapter. It is important to note that the extremum-seeking algorithm in this chapter generally does not drive the input u towards u^* if the steady-state responses of the dynamical subsystems are not exponentially stable. For perturbation-based extremum-seeking schemes, on the other hand, often only asymptotic stability is required; see for example Tan et al. (2006).*

4.3 Self-driving extremum-seeking controller

In this section, we will introduce a self-driving extremum-seeking controller to steer the input u of the plant (4.1) towards its performance-optimizing value u^*. From Assumption 4.4, it follows that the input u will converge to u^* if u is steered in the gradient-descent direction of the objective function F in (4.10). The gradient of the objective function is unknown and needs to be estimated before it can be used for such purpose. To estimate the gradient of the objective function, we model the plant in a general form, where we assume that the plant input u is a continuously differentiable function of time. We define

$$\begin{aligned} m_1(t) &= F(u(t)) - Q_1(t)\frac{dF}{du}(u(t)), \\ m_2(t) &= \frac{dF}{du}(u(t)), \end{aligned} \tag{4.15}$$

where $Q_1(t)$ is a known function of time. In particular, we define $Q_1(t)$ as the solution of the differential equation

$$\dot{Q}_1(t) = -\eta Q_1(t) + \dot{u}(t), \tag{4.16}$$

with tuning parameter $\eta \in \mathbb{R}_{>0}$, where $\dot{u}$ is known and will be defined in (4.21). By taking the time derivatives of m_1 and m_2, and taking into account the plant dynamics (4.2)-(4.3), we obtain

$$\begin{aligned} \dot{m}_1(t) &= -Q_1(t)w(t) + \eta Q_1(t)m_2(t) \\ \dot{m}_2(t) &= w(t) \\ y(t) &= m_1(t) + Q_1(t)m_2(t) + z(t), \end{aligned} \tag{4.17}$$

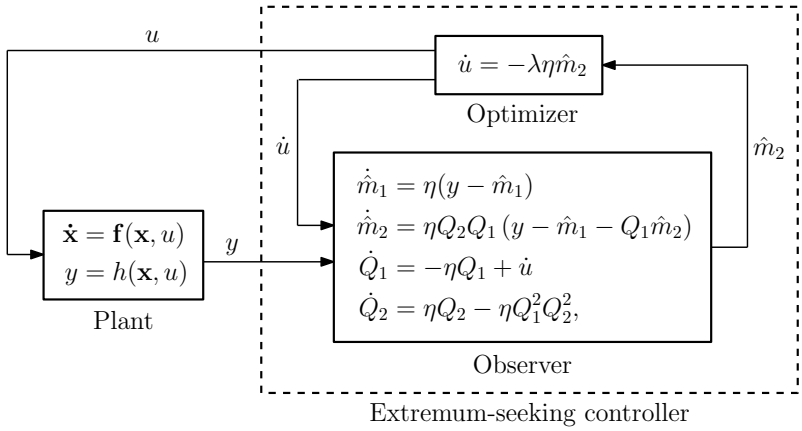

Figure 4.2: Self-driving extremum-seeking scheme.

with

$$\begin{aligned} w(t) &= \frac{d^2F}{du^2}(u(t))\dot{u}(t), \\ z(t) &= y(t) - F(u(t)). \end{aligned} \tag{4.18}$$

The signals w and z can be regarded as disturbances to the plant. We introduce the following observer for the plant (4.17):

$$\begin{aligned} \dot{\hat{m}}_1(t) &= \eta(y(t) - \hat{m}_1(t)) \\ \dot{\hat{m}}_2(t) &= \eta Q_2(t) Q_1(t) \left(y(t) - \hat{m}_1(t) - Q_1(t)\hat{m}_2(t)\right), \end{aligned} \tag{4.19}$$

where $Q_2(t)$ is the solution of the differential equation

$$\dot{Q}_2(t) = \eta Q_2(t) - \eta Q_1^2(t) Q_2^2(t), \tag{4.20}$$

with $Q_2(0) > 0$. We note that $\hat{m}_1$ and $\hat{m}_2$ are estimates for m_1 and m_2, respectively. Hence, $\hat{m}_2$ is an estimate for the gradient of the objective function.

To steer the input u of the plant (4.1) towards its performance-optimizing value, we introduce the gradient-descent optimizer

$$\dot{u}(t) = -\lambda\eta\hat{m}_2(t), \tag{4.21}$$

with tuning parameter $\lambda \in \mathbb{R}_{>0}$ and employing the gradient estimate $\hat{m}_2$. The resulting extremum-seeking scheme consisting of the plant and the extremum-seeking controller (that is, the observer and the optimizer) is illustrated in Figure 4.2.

4.4 Stability analysis

As for self-driving systems in general, selecting suitable initial condition and tuning-parameter values is essential for a successful convergence of the input u

to its performance-optimal value u^*. For example, if we choose the initial values of $\hat{m}_2$ and Q_1 equal to zero, u remains constant and will not converge to u^*. To identify suitable initial conditions $\mathbf{x}_1(0)$, $\mathbf{x}_2(0)$, $\hat{m}_1(0)$, $\hat{m}_2(0)$, $Q_1(0)$, $Q_2(0)$, $u(0)$ and tuning-parameter values λ, η, we present an in-depth stability analysis of the presented extremum-seeking scheme.

Let us define the following coordinate transformation:

$$\begin{aligned}
\tilde{\mathbf{x}}_i(t) &= \mathbf{x}_i(t) - \mathbf{X}_i(u_i(t)),\\
\tilde{m}_i(t) &= \hat{m}_i(t) - m_i(t),\\
\tilde{Q}_1(t) &= Q_1(t) + \lambda \frac{dF}{du}(u(t)),\\
\tilde{Q}_2(t) &= Q_2^{-1}(t) - \left(\lambda \frac{dF}{du}(u(t))\right)^2,\\
\tilde{u}(t) &= u(t) - u^*
\end{aligned} \tag{4.22}$$

for $i = 1, 2$. For notational convenience, we additionally introduce the transformation

$$\begin{aligned}
\tilde{\mathbf{x}}_1^u(t) &= \frac{\tilde{\mathbf{x}}_1(t)}{\tilde{u}(t)}, \qquad \tilde{\mathbf{x}}_2^u(t) = \frac{\tilde{\mathbf{x}}_2(t)}{\tilde{u}^2(t)}, \qquad \tilde{m}_1^u(t) = \frac{\tilde{m}_1(t)}{\tilde{u}^2(t)},\\
\tilde{m}_2^u(t) &= \frac{\tilde{m}_2(t)}{\tilde{u}(t)}, \qquad \tilde{Q}_1^u(t) = \frac{\tilde{Q}_1(t)}{\tilde{u}(t)}, \qquad \tilde{Q}_2^u(t) = \frac{\tilde{Q}_2(t)}{\tilde{u}^2(t)}.
\end{aligned} \tag{4.23}$$

We note that the transformation (4.23) is well defined if $\tilde{u}(t) \neq 0$. To specify the time domain for which the transformation is well defined, we introduce

$$t_f = \max\left\{\tau \in \mathbb{R}_{\geq 0} \cup \{\infty\} : \tilde{u}(t) \neq 0, \forall t \in [0, \tau)\right\}. \tag{4.24}$$

Hence, $t = t_f$ is the first time instance for which $\tilde{u}(t) = 0$, which implies that the transformation (4.23) is well defined for $0 \leq t < t_f$. We will show that the states in (4.23) remain arbitrarily small under suitable initial conditions and tuning conditions. We will do this in two steps: first, we show in Lemma 4.6 that the solutions of the dynamics governing the states in (4.23) satisfy bounds that imply local input-to-state stability if t_f is infinite; second, we invoke a local small-gain argument to show in Lemma 4.7 that the corresponding interconnection of the states in (4.23) is stable and that the bound on the solutions of $\tilde{m}_2^u$ can be made arbitrarily small under suitable initial conditions and tuning conditions.

Lemma 4.6. *Under Assumptions 4.1-4.4, there exist constants* $c_{\mathbf{x}11}, c_{\mathbf{x}12}, c_{\mathbf{x}21}, c_{\mathbf{x}22}, c_{\mathbf{x}23}, c_{\mathbf{x}24}, c_{Q11}, c_{Q12},$ $c_{Q21}, c_{Q22}, c_{Q23}, c_{Q24}, c_{m21}, c_{m22}, \ldots, c_{m27}, \rho_\lambda, \rho_\eta \in \mathbb{R}_{>0}$ *such that for any* $0 \leq t_1 \leq$

t_f the following bounds holds:

$$
\begin{aligned}
\sup_{0\le t<t_1} \|\tilde{\mathbf{x}}_1^u(t)\| &\le \max\left\{c_{\mathbf{x}11}\|\tilde{\mathbf{x}}_1^u(0)\|, \lambda\eta c_{\mathbf{x}12}\right\},\\
\sup_{0\le t<t_1} \|\tilde{\mathbf{x}}_2^u(t)\| &\le \max\Bigg\{c_{\mathbf{x}21}\|\tilde{\mathbf{x}}_2^u(0)\|, c_{\mathbf{x}22}\sup_{0\le t<t_1}\|\tilde{\mathbf{x}}_1^u(t)\|,\\
&\qquad c_{\mathbf{x}23}\sup_{0\le t<t_1}\|\tilde{\mathbf{x}}_1^u(t)\|^2, \lambda\eta c_{\mathbf{x}24}\Bigg\},\\
\sup_{0\le t<t_1} |\tilde{Q}_1^u(t)| &\le \max\Bigg\{c_{Q11}|\tilde{Q}_1^u(0)|, \lambda c_{Q12}\sup_{0\le t<t_1}|\tilde{m}_2^u(t)|, \lambda^2 c_{Q13}\Bigg\},\\
\sup_{0\le t<t_1} |\tilde{Q}_2^u(t)| &\le \max\Bigg\{c_{Q21}|\tilde{Q}_2^u(0)|, c_{Q22}\sup_{0\le t<t_1}|\tilde{Q}_1^u(t)|^2,\\
&\qquad \lambda c_{Q23}\sup_{0\le t<t_1}|\tilde{Q}_1^u(t)|, \lambda^3 c_{Q24}\Bigg\},\\
\sup_{0\le t<t_1} |\tilde{m}_2^u(t)\| &\le \max\Bigg\{\frac{1}{\lambda}c_{m21}|\tilde{m}_1^u(0)|, c_{m22}|\tilde{m}_2^u(0)|,\\
&\qquad \frac{1}{\lambda}c_{m23}\sup_{0\le t<t_1}\|\tilde{\mathbf{x}}_1^u(t)\|, \frac{1}{\lambda}c_{m24}\sup_{0\le t<t_1}\|\tilde{\mathbf{x}}_1^u(t)\|^2,\\
&\qquad \frac{1}{\lambda}c_{m25}\sup_{0\le t<t_1}\|\tilde{\mathbf{x}}_2^u(t)\|, c_{m26}\sup_{0\le t<t_1}|\tilde{Q}_1^u(t)|, \lambda c_{m27}\Bigg\}
\end{aligned}
\tag{4.25}
$$

for all $\lambda < \rho_\lambda$ and all $\eta < \rho_\eta$, if

$$
|\tilde{m}_2^u(t)| < 1 \quad \textit{and} \quad |\tilde{Q}_2^u(t)| < \lambda^2\frac{L_{F1}^2}{2} \tag{4.26}
$$

for all $0 \le t < t_1$.

Proof. See Section 4.7.1. □

Lemma 4.7. *Under Assumptions 4.1-4.4, for any constant $C \in \mathbb{R}_{>0}$, there exist constants $\varepsilon_{\mathbf{x}1}, \varepsilon_{\mathbf{x}2}, \varepsilon_{m1}, \varepsilon_{m_2}, \varepsilon_{Q1}$, $\varepsilon_{Q2}, \varepsilon_\eta, \varepsilon_\lambda \in \mathbb{R}_{>0}$ such that*

$$
\sup_{0\le t<t_f}|\tilde{m}_2^u(t)| < C \tag{4.27}
$$

for all $\|\tilde{\mathbf{x}}_1^u(0)\| < \lambda\varepsilon_{\mathbf{x}1}$, all $\|\tilde{\mathbf{x}}_2^u(0)\| < \lambda\varepsilon_{\mathbf{x}2}$, all $|\tilde{m}_1^u(0)| < \lambda\varepsilon_{m1}$, all $|\tilde{m}_2^u(0)| < \varepsilon_{m2}$, all $|\tilde{Q}_1^u(0)| < \lambda\varepsilon_{Q1}$, all $|\tilde{Q}_2^u(0)| < \lambda^2\varepsilon_{Q2}$, all $\eta < \varepsilon_\eta$ and all $\lambda < \varepsilon_\lambda$.

Proof. See Section 4.7.2. □

We note that (4.23) and (4.27) imply that $|\tilde{m}_2(t)| < C|\tilde{u}(t)|$ for $0 \le t < t_f$. Because the constant C can be chosen arbitrarily small, from (4.22), we obtain that the gradient estimate $\hat{m}_2$ remains arbitrarily close to the gradient $m_2 = \frac{dF}{du}(u)$ under the initial conditions and tuning conditions given in Lemma 4.7.

The gradient-descent optimizer in (4.21) steers the input u to its performance-optimizing value u^* if the gradient estimate $\hat{m}_2$ is sufficiently accurate. As a result, exponential convergence to the optimum is obtained in Theorem 4.8 for a sufficiently small constant C, with $t_f = \infty$.

Theorem 4.8. *Under Assumptions 4.1-4.4, there exist constants* $\mu_u, \varepsilon_{\mathbf{x}1}, \varepsilon_{\mathbf{x}2}, \varepsilon_{m1}, \varepsilon_{m_2}, \varepsilon_{Q1}, \varepsilon_{Q2}, \varepsilon_\eta, \varepsilon_\lambda \in \mathbb{R}_{>0}$ *such that*

$$|\tilde{u}(t)| \leq |\tilde{u}(0)| e^{-\lambda\eta\mu_u t} \tag{4.28}$$

for all $t \geq 0$, *all* $\tilde{u}(0) \in \mathbb{R} \setminus \{0\}$, *all* $\|\tilde{\mathbf{x}}_1(0)\| < \lambda\varepsilon_{\mathbf{x}1}|\tilde{u}(0)|$, *all* $\|\tilde{\mathbf{x}}_2(0)\| < \lambda\varepsilon_{\mathbf{x}2}|\tilde{u}(0)|^2$, *all* $|\tilde{m}_1(0)| < \lambda\varepsilon_{m1}|\tilde{u}(0)|^2$, *all* $|\tilde{m}_2(0)| < \varepsilon_{m2}|\tilde{u}(0)|$, *all* $|\tilde{Q}_1(0)| < \lambda\varepsilon_{Q1}|\tilde{u}(0)|$, *all* $|\tilde{Q}_2(0)| < \lambda^2\varepsilon_{Q2}|\tilde{u}(0)|^2$, *all* $\eta < \varepsilon_\eta$ *and all* $\lambda < \varepsilon_\lambda$.

Proof. From (4.15), (4.21) and (4.22), it follows that

$$\dot{\tilde{u}} = -\lambda\eta\frac{dF}{du}(u) - \lambda\eta\tilde{m}_2. \tag{4.29}$$

We introduce the Lyapunov-function candidate

$$V_u(\tilde{u}) = \tilde{u}^2. \tag{4.30}$$

From (4.29), we obtain that the time derivative of V_u is given by

$$\dot{V}_u(\tilde{u}) = -2\lambda\eta\tilde{u}\frac{dF}{du}(u) - 2\lambda\eta\tilde{u}\tilde{m}_2. \tag{4.31}$$

Now, let the constant C in Lemma 4.7 be given by $C = \frac{L_{F1}}{2}$, such that

$$|\tilde{m}_2| < \frac{L_{F1}}{2}|\tilde{u}| \tag{4.32}$$

under the conditions of Lemma 4.7, where we used $\tilde{m}_2^u = \frac{\tilde{m}_2}{\tilde{u}}$. From Assumption 4.4, (4.31) and (4.32), we obtain

$$-\lambda\eta(L_{F1} + 2L_{F2})\tilde{u}^2 \leq \dot{V}_u(\tilde{u}) \leq -\lambda\eta L_{F1}\tilde{u}^2. \tag{4.33}$$

From (4.30) and (4.33), it follows that

$$-\lambda\eta(L_{F1} + 2L_{F2})V_u(\tilde{u}) \leq \dot{V}_u(\tilde{u}) \leq -\lambda\eta L_{F1}V_u(\tilde{u}). \tag{4.34}$$

By applying the comparison lemma (Khalil, 2002, Lemma 3.4), we obtain

$$V_u(\tilde{u}(0))e^{-\lambda\eta(L_{F1}+2L_{F2})t} \leq V_u(\tilde{u}(t)) \leq V_u(\tilde{u}(0))e^{-\lambda\eta L_{F1}t} \tag{4.35}$$

for all $0 \leq t < t_f$.

We will prove by contradiction that $t_f = \infty$ if $\tilde{u}(0) \neq 0$. From the definition of t_f in (4.24) and the continuity of the solutions of $\tilde{u}$, it follows that $t_f > 0$ if

$\tilde{u}(0) \neq 0$. Suppose that t_f is a finite positive number. We note that $V_u(\tilde{u}) = 0$ if and only if $\tilde{u} = 0$. If $t_f > 0$, we must have that $\tilde{u}(0) \neq 0$, which implies that $V_u(\tilde{u}(0)) > 0$. Under the conditions of Lemma 4.7, we have that the bounds in (4.35) are satisfied for all $0 \leq t < t_f$. From (4.35) and the continuity of the solutions of V_u, it therefore follows that $V_u(\tilde{u}(t_f)) \geq V_u(\tilde{u}(0))e^{-\lambda\eta(L_{F1}+2L_{F2})t_f} > 0$, which implies that $\tilde{u}(t_f) \neq 0$. Therefore, we have that $\tilde{u}(t) \neq 0$ for all $0 \leq t \leq t_f$. From this and the continuity of the solutions of $\tilde{u}$, we conclude that there must exist some $t^* > t_f$ for which $\tilde{u}(t) \neq 0$ for all $0 \leq t < t^*$. This contradicts the definition of t_f in (4.24). Hence, t_f cannot be zero or a finite positive number and must be infinite. Theorem 4.8 follows from (4.23), (4.30) and (4.35), with $\mu_u = \frac{L_{F1}}{2}$ and $\varepsilon_{\mathbf{x}1}, \varepsilon_{\mathbf{x}2}, \varepsilon_{m1}, \varepsilon_{m_2}, \varepsilon_{Q1}, \varepsilon_{Q2}, \varepsilon_\eta, \varepsilon_\lambda$ as defined in Lemma 4.7. □

4.4.1 Discussion

From (4.22) and Theorem 4.8, it follows that, for any $u(0) \neq u^*$, the input u of the plant (4.1) exponentially converges to its performance-optimal value u^* under the initial conditions and tuning conditions of Theorem 4.8. Moreover, we obtain that the closer $u(0)$ is to u^* and the smaller the tuning parameter λ is, the closer $\mathbf{x}_1(0)$, $\mathbf{x}_2(0)$, $\hat{m}_1(0)$, $\hat{m}_2(0)$, $Q_1(0)$ and $Q_2(0)$ are required to be to $\mathbf{X}_1(u(0))$, $\mathbf{X}_2(u(0))$, $m_1(0)$, $m_2(0)$, $-\lambda\frac{dF}{du}(u(0))$ and $\left(\lambda\frac{dF}{du}(u(0))\right)^{-2}$, respectively, to guarantee exponential convergence. To obtain a fast convergence, high values of the tuning parameters λ and η should be chosen. However, too high values may result in an unstable extremum-seeking scheme.

From Assumption 4.3, it follows that the steady-state solutions of the dynamical subsystems of the plant are exponentially stable. Therefore, one can ensure that $\mathbf{x}_1(0)$ and $\mathbf{x}_2(0)$ are sufficiently close to $\mathbf{X}_1(u(0))$ and $\mathbf{X}_2(u(0))$, respectively, by keeping the plant parameter constant for a sufficiently long time before the adaptation of the extremum-seeking scheme is turned on at time $t = 0$. Similarly, by keeping the plant parameter constant, the (measured) output y converges to its steady-state value $F(u(0))$. Therefore, y is an accurate estimate of $F(u(0))$ if the plant parameter is kept constant for a sufficiently long time. To ensure that $\hat{m}_1(0)$, $\hat{m}_2(0)$, $Q_1(0)$ and $Q_2(0)$ are sufficiently close to $m_1(0)$, $m_2(0)$, $-\lambda\frac{dF}{du}(u(0))$ and $\left(\lambda\frac{dF}{du}(u(0))\right)^{-2}$, respectively, we additionally require a sufficiently accurate initial estimate of gradient of the map F. An accurate initial gradient estimate can be obtained using a finite-difference approach or by using the observer of the extremum-seeking controller while slowly perturbing the plant parameter.

4.4.2 Aspects of numerical implementation and measurement noise

The time derivative of u converges to zero as u exponentially converges to u^*. As a result, Q_1 becomes increasingly smaller and Q_2 continuously grows as the plant parameter u converges to u^*; see (4.16) and (4.20). A too large value of Q_2 may affect the numerical stability of the extremum-seeking algorithm. Moreover,

because Q_2 serves as an amplification gain for measurement noise in the system (see the second equation of (4.19)), noise-related issues may arise if Q_2 becomes too large. To maintain numerical stability and limit the effect of measurement noise, one could turn off the adaptation of the plant parameter if Q_2 become too large, as suggested in Hunnekens et al. (2014). Alternatively, one could add a regularization term to the observer to bound Q_2, similar to Guay and Dochain (2015) and Chapter 2, which leads to

$$\dot{\hat{m}}_2(t) = \eta Q_2(t) Q_1(t) \left(y(t) - \hat{m}_1(t) - Q_1(t)\hat{m}_2(t)\right) - \sigma \eta Q_2(t) \hat{m}_2(t) \tag{4.36}$$

and

$$\dot{Q}_2(t) = \eta Q_2(t) - \eta Q_1^2(t) Q_2^2(t) - \sigma \eta Q_2^2(t), \tag{4.37}$$

where $\sigma \in \mathbb{R}_{>0}$ is a (small) regularization constant. It should be noted that turning off the adaptation or adding a regularization term prevents the plant parameter u from converging to u^*. In the absence of numerical discrepancies and measurement noise, with any of these two modifications, the plant parameter u converges to a neighborhood of the optimal value u^*, where the size of the neighborhood can be made arbitrarily small by turning off the adaptation only for sufficiently large values of Q_2 or by making the regularization constant σ sufficiently small, respectively. The level of numerical discrepancies and the level of measurement noise determine which turn-off values of Q_2 or which values of the regularization constant are appropriate.

4.5 Example

Consider a nonlinear plant of the form (4.2)-(4.3) (with the cascaded structure as in Figure 4.1), with $u = u_1$, $y = y_2$ and

$$\begin{aligned}
\dot{x}_1(t) &= -x_1(t) - x_1^3(t) + u_1(t) \\
y_1(t) &= x_1(t) \\
u_2(t) &= (y_1(t) - 2)^2 \\
\dot{x}_2(t) &= -x_2(t) - \arctan(x_2(t)) + u_2(t) \\
y_2(t) &= x_2(t).
\end{aligned} \tag{4.38}$$

Note that this system satisfies Assumption 4.1 for arbitrarily large compact sets; see also Remark 4.5. From (4.38) and the implicit function theorem, we have that

$$\frac{dX_1}{du_1}(u_1) = \frac{1}{1 + 3X_1^2(u_1)}, \qquad \frac{dX_2}{du_2}(u_2) = \frac{1 + X_2^2(u_2)}{2 + X_2^2(u_2)}, \tag{4.39}$$

with $X_1(0) = X_2(0) = 0$. This implies that Assumption 4.2 is satisfied. Assumption 4.3 is satisfied because both the x_1- and x_2-dynamics exhibit a unique globally exponentially stable equilibrium point for constant values of u. Finally,

because $F_1(u_1) = X_1(u_1)$ and $F_2(u_2) = X_2(u_2)$ are monotonic functions, Assumption 4.4 on the existence of a unique minimum for the objective function $F(u) = F_2(G(F_1(u)))$, with $G(y_1) = (y_1 - 2)^2$, is also satisfied for arbitrarily large compact sets.

Next, in Figures 4.3-4.7 we present simulation results for the following parameter setting for the extremum seeking controller: $\lambda = 40$, $\eta = 1$. Moreover, the regularization constant in the observer for the gradient estimate, see Section 4.4.2, has been set to $\sigma = 10^{-12}$. We observe in Figure 4.3 that the performance variable y indeed converges to a very small neighborhood of the optimum (minimum). Figure 4.4 shows the asymptotic convergence of the input u to its optimal value $u^* = 10$. Figures 4.5 and 4.6 display the convergence of the states x_1 and x_2 of the plant to their optimal steady states. Figure 4.7 illustrates the quality of the gradient estimate using the proposed observer. Clearly, the absence of (dither) perturbations in the proposed self-driving extremum seeking controller allows for such a smooth asymptotic convergence towards the optimum.

4.6 Conclusion

In this chapter, we have presented a self-driving extremum-seeking controller that optimizes the steady-state performance of a class of nonlinear dynamical plants under the given assumptions. The stability analysis in this chapter shows that exponential convergence to the performance-optimal condition can be achieved under suitable initial conditions and tuning conditions. To the best of our knowledge, this is the first rigorous stability proof for self-driving extremum-seeking schemes with dynamical plants. A simulation example displays the effectiveness of the presented extremum-seeking approach.

4.7 Appendix

4.7.1 Proof of Lemma 4.6

We will derive the bounds in Lemma 4.6 one by one. Although, we do not explicitly mention it for every step of the derivations below, we note that the bounds are derived for $0 \leq t < t_1 \leq t_f$, which implies that $\tilde{u}(t) \neq 0$ for all $0 \leq t < t_1$. Moreover, we note that the following lemma (converse stability result) holds under Assumptions 4.1-4.3 for constant u_i, with $i = 1, 2$.

Lemma 4.9. *For $i = 1, 2$, under Assumptions 4.1-4.3, there exist functions $W_{\mathbf{x}i} : \mathbb{R}^{n_{\mathbf{x}i}} \times \mathbb{R} \to \mathbb{R}$ and constants $\gamma_{Wi1}, \gamma_{Wi2}, \gamma_{Wi3}, \gamma_{Wi4}, \gamma_{Wi5} \in \mathbb{R}_{>0}$ such that the inequalities*

$$\gamma_{Wi1}\|\tilde{\mathbf{x}}_i\|^2 \leq W_{\mathbf{x}i}(\tilde{\mathbf{x}}_i, u_i) \leq \gamma_{Wi2}\|\tilde{\mathbf{x}}_i\|^2, \tag{4.40}$$

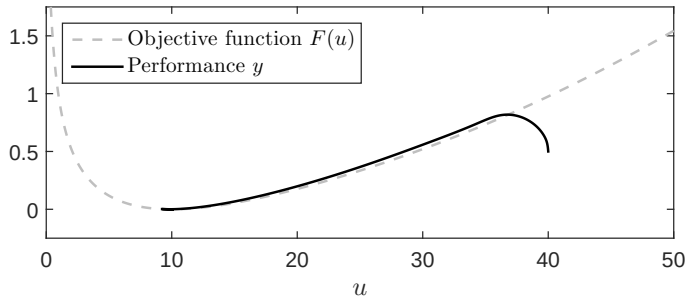

Figure 4.3: Plant performance as a function of time.

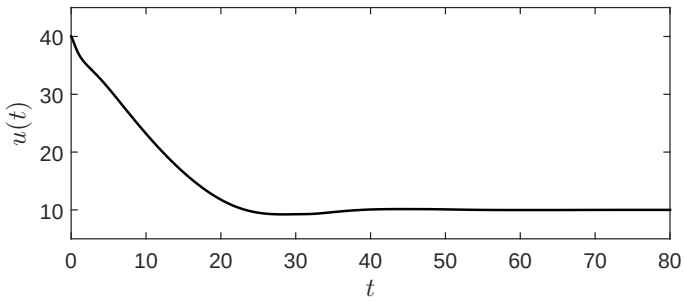

Figure 4.4: Plant parameter as a function of time.

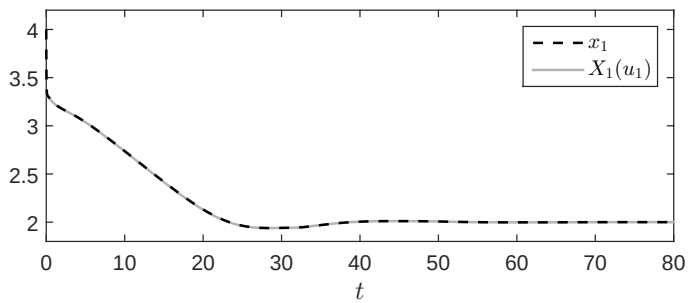

Figure 4.5: State x_1 and $X_1(u_1)$ as a function of time.

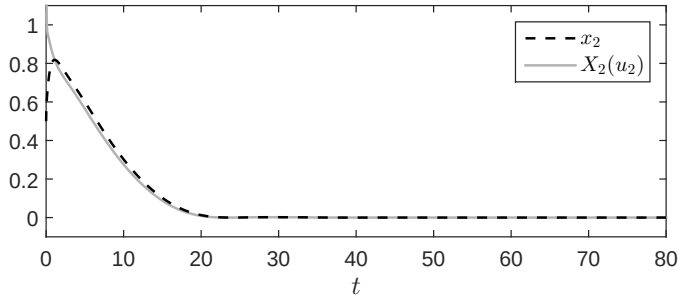

Figure 4.6: State x_2 and $X_2(u_2)$ as a function of time.

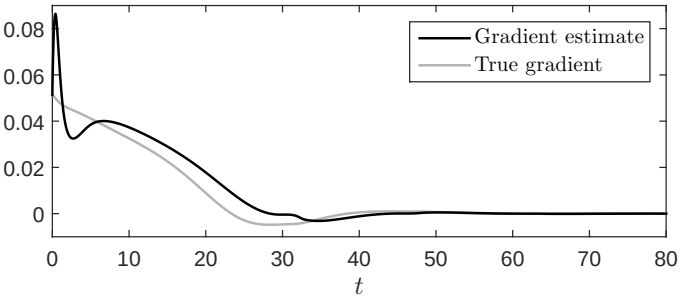

Figure 4.7: Gradient estimate and the true gradient as a function of time.

$$\frac{\partial W_{\mathbf{x}i}}{\partial \tilde{\mathbf{x}}_i}(\tilde{\mathbf{x}}_i, u_i)\mathbf{f}_i(\tilde{\mathbf{x}}_i + \mathbf{X}_i(u_i), u_i) \leq -\gamma_{Wi3}\|\tilde{\mathbf{x}}_i(t)\|^2, \tag{4.41}$$

$$\left\|\frac{\partial W_{\mathbf{x}i}}{\partial \tilde{\mathbf{x}}_i}(\tilde{\mathbf{x}}_i, u_i)\right\| \leq \gamma_{Wi4}\|\tilde{\mathbf{x}}_i\|, \tag{4.42}$$

$$\left\|\frac{\partial W_{\mathbf{x}i}}{\partial u_i}(\tilde{\mathbf{x}}_i, u_i)\right\| \leq \gamma_{Wi5}\|\tilde{\mathbf{x}}_i\| \tag{4.43}$$

are satisfied for all $\tilde{\mathbf{x}}_i \in \mathbb{R}^{n_{\mathbf{x}i}}$ *and all* $u_i \in \mathbb{R}$.

Proof. The proof follows similar lines as the proof of Lemma 2.15 in Section 2.7.1. □

To derive the bound on $\tilde{\mathbf{x}}_1^u$, we introduce the Lyapunov-function candidate

$$V_{\mathbf{x}1}(\tilde{\mathbf{x}}_1, \tilde{u}) = \frac{1}{\tilde{u}^2}W_{\mathbf{x}1}(\tilde{\mathbf{x}}_1, u_1), \tag{4.44}$$

with $u_1 = \tilde{u} + u^*$, where $W_{\mathbf{x}1}$ is defined in Lemma 4.9. We note that, from Lemma 4.9, it follows that

$$\gamma_{W11}\|\tilde{\mathbf{x}}_1^u\|^2 \leq V_{\mathbf{x}1}(\tilde{\mathbf{x}}_1, \tilde{u}) \leq \gamma_{W12}\|\tilde{\mathbf{x}}_1^u\|^2. \tag{4.45}$$

From (4.2) and (4.22), we have

$$\dot{\tilde{\mathbf{x}}}_1 = \mathbf{f}_1(\tilde{\mathbf{x}}_1 + \mathbf{X}_1(u_1), u_1) - \frac{d\mathbf{X}_1}{du_1}(u_1)\dot{u}_1. \tag{4.46}$$

By taking the time derivative of $V_{\mathbf{x}1}$ and substituting (4.46), we obtain

$$\begin{aligned}\dot{V}_{\mathbf{x}1}(\tilde{\mathbf{x}}_1, \tilde{u}) = {} & \frac{1}{\tilde{u}^2}\frac{\partial W_{\mathbf{x}1}}{\partial \tilde{\mathbf{x}}_1}(\tilde{\mathbf{x}}_1, u_1)\mathbf{f}_1(\tilde{\mathbf{x}}_1 + \mathbf{X}_1(u_1), u_1) \\ & + \frac{1}{\tilde{u}}\left(\frac{\partial W_{\mathbf{x}1}}{\partial u_1} - \frac{\partial W_{\mathbf{x}1}}{\partial \tilde{\mathbf{x}}_1}(\tilde{\mathbf{x}}_1, u_1)\frac{d\mathbf{X}_1}{du_1}(u_1)\right)\frac{\dot{u}_1}{\tilde{u}} - 2V_{\mathbf{x}1}(\tilde{\mathbf{x}}_1, \tilde{u})\frac{\dot{\tilde{u}}}{\tilde{u}}.\end{aligned} \tag{4.47}$$

From Assumption 4.4, it follows that $\left|\frac{dF}{du}(u)\right| \leq L_{F2}|\tilde{u}|$. Then, from (4.23) and (4.29), we obtain

$$\left|\frac{\dot{\tilde{u}}}{\tilde{u}}\right| \leq \lambda\eta(L_{F2} + |\tilde{m}_2^u|). \tag{4.48}$$

By noting that $\dot{u}_1 = \dot{\tilde{u}}$, from Assumption 4.2, Lemma 4.9, (4.47) and (4.48), we obtain

$$\begin{aligned}\dot{V}_{\mathbf{x}1}(\tilde{\mathbf{x}}_1, \tilde{u}) \leq {} & -\gamma_{W13}\|\tilde{\mathbf{x}}_1^u\|^2 + 2\lambda\eta V_{\mathbf{x}1}(\tilde{\mathbf{x}}_1, \tilde{u})\left(L_{F2} + |\tilde{m}_2^u|\right) \\ & + \lambda\eta\left(\gamma_{W15} + \gamma_{W14}L_{\mathbf{X}1}\right)\|\tilde{\mathbf{x}}_1^u\|\left(L_{F2} + |\tilde{m}_2^u|\right).\end{aligned} \tag{4.49}$$

From (4.45) and Young's inequality, it subsequently follows that

$$\begin{aligned}\dot{V}_{\mathbf{x}1}(\tilde{\mathbf{x}}_1,\tilde{u}) \leq & -\frac{\gamma_{W13}}{2\gamma_{W12}}V_{\mathbf{x}1}(\tilde{\mathbf{x}}_1,\tilde{u}) + 2\lambda\eta V_{\mathbf{x}1}(\tilde{\mathbf{x}}_1,\tilde{u})\left(L_{F2}+|\tilde{m}_2^u|\right) \\ & + \lambda^2\eta^2\frac{1}{2\gamma_{W13}}\left(\gamma_{W15}+\gamma_{W14}L_{\mathbf{X}1}\right)^2\left(L_{F2}+|\tilde{m}_2^u|\right)^2.\end{aligned} \tag{4.50}$$

From this, it follows that

$$\dot{V}_{\mathbf{x}1}(\tilde{\mathbf{x}}_1,\tilde{u}) \leq -\frac{\gamma_{W13}}{4\gamma_{W12}}V_{\mathbf{x}1}(\tilde{\mathbf{x}}_1,\tilde{u}) + \lambda^2\eta^2\frac{1}{2\gamma_{W13}}\left(\gamma_{W15}+\gamma_{W14}L_{\mathbf{X}1}\right)^2\left(L_{F2}+1\right)^2, \tag{4.51}$$

if $|\tilde{m}_2^u| < 1$, which holds by (4.26) in the lemma, and $\lambda\eta < \frac{\gamma_{W13}}{8\gamma_{W12}(L_{F2}+1)}$. By applying the comparison lemma (Khalil, 2002, Lemma 3.4), we obtain

$$\begin{aligned}V_{\mathbf{x}1}(\tilde{\mathbf{x}}_1(t),\tilde{u}(t)) \leq & \, V_{\mathbf{x}1}(\tilde{\mathbf{x}}_1(0),\tilde{u}(0))e^{-\frac{\gamma_{W13}}{4\gamma_{W12}}t} \\ & + \lambda^2\eta^2\frac{2\gamma_{W12}}{\gamma_{W13}^2}\left(\gamma_{W15}+\gamma_{W14}L_{\mathbf{X}1}\right)^2\left(L_{F2}+1\right)^2,\end{aligned} \tag{4.52}$$

for all $0 \leq t < t_1$, if $\sup_{0\leq t<t_1}|\tilde{m}_2^u(t)| < 1$ and $\lambda\eta < \frac{\gamma_{W13}}{8\gamma_{W12}(L_{F2}+1)}$. The bound on $\tilde{\mathbf{x}}_1^u$ of Lemma 4.6 follows from (4.45) and (4.52), with $c_{\mathbf{x}11} = \sqrt{\frac{2\gamma_{W12}}{\gamma_{W11}}}$ and $c_{\mathbf{x}12} = \frac{2}{\gamma_{W13}}\sqrt{\frac{\gamma_{W12}}{\gamma_{W11}}}\left(\gamma_{W15}+\gamma_{W14}L_{\mathbf{X}1}\right)\left(L_{F2}+1\right)$.

Similarly, to derive the bound on $\tilde{\mathbf{x}}_2^u$, we introduce the Lyapunov-function candidate

$$V_{\mathbf{x}2}(\tilde{\mathbf{x}}_1,\tilde{\mathbf{x}}_2,\tilde{u}) = \frac{1}{\tilde{u}^4}W_{\mathbf{x}2}(\tilde{\mathbf{x}}_2,u_2), \tag{4.53}$$

with $u_2 = G(h_1(\mathbf{x}_1,u_1))$, $\mathbf{x}_1 = \tilde{\mathbf{x}}_1 + \mathbf{X}_1(u_1)$ and $u_1 = \tilde{u}+u^*$, where $W_{\mathbf{x}2}$ is defined in Lemma 4.9. Similar to (4.45), we note that

$$\gamma_{W21}\|\tilde{\mathbf{x}}_2^u\|^2 \leq V_{\mathbf{x}2}(\tilde{\mathbf{x}}_1,\tilde{\mathbf{x}}_2,\tilde{u}) \leq \gamma_{W22}\|\tilde{\mathbf{x}}_2^u\|^2. \tag{4.54}$$

From (4.2) and (4.22), we have

$$\dot{\tilde{\mathbf{x}}}_2 = \mathbf{f}_2(\tilde{\mathbf{x}}_2+\mathbf{X}_2(u_2),u_2) - \frac{d\mathbf{X}_2}{du_2}(u_2)\dot{u}_2. \tag{4.55}$$

Taking the time derivative of $V_{\mathbf{x}2}$ and substituting (4.55) yields

$$\begin{aligned}\dot{V}_{\mathbf{x}2}(\tilde{\mathbf{x}}_1,\tilde{\mathbf{x}}_2,\tilde{u}) = & \frac{1}{\tilde{u}^4}\frac{\partial W_{\mathbf{x}2}}{\partial\tilde{\mathbf{x}}_2}(\tilde{\mathbf{x}}_2,u_2)\mathbf{f}_2(\tilde{\mathbf{x}}_2+\mathbf{X}_2(u_2),u_2) - 4V_{\mathbf{x}2}(\tilde{\mathbf{x}}_1,\tilde{\mathbf{x}}_2,\tilde{u})\frac{\dot{\tilde{u}}}{\tilde{u}} \\ & + \frac{1}{\tilde{u}^2}\left(\frac{\partial W_{\mathbf{x}2}}{\partial u_2}(\tilde{\mathbf{x}}_2,u_2) - \frac{\partial W_{\mathbf{x}2}}{\partial\tilde{\mathbf{x}}_2}(\tilde{\mathbf{x}}_2,u_2)\frac{d\mathbf{X}_2}{du_2}(u_2)\right)\frac{\dot{u}_2}{\tilde{u}^2}.\end{aligned} \tag{4.56}$$

From $u_2 = G(h_1(\mathbf{x}_1,u_1))$, it follows that

$$\dot{u}_2 = \frac{dG}{dy_1}(h_1(\mathbf{x}_1,u_1))\left(\frac{\partial h_1}{\partial\mathbf{x}_1}(\mathbf{x}_1,u_1)\dot{\mathbf{x}}_1 + \frac{\partial h_1}{\partial u_1}(\mathbf{x}_1,u_1)\dot{u}_1\right). \tag{4.57}$$

Using Assumption 4.4 and (4.9), we note that

$$\begin{aligned}\frac{dG}{dy_1}(h_1(\mathbf{x}_1,u)) = \frac{dG}{dy_1}(h_1(\mathbf{x}_1,u)) - \frac{dG}{dy_1}(h_1(\mathbf{X}_1(u),u)) \\ + \frac{dG}{dy_1}(F_1(u)) - \frac{dG}{dy_1}(F_1(u^*)).\end{aligned} \tag{4.58}$$

From Assumptions 4.1 and 4.4 and from (4.22), we have

$$\begin{aligned}&\left|\frac{dG}{dy_1}(h_1(\mathbf{x}_1,u)) - \frac{dG}{dy_1}(h_1(\mathbf{X}_1(u),u))\right| \\ &= \left|\int_0^1 \frac{d^2G}{dy_1^2}(h_1(\tilde{\mathbf{x}}_1\sigma + \mathbf{X}_1(u),u))\frac{\partial h_1}{\partial \tilde{\mathbf{x}}_1}(\tilde{\mathbf{x}}_1\sigma + \mathbf{X}_1(u),u)d\sigma\tilde{\mathbf{x}}_1\right| \leq L_G L_{h\mathbf{x}1}\|\tilde{\mathbf{x}}_1\|.\end{aligned} \tag{4.59}$$

From Assumptions 4.1-4.2 and (4.9), it follows that

$$\left|\frac{dF_1}{du_1}(u_1)\right| = \left|\frac{\partial h_1}{\partial \mathbf{x}_1}(\mathbf{X}_1(u_1),u_1)\frac{d\mathbf{X}_i}{du_1}(u_1) + \frac{\partial h_1}{\partial u_1}(\mathbf{X}_1(u_1),u_1)\right| \leq L_{F3} \tag{4.60}$$

for all $u_1 \in \mathbb{R}$, with $L_{F3} = L_{h\mathbf{x}1}L_{\mathbf{X}1} + L_{hu1}$. Therefore, from Assumption 4.4 and (4.60) and from (4.22), we obtain

$$\begin{aligned}\left|\frac{dG}{dy_1}(F_1(u)) - \frac{dG}{dy_1}(F_1(u^*))\right| &= \left|\int_0^1 \frac{d^2G}{dy_1^2}(F_1(\tilde{u}\sigma + u^*))\frac{dF_1}{du_1}(\tilde{u}\sigma + u^*)d\sigma\tilde{u}\right| \\ &\leq L_G L_{F3}|\tilde{u}|.\end{aligned} \tag{4.61}$$

By combining (4.58), (4.59) and (4.61), we obtain

$$\left|\frac{dG}{dy_1}(h_1(\mathbf{x}_1,u))\right| \leq L_G(L_{h\mathbf{x}1}\|\tilde{\mathbf{x}}_1\| + L_{F3}|\tilde{u}|). \tag{4.62}$$

From Assumptions 4.1-4.2, (4.2) and (4.22), we have

$$\begin{aligned}|\dot{\mathbf{x}}_1| &= |\mathbf{f}(\mathbf{x}_1,u_1) - \mathbf{f}_1(\mathbf{X}_1(u_1),u_1)| \\ &= \left|\int_0^1 \frac{\partial \mathbf{f}_1}{\partial \mathbf{x}_1}(\tilde{\mathbf{x}}_1\sigma + \mathbf{X}_1(u_1),u_1)d\sigma\tilde{\mathbf{x}}_1\right| \leq L_{\mathbf{f}\mathbf{x}1}\|\tilde{\mathbf{x}}_1\|.\end{aligned} \tag{4.63}$$

Then, from Assumption 4.1, (4.23), (4.48), (4.57), (4.62), (4.63) and $\dot{u}_1 = \dot{\tilde{u}}$, it follows that

$$\left|\frac{\dot{u}_2}{\tilde{u}^2}\right| \leq L_G(L_{h\mathbf{x}1}\|\tilde{\mathbf{x}}_1^u\| + L_{F3})\left(L_{h\mathbf{x}1}L_{\mathbf{f}\mathbf{x}1}\|\tilde{\mathbf{x}}_1^u\| + \lambda\eta L_{hu1}(L_{F2} + |\tilde{m}_2^u|)\right) \tag{4.64}$$

Now, by applying the bounds in Lemma 4.9, (4.48) and (4.64) to (4.56), we obtain

$$\begin{aligned}\dot{V}_{\mathbf{x}2}(\tilde{\mathbf{x}}_1,\tilde{\mathbf{x}}_2,\tilde{u}) \leq -\gamma_{W23}\|\tilde{\mathbf{x}}_2^u\|^2 + (\gamma_{W25} + \gamma_{W24}L_{\mathbf{X}2})\|\tilde{\mathbf{x}}_2^u\|L_G(L_{h\mathbf{x}1}\|\tilde{\mathbf{x}}_1^u\| + L_{F3}) \\ \times (L_{h\mathbf{x}1}L_{\mathbf{f}\mathbf{x}1}\|\tilde{\mathbf{x}}_1^u\| + \lambda\eta L_{hu1}(L_{F2} + |\tilde{m}_2^u|)) \\ + 4\lambda\eta V_{\mathbf{x}2}(\tilde{\mathbf{x}}_1,\tilde{\mathbf{x}}_2,\tilde{u})(L_{F2} + |\tilde{m}_2^u|).\end{aligned} \tag{4.65}$$

From (4.54) and Young's inequality, it subsequently follows that

$$\begin{aligned}\dot{V}_{\mathbf{x}2}(\tilde{\mathbf{x}}_1,\tilde{\mathbf{x}}_2,\tilde{u}) \leq & -\frac{\gamma_{W23}}{2\gamma_{W22}}V_{\mathbf{x}2}(\tilde{\mathbf{x}}_1,\tilde{\mathbf{x}}_2,\tilde{u})+\frac{1}{2\gamma_{W23}}L_G^2\left(\gamma_{W25}+\gamma_{W24}L_{\mathbf{X}2}\right)^2\\ &\times\left(L_{h\mathbf{x}1}\|\tilde{\mathbf{x}}_1^u\|+L_{F3}\right)^2\left(L_{h\mathbf{x}1}L_{\mathbf{fx}1}\|\tilde{\mathbf{x}}_1^u\|+\lambda\eta L_{hu1}(L_{F2}+|\tilde{m}_2^u|)\right)^2\\ &+4\lambda\eta V_{\mathbf{x}2}(\tilde{\mathbf{x}}_1,\tilde{\mathbf{x}}_2,\tilde{u})(L_{F2}+|\tilde{m}_2^u|).\end{aligned} \tag{4.66}$$

From this, we obtain that

$$\begin{aligned}\dot{V}_{\mathbf{x}2}(\tilde{\mathbf{x}}_1,\tilde{\mathbf{x}}_2,\tilde{u}) \leq & -\frac{\gamma_{W23}}{4\gamma_{W22}}V_{\mathbf{x}2}(\tilde{\mathbf{x}}_1,\tilde{\mathbf{x}}_2,\tilde{u})+\frac{1}{2\gamma_{W23}}L_G^2\left(\gamma_{W25}+\gamma_{W24}L_{\mathbf{X}2}\right)^2\\ &\times\left(L_{h\mathbf{x}1}\|\tilde{\mathbf{x}}_1^u\|+L_{F3}\right)^2\left(L_{h\mathbf{x}1}L_{\mathbf{fx}1}\|\tilde{\mathbf{x}}_1^u\|+\lambda\eta L_{hu1}(L_{F2}+1)\right)^2\end{aligned} \tag{4.67}$$

if $|\tilde{m}_2^u|<1$ and $\lambda\eta<\frac{\gamma_{W23}}{16\gamma_{W22}(L_{F2}+1)}$. By applying the comparison lemma (Khalil, 2002, Lemma 3.4), we obtain

$$\begin{aligned}V_{\mathbf{x}2}(\tilde{\mathbf{x}}_1(t),\tilde{\mathbf{x}}_2(t),\tilde{u}(t)) \leq & \, V_{\mathbf{x}2}(\tilde{\mathbf{x}}_1(0),\tilde{\mathbf{x}}_2(0),\tilde{u}(0))e^{-\frac{\gamma_{W23}}{4\gamma_{W22}}t}\\ &+\frac{2\gamma_{W22}}{\gamma_{W23}^2}L_G^2\left(\gamma_{W25}+\gamma_{W24}L_{\mathbf{X}2}\right)^2\left(L_{h\mathbf{x}1}\sup_{0\leq t<t_1}\|\tilde{\mathbf{x}}_1^u(t)\|+L_{F3}\right)^2\\ &\times\left(L_{h\mathbf{x}1}L_{\mathbf{fx}1}\sup_{0\leq t<t_1}\|\tilde{\mathbf{x}}_1^u(t)\|+\lambda\eta L_{hu1}(L_{F2}+1)\right)^2\end{aligned} \tag{4.68}$$

for all $0\leq t<t_1$, if $\sup_{0\leq t<t_1}|\tilde{m}_2^u(t)|<1$ as guaranteed by (4.26) and $\lambda\eta<\frac{\gamma_{W23}}{16\gamma_{W22}(L_{F2}+1)}$. The bound on $\tilde{\mathbf{x}}_2^u$ of Lemma 4.6 follows from (4.54) and (4.68), with $c_{\mathbf{x}21}=\sqrt{\frac{2\gamma_{W22}}{\gamma_{W21}}}$, $c_{\mathbf{x}22}=\frac{6}{\gamma_{W23}}\sqrt{\frac{\gamma_{W22}}{\gamma_{W21}}}(\gamma_{W25}+\gamma_{W24}L_{\mathbf{X}2})L_GL_{h\mathbf{x}1}\left(\frac{\gamma_{W23}}{16\gamma_{W22}}+L_{F3}L_{\mathbf{fx}1}\right)$, $c_{\mathbf{x}23}=\frac{6}{\gamma_{W23}}\times\sqrt{\frac{\gamma_{W22}}{\gamma_{W21}}}(\gamma_{W25}+\gamma_{W24}L_{\mathbf{X}2})L_GL_{h\mathbf{x}1}^2L_{\mathbf{fx}1}$ and $c_{\mathbf{x}24}=\frac{6}{\gamma_{W23}}\sqrt{\frac{\gamma_{W22}}{\gamma_{W21}}}(\gamma_{W25}+\gamma_{W24}L_{\mathbf{X}2})L_GL_{F3}L_{hu1}(L_{F2}+1)$.

Next, we derive the bound on $\tilde{Q}_1^u$. From (4.15), (4.16), (4.21), (4.22) and (4.23), we have

$$\dot{\tilde{Q}}_1^u=-\eta\tilde{Q}_1^u-\lambda\eta\tilde{m}_2^u+\lambda\frac{d^2F}{du^2}(u)\frac{\dot{u}}{\tilde{u}}-\tilde{Q}_1^u\frac{\dot{\tilde{u}}}{\tilde{u}}. \tag{4.69}$$

We introduce the Lyapunov-function candidate

$$V_{Q1}(\tilde{Q}_1^u)=(\tilde{Q}_1^u)^2. \tag{4.70}$$

By substituting (4.69), the time derivative of V_{Q1} can be written as

$$\dot{V}_{Q1}(\tilde{Q}_1^u)=-2\eta(\tilde{Q}_1^u)^2-2\lambda\eta\tilde{Q}_1^u\tilde{m}_2^u+2\lambda\tilde{Q}_1^u\frac{d^2F}{du^2}(u)\frac{\dot{u}}{\tilde{u}}-2V_{Q1}(\tilde{Q}_1^u)\frac{\dot{\tilde{u}}}{\tilde{u}}. \tag{4.71}$$

By noting that $\dot{u}=\dot{\tilde{u}}$, from Assumption 4.4, (4.48) and Young's inequality, it follows that

$$\begin{aligned}\dot{V}_{Q1}(\tilde{Q}_1^u)=&-\eta V_{Q1}(\tilde{Q}_1^u)+2\lambda\eta V_{Q1}(\tilde{Q}_1^u)(L_{F2}+|\tilde{m}_2^u|)\\ &+\lambda^2\eta\left(\lambda L_{F2}(L_{F2}+|\tilde{m}_2^u|)+|\tilde{m}_2^u|\right)^2.\end{aligned} \tag{4.72}$$

From this, it follows that

$$\dot{V}_{Q1}(\tilde{Q}_1^u) = -\frac{\eta}{2}V_{Q1}(\tilde{Q}_1^u) + \lambda^2\eta\left(\lambda L_{F2}(L_{F2}+1) + |\tilde{m}_2^u|\right)^2. \tag{4.73}$$

if $|\tilde{m}_2^u| < 1$ and $\lambda < \frac{1}{4(L_{F2}+1)}$. From the comparison lemma (Khalil, 2002, Lemma 3.4), we obtain

$$\dot{V}_{Q1}(\tilde{Q}_1^u(t)) = V_{Q1}(\tilde{Q}_1^u(0))e^{-\frac{\eta}{2}t} + 2\lambda^2\left(\lambda L_{F2}(L_{F2}+1) + \sup_{0\le t<t_1}|\tilde{m}_2^u(t)|\right)^2 \tag{4.74}$$

for all $0 \le t < t_1$, if $\sup_{0\le t<t_1}|\tilde{m}_2^u(t)| < 1$ as guaranteed by (4.26) and $\lambda < \frac{1}{4(L_{F2}+1)}$. The bound on $\tilde{Q}_1^u$ of Lemma 4.6 follows from (4.70) and (4.74), with $c_{Q11} = \sqrt{2}$, $c_{Q12} = 4$ and $c_{Q13} = 4L_{F2}(L_{F2}+1)$.

To derive the bound on $\tilde{Q}_2^u$, we note that from (4.20), (4.22) and (4.23), we have

$$\dot{\tilde{Q}}_2^u = -\eta\tilde{Q}_2^u + \eta(\tilde{Q}_1^u)^2 - 2\lambda\eta\tilde{Q}_1^u\frac{1}{\tilde{u}}\frac{dF}{du}(u) - 2\lambda^2\frac{1}{\tilde{u}}\frac{dF}{du}(u)\frac{d^2F}{du^2}(u)\frac{\dot{u}}{\tilde{u}} - 2\tilde{Q}_2^u\frac{\dot{\tilde{u}}}{\tilde{u}}. \tag{4.75}$$

We introduce the Lyapunov-function candidate

$$V_{Q2}(\tilde{Q}_2^u) = (\tilde{Q}_2^u)^2. \tag{4.76}$$

Using (4.75), its time derivative is given by

$$\begin{aligned}\dot{V}_{Q2}(\tilde{Q}_2^u) = &-2\eta(\tilde{Q}_2^u)^2 + 2\eta\tilde{Q}_2^u(\tilde{Q}_1^u)^2 - 4V_{Q2}(\tilde{Q}_2^u)\frac{\dot{\tilde{u}}}{\tilde{u}}\\ &- 4\lambda\eta\tilde{Q}_2^u\tilde{Q}_1^u\frac{1}{\tilde{u}}\frac{dF}{du}(u) - 4\lambda^2\tilde{Q}_2^u\frac{1}{\tilde{u}}\frac{dF}{du}(u)\frac{d^2F}{du^2}(u)\frac{\dot{u}}{\tilde{u}}.\end{aligned} \tag{4.77}$$

Subsequently, from Assumption 4.4, (4.48) and Young's inequality, we obtain

$$\begin{aligned}\dot{V}_{Q2}(\tilde{Q}_2^u) \le &-\eta V_{Q2}(\tilde{Q}_2^u) + 4\lambda\eta V_{Q2}(\tilde{Q}_2^u)(L_{F2} + |\tilde{m}_2^u|)\\ &+ \eta\left(|\tilde{Q}_1^u|^2 + 2\lambda L_{F2}|\tilde{Q}_1^u| + 2\lambda^3 L_{F2}^2(L_{F2} + |\tilde{m}_2^u|)\right)^2.\end{aligned} \tag{4.78}$$

From this, it follows that

$$\dot{V}_{Q2}(\tilde{Q}_2^u) \le -\frac{\eta}{2}V_{Q2}(\tilde{Q}_2^u) + \eta\left(|\tilde{Q}_1^u|^2 + 2\lambda L_{F2}|\tilde{Q}_1^u| + 2\lambda^3 L_{F2}^2(L_{F2}+1)\right)^2 \tag{4.79}$$

if $|\tilde{m}_2^u| < 1$ and $\lambda < \frac{1}{8(L_{F2}+1)}$. From the comparison lemma (Khalil, 2002, Lemma 3.4), we obtain

$$\begin{aligned}V_{Q2}(\tilde{Q}_2^u(t)) \le &\, V_{Q2}(\tilde{Q}_2^u(0))e^{-\frac{\eta}{2}t}\\ &+ 2\left(\sup_{0\le t<t_1}|\tilde{Q}_1^u(t)|^2 + 2\lambda L_{F2}\sup_{0\le t<t_1}|\tilde{Q}_1^u(t)| + 2\lambda^3 L_{F2}^2(L_{F2}+1)\right)^2\end{aligned} \tag{4.80}$$

for all $0 \leq t < t_1$, if $\sup_{0\leq t<t_1} |\tilde{m}_2^u(t)| < 1$ as guaranteed by (4.26) and $\lambda < \frac{1}{8(L_{F2}+1)}$. The bound on $\tilde{Q}_2^u$ of Lemma 4.6 follows from (4.76) and (4.80), with $c_{Q21} = \sqrt{2}$, $c_{Q22} = 6$, $c_{Q23} = 12L_{F2}$ and $c_{Q24} = 12L_{F2}^2(L_{F2}+1)$.

To derive the bounds on $\tilde{m}_1^u$ and $\tilde{m}_2^u$, we introduce the Lyapunov-function candidate

$$V_m(\tilde{m}_1^u, \tilde{m}_2^u, Q_2, \tilde{u}) = (\tilde{m}_1^u)^2 + \frac{1}{\tilde{u}^2} Q_2^{-1} (\tilde{m}_2^u)^2. \tag{4.81}$$

From (4.22) and (4.23), we have

$$\frac{1}{\tilde{u}^2} Q_2^{-1} = \tilde{Q}_2^u + \left(\lambda \frac{1}{\tilde{u}} \frac{dF}{du}(u) \right)^2. \tag{4.82}$$

From Assumption 4.4, we have that

$$L_{F1} \leq \frac{1}{\tilde{u}} \frac{dF}{du}(u) \leq L_{F2}. \tag{4.83}$$

Therefore, we have

$$\lambda^2 \frac{L_{F1}^2}{2} \leq \frac{1}{\tilde{u}^2} Q_2^{-1} \leq \lambda^2 \left(L_{F2}^2 + \frac{L_{F1}^2}{2} \right) \tag{4.84}$$

if $|\tilde{Q}_2^u| < \lambda^2 \frac{L_{F1}^2}{2}$. From this, we obtain the following bound on V_m:

$$\lambda^2 \frac{L_{F1}^2}{2} (\tilde{m}_2^u)^2 \leq V_m(\tilde{m}_1^u, \tilde{m}_2^u, Q_2, \tilde{u}) \tag{4.85}$$

and

$$V_m(\tilde{m}_1^u, \tilde{m}_2^u, Q_2, \tilde{u}) \leq (\tilde{m}_1^u)^2 + \lambda^2 \left(L_{F2}^2 + \frac{L_{F1}^2}{2} \right) (\tilde{m}_2^u)^2 \tag{4.86}$$

if $|\tilde{Q}_2^u| < \lambda^2 \frac{L_{F1}^2}{2}$. From (4.17), (4.19), (4.22) and (4.23), it follows that

$$\dot{\tilde{m}}_1^u = -\eta \tilde{m}_1^u + \eta \frac{z}{\tilde{u}^2} + \frac{1}{\tilde{u}} Q_1 \frac{w}{\tilde{u}} - 2\tilde{m}_1^u \frac{\dot{\tilde{u}}}{\tilde{u}} \tag{4.87}$$

and

$$\dot{\tilde{m}}_2^u = -\eta \tilde{u}^2 Q_2 \frac{1}{\tilde{u}} Q_1 \left(\tilde{m}_1^u + \frac{1}{\tilde{u}} Q_1 \tilde{m}_2^u \right) + \eta \tilde{u}^2 Q_2 \frac{1}{\tilde{u}} Q_1 \frac{z}{\tilde{u}^2} - \frac{w}{\tilde{u}} - \tilde{m}_2^u \frac{\dot{\tilde{u}}}{\tilde{u}}. \tag{4.88}$$

Moreover, from (4.20), we have

$$\frac{d}{dt} \left(\frac{1}{\tilde{u}^2} Q_2^{-1} \right) = -\eta \frac{1}{\tilde{u}^2} Q_2^{-1} + \eta \left(\frac{1}{\tilde{u}} Q_1 \right)^2 - 2 \frac{1}{\tilde{u}^2} Q_2^{-1} \frac{\dot{\tilde{u}}}{\tilde{u}}. \tag{4.89}$$

Using (4.87)-(4.89), the time derivative of V_m can be written as

$$\begin{aligned}\dot{V}_m(\tilde{m}_1^u,\tilde{m}_2^u,Q_2,\tilde{u}) = &-\eta(\tilde{m}_1^u)^2-\eta\left(\tilde{m}_1^u+\frac{1}{\tilde{u}}Q_1\tilde{m}_2^u\right)^2\\ &-\eta\frac{1}{\tilde{u}^2}Q_2^{-1}(\tilde{m}_2^u)^2+2\tilde{m}_1^u\frac{1}{\tilde{u}}Q_1\frac{w}{\tilde{u}}-2\frac{1}{\tilde{u}^2}Q_2^{-1}\tilde{m}_2^u\frac{w}{\tilde{u}}\\ &+2\eta\left(\tilde{m}_1^u+\frac{1}{\tilde{u}}Q_1\tilde{m}_2^u\right)\frac{z}{\tilde{u}^2}-4V_m(\tilde{m}_1^u,\tilde{m}_2^u,Q_2,\tilde{u})\frac{\dot{\tilde{u}}}{\tilde{u}}.\end{aligned} \tag{4.90}$$

From Young's inequality, it follows that

$$\begin{aligned}\dot{V}_m(\tilde{m}_1^u,\tilde{m}_2^u,Q_2,\tilde{u}) \le &-\frac{\eta}{2}(\tilde{m}_1^u)^2-\frac{\eta}{2}\frac{1}{\tilde{u}^2}Q_2^{-1}(\tilde{m}_2^u)^2+4V_m(\tilde{m}_1^u,\tilde{m}_2^u,Q_2,\tilde{u})\left|\frac{\dot{\tilde{u}}}{\tilde{u}}\right|\\ &+\eta\left|\frac{z}{\tilde{u}^2}\right|^2+\frac{2}{\eta}\left|\frac{1}{\tilde{u}}Q_1\right|^2\left|\frac{w}{\tilde{u}}\right|^2+\frac{2}{\eta}\left|\frac{1}{\tilde{u}^2}Q_2^{-1}\right|\left|\frac{w}{\tilde{u}}\right|^2.\end{aligned} \tag{4.91}$$

From Assumption 4.4, (4.22) and (4.23), we have

$$\left|\frac{1}{\tilde{u}}Q_1\right| \le |\tilde{Q}_1^u|+\lambda L_{F2}. \tag{4.92}$$

From Assumption 4.4, (4.18), $\dot{u}=\dot{\tilde{u}}$ and (4.48), we obtain

$$\left|\frac{w}{\tilde{u}}\right| \le \lambda\eta L_{F2}(L_{F2}+|\tilde{m}_2^u|). \tag{4.93}$$

From (4.2), (4.9), (4.18), (4.22) and $y=y_2$, it follows that

$$z = h_2(\mathbf{x}_2,u_2)-h_2(\mathbf{X}_2(u_2),u_2)+F_2(u_2)-F(u). \tag{4.94}$$

Using Assumption 4.1, we obtain

$$|h_2(\mathbf{x}_2,u_2)-h_2(\mathbf{X}_2(u_2),u_2)| = \left|\int_0^1\frac{\partial h_2}{\partial\mathbf{x}_2}(\tilde{\mathbf{x}}_2\sigma+\mathbf{X}_2(u_2),u_2)d\sigma\tilde{\mathbf{x}}_2\right| \le L_{h\mathbf{x}2}\|\tilde{\mathbf{x}}_2\|. \tag{4.95}$$

From (4.2), (4.3), (4.9), (4.10), (4.22) and $u=u_1$, it follows that

$$\begin{aligned}F_2(u_2)-F(u) &= F_2(G(h_1(\tilde{\mathbf{x}}_1+\mathbf{X}_1(u),u)))-F_2(G(h_1(\mathbf{X}_1(u),u)))\\ &= \int_0^1\frac{dF_2}{du_2}(G(h_1(\tilde{\mathbf{x}}_1\sigma+\mathbf{X}_1(u),u)))\frac{dG}{dy_1}(h_1(\tilde{\mathbf{x}}_1\sigma+\mathbf{X}_1(u),u))\\ &\quad\times\frac{\partial h_1}{\partial\mathbf{x}_1}(\tilde{\mathbf{x}}_1\sigma+\mathbf{X}_1(u),u)d\sigma\tilde{\mathbf{x}}_1.\end{aligned} \tag{4.96}$$

From Assumptions 4.1-4.2 and (4.9), we have

$$\left|\frac{dF_2}{du_2}(u_2)\right| = \left|\frac{\partial h_2}{\partial\mathbf{x}_2}(\mathbf{X}_2(u_2),u_2)\frac{d\mathbf{X}_2}{du_2}(u_2)+\frac{\partial h_2}{\partial u_2}(\mathbf{X}_2(u_2),u_2)\right| \le L_{F4} \tag{4.97}$$

for all $u_2 \in \mathbb{R}$, with $L_{F4} = L_{h\mathbf{x}2}L_{\mathbf{X}2} + L_{hu2}$. From (4.22), $u_1 = u$ and (4.62), it follows that

$$\left|\frac{dG}{dy_1}(h_1(\tilde{\mathbf{x}}_1 + \mathbf{X}_1(u), u))\right| \leq L_G(L_{h\mathbf{x}1}\|\tilde{\mathbf{x}}_1\| + L_{F3}|\tilde{u}|). \tag{4.98}$$

for any $\tilde{\mathbf{x}}_1 \in \mathbb{R}^{n_{\mathbf{x}1}}$. Now, from Assumption 4.1 and (4.96)-(4.98), we obtain

$$\begin{aligned} |F_2(u_2) - F(u)| &\leq \int_0^1 L_{F4}L_G(L_{h\mathbf{x}1}\|\tilde{\mathbf{x}}_1\|\sigma + L_{F3}|\tilde{u}|)L_{h\mathbf{x}1}d\sigma\|\tilde{\mathbf{x}}_1\| \\ &\leq L_{F4}L_GL_{h\mathbf{x}1}\|\tilde{\mathbf{x}}_1\|\left(\frac{1}{2}L_{h\mathbf{x}1}\|\tilde{\mathbf{x}}_1\| + L_{F3}|\tilde{u}|\right). \end{aligned} \tag{4.99}$$

Subsequently, from (4.23), (4.94), (4.95) and (4.99), we have

$$\left|\frac{z}{\tilde{u}^2}\right| \leq L_{h\mathbf{x}2}\|\tilde{\mathbf{x}}_2^u\| + L_{F4}L_GL_{h\mathbf{x}1}\|\tilde{\mathbf{x}}_1^u\|\left(\frac{1}{2}L_{h\mathbf{x}1}\|\tilde{\mathbf{x}}_1^u\| + L_{F3}\right). \tag{4.100}$$

Substituting the bounds in (4.48), (4.84), (4.92), (4.93) and (4.100) into (4.91) yields

$$\begin{aligned} \dot{V}_m(\tilde{m}_1^u, \tilde{m}_2^u, Q_2, \tilde{u}) \leq& -\frac{\eta}{2}(\tilde{m}_1^u)^2 - \frac{\eta}{2}\frac{1}{\tilde{u}^2}Q_2^{-1}(\tilde{m}_2^u)^2 \\ &+ 4\lambda\eta V_m(\tilde{m}_1^u, \tilde{m}_2^u, Q_2, \tilde{u})(L_{F2} + |\tilde{m}_2^u|) \\ &+ \eta\left(L_{h\mathbf{x}2}\|\tilde{\mathbf{x}}_2^u\| + L_{F4}L_GL_{h\mathbf{x}1}\|\tilde{\mathbf{x}}_1^u\|\left(\frac{1}{2}L_{h\mathbf{x}1}\|\tilde{\mathbf{x}}_1^u\| + L_{F3}\right)\right)^2 \\ &+ 2\lambda^2\eta\left(|\tilde{Q}_1^u| + \lambda L_{F2}\right)^2 L_{F2}^2(L_{F2} + |\tilde{m}_2^u|)^2 \\ &+ 2\lambda^4\eta\left(L_{F2}^2 + \frac{L_{F1}^2}{2}\right)L_{F2}^2(L_{F2} + |\tilde{m}_2^u|)^2 \end{aligned} \tag{4.101}$$

if $|\tilde{Q}_2^u| < \lambda^2\frac{L_{F1}^2}{2}$. From this and (4.81), it follows that

$$\begin{aligned} \dot{V}_m(\tilde{m}_1^u, \tilde{m}_2^u, Q_2, \tilde{u}) \leq& -\frac{\eta}{4}V_m(\tilde{m}_1^u, \tilde{m}_2^u, Q_2, \tilde{u}) \\ &+ \eta\left(L_{h\mathbf{x}2}\|\tilde{\mathbf{x}}_2^u\| + L_{F4}L_GL_{h\mathbf{x}1}\|\tilde{\mathbf{x}}_1^u\|\left(\frac{1}{2}L_{h\mathbf{x}1}\|\tilde{\mathbf{x}}_1^u\| + L_{F3}\right)\right)^2 \\ &+ 2\lambda^2\eta\left(|\tilde{Q}_1^u| + \lambda L_{F2}\right)^2 L_{F2}^2(L_{F2}+1)^2 + 2\lambda^4\eta\left(L_{F2}^2 + \frac{L_{F1}^2}{2}\right)L_{F2}^2(L_{F2}+1)^2 \end{aligned} \tag{4.102}$$

if $|\tilde{Q}_2^u| < \lambda^2\frac{L_{F1}^2}{2}$, $|\tilde{m}_2^u| < 1$ and $\lambda < \frac{1}{16(L_{F2}+1)}$. By applying the comparison lemma

(Khalil, 2002, Lemma 3.4), we obtain

$$\begin{aligned} V_m(\tilde{m}_1^u(t),\tilde{m}_2^u(t),Q_2(t),\tilde{u}(t)) &\leq V_m(\tilde{m}_1^u(0),\tilde{m}_2^u(0),Q_2(0),\tilde{u}(0))e^{-\frac{\eta}{4}t} \\ &+ 4\Bigg(L_{h\mathbf{x}2}\sup_{0\leq t<t_1}\|\tilde{\mathbf{x}}_2^u(t)\| + L_{F4}L_GL_{h\mathbf{x}1} \\ &\times \sup_{0\leq t<t_1}\|\tilde{\mathbf{x}}_1^u(t)\|\left(\frac{1}{2}L_{h\mathbf{x}1}\sup_{0\leq t<t_1}\|\tilde{\mathbf{x}}_1^u(t)\| + L_{F3}\right)\Bigg)^2 \\ &+ 8\lambda^2\left(\sup_{0\leq t<t_1}|\tilde{Q}_1^u(t)| + \lambda L_{F2}\right)^2 L_{F2}^2(L_{F2}+1)^2 \\ &+ 8\lambda^4\left(L_{F2}^2 + \frac{L_{F1}^2}{2}\right)L_{F2}^2(L_{F2}+1)^2 \end{aligned} \tag{4.103}$$

for all $0 \leq t < t_1$, if $\sup_{0\leq t<t_1}|\tilde{Q}_2^u(t)| < \lambda^2\frac{L_{F1}^2}{2}$, $\sup_{0\leq t<t_1}|\tilde{m}_2^u(t)| < 1$ and $\lambda < \frac{1}{16(L_{F2}+1)}$. The bounds on $\tilde{m}_1^u$ and $\tilde{m}_2^u$ follow from (4.85), (4.86) and (4.103), with $c_{m21} = \frac{\sqrt{10}}{L_{F1}}$, $c_{m22} = \frac{1}{L_{F1}}\sqrt{10\left(L_{F2}^2 + \frac{L_{F1}^2}{2}\right)}$, $c_{m23} = 8\frac{\sqrt{10}}{L_{F1}}L_{F3}L_{F4}L_GL_{h\mathbf{x}1}$, $c_{m24} = 4\frac{\sqrt{10}}{L_{F1}}L_{F4}L_GL_{h\mathbf{x}1}^2$, $c_{m25} = 4\frac{\sqrt{10}}{L_{F1}}L_{h\mathbf{x}2}$, $c_{m26} = 8\frac{\sqrt{5}}{L_{F1}}L_{F2}(L_{F2}+1)$ and $c_{m27} = 4\frac{\sqrt{5}}{L_{F1}}\left(2L_{F2} + \sqrt{L_{F2}^2 + \frac{L_{F1}^2}{2}}\right)L_{F2}(L_{F2}+1)$.

The proof of Lemma 4.6 is complete by defining $\rho_\lambda = \frac{1}{16(L_{F2}+1)}$ and $\rho_\eta = \min\left\{\frac{2\gamma_{W13}}{\gamma_{W12}}, \frac{\gamma_{W23}}{\gamma_{W22}}\right\}$.

4.7.2 Proof of Lemma 4.7

For simplicity of the proof, let $\varepsilon_{\mathbf{x}1} = \varepsilon_{\mathbf{x}2} = \varepsilon_{m1} = \varepsilon_{m2} = \varepsilon_{Q1} = \varepsilon_{Q2} = \varepsilon_0$ for some constant $\varepsilon_0 \in \mathbb{R}_{>0}$, with $\varepsilon_0 \leq C$. Moreover, let $\varepsilon_\lambda \leq \rho_\lambda$ and $\varepsilon_\eta \leq \rho_\eta$, such that the bounds in Lemma 4.6 on λ and η are satisfied for $\lambda < \varepsilon_\lambda$ and $\eta < \varepsilon_\eta$. The exact values of ε_0, ε_λ and ε_η will be assigned later. From the first bound in Lemma 4.6, it follows that

$$\sup_{0\leq t<t_1}\|\tilde{\mathbf{x}}_1^u(t)\| < \lambda\max\{\varepsilon_0,\varepsilon_\eta\}c_{\mathbf{x}1}, \tag{4.104}$$

with $c_{\mathbf{x}1} = \max\{c_{\mathbf{x}11}, c_{\mathbf{x}21}\}$, if $\|\tilde{\mathbf{x}}_1^u(0)\| < \lambda\varepsilon_{\mathbf{x}1}$ and $\eta < \varepsilon_\eta$. From the second bound of Lemma 4.6 and (4.104), we have

$$\sup_{0\leq t<t_1}\|\tilde{\mathbf{x}}_2^u(t)\| < \lambda\max\{\varepsilon_0,\varepsilon_\eta\}c_{\mathbf{x}2}, \tag{4.105}$$

with $c_{\mathbf{x}2} = \max\{c_{\mathbf{x}21}, c_{\mathbf{x}22}c_{\mathbf{x}1}, c_{\mathbf{x}23}\rho_\lambda\max\{C,\rho_\eta\}c_{\mathbf{x}1}^2, c_{\mathbf{x}24}\}$, if $\|\tilde{\mathbf{x}}_2^u(0)\| < \lambda\varepsilon_{\mathbf{x}2}$, $\lambda < \varepsilon_\lambda$ and $\eta < \varepsilon_\eta$, where we used that $\varepsilon_0 \leq C$, $\varepsilon_\lambda \leq \rho_\lambda$ and $\varepsilon_\eta \leq \rho_\eta$. From the bound on $\tilde{Q}_1^u$ in Lemma 4.6, we obtain

$$\sup_{0\leq t<t_1}|\tilde{Q}_1^u(t)| < \lambda\max\left\{\varepsilon_0,\varepsilon_\lambda,\sup_{0\leq t<t_1}|\tilde{m}_2^u(t)|\right\}c_{Q1}, \tag{4.106}$$

with $c_{Q1} = \max\{c_{Q11}, c_{Q12}, c_{Q13}\}$, if $|\tilde{Q}_1^u(0)| < \lambda\varepsilon_{Q1}$ and $\lambda < \varepsilon_\lambda$. Similarly, from the bound on $\tilde{m}_2^u$ in Lemma 4.6, (4.104) and (4.105), it follows that

$$\sup_{0\le t<t_1} |\tilde{m}_2^u(t)| < \max\left\{\varepsilon_0, \varepsilon_\lambda, \varepsilon_\eta, \sup_{0\le t<t_1} |\tilde{Q}_1^u(t)|\right\} c_{m2}, \tag{4.107}$$

with $c_{m2} = \max\{c_{m21}, c_{m22}, c_{m23}c_{\mathbf{x}1}, c_{m25}c_{\mathbf{x}2}, c_{m26}, c_{m27}, c_{m24}\rho_\lambda \max\{C, \rho_\eta\}c_{\mathbf{x}1}^2\}$, if $|\tilde{m}_1^u(0)| < \lambda\varepsilon_{m1}$, $|\tilde{m}_2^u(0)| < \lambda\varepsilon_{m2}$ and $\lambda < \varepsilon_\lambda$, where we again used that $\varepsilon_0 \le C$, $\varepsilon_\lambda \le \rho_\lambda$ and $\varepsilon_\eta \le \rho_\eta$. By combining (4.106) and (4.107), we obtain that

$$\sup_{0\le t<t_1} |\tilde{Q}_1^u(t)| < \lambda \max\{\varepsilon_0, \varepsilon_\lambda, \varepsilon_\eta\} c_{m2}c_{Q1} \tag{4.108}$$

and

$$\sup_{0\le t<t_1} |\tilde{m}_2^u(t)| < \max\{\varepsilon_0, \varepsilon_\lambda, \varepsilon_\eta\} c_{m2}c_{Q1}, \tag{4.109}$$

if the small-gain condition $\lambda < \varepsilon_\lambda \le \frac{1}{c_{Q1}c_{m2}}$ holds, where we assume without loss of generality that $c_{m2} \ge 1$ and $c_{Q1} \ge 1$. Now, from the bound on $\tilde{Q}_2^u$ in Lemma 4.6 and (4.108), it follows that

$$\sup_{0\le t<t_1} |\tilde{Q}_2^u(t)| < \lambda^2 \max\{\varepsilon_0, \varepsilon_\lambda, \varepsilon_\eta\} c_{Q2}, \tag{4.110}$$

with $c_{Q2} = \max\{c_{Q21}, c_{Q22}\max\{C, \rho_\lambda, \rho_\eta\}c_{m2}^2c_{Q1}^2,\ c_{Q23}c_{m2}c_{Q1}, c_{Q24}\}$, if $|\tilde{Q}_2^u| < \lambda^2\varepsilon_{Q2}$ and $\lambda < \varepsilon_\lambda$. Now, let ε_0, ε_λ and ε_η be given by

$$\begin{aligned}
\varepsilon_0 &= \min\left\{\frac{\min\{1, C\}}{c_{m2}c_{Q1}}, \frac{L_{F1}^2}{2c_{Q2}}\right\},\\
\varepsilon_\lambda &= \min\left\{\rho_\lambda, \frac{\min\{1, C\}}{c_{m2}c_{Q1}}, \frac{L_{F1}^2}{2c_{Q2}}\right\},\\
\varepsilon_\eta &= \min\left\{\rho_\eta, \frac{\min\{1, C\}}{c_{m2}c_{Q1}}, \frac{L_{F1}^2}{2c_{Q2}}\right\}.
\end{aligned} \tag{4.111}$$

We note that, from (4.111), it follows that $\max\{\varepsilon_0, \varepsilon_\lambda, \varepsilon_\eta\} \le \frac{\min\{1,C\}}{c_{m2}c_{Q1}}$ and $\max\{\varepsilon_0, \varepsilon_\lambda, \varepsilon_\eta\} \le \frac{L_{F1}^2}{2c_{Q2}}$. Then, from (4.109)-(4.111), we obtain

$$\sup_{0\le t<t_1} |\tilde{m}_2^u(t)| < \min\{1, C\} \tag{4.112}$$

and

$$\sup_{0\le t<t_1} |\tilde{Q}_2^u(t)| < \lambda^2 \frac{L_{F1}^2}{2}, \tag{4.113}$$

if $\|\tilde{\mathbf{x}}_1^u(0)\| < \lambda\varepsilon_{\mathbf{x}1}$, $\|\tilde{\mathbf{x}}_2^u(0)\| < \lambda\varepsilon_{\mathbf{x}2}$, $|\tilde{m}_1^u(0)| < \lambda\varepsilon_{m1}$, $|\tilde{m}_2^u(0)| < \varepsilon_{m2}$, $|\tilde{Q}_1^u(0)| < \lambda\varepsilon_{Q1}$, $|\tilde{Q}_2^u(0)| < \lambda^2\varepsilon_{Q2}$, $\eta < \varepsilon_\eta$ and $\lambda < \varepsilon_\lambda$, with $\varepsilon_{\mathbf{x}1} = \varepsilon_{\mathbf{x}2} = \varepsilon_{m1} = \varepsilon_{m2} = \varepsilon_{Q1} = \varepsilon_{Q2} = \varepsilon_0$.

We note that the bounds in (4.112) and (4.113) are obtained with the help of Lemma 4.6 under the assumption that $|\tilde{m}_2^u(t)| < 1$ and $|\tilde{Q}_2^u(t)| < \lambda^2 \frac{L_{F1}^2}{2}$ for all $0 \leq t < t_1$. We will prove by contradiction that $|\tilde{m}_2^u(t)| < 1$ and $|\tilde{Q}_2^u(t)| < \lambda^2 \frac{L_{F1}^2}{2}$ for all $0 \leq t < t_f$ under the conditions of the lemma. First, we assume without loss of generality that $c_{m2} \geq 1$, $c_{Q1} \geq 1$ (as above) and $c_{Q2} \geq 1$. From (4.111), it follows that $\varepsilon_0 \leq \min\{1, C\}$ and $\varepsilon_0 \leq \frac{L_F 1^2}{2}$ for $c_{m2} \geq 1$, $c_{Q1} \geq 1$ and $c_{Q2} \geq 1$, such that $|\tilde{m}_2^u(0)| < 1$ and $|\tilde{Q}_2^u(0)| < \lambda^2 \frac{L_{F1}^2}{2}$ if $|\tilde{m}_2^u(0)| < \varepsilon_{m2}$ and $|\tilde{Q}_2^u(0)| < \lambda^2 \varepsilon_{Q2}$, with $\varepsilon_{m2} = \varepsilon_{Q2} = \varepsilon_0$. From this and the continuity of the solutions of $\tilde{m}_2^u$ and $\tilde{Q}_2^u$, we obtain that there must exist some t^*, with $0 \leq t^* < t_f$, such that $|\tilde{m}_2^u(t^*)| = 1$ and/or $|\tilde{Q}_2^u(t^*)| = \lambda^2 \frac{L_{F1}^2}{2}$ and such that $|\tilde{m}_2^u(t)| < 1$ and $|\tilde{Q}_2^u(t)| < \lambda^2 \frac{L_{F1}^2}{2}$ for all $0 \leq t < t^*$, if $|\tilde{m}_2^u(t)| < 1$ and/or $|\tilde{Q}_2^u(t)| < \lambda^2 \frac{L_{F1}^2}{2}$ do not hold for all $0 \leq t < t_f$. Now, suppose there exists some t^*, with $0 \leq t^* < t_f$, such that $|\tilde{m}_2^u(t^*)| = 1$ and/or $|\tilde{Q}_2^u(t^*)| = \lambda^2 \frac{L_{F1}^2}{2}$ and such that $|\tilde{m}_2^u(t)| < 1$ and $|\tilde{Q}_2^u(t)| < \lambda^2 \frac{L_{F1}^2}{2}$ for all $0 \leq t < t^*$. From the bounds in (4.112) and (4.113), we have that $\sup_{0 \leq t < t^*} |\tilde{m}_2^u(t)| < 1$ and $\sup_{0 \leq t < t^*} |\tilde{Q}_2^u(t)| < \lambda^2 \frac{L_{F1}^2}{2}$ under the conditions of the lemma. From this and the continuity of the solutions of $\tilde{m}_2^u$ and $\tilde{Q}_2^u$, we obtain that $|\tilde{m}_2^u(t^*)| < 1$ and $|\tilde{Q}_2^u(t^*)| < \lambda^2 \frac{L_{F1}^2}{2}$, which contradicts that $|\tilde{m}_2^u(t^*)| = 1$ and/or $|\tilde{Q}_2^u(t^*)| = \lambda^2 \frac{L_{F1}^2}{2}$. Hence, we conclude that $|\tilde{m}_2^u(t)| < 1$ and $|\tilde{Q}_2^u(t)| < \lambda^2 \frac{L_{F1}^2}{2}$ for all $0 \leq t < t_f$ under the conditions of the lemma. Therefore, the bounds in (4.112) and (4.113) hold for all $0 \leq t_1 \leq t_f$. The bound on $\tilde{m}_2^u$ in (4.27) follows from (4.112).

Chapter 5

Asymptotic stability of perturbation-based extremum-seeking control for nonlinear plants

We introduce a perturbation-based extremum-seeking controller for general nonlinear dynamical plants with an arbitrary number of tunable plant parameters. The controller ensures asymptotic convergence of the plant parameters to their performance-optimizing values for any initial plant condition under the assumptions in this chapter. The key to this result is that the amplitude and the frequencies of the perturbations, as well as other tuning parameters of the controller, are time varying. Remarkably, the time-varying tuning parameters can be chosen such that asymptotic convergence is achieved for all plants that satisfy the assumptions, thereby guaranteeing stability of the resulting closed-loop system of plant and controller regardless of tuning.

5.1 Introduction

Although extremum-seeking methods aim to tune the plant parameters such that the steady-state performance of the plant is optimal, commonly only near-optimal values are obtained due to the effects of plant dynamics, measurement noise and added perturbations. Therefore, practical convergence with respect to the optimal steady-state plant performance is the standard for many extremum-seeking methods; see for example Khong et al. (2013b); Krstić and Wang (2000); Nešić et al. (2012); Tan et al. (2006). Asymptotic convergence results are relatively rare. It is shown in Moura and Chang (2013) that local exponential convergence to the optimal steady-state performance can be achieved for static plants by exponentially decaying the amplitude of the added perturbations once the plant parameters enter a neighborhood of the performance-optimizing values. Similarly, local exponential convergence to the optimal steady-state performance for dynamical plants is claimed in Wang et al. (2016) by regulating the perturbation amplitude. In Stanković and Stipanović (2010), asymptotic convergence for Wiener-Hammerstein-type plants is obtained by letting the perturbation amplitude and the adaptation gain of the controller asymptotically converge to

zero as time goes to infinity.

In addition, a few references describe asymptotic behavior for extremum-seeking methods that do not rely on added perturbations; see for example Guay and Dochain (2015); Hunnekens et al. (2014). It is shown in Hunnekens et al. (2014) that asymptotic convergence to the optimal plant performance can be obtained with an extremum-seeking controller that uses first-order least-squares fits if the plant is static. Moreover, simulation results for a Hammerstein-type plant indicate that asymptotic convergence can also be obtained for certain dynamical plants. In Guay and Dochain (2015), a simulation example of a Wiener-type plant displays asymptotic convergence to the optimal steady-state performance if the perturbation of the extremum-seeking controller in Guay and Dochain (2015) is omitted.

The main contributions of this chapter can be summarized as follows. First, we introduce a novel perturbation-based extremum-seeking controller for general nonlinear dynamical plants with an arbitrary number of plant parameters. From the stability analysis in this chapter, it follows that, under given assumptions and appropriate tuning of the controller, the closed-loop system of plant and controller is globally asymptotically stable with respect to the optimal steady-state plant performance in the sense that the solutions of the closed-loop system are bounded and asymptotically converge to the steady-state values for which the plant performance is optimal for any initial condition of the plant. The key to this result is that the amplitude and the frequencies of the perturbations, as well as other tuning parameters of the controller, are time varying and asymptotically decay to zero as time goes to infinity. To the best of our knowledge, this is the first work about extremum-seeking control in which global asymptotic stability with respect to the optimal steady-state performance of general nonlinear dynamical plants is proved. Second, we prove that global asymptotic stability can even be obtained if the plant is subjected to a time-varying disturbance under the assumption that the perturbations of the controller and the zero-mean component of the disturbance are uncorrelated. Third, there exist time-varying tuning-parameter values of the controller that ensure global asymptotic stability of the closed-loop system for all plants that satisfy the assumptions in this chapter. Application of these values eliminates the necessity (in Krstić and Wang (2000); Tan et al. (2006) for example) to tune the extremum-seeking controller in order to obtain a stable closed-loop system.

The organization of this chapter is as follows. The extremum-seeking problem is formulated in Section 5.2. Our extremum-seeking controller is introduced in Section 5.3. The stability analysis of the resulting closed-loop system of plant and controller is given in Section 5.4. We demonstrate our findings with two simulation examples in Section 5.5, after which this chapter is concluded in Section 5.6.

5.2 Problem formulation

We consider the following mulit-input-single-ouput nonlinear plant:

$$\begin{aligned} \dot{\mathbf{x}}(t) &= \mathbf{f}(\mathbf{x}(t), \mathbf{u}(t)) \\ y(t) &= h(\mathbf{x}(t), \mathbf{u}(t)) + d(t), \end{aligned} \tag{5.1}$$

where $\mathbf{x} \in \mathbb{R}^{n_\mathbf{x}}$ is the state, $\mathbf{u} \in \mathbb{R}^{n_\mathbf{u}}$ is the input, $y \in \mathbb{R}$ is the output and where $t \in \mathbb{R}_{\geq 0}$ is the time. The dimensions of the state and the input are denoted by $n_\mathbf{x}, n_\mathbf{u} \in \mathbb{N}_{>0}$, respectively. The input $\mathbf{u}$ can be regarded as a vector of tunable plant parameters. The output of the function h can be seen as a measure for the performance of the plant. We refer to the output of h as the performance cost. The performance cost is measured by the imperfect measurement y. The discrepancy between the performance cost and the measurement is denoted by the disturbance d. Our aim is to find the constant plant-parameter values that optimize the steady-state plant performance by minimizing the steady-state performance cost. However, the exact relation between the plant parameters and the performance cost is unknown, meaning that the state $\mathbf{x}$, the functions $\mathbf{f}$ and h, the state dimension $n_\mathbf{x}$ and the disturbance d are unknown. To identify for which plant-parameter values the steady-state plant performance is optimal, we rely on the plant-parameter values $\mathbf{u}$, the measurement y and a set of general assumptions about the plant, which we introduce next.

Our first assumption is that there exist a constant (unknown) steady-state solution of the plant denoted by $\mathbf{x} = \mathbf{X}(\mathbf{u})$ for each set of constant plant-parameter values $\mathbf{u}$. This is formalized as follows.

Assumption 5.1. *There exists a twice continuously differentiable map* $\mathbf{X} : \mathbb{R}^{n_\mathbf{u}} \to \mathbb{R}^{n_\mathbf{u}}$ *and a constant* $L_\mathbf{X} \in \mathbb{R}_{>0}$ *such that*

$$\mathbf{0} = \mathbf{f}(\mathbf{X}(\mathbf{u}), \mathbf{u}) \tag{5.2}$$

and

$$\left\| \frac{d\mathbf{X}}{d\mathbf{u}}(\mathbf{u}) \right\| \leq L_\mathbf{X} \tag{5.3}$$

for all $\mathbf{u} \in \mathbb{R}^{n_\mathbf{u}}$.

We note that $\mathbf{X}(\mathbf{u})$ is the explicit solution of the implicit equation (5.2) for any $\mathbf{u} \in \mathbb{R}^{n_\mathbf{u}}$. Our second assumption is that the plant is globally exponentially stable with respect to the steady-state solution $\mathbf{X}(\mathbf{u})$ if $\mathbf{u}$ is constant.

Assumption 5.2. *There exist constants* $\mu_\mathbf{x}, \nu_\mathbf{x} \in \mathbb{R}_{>0}$ *such that, for each constant* $\mathbf{u} \in \mathbb{R}^{n_\mathbf{u}}$*, the solutions of (5.1) satisfy*

$$\|\tilde{\mathbf{x}}(t)\| \leq \mu_\mathbf{x} \|\tilde{\mathbf{x}}(t_0)\| e^{-\nu_\mathbf{x}(t-t_0)}, \tag{5.4}$$

with

$$\tilde{\mathbf{x}}(t) = \mathbf{x}(t) - \mathbf{X}(\mathbf{u}), \tag{5.5}$$

for all $\mathbf{x}(t_0) \in \mathbb{R}^{n_\mathbf{x}}$ *and all* $t \geq t_0 \geq 0$.

From Assumptions 5.1 and 5.2 and the output function of the plant, we obtain that steady-state relation between the plant-parameter values and the performance cost can be written as

$$F(\mathbf{u}) = h(\mathbf{X}(\mathbf{u}), \mathbf{u}). \tag{5.6}$$

We refer to F as the objective function. In order to minimize the steady-state performance cost and to optimize the steady-state plant performance, we aim to find the plant-parameter values for which the output of objective function is minimal. Because the functions $\mathbf{f}$ and h are unknown, the objective function is also unknown. Nonetheless, we assume that $F(\mathbf{u})$ exhibits a unique minimum for some unknown value $\mathbf{u} = \mathbf{u}^*$ for which the steady-state plant performance is optimal. This is formulated in the following assumption.

Assumption 5.3. *The objective function $F : \mathbb{R}^{n_\mathbf{u}} \to \mathbb{R}$ is twice continuously differentiable and exhibits a unique minimum on the domain $\mathbb{R}^{n_\mathbf{u}}$. Let the corresponding minimizer be denoted by $\mathbf{u}^*$. There exist constants $L_{F1}, L_{F2} \in \mathbb{R}_{>0}$ such that*

$$\frac{dF}{d\mathbf{u}}(\mathbf{u})(\mathbf{u} - \mathbf{u}^*) \geq L_{F1}\|\mathbf{u} - \mathbf{u}^*\|^2 \tag{5.7}$$

and

$$\left\| \frac{d^2F}{d\mathbf{u}d\mathbf{u}^T}(\mathbf{u}) \right\| \leq L_{F2} \tag{5.8}$$

for all $\mathbf{u} \in \mathbb{R}^{n_\mathbf{u}}$.

We note that, although (5.7) implies that $F(\mathbf{u}^*)$ is a unique minimum of the objective function, it does not imply that the objective function is convex. A similar assumption to (5.7) for a single-parameter plants is stated in Tan et al. (2006).

The existence of a steady-state solution, the stability of the plant and the existence of a minimum of the objective function are common assumptions in the extremum-seeking literature; see for example Krstić and Wang (2000); Tan et al. (2006). Additionally, we require the following bounds on the derivatives of the functions $\mathbf{f}$ and h for analytical purposes.

Assumption 5.4. *The function $\mathbf{f} : \mathbb{R}^{n_\mathbf{x}} \times \mathbb{R}^{n_\mathbf{u}} \to \mathbb{R}^{n_\mathbf{x}}$ and $h : \mathbb{R}^{n_\mathbf{x}} \times \mathbb{R}^{n_\mathbf{u}} \to \mathbb{R}$ are twice continuously differentiable. Moreover, there exist constants $L_{\mathbf{fx}}, L_{\mathbf{fu}}, L_{h\mathbf{x}}, L_{h\mathbf{u}} \in \mathbb{R}_{>0}$ such that*

$$\left\| \frac{\partial \mathbf{f}}{\partial \mathbf{x}}(\mathbf{x}, \mathbf{u}) \right\| \leq L_{\mathbf{fx}}, \qquad \left\| \frac{\partial \mathbf{f}}{\partial \mathbf{u}}(\mathbf{x}, \mathbf{u}) \right\| \leq L_{\mathbf{fu}} \tag{5.9}$$

and

$$\left\| \frac{\partial^2 h}{\partial \mathbf{x} \partial \mathbf{x}^T}(\mathbf{x}, \mathbf{u}) \right\| \leq L_{h\mathbf{x}}, \qquad \left\| \frac{\partial^2 h}{\partial \mathbf{x} \partial \mathbf{u}^T}(\mathbf{x}, \mathbf{u}) \right\| \leq L_{h\mathbf{u}} \tag{5.10}$$

for all $\mathbf{x} \in \mathbb{R}^{n_\mathbf{x}}$ and all $\mathbf{u} \in \mathbb{R}^{n_\mathbf{u}}$.

Remark 5.5. *We note that Assumptions 5.1-5.4 are the same as Assumptions 2.1-2.4 in Chapter 2. Similarly to Remark 2.7, for a local result, it is sufficient to assume that Assumptions 5.1-5.4 hold for compact sets of* $\mathbf{x}$ *and* $\mathbf{u}$*, where the steady-state solution* $\mathbf{X}(\mathbf{u})$ *is in the interior of the compact set of* $\mathbf{x}$ *and the minimizer* $\mathbf{u}^*$ *is in the interior of the compact set of* $\mathbf{u}$*. Assumption 5.4 holds for any compact sets of* $\mathbf{x}$ *and* $\mathbf{u}$ *if the functions* $\mathbf{f}$ *and* h *are twice continuously differentiable.*

Because the objective function is unknown, any information about the objective function is obtained via the measurement y. We note that the measurement y differs from the output of the objective function F (which is equal to the steady-state performance cost) in two ways: first, the measurement is not equal to the performance cost due to the disturbance d; second, the performance cost is not equal to the output of the objective function due to the plant dynamics. Nonetheless, we aim to steer the plant parameters $\mathbf{u}$ to their performance-optimizing values $\mathbf{u}^*$ under the given assumptions by using the measurement y as feedback.

5.3 Proposed controller

From Assumption 5.3, it follows that the plant parameters $\mathbf{u}$ converge to their performance-optimizing values $\mathbf{u}^*$ if they are steered in the direction opposite to the gradient of the objective function. Because the objective function is unknown, we estimate (a scaled version of) its gradient and use this gradient estimate to steer $\mathbf{u}$ to $\mathbf{u}^*$. We introduce the following sinusoidal perturbations to provide sufficient excitation to the plant-parameter signals to accurately estimate the gradient of the objective function:

$$\boldsymbol{\omega}(t) = [\omega_1(t),\ \omega_2(t),\ \ldots,\ \omega_{n_\mathbf{u}}(t)]^T, \tag{5.11}$$

with

$$\omega_i(t) = \begin{cases} \sin\left(\dfrac{i+1}{2}\displaystyle\int_0^t \eta_{\boldsymbol{\omega}}(\tau)d\tau\right), & \text{if } i \text{ is odd,} \\ \cos\left(\dfrac{i}{2}\displaystyle\int_0^t \eta_{\boldsymbol{\omega}}(\tau)d\tau\right), & \text{if } i \text{ is even} \end{cases} \tag{5.12}$$

for $i = 1, 2, \ldots, n_\mathbf{u}$, where $\eta_{\boldsymbol{\omega}} \in \mathbb{R}_{>0}$ is a time-varying tuning parameter. We note that if $\eta_{\boldsymbol{\omega}}$ is constant, the perturbation signals in (5.12) are given by $\omega_1 = \sin(\eta_{\boldsymbol{\omega}} t)$, $\omega_2 = \cos(\eta_{\boldsymbol{\omega}} t)$, $\omega_3 = \sin(2\eta_{\boldsymbol{\omega}} t)$, etcetera. The use of sinusoidal perturbations with constant angular frequencies is common in extremum-seeking control; see for example Ariyur and Krstić (2003); Tan et al. (2010) and references therein. The corresponding plant-parameter signals are given by

$$\mathbf{u}(t) = \hat{\mathbf{u}}(t) + \alpha_{\boldsymbol{\omega}}(t)\boldsymbol{\omega}(t), \tag{5.13}$$

where $\hat{\mathbf{u}} \in \mathbb{R}^{n_{\mathbf{u}}}$ is the nominal value of the plant parameters and $\alpha_{\boldsymbol{\omega}} \in \mathbb{R}_{>0}$ is the time-varying amplitude of the perturbation signals. The tuning parameters $\alpha_{\boldsymbol{\omega}}$ and $\eta_{\boldsymbol{\omega}}$ satisfy the differential equations

$$\dot{\alpha}_{\boldsymbol{\omega}}(t) = -g_{\alpha}(t)\alpha_{\boldsymbol{\omega}}(t), \quad \dot{\eta}_{\boldsymbol{\omega}}(t) = -g_{\boldsymbol{\omega}}(t)\eta_{\boldsymbol{\omega}}(t), \tag{5.14}$$

with initial conditions $\alpha_{\boldsymbol{\omega}}(0), \eta_{\boldsymbol{\omega}}(0) \in \mathbb{R}_{>0}$ and time-varying parameters $g_{\alpha}, g_{\boldsymbol{\omega}} \in \mathbb{R}_{\geq 0}$. This is not the first work about extremum-seeking control for which the amplitude of the perturbations is time varying. Sinusoidal perturbations with a time-varying amplitude are also used to optimize the plant performance in the presence of multiple local extrema in Tan et al. (2009), to increase the convergence rate of the extremum-seeking controller in Moase et al. (2010), to obtain local exponential convergence for static plants in Moura and Chang (2013) and for dynamical plant in Wang et al. (2016), and to achieve nonlocal asymptotic convergence for Wiener-Hammerstein-type plants in Stanković and Stipanović (2010). In this chapter, we utilize sinusoidal perturbations with a time-varying amplitude and time-varying frequencies to obtain asymptotic convergence of the plant parameters to their performance-optimizing values by letting the value of $\alpha_{\boldsymbol{\omega}}$ and $\eta_{\boldsymbol{\omega}}$ asymptotically decay to zero as time goes to infinity. Here, the novelty lies in the decay of the frequencies in addition to the decay of the amplitude of the perturbations, which allows us to extend the results in Stanković and Stipanović (2010) to the general nonlinear plant in (5.1).

In this chapter, we introduce an extremum-seeking controller that asymptotically regulates the nominal plant parameters $\hat{\mathbf{u}}$ to $\mathbf{u}^*$ with the help of an estimate of the gradient of the objective function. To be able to estimate the gradient of the objective function from the measurement y, we impose the following assumption on the disturbance d.

Assumption 5.6. *The disturbance $d : \mathbb{R}_{\geq 0} \to \mathbb{R}$ is integrable. Moreover, there exists a constant $b_d \in \mathbb{R}$ for which*

$$b_d = \lim_{T \to \infty} \frac{1}{T} \int_0^T d(t)dt. \tag{5.15}$$

We define

$$\tilde{d}(t) = d(t) - b_d. \tag{5.16}$$

In addition, there exists a vector $\mathbf{b}_{\boldsymbol{\omega}d} \in \mathbb{R}^{n_{\mathbf{u}}}$ for which

$$\mathbf{b}_{\boldsymbol{\omega}d} = \lim_{T \to \infty} \frac{1}{T} \int_0^T \boldsymbol{\omega}(t)\tilde{d}(t)dt. \tag{5.17}$$

Furthermore, there exist constants $q_d, q_{\boldsymbol{\omega}d} \in \mathbb{R}_{\geq 0}$ such that

$$\left| \int_0^t \tilde{d}(\tau)d\tau \right| \leq q_d \tag{5.18}$$

and

$$\left\| \int_0^t \left(\boldsymbol{\omega}(\tau)\tilde{d}(\tau) - \mathbf{b}_{\boldsymbol{\omega}d} \right) d\tau \right\| \leq q_{\boldsymbol{\omega}d} \tag{5.19}$$

for all $t \geq 0$.

We note that the disturbance d is allowed to be discontinuous and unbounded as long as the bounds on the integrals in (5.18) and (5.19) exist. The constant b_d is a bias in the measurement. We refer to $\tilde{d}$ as the zero-mean component of the disturbance. The vector $\mathbf{b}_{\boldsymbol{\omega}d}$ is a measure for the correlation between $\boldsymbol{\omega}$ and $\tilde{d}$. We refer to $\boldsymbol{\omega}$ and $\tilde{d}$ as uncorrelated if $\mathbf{b}_{\boldsymbol{\omega}d}$ is equal to the zero vector. Uncorrelation between the perturbations and the zero-mean component of the disturbance is used to prove the practical stability results in Ariyur and Krstić (2003); Tan et al. (2010), where (5.17) is equivalent to the noise assumption in Tan et al. (2010) for $\mathbf{b}_{\boldsymbol{\omega}d} = \mathbf{0}$. Similarly, the asymptotic stability result in this chapter can only be obtained if the perturbations and the zero-mean component of the disturbance are uncorrelated.

5.3.1 Model of the input-to-output behavior of the plant

To obtain an estimate of the gradient of the objective function from the measurement signal y, we model the input-to-output behavior of the plant. The state of the model is given by

$$m_1(t) = F(\hat{\mathbf{u}}(t)) + b_d, \qquad \mathbf{m}_2(t) = \alpha_{\boldsymbol{\omega}}(t)\frac{dF}{d\mathbf{u}^T}(\hat{\mathbf{u}}(t)). \tag{5.20}$$

By combining the output equation in (5.1) and the expression for objective function in (5.6), the measurement y can be expressed as

$$y = h(\mathbf{x}, \mathbf{u}) - h(\mathbf{X}(\mathbf{u}), \mathbf{u}) + F(\mathbf{u}) + d. \tag{5.21}$$

With the help of Taylor's theorem and (5.13), the steady-state performance cost can be written as

$$\begin{aligned} F(\mathbf{u}) &= F(\hat{\mathbf{u}} + \alpha_{\boldsymbol{\omega}}\boldsymbol{\omega}) \\ &= F(\hat{\mathbf{u}}) + \alpha_{\boldsymbol{\omega}}\frac{dF}{d\mathbf{u}}(\hat{\mathbf{u}})\boldsymbol{\omega} + \alpha_{\boldsymbol{\omega}}^2\boldsymbol{\omega}^T\int_0^1 (1-s)\frac{d^2F}{d\mathbf{u}d\mathbf{u}^T}(\hat{\mathbf{u}} + s\alpha_{\boldsymbol{\omega}}\boldsymbol{\omega})ds\boldsymbol{\omega}. \end{aligned} \tag{5.22}$$

By combining (5.14), (5.16) and (5.20)-(5.22), we obtain the following input-to-output behavior of the plant:

$$\begin{aligned} \dot{m}_1(t) &= \frac{\dot{\hat{\mathbf{u}}}^T(t)}{\alpha_{\boldsymbol{\omega}}(t)}\mathbf{m}_2(t) \\ \dot{\mathbf{m}}_2(t) &= -g_\alpha(t)\mathbf{m}_2(t) + \alpha_{\boldsymbol{\omega}}^2(t)\mathbf{w}(t) \\ y(t) &= m_1(t) + \boldsymbol{\omega}^T(t)\mathbf{m}_2(t) + \alpha_{\boldsymbol{\omega}}^2(t)v(t) + z(t) + \tilde{d}(t), \end{aligned} \tag{5.23}$$

with

$$\begin{aligned} \mathbf{w} &= \frac{d^2F}{d\mathbf{u}d\mathbf{u}^T}(\hat{\mathbf{u}})\frac{\dot{\hat{\mathbf{u}}}}{\alpha_{\boldsymbol{\omega}}}, \\ v &= \boldsymbol{\omega}^T \int_0^1 (1-s)\frac{d^2F}{d\mathbf{u}d\mathbf{u}^T}(\hat{\mathbf{u}} + s\alpha_{\boldsymbol{\omega}}\boldsymbol{\omega})ds\boldsymbol{\omega}, \\ z &= h(\mathbf{x},\mathbf{u}) - h(\mathbf{X}(\mathbf{u}),\mathbf{u}). \end{aligned} \tag{5.24}$$

The signals $\mathbf{w}$, v and z can be regarded as unknown disturbances. The influences of $\mathbf{w}$, v and z on the state and output of the model are small if $\hat{\mathbf{u}}$ is slowly time varying, if $\alpha_{\boldsymbol{\omega}}$ is small and if the state $\mathbf{x}$ of the plant is close to its steady-state value $\mathbf{X}(\mathbf{u})$. We note that the state $\mathbf{m}_2$ in (5.20) is equal to the gradient of the objective function scaled by the perturbation amplitude $\alpha_{\boldsymbol{\omega}}$. Hence, an estimate of the gradient of the objective function can be obtained from an estimate of the state $\mathbf{m}_2$.

5.3.2 Controller design

We introduce an extremum-seeking controller that consists of an observer to estimate the state of the model in (5.23) and an optimizer that uses the estimate of the state $\mathbf{m}_2$ of the observer to regulate the nominal plant parameters $\hat{\mathbf{u}}$ to their performance-optimizing values $\mathbf{u}^*$. Let the observer be given by

$$\begin{aligned} \dot{\hat{m}}_1(t) &= \eta_{\mathbf{m}}(t)\left(y(t) - \hat{m}_1(t)\right) \\ \dot{\hat{\mathbf{m}}}_2(t) &= -g_\alpha(t)\hat{\mathbf{m}}_2(t) + \eta_{\mathbf{m}}(t)\mathbf{Q}(t)\boldsymbol{\omega}(t)\left(y(t) - \hat{m}_1(t) - \boldsymbol{\omega}^T(t)\hat{\mathbf{m}}_2(t)\right) \\ \dot{\mathbf{Q}}(t) &= \eta_{\mathbf{m}}(t)\mathbf{Q}(t) - 2g_\alpha(t)\mathbf{Q}(t) - \eta_{\mathbf{m}}(t)\mathbf{Q}(t)\boldsymbol{\omega}(t)\boldsymbol{\omega}^T(t)\mathbf{Q}(t), \end{aligned} \tag{5.25}$$

with time-varying tuning parameter $\eta_{\mathbf{m}} \in \mathbb{R}_{>0}$ and state $\hat{m}_1 \in \mathbb{R}$, $\hat{\mathbf{m}}_2 \in \mathbb{R}^{n_{\mathbf{u}}}$ and $\mathbf{Q} \in \mathbb{R}^{n_{\mathbf{u}} \times n_{\mathbf{u}}}$, where $\mathbf{Q}$ is symmetric and positive definite. Similar to (5.14), the tuning parameter $\eta_{\mathbf{m}}$ satisfies the differential equation

$$\dot{\eta}_{\mathbf{m}}(t) = -g_{\mathbf{m}}(t)\eta_{\mathbf{m}}(t), \tag{5.26}$$

with initial condition $\eta_{\mathbf{m}}(0) \in \mathbb{R}_{>0}$ and time-varying parameter $g_{\mathbf{m}} \in \mathbb{R}_{\geq 0}$. We note that $\hat{m}_1$ and $\hat{\mathbf{m}}_2$ are estimates of m_1 and $\mathbf{m}_2$ in (5.20), respectively. Therefore, $\hat{\mathbf{m}}_2$ is an estimate of the scaled gradient of the objective function. We define the following gradient-descent optimizer to steer the nominal plant parameters $\hat{\mathbf{u}}$ to their performance optimizing values $\mathbf{u}^*$:

$$\dot{\hat{\mathbf{u}}}(t) = -\lambda_{\mathbf{u}}(t)\frac{\eta_{\mathbf{u}}(t)\hat{\mathbf{m}}_2(t)}{\eta_{\mathbf{u}}(t) + \lambda_{\mathbf{u}}(t)\|\hat{\mathbf{m}}_2(t)\|}, \tag{5.27}$$

where $\lambda_{\mathbf{u}}, \eta_{\mathbf{u}} \in \mathbb{R}_{>0}$ are time-varying tuning parameters that satisfy the differential equations

$$\dot{\lambda}_{\mathbf{u}}(t) = -g_\lambda(t)\lambda_{\mathbf{u}}(t), \qquad \dot{\eta}_{\mathbf{u}}(t) = -g_{\mathbf{u}}(t)\eta_{\mathbf{u}}(t), \tag{5.28}$$

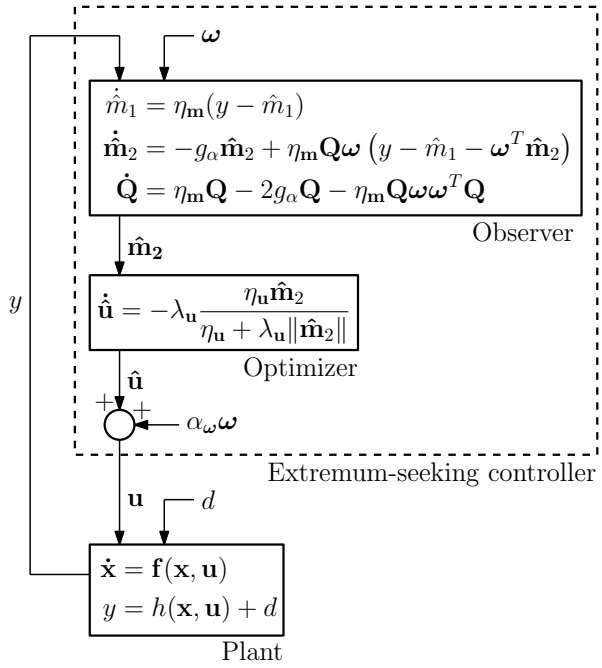

Figure 5.1: Closed-loop system of plant and extremum-seeking controller.

with initial conditions $\lambda_{\mathbf{u}}(0), \eta_{\mathbf{u}}(0) \in \mathbb{R}_{>0}$ and time-varying parameters $g_\lambda, g_{\mathbf{u}} \in \mathbb{R}_{\geq 0}$. We note that the adaptation gain of the optimizer in (5.27) is normalized to preclude a finite escape time of the solutions of the closed-loop system of plant and extremum-seeking controller if the estimate $\hat{\mathbf{m}}_2$ is inaccurate.

5.3.3 Closed-loop system

The closed-loop system of the plant in (5.1) and the extremum-seeking controller in (5.25) and (5.27) is illustrated in Figure 5.1. To accurately estimate the state of the model in (5.23) with the observer in (5.25), it is assumed that the following design assumptions are satisfied: first, the plant parameters (that is, the sum of the nominal plant parameters and the perturbations) are slowly time varying with respect to the plant dynamics so that the performance cost remains close to its steady-state value (that is, the disturbance z in (5.24) is small); second, the observer uses a sufficiently long time history of the perturbation signals and measurement signal to be able to accurately extract the state of the model from these signals, which requires the observer to be slow compared to the perturbations; third, the nominal plant parameters are slowly time varying with respect to the observer so that an accurate state estimate is obtained (that is, the disturbance $\mathbf{w}$ in (5.24) is small). Under these design assumptions, different

time scales can be assigned to the various components of the closed-loop system of plant and controller, similar to Krstić and Wang (2000); Moase and Manzie (2011); Tan et al. (2006). We conclude that the closed-loop system should be tuned to exhibit four time scales under these assumptions:

- fast – the plant;
- medium fast – the perturbations of the controller;
- medium slow – the observer of the controller;
- slow – the optimizer of the controller.

The time scales of the perturbations, the observer and the optimizer are dependent on the tuning parameters $\alpha_{\boldsymbol{\omega}}$, $\eta_{\boldsymbol{\omega}}$, $\eta_{\mathbf{m}}$, $\lambda_{\mathbf{u}}$ and $\eta_{\mathbf{u}}$. As mentioned above, we let $\alpha_{\boldsymbol{\omega}}$ and $\eta_{\boldsymbol{\omega}}$ asymptotically converge to zero to obtain asymptotic convergence of the plant parameters to their performance-optimizing values. This implies that the perturbations become slower as time progresses. To ensure that the observer and the controller are sufficiently slow compared to the perturbations, the tuning parameters $\eta_{\mathbf{m}}$, $\lambda_{\mathbf{u}}$ and $\eta_{\mathbf{u}}$ are required to be time varying and asymptotically decay to zero as well.

5.4 Stability analysis

To investigate under which initial conditions and tuning conditions the plant parameters converge to their performance-optimizing values, we analyse the stability of the closed-loop system of the plant in (5.1) and the extremum-seeking controller in (5.25) and (5.27). Contrary to extremum-seeking controllers with constant tuning parameters in Krstić and Wang (2000); Tan et al. (2006), for example, we allow our choice of tuning-parameter values to be bad initially, as long as suitable tuning-parameter values are obtained after a finite time $t_1 \geq 0$. Our main result is presented next.

Theorem 5.7. *Suppose that the parameters g_α, $g_{\boldsymbol{\omega}}$, $g_{\mathbf{m}}$, g_λ and $g_{\mathbf{u}}$ in (5.14), (5.26) and (5.28) are chosen such that*

$$\begin{aligned} \int_0^\infty e^{-\int_0^t g_{\mathbf{m}}(\tau)d\tau} dt = \infty, \\ \int_0^\infty \min\left\{ e^{-\int_0^t (g_\alpha(\tau)+g_\lambda(\tau))d\tau}, e^{-\int_0^t g_{\mathbf{u}}(\tau)d\tau} \right\} dt = \infty \end{aligned} \tag{5.29}$$

and

$$\max\left\{ g_\alpha(t), g_{\boldsymbol{\omega}}(t), g_{\mathbf{m}}(t), g_\lambda(t), g_{\mathbf{u}}(t) \right\} \leq c_g \tag{5.30}$$

for all $t \geq 0$ and some constant $c_g \in \mathbb{R}_{>0}$. Moreover, suppose that

$$\max\left\{ \frac{\eta_{\mathbf{m}}(t)}{\alpha_{\boldsymbol{\omega}}(t)} q_d, \frac{\eta_{\mathbf{m}}(t)}{\alpha_{\boldsymbol{\omega}}(t)} q_{\boldsymbol{\omega}d}, \frac{1}{\alpha_{\boldsymbol{\omega}}(t)} \|\mathbf{b}_{\boldsymbol{\omega}d}\| \right\} \leq c_d \tag{5.31}$$

for all $t \geq 0$ and for some constant $c_d \in \mathbb{R}_{>0}$. Let $\alpha_{\boldsymbol{\omega}}(0), \eta_{\boldsymbol{\omega}}(0), \lambda_{\mathbf{m}}(0), \lambda_{\mathbf{u}}(0), \eta_{\mathbf{u}}(0) \in \mathbb{R}_{>0}$. Under these assumptions and Assumptions 5.1-5.4 and 5.6, there exist (sufficiently large) constants $c_1, c_2, \ldots, c_5 \in \mathbb{R}_{>0}$ and (sufficiently small) constants $\varepsilon_1, \varepsilon_2, \ldots, \varepsilon_7 \in \mathbb{R}_{>0}$ such that, if there exists a time $t_1 \in \mathbb{R}_{\geq 0}$ for which

$$\begin{aligned} g_\alpha(t) + g_{\boldsymbol{\omega}}(t) &\leq \varepsilon_1, & g_\alpha(t) &\leq \eta_{\mathbf{m}}(t)\varepsilon_2, \\ |g_{\mathbf{m}}(t) - g_{\boldsymbol{\omega}}(t)| &\leq \eta_{\mathbf{m}}(t)\varepsilon_3, & \eta_{\boldsymbol{\omega}}(t) &\leq \varepsilon_4, \\ \eta_{\mathbf{m}}(t) &\leq \eta_{\boldsymbol{\omega}}(t)\varepsilon_5, & \eta_{\mathbf{u}}(t) &\leq \alpha_{\boldsymbol{\omega}}(t)\eta_{\mathbf{m}}(t)\varepsilon_6, \\ \alpha_{\boldsymbol{\omega}}(t)\lambda_{\mathbf{u}}(t) &\leq \eta_{\mathbf{m}}(t)\varepsilon_7 \end{aligned} \tag{5.32}$$

for all $t \geq t_1$, then the solutions of the closed-loop system of the plant in (5.1) and the extremum-seeking controller in (5.25) and (5.27) are bounded for all $t \geq 0$, all $\mathbf{x}(0) \in \mathbb{R}^{n_{\mathbf{x}}}$, all $\hat{m}_1(0) \in \mathbb{R}$, all $\hat{\mathbf{m}}_2(0) \in \mathbb{R}^{n_{\mathbf{u}}}$, all symmetric positive-definite $\mathbf{Q}(0) \in \mathbb{R}^{n_{\mathbf{u}} \times n_{\mathbf{u}}}$ and all $\hat{\mathbf{u}}(0) \in \mathbb{R}^{n_{\mathbf{u}}}$. In addition, the solutions of $\hat{\mathbf{u}}$ satisfy

$$\begin{aligned} \limsup_{t\to\infty} \|\hat{\mathbf{u}}(t) - \mathbf{u}^*\| \leq \limsup_{t\to\infty} \max \Bigg\{ & \alpha_{\boldsymbol{\omega}}(t)c_1, \eta_{\boldsymbol{\omega}}(t)c_2, \\ & \frac{\eta_{\mathbf{m}}(t)}{\alpha_{\boldsymbol{\omega}}(t)} c_3 q_d, \frac{\eta_{\mathbf{m}}(t)}{\alpha_{\boldsymbol{\omega}}(t)} c_4 q_{\boldsymbol{\omega}d}, \frac{1}{\alpha_{\boldsymbol{\omega}}(t)} c_5 \|\mathbf{b}_{\boldsymbol{\omega}d}\| \Bigg\}. \end{aligned} \tag{5.33}$$

5.4.1 Proof of Theorem 5.7

To prove Theorem 5.7, we define the following coordinate transformation:

$$\begin{aligned} \tilde{\mathbf{x}}(t) &= \mathbf{x}(t) - \mathbf{X}(\mathbf{u}(t)), \\ \tilde{m}_1(t) &= \hat{m}_1(t) - m_1(t) \\ &\quad - \eta_{\mathbf{m}}(t)k_1(t) - \frac{\eta_{\mathbf{m}}(t)}{\eta_{\boldsymbol{\omega}}(t)} \mathbf{l}_1^T(t)\mathbf{m}_2(t), \\ \tilde{\mathbf{m}}_2(t) &= \hat{\mathbf{m}}_2(t) - \mathbf{m}_2(t) - \eta_{\mathbf{m}}(t)\mathbf{Q}(t)\mathbf{k}_2(t), \\ \tilde{\mathbf{Q}}(t) &= \mathbf{Q}^{-1}(t) - \frac{1}{2}\mathbf{I} - \frac{\eta_{\mathbf{m}}(t)}{\eta_{\boldsymbol{\omega}}(t)} \mathbf{l}_2(t), \\ \tilde{\mathbf{u}}(t) &= \hat{\mathbf{u}}(t) - \mathbf{u}^*, \end{aligned} \tag{5.34}$$

with

$$\begin{aligned} k_1(t) &= \int_0^t \tilde{d}(\tau) d\tau, \\ \mathbf{k}_2(t) &= \int_0^t \left(\boldsymbol{\omega}(\tau)\tilde{d}(\tau) - b_{\boldsymbol{\omega}d} \right) d\tau \end{aligned} \tag{5.35}$$

and

$$\begin{aligned} \mathbf{l}_1(t) &= \int_0^t \eta_{\boldsymbol{\omega}}(\tau)\boldsymbol{\omega}(\tau) d\tau, \\ \mathbf{l}_2(t) &= \int_0^t \eta_{\boldsymbol{\omega}}(\tau) \left(\boldsymbol{\omega}(\tau)\boldsymbol{\omega}^T(\tau) - \frac{1}{2}\mathbf{I} \right) d\tau. \end{aligned} \tag{5.36}$$

We note that k_1 and $\mathbf{k}_2$ in (5.35) are bounded; see Assumption 5.6. Moreover, from the definition of $\boldsymbol{\omega}$ in (5.11), it follows that $\mathbf{l}_1$ and $\mathbf{l}_2$ in (5.36) are also bounded. Loosely speaking, the convergence of the closed-loop system can be divided in three stages:

- for $0 \leq t < t_1$, the tuning parameters converge to the bounds in (5.32), while the state (5.34) of the closed-loop system may drift;
- for $t_1 \leq t < t_2$, the variables $\tilde{\mathbf{x}}$ and $\tilde{\mathbf{Q}}$ converge to a region of the origin and remain there, while the rest of the state (5.34) of the closed-loop system may drift;
- for $t \geq t_2$, the variables $\tilde{m}_1$, $\tilde{\mathbf{m}}_2$ and $\tilde{\mathbf{u}}$ converge to a region of the origin and remain there.

Next, we derive bounds on solutions of the individual variables in (5.34) in accordance with the three stages. First, we derive bounds on $\tilde{\mathbf{x}}$ and $\tilde{\mathbf{Q}}$ in Lemmas 5.8 and 5.9, respectively.

Lemma 5.8. *Under the conditions of Theorem 5.7, there exist constants $c_{\mathbf{x}1}, c_{\mathbf{x}2}, \beta_{\mathbf{x}} \in \mathbb{R}_{>0}$ such that the solutions of $\tilde{\mathbf{x}}$ are bounded for all $t \geq 0$ and all $\tilde{\mathbf{x}}(0) \in \mathbb{R}^{n_{\mathbf{x}}}$. Moreover, the solutions of $\tilde{\mathbf{x}}$ satisfy*

$$\|\tilde{\mathbf{x}}(t)\| \leq \max\left\{c_{\mathbf{x}1}\|\tilde{\mathbf{x}}(t_1)\|e^{-\beta_{\mathbf{x}}(t-t_1)}, \alpha_{\boldsymbol{\omega}}(t)\eta_{\boldsymbol{\omega}}(t)c_{\mathbf{x}2}\right\} \tag{5.37}$$

for all $t \geq t_1$.

Proof. See Section 5.7.1. □

Lemma 5.9. *Under the conditions of Theorem 5.7, there exist constants $c_{\mathbf{Q}}, \beta_{\mathbf{Q}} \in \mathbb{R}_{>0}$ such that the solutions of $\tilde{\mathbf{Q}}$ are bounded for all $t \geq 0$ and all $\tilde{\mathbf{Q}}(0) \in \mathbb{R}^{n_{\mathbf{u}} \times n_{\mathbf{u}}}$ for which $\mathbf{Q}(0)$ is symmetric and positive definite. Moreover, the solutions of $\tilde{\mathbf{Q}}$ satisfy*

$$\|\tilde{\mathbf{Q}}(t)\| \leq \max\left\{c_{\mathbf{Q}}\|\tilde{\mathbf{Q}}(t_1)\|e^{-\beta_{\mathbf{Q}}\int_{t_1}^{t}\eta_{\mathbf{m}}(\tau)d\tau}, \frac{1}{8}\right\} \tag{5.38}$$

for all $t \geq t_1$.

Proof. See Section 5.7.2. □

From Lemmas 5.8 and 5.9, we have that the solutions of $\tilde{\mathbf{x}}$ and $\tilde{\mathbf{Q}}$ are bounded for all time under the given assumptions. Moreover, it follows that there exists a time $t_2 \geq t_1$ such that $\|\tilde{\mathbf{x}}(t)\| \leq \alpha_{\boldsymbol{\omega}}(t)\eta_{\boldsymbol{\omega}}(t)c_{\mathbf{x}2}$ and $\|\tilde{\mathbf{Q}}(t)\| \leq \frac{1}{8}$ for all $t \geq t_2$ under the conditions of Theorem 5.7. We use these bounds on $\tilde{\mathbf{x}}$ and $\tilde{\mathbf{Q}}$ to obtain the results in Lemmas 5.10 and 5.11 regarding the solutions of $\tilde{m}_1$, $\tilde{\mathbf{m}}_2$ and $\tilde{\mathbf{u}}$.

Lemma 5.10. *Under the conditions of Theorem 5.7, there exists a time $t_2 \geq t_1$ such that the solutions of $\tilde{m}_1$ and $\tilde{\mathbf{m}}_2$ are bounded for all $0 \leq t \leq t_2$, all $\tilde{m}_1(0) \in \mathbb{R}$ and all $\tilde{\mathbf{m}}_2(0) \in \mathbb{R}^{n_\mathbf{u}}$. In addition, there exist a function $V_\mathbf{m} : \mathbb{R} \times \mathbb{R}^{n_\mathbf{u}} \times \mathbb{R}^{n_\mathbf{u} \times n_\mathbf{u}} \to \mathbb{R}_{\geq 0}$ and constants $\gamma_{\mathbf{m}1}, \gamma_{\mathbf{m}2}, \ldots, \gamma_{\mathbf{m}5}, c_{\mathbf{m}1}, c_{\mathbf{m}2}, \ldots, c_{\mathbf{m}9} \in \mathbb{R}_{>0}$ such that*

$$\begin{aligned} \max\left\{\gamma_{\mathbf{m}1}|\tilde{m}_1(t)|^2, \gamma_{\mathbf{m}2}\|\tilde{\mathbf{m}}_2(t)\|^2\right\} &\leq V_\mathbf{m}(\tilde{m}_1(t), \tilde{\mathbf{m}}_2(t), \mathbf{Q}(t)) \\ &\leq \max\{\gamma_{\mathbf{m}3}|\tilde{m}_1(t)|^2, \gamma_{\mathbf{m}4}\|\tilde{\mathbf{m}}_2(t)\|^2\} \end{aligned} \tag{5.39}$$

for all $t \geq t_2$. Moreover, for all $t \geq t_2$, we have that

$$\dot{V}_\mathbf{m}(\tilde{m}_1(t), \tilde{\mathbf{m}}_2(t), \mathbf{Q}(t)) \leq -\eta_\mathbf{m}(t)\gamma_{\mathbf{m}5} V_\mathbf{m}(\tilde{m}_1(t), \tilde{\mathbf{m}}_2(t), \mathbf{Q}(t)) \tag{5.40}$$

if

$$\begin{aligned} V_\mathbf{m}(\tilde{m}_1(t), \tilde{\mathbf{m}}_2(t), \mathbf{Q}(t)) \geq \max\Bigg\{ &\alpha_{\boldsymbol{\omega}}^4(t) c_{\mathbf{m}1}, \alpha_{\boldsymbol{\omega}}^2(t)\eta_{\boldsymbol{\omega}}^2(t) c_{\mathbf{m}2}, \\ &\alpha_{\boldsymbol{\omega}}^2(t)\eta_{\boldsymbol{\omega}}^2(t) c_{\mathbf{m}3}\|\tilde{\mathbf{u}}(t)\|^2, \frac{\alpha_{\boldsymbol{\omega}}^2(t)\eta_\mathbf{m}^2(t)}{\eta_{\boldsymbol{\omega}}^2(t)} c_{\mathbf{m}4}\|\tilde{\mathbf{u}}(t)\|^2, \frac{\alpha_{\boldsymbol{\omega}}^4(t)\lambda_\mathbf{u}^2(t)}{\eta_\mathbf{m}^2(t)} c_{\mathbf{m}5}\|\tilde{\mathbf{u}}(t)\|^2, \\ &\frac{\eta_\mathbf{u}^2(t)}{\eta_\mathbf{m}^2(t)} c_{\mathbf{m}6}\|\tilde{\mathbf{u}}(t)\|^2, \eta_\mathbf{m}^2(t) c_{\mathbf{m}7} q_d^2, \eta_\mathbf{m}^2(t) c_{\mathbf{m}8} q_{\boldsymbol{\omega}d}^2, c_{\mathbf{m}9}\|\mathbf{b}_{\boldsymbol{\omega}d}\|^2 \Bigg\}. \end{aligned} \tag{5.41}$$

Proof. See Section 5.7.3. □

Lemma 5.11. *Under the conditions of Theorem 5.7, there exists a time $t_2 \geq t_1$ such that the solutions of $\tilde{\mathbf{u}}$ are bounded for all $0 \leq t \leq t_2$ and all $\tilde{\mathbf{u}}(0) \in \mathbb{R}^{n_\mathbf{u}}$. In addition, there exist a function $V_\mathbf{u} : \mathbb{R}^{n_\mathbf{u}} \to \mathbb{R}_{\geq 0}$ and constants $\gamma_{\mathbf{u}1}, \gamma_{\mathbf{u}2}, \gamma_{\mathbf{u}3}, \gamma_{\mathbf{u}4}, c_{\mathbf{u}1}, c_{\mathbf{u}2} \in \mathbb{R}_{>0}$ such that*

$$\gamma_{\mathbf{u}1}\|\tilde{\mathbf{u}}(t)\|^2 \leq V_\mathbf{u}(\tilde{\mathbf{u}}(t)) \leq \gamma_{\mathbf{u}2}\|\tilde{\mathbf{u}}(t)\|^2 \tag{5.42}$$

for all $t \geq t_2$. Moreover, for all $t \geq t_2$, we have that

$$\dot{V}_\mathbf{u}(\tilde{\mathbf{u}}(t)) \leq -\min\Big\{\alpha_{\boldsymbol{\omega}}(t)\lambda_\mathbf{u}(t)\gamma_{\mathbf{u}3} V_\mathbf{u}(\tilde{\mathbf{u}}(t)), \eta_\mathbf{u}(t)\gamma_{\mathbf{u}4}\sqrt{V_\mathbf{u}(\tilde{\mathbf{u}}(t))}\Big\} \tag{5.43}$$

if

$$V_\mathbf{u}(\tilde{\mathbf{u}}(t)) \geq \max\left\{\frac{1}{\alpha_{\boldsymbol{\omega}}^2(t)} c_{\mathbf{u}1}\|\tilde{\mathbf{m}}_2(t)\|^2, \frac{\eta_\mathbf{m}^2(t)}{\alpha_{\boldsymbol{\omega}}^2(t)} c_{\mathbf{u}2} q_{\boldsymbol{\omega}d}^2\right\}. \tag{5.44}$$

Proof. See Section 5.7.4. □

To prove that the solutions of $\tilde{m}_1$, $\tilde{\mathbf{m}}_2$ and $\tilde{\mathbf{u}}$ remain bounded for all $t \geq t_2$ and to show that bound in (5.33) holds, we introduce the following Lyapunov-function candidate as proposed in Dashkovskiy et al. (2010); Jiang et al. (1996); Liu et al. (2011):

$$V(\tilde{m}_1, \tilde{\mathbf{m}}_2, \tilde{\mathbf{u}}, \mathbf{Q}, \alpha_{\boldsymbol{\omega}}) = \max\left\{V_\mathbf{u}(\tilde{\mathbf{u}}), \frac{1}{\alpha_{\boldsymbol{\omega}}^2}\frac{c_{\mathbf{u}1}}{\gamma_{\mathbf{m}2}} V_\mathbf{m}(\tilde{m}_1, \tilde{\mathbf{m}}_2, \mathbf{Q})\right\}, \tag{5.45}$$

where the functions $V_{\mathbf{m}}$ and $V_{\mathbf{u}}$ are defined in Lemmas 5.10 and 5.11, respectively. By following similar lines as in Jiang et al. (1996), we obtain the following result regarding the solutions of $\tilde{m}_1$, $\tilde{\mathbf{m}}_2$ and $\tilde{\mathbf{u}}$.

Lemma 5.12. *Under the conditions of Theorem 5.7, there exist constants* $\gamma_{V1}, \gamma_{V2}, \gamma_{V3}, c_{V1}, c_{V2}, \ldots, c_{V5} \in \mathbb{R}_{>0}$ *such that the solutions of* $\tilde{m}_1$, $\tilde{\mathbf{m}}_2$ *and* $\tilde{\mathbf{u}}$ *are bounded for all* $t \geq t_2$, *all* $\tilde{m}_1(t_2) \in \mathbb{R}$, $\tilde{\mathbf{m}}_2(t_2) \in \mathbb{R}^{n_{\mathbf{u}}}$ *and all* $\tilde{\mathbf{u}}(t_2) \in \mathbb{R}^{n_{\mathbf{u}}}$, *where* $t_2 \in \mathbb{R}_{\geq 0}$ *is defined in Lemmas 5.10 and 5.11. In addition, the solutions of* $\tilde{m}_1$, $\tilde{\mathbf{m}}_2$ *and* $\tilde{\mathbf{u}}$ *satisfy*

$$\begin{aligned}\limsup_{t\to\infty} \max\left\{ \frac{\gamma_{V1}}{\alpha_{\boldsymbol{\omega}}(t)}|\tilde{m}_1(t)|, \frac{\gamma_{V2}}{\alpha_{\boldsymbol{\omega}}(t)}\|\tilde{\mathbf{m}}_2(t)\|, \gamma_{V3}\|\tilde{\mathbf{u}}(t)\| \right\} \\ \leq \limsup_{t\to\infty} \max\Bigg\{ \alpha_{\boldsymbol{\omega}}(t)c_{V1}, \eta_{\boldsymbol{\omega}}(t)c_{V2}, \frac{\eta_{\mathbf{m}}(t)}{\alpha_{\boldsymbol{\omega}}(t)}c_{V3}q_d, \\ \frac{\eta_{\mathbf{m}}(t)}{\alpha_{\boldsymbol{\omega}}(t)}c_{V4}q_{\boldsymbol{\omega}d}, \frac{1}{\alpha_{\boldsymbol{\omega}}(t)}c_{V5}\|\mathbf{b}_{\boldsymbol{\omega}d}\| \Bigg\}.\end{aligned} \tag{5.46}$$

Proof. See Section 5.7.5. □

The proof of Theorem 5.7 follows from Lemmas 5.8-5.12 and the coordinate transformation in (5.34).

5.4.2 Choice of tuning parameters

We explore the implications of Theorem 5.7 for different choices of the tuning parameters $\alpha_{\boldsymbol{\omega}}$, $\eta_{\boldsymbol{\omega}}$, $\eta_{\mathbf{m}}$, $\lambda_{\mathbf{u}}$ and $\eta_{\mathbf{u}}$. First, we consider constant tuning parameters, in which case Theorem 5.7 reduces to the following result.

Corollary 5.13. *Let the tuning parameters* $\alpha_{\boldsymbol{\omega}}, \eta_{\boldsymbol{\omega}}, \eta_{\mathbf{m}}, \lambda_{\mathbf{u}}, \eta_{\mathbf{u}} \in \mathbb{R}_{>0}$ *be constant (that is,* $g_\alpha = g_{\boldsymbol{\omega}} = g_{\mathbf{m}} = g_\lambda = g_{\mathbf{u}} = 0$*). Under Assumptions 5.1-5.4 and 5.6, there exist (sufficiently large) constants* $c_1, c_2, \ldots, c_5 \in \mathbb{R}_{>0}$ *and (sufficiently small) constants* $\varepsilon_1, \varepsilon_2, \varepsilon_3, \varepsilon_4 \in \mathbb{R}_{>0}$ *such that the solutions of the closed-loop system of the plant in (5.1) and the extremum-seeking controller in (5.25) and (5.27) are bounded for all* $t \geq 0$, *all* $\mathbf{x}(0) \in \mathbb{R}^{n_{\mathbf{x}}}$, *all* $\hat{m}_1(0) \in \mathbb{R}$, *all* $\hat{\mathbf{m}}_2(0) \in \mathbb{R}^{n_{\mathbf{u}}}$, *all symmetric positive-definite* $\mathbf{Q}(0) \in \mathbb{R}^{n_{\mathbf{u}}\times n_{\mathbf{u}}}$, *all* $\hat{\mathbf{u}}(0) \in \mathbb{R}^{n_{\mathbf{u}}}$ *and all* $\alpha_{\boldsymbol{\omega}}, \eta_{\boldsymbol{\omega}}, \eta_{\mathbf{m}}, \lambda_{\mathbf{u}}, \eta_{\mathbf{u}} \in \mathbb{R}_{>0}$ *that satisfy* $\eta_{\boldsymbol{\omega}} < \varepsilon_1$, $\eta_{\mathbf{m}} < \eta_{\boldsymbol{\omega}}\varepsilon_2$, $\eta_{\mathbf{u}} < \alpha_{\boldsymbol{\omega}}\eta_{\mathbf{m}}\varepsilon_3$ *and* $\alpha_{\boldsymbol{\omega}}\lambda_{\mathbf{u}} < \eta_{\mathbf{m}}\varepsilon_4$. *In addition, the solutions of* $\hat{\mathbf{u}}$ *satisfy*

$$\limsup_{t\to\infty} \|\hat{\mathbf{u}}(t) - \mathbf{u}^*\| \leq \max\left\{ \alpha_{\boldsymbol{\omega}}c_1, \eta_{\boldsymbol{\omega}}c_2, \frac{\eta_{\mathbf{m}}}{\alpha_{\boldsymbol{\omega}}}c_3q_d, \frac{\eta_{\mathbf{m}}}{\alpha_{\boldsymbol{\omega}}}c_4q_{\boldsymbol{\omega}d}, \frac{1}{\alpha_{\boldsymbol{\omega}}}c_5\|\mathbf{b}_{\boldsymbol{\omega}d}\| \right\}. \tag{5.47}$$

Proof. The proof follows directly from Theorem 5.7 for $g_\alpha = g_{\boldsymbol{\omega}} = g_{\mathbf{m}} = g_\lambda = g_{\mathbf{u}} = 0$. □

From Corollary 5.13, we obtain that $\hat{\mathbf{u}}$ converges to a region of performance-optimizing value $\mathbf{u}^*$, where the size of the region is dependent on the tuning parameters $\alpha_{\boldsymbol{\omega}}$, $\eta_{\boldsymbol{\omega}}$ and $\eta_{\mathbf{m}}$ and the disturbance-related constants q_d, $q_{\boldsymbol{\omega}d}$ and $\mathbf{b}_{\boldsymbol{\omega}d}$. If the perturbations and the zero-mean component of the disturbance are uncorrelated (that is, $\mathbf{b}_{\boldsymbol{\omega}d} = \mathbf{0}$), the size of the region of $\mathbf{u}^*$ to which $\hat{\mathbf{u}}$ converges can be made arbitrarily small by selecting suitable tuning parameters. This result is similar to the results for plants with output disturbances in Ariyur and Krstić (2003); Tan et al. (2010). It is generally not possible to make the size of the region of $\mathbf{u}^*$ to which $\hat{\mathbf{u}}$ converges arbitrarily small if the perturbations and the zero-mean component of the disturbance are correlated. We note that, because $\mathbf{b}_{\boldsymbol{\omega}d}$ depends on the tuning parameter $\eta_{\boldsymbol{\omega}}$ (see Assumption 5.6), correlation of the perturbations and the zero-mean component of the disturbance may be avoided by choosing a different value of $\eta_{\boldsymbol{\omega}}$.

Now, let us consider time-varying tuning parameters. In particular, let the time-varying parameters g_α, $g_{\boldsymbol{\omega}}$, $g_{\mathbf{m}}$, g_λ and $g_{\mathbf{u}}$ be defined as follows.

Corollary 5.14. *Let the parameters g_α, $g_{\boldsymbol{\omega}}$, $g_{\mathbf{m}}$, g_λ and $g_{\mathbf{u}}$ in (5.14), (5.26) and (5.28) be given by*

$$\begin{aligned} g_\alpha(t) &= \frac{r_\alpha}{r_0 + t}, \qquad g_{\boldsymbol{\omega}}(t) = \frac{r_{\boldsymbol{\omega}}}{r_0 + t}, \qquad g_{\mathbf{m}}(t) = \frac{r_{\mathbf{m}}}{r_0 + t}, \\ g_\lambda(t) &= \frac{r_\lambda}{r_0 + t}, \qquad g_{\mathbf{u}}(t) = \frac{r_{\mathbf{u}}}{r_0 + t}, \end{aligned} \tag{5.48}$$

where the constants $r_0 \in \mathbb{R}_{>0}$ and $r_\alpha, r_{\boldsymbol{\omega}}, r_{\mathbf{m}}, r_\lambda, r_{\mathbf{u}} \in \mathbb{R}_{\geq 0}$ satisfy

$$\begin{aligned} 0 < r_\alpha < r_{\mathbf{m}}, \qquad & 0 < r_{\boldsymbol{\omega}} < r_{\mathbf{m}}, \\ r_{\mathbf{m}} < r_\alpha + r_\lambda \leq 1, \qquad & r_\alpha + r_{\mathbf{m}} < r_{\mathbf{u}} \leq 1. \end{aligned} \tag{5.49}$$

Suppose that the perturbations and the zero-mean component of the disturbance are uncorrelated (that is, $\mathbf{b}_{\boldsymbol{\omega}d} = \mathbf{0}$). Under this assumption and Assumptions 5.1-5.4 and 5.6, the solutions of the closed-loop system of the plant in (5.1) and the extremum-seeking controller in (5.25) and (5.27) are bounded for all $t \geq 0$, all $\mathbf{x}(0) \in \mathbb{R}^{n_{\mathbf{x}}}$, all $\hat{m}_1(0) \in \mathbb{R}$, all $\hat{\mathbf{m}}_2(0) \in \mathbb{R}^{n_{\mathbf{u}}}$, all symmetric positive-definite $\mathbf{Q}(0) \in \mathbb{R}^{n_{\mathbf{u}} \times n_{\mathbf{u}}}$, all $\hat{\mathbf{u}}(0) \in \mathbb{R}^{n_{\mathbf{u}}}$ and all $\alpha_{\boldsymbol{\omega}}(0), \eta_{\boldsymbol{\omega}}(0), \eta_{\mathbf{m}}(0), \lambda_{\mathbf{u}}(0), \eta_{\mathbf{u}}(0) \in \mathbb{R}_{>0}$. In addition, the solutions of $\hat{\mathbf{u}}$ satisfy $\lim_{t\to\infty} \hat{\mathbf{u}}(t) = \mathbf{u}^*$.

Proof. The proof follows from Theorem 5.7 for g_α, $g_{\boldsymbol{\omega}}$, $g_{\mathbf{m}}$, g_λ and $g_{\mathbf{u}}$ defined in (5.48) and (5.49). We note that, for any $\alpha_{\boldsymbol{\omega}}(0), \eta_{\boldsymbol{\omega}}(0), \eta_{\mathbf{m}}(0), \lambda_{\mathbf{u}}(0), \eta_{\mathbf{u}}(0) \in \mathbb{R}_{>0}$, there exists a time $t_1 \in \mathbb{R}_{\geq 0}$ such that (5.32) in Theorem 5.7 holds for all $t \geq t_1$. □

Under the conditions of Corollary 5.14, $\hat{\mathbf{u}}$ converges to $\mathbf{u}^*$, even in the presence of an unknown disturbance (if the perturbations and the zero-mean component of the disturbance are uncorrelated). It is not difficult to show that the state $\mathbf{x}$ of the plant converges to $\mathbf{X}(\mathbf{u}^*)$ under the conditions of Corollary 5.14, which implies

that the plant performance converges to the optimal steady-state performance as time goes to infinity. We note that the closed-loop system is globally asymptotically stable with respect to the optimal steady-state plant performance under the conditions of Corollary 5.14 in the sense that the solutions of the closed-loop system are bounded and asymptotically converge to the steady-state values for which the plant performance is optimal for any initial condition of the plant. To the best of our knowledge, this is the first work about extremum-seeking control in which global asymptotic stability to the optimal steady-state performance of the general nonlinear plant in (5.1) is proved. Because global asymptotic stability with respect to the optimal steady-state plant performance is ensured for any plant that satisfies the assumptions in Corollary 5.14, selecting any set of tuning parameters that satisfy (5.48) and (5.49) eliminates the necessity (in Krstić and Wang (2000); Tan et al. (2006) for example) to tune the extremum-seeking controller in order to guarantee stability of the resulting closed-loop system. Nonetheless, plant-specific tuning of the controller is often desirable as suitably chosen tuning parameters can significantly enhance the overall convergence rate of the extremum-seeking scheme. Moreover, we note that $\mathbf{b}_{\boldsymbol{\omega} d}$ is the time average of the product of the perturbations, whose frequencies asymptotically converge to zero, and the zero-mean component of the disturbance. Hence, $\mathbf{b}_{\boldsymbol{\omega} d} = \mathbf{0}$ for a large class of disturbances. Corollary 5.14 does not guarantee convergence or boundedness of the solutions of the closed-loop system if $\mathbf{b}_{\boldsymbol{\omega} d} \neq \mathbf{0}$. To guarantee robustness of the closed-loop system for time-varying tuning of the controller if $\mathbf{b}_{\boldsymbol{\omega} d} \neq \mathbf{0}$, the perturbation amplitude should be chosen such that $\lim_{t\to\infty} \alpha_{\boldsymbol{\omega}}(t) > 0$, which precludes asymptotic convergence to the optimal steady-state plant performance.

5.5 Simulation examples

We introduce two examples to illustrate the results in this chapter.

5.5.1 Example 1

Consider the following double-input-single-output plant

$$\begin{aligned} \dot{x}_1(t) &= -x_1(t) + u_1^2(t) \\ \dot{x}_2(t) &= -x_2(t) + u_2(t) \\ \dot{x}_3(t) &= -x_3(t) + u_1(t)x_2(t) \\ y(t) &= 2(x_1(t) + x_2(t) - u_2(t)) + (x_2(t) + x_3(t))^2, \end{aligned} \tag{5.50}$$

with state $\mathbf{x} = [x_1, x_2, x_3]^T$ and plant-parameter vector $\mathbf{u} = [u_1, u_2]^T$. The corresponding objective function of the plant is given by $F(\mathbf{u}) = 2u_1^2 + (1+u_1)^2 u_2^2$. We apply the extremum-seeking controller in Section 5.3 to the plant (5.50). The tuning parameters of the controller are chosen as defined in Corollary 5.13

and Corollary 5.14, where the tuning constants in Corollary 5.14 are set to $r_0 = 200$, $r_\alpha = 0.4$, $r_{\boldsymbol{\omega}} = 0.4$, $r_{\mathbf{m}} = 0.45$, $r_\lambda = 0.1$ and $r_{\mathbf{u}} = 0.9$. The initial tuning-parameter values are set to $\alpha_{\boldsymbol{\omega}}(0) = 0.1$, $\eta_{\boldsymbol{\omega}}(0) = 1$, $\eta_{\mathbf{m}}(0) = 1$, $\lambda_{\mathbf{u}}(0) = 0.5$ and $\eta_{\mathbf{u}}(0) = 0.04$ for both tuning conditions. The trajectories of the plant parameters are illustrated in Figure 5.2. Figure 5.3 displays the corresponding measurement y of the performance cost for the first 2000 time units. From Figure 5.2, we obtain that the plant parameters asymptotically converge to the performance-optimizing values $\mathbf{u}^* = \mathbf{0}$ if the time-varying tuning in Corollary 5.14 is applied. The corresponding measurement y in Figure 5.3 asymptotically converges to the minimum $F(\mathbf{u}^*) = 0$ of the objective function. This implies that the optimal steady-state performance of the plant is obtained as time goes to infinity. Contrarily, the plant parameters converge to a region of $\mathbf{u}^* = \mathbf{0}$ for the constant tuning in Corollary 5.13 (see Figure 5.2) for which the obtained plant performance is suboptimal. As a result, we observe in Figure 5.3 that the measurement y converges to the value 0.5 instead of zero.

5.5.2 Example 2

To illustrate the influence of a time-varying disturbance on the convergence of the plant parameters for the time-varying tuning in Corollary 5.14, we consider the plant

$$\begin{aligned} \dot{x}(t) &= -x(t) + u(t) \\ y(t) &= (x(t) - 1)^2 + d(t), \end{aligned} \tag{5.51}$$

with disturbance $d(t) = \sin(0.2t)$. The objective function is given by $F(u) = (u-1)^2$. We note that the perturbation ω in (5.11) and the zero-mean component of the disturbance $\tilde{d} = d$ are uncorrelated for any values $r_0, r_{\boldsymbol{\omega}} > 0$ in Corollary 5.14. We let $r_0 = 10$, $r_\alpha = 0.15$, $r_\omega = 0.25$, $r_{\mathbf{m}} = 0.4$, $r_\lambda = 0.3$ and $r_u = 0.6$. Figures 5.4 and 5.5 illustrate the evolution of the plant parameter u, the performance cost $(x-2)^2$ and the measurement y as a function of time for the initial tuning-parameter values $\alpha_\omega(0) = 0.2$, $\eta_\omega(0) = 0.8$, $\eta_{\mathbf{m}}(0) = 0.6$, $\lambda_u(0) = 0.2$ and $\eta_u(0) = 0.4$. We observe in Figure 5.4 that the plant parameter u converges to its performance-optimizing values $u^* = 1$ as time progresses. However, the convergence of the plant parameter is momentarily disrupted when the angular frequency η_ω of the perturbation is equal to the angular frequency of the disturbance (that is, $\eta_\omega = 0.2$). A similar observation can be made in Figure 5.5 where the performance cost rises as η_ω reaches the value 0.2. We note that this disruption can be contributed to a "momentary correlation" of the perturbation and the zero-mean component of the disturbance for $\eta_\omega = 0.2$. We note that the effect of the momentary correlation can be diminished by increasing the perturbation amplitude. Alternatively, the disruption can be prevented by choosing $\eta_\omega(0)$ smaller than 0.2. Figure 5.5 shows that the performance cost converges to the optimal value $F(u^*) = 0$ as time elapses. This implies that the optimal steady-state performance is achieved despite that the measurement y of

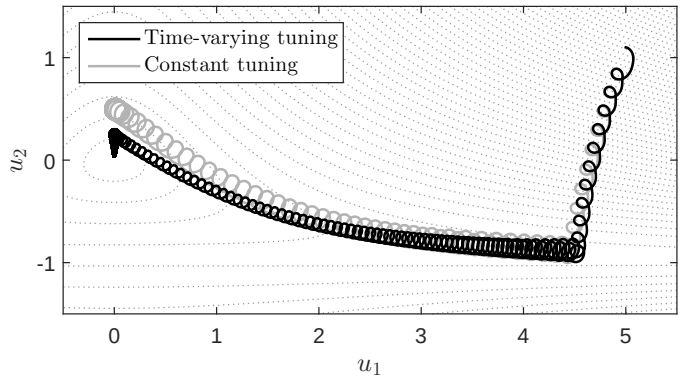

Figure 5.2: Trajectory of the plant parameters $\mathbf{u} = [u_1, u_2]^T$ for Example 1 using the constant tuning in Corollary 5.13 and the time-varying tuning in Corollary 5.14.

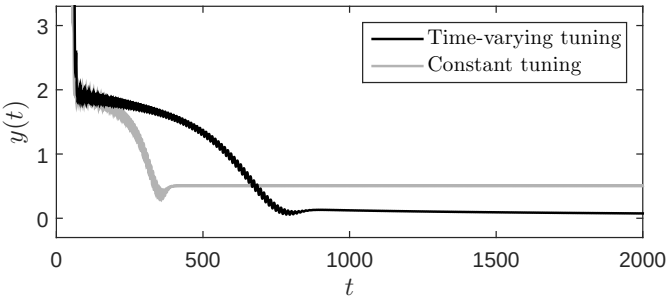

Figure 5.3: Measurement y of the performance cost as a function of time for Example 1 using the constant tuning in Corollary 5.13 and the time-varying tuning in Corollary 5.14.

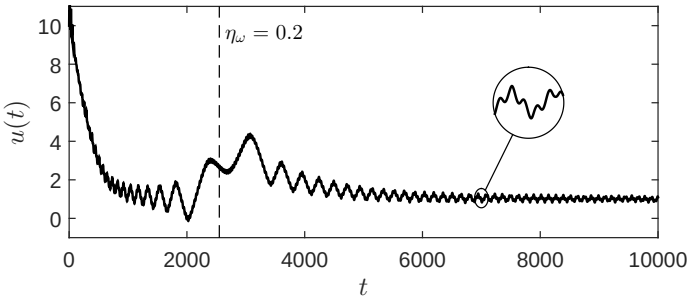

Figure 5.4: Plant parameter u as a function of time for Example 2.

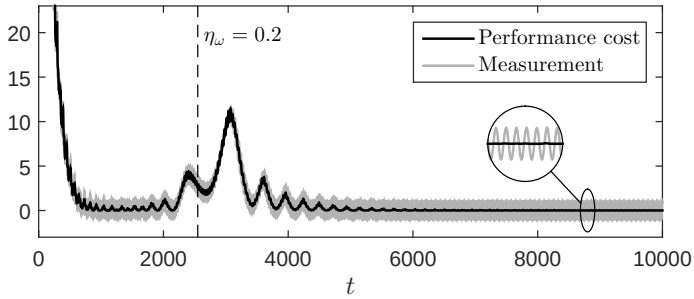

Figure 5.5: Performance cost $(x-1)^2$ and measurement y as a function of time for Example 2.

the performance cost is corrupted by the disturbance d.

5.6 Conclusion

In this chapter, we have introduced a perturbation-based extremum-seeking controller to optimize the steady-state performance of nonlinear dynamical plants. We have shown that global asymptotic stability of the closed-loop system of plant and controller with respect to the optimal steady-state plant performance can be obtained for any plant that satisfies the assumptions in the chapter. The key to this result is that the tuning parameters of the controller are time varying and asymptotically decay to zero as time goes to infinity. We note that global asymptotic stability can even be obtained if the plant is subjected to a time-varying disturbance under the assumption that the perturbations of the controller and the zero-mean component of the disturbance are uncorrelated. Moreover, we have identified time-varying tuning-parameter values of the controller for which the closed-loop system is globally asymptotically stable for all plants that satisfy the assumptions in this chapter. Two simulation examples illustrate the effectiveness of the proposed extremum-seeking controller.

5.7 Appendix

5.7.1 Proof of Lemma 5.8

From (5.1) and (5.34), we obtain that the state equation for $\tilde{\mathbf{x}}$ is given by

$$\dot{\tilde{\mathbf{x}}} = \mathbf{f}(\tilde{\mathbf{x}} + \mathbf{X}(\mathbf{u}), \mathbf{u}) - \frac{d\mathbf{X}}{d\mathbf{u}}(\mathbf{u})\dot{\mathbf{u}}. \tag{5.52}$$

Because the plant is globally exponentially stable with respect to the steady-state solution $\mathbf{X}(\mathbf{u})$ for constant $\mathbf{u}$, the following converse lemma holds.

Lemma 5.15. *Under Assumptions 5.1, 5.2 and 5.4, there exists a function* $V_{\mathbf{x}} : \mathbb{R}^{n_{\mathbf{x}}} \times \mathbb{R}^{n_{\mathbf{u}}} \to \mathbb{R}$ *and constants* $\gamma_{\mathbf{x}1}, \gamma_{\mathbf{x}2}, \gamma_{\mathbf{x}3}, \gamma_{\mathbf{x}4}, \gamma_{\mathbf{x}5} \in \mathbb{R}_{>0}$ *such that the inequalities*

$$\gamma_{\mathbf{x}1}\|\tilde{\mathbf{x}}\|^2 \leq V_{\mathbf{x}}(\tilde{\mathbf{x}}, \mathbf{u}) \leq \gamma_{\mathbf{x}2}\|\tilde{\mathbf{x}}\|^2, \tag{5.53}$$

$$\frac{\partial V_{\mathbf{x}}}{\partial \tilde{\mathbf{x}}}(\tilde{\mathbf{x}}, \mathbf{u})\mathbf{f}(\tilde{\mathbf{x}} + \mathbf{X}(\mathbf{u}), \mathbf{u}) \leq -\gamma_{\mathbf{x}3}\|\tilde{\mathbf{x}}\|^2 \tag{5.54}$$

and

$$\left\| \frac{\partial V_{\mathbf{x}}}{\partial \tilde{\mathbf{x}}}(\tilde{\mathbf{x}}, \mathbf{u}) \right\| \leq \gamma_{\mathbf{x}4}\|\tilde{\mathbf{x}}\|, \qquad \left\| \frac{\partial V_{\mathbf{x}}}{\partial \mathbf{u}}(\tilde{\mathbf{x}}, \mathbf{u}) \right\| \leq \gamma_{\mathbf{x}5}\|\tilde{\mathbf{x}}\| \tag{5.55}$$

are satisfied for all $\tilde{\mathbf{x}} \in \mathbb{R}^{n_{\mathbf{x}}}$ *and all* $\mathbf{u} \in \mathbb{R}^{n_{\mathbf{u}}}$.

Proof. We note that Assumptions 5.1, 5.2 and 5.4 are the same as Assumptions 2.1-2.3 in Chapter 2. Therefore, the proof follows from the proof of Lemma 2.15 in Section 2.7.1. □

We use the function $V_{\mathbf{x}}$ as a Lyapunov-function candidate for the $\tilde{\mathbf{x}}$-dynamics for time-varying plant parameters $\mathbf{u}$. By using (5.52), the time derivative of $V_{\mathbf{x}}$ for time-varying plant parameters can be written as

$$\dot{V}_{\mathbf{x}}(\tilde{\mathbf{x}}, \mathbf{u}) = \frac{\partial V_{\mathbf{x}}}{\partial \tilde{\mathbf{x}}}(\tilde{\mathbf{x}}, \mathbf{u})\mathbf{f}(\tilde{\mathbf{x}} + \mathbf{X}(\mathbf{u}), \mathbf{u}) + \left(\frac{\partial V_{\mathbf{x}}}{\partial \mathbf{u}}(\tilde{\mathbf{x}}, \mathbf{u}) - \frac{\partial V_{\mathbf{x}}}{\partial \tilde{\mathbf{x}}}(\tilde{\mathbf{x}}, \mathbf{u})\frac{d\mathbf{X}}{d\mathbf{u}}(\mathbf{u}) \right) \dot{\mathbf{u}}. \tag{5.56}$$

From Assumption 5.1 and Lemma 5.15, we obtain that the time derivative of $V_{\mathbf{x}}$ can be bounded by

$$\dot{V}_{\mathbf{x}}(\tilde{\mathbf{x}}, \mathbf{u}) \leq -\gamma_{\mathbf{x}3}\|\tilde{\mathbf{x}}\|^2 + (\gamma_{\mathbf{x}5} + \gamma_{\mathbf{x}4}L_{\mathbf{X}})\|\tilde{\mathbf{x}}\|\|\dot{\mathbf{u}}\|. \tag{5.57}$$

Subsequently, from Lemma 5.15 and Young's inequality, it follows that

$$\dot{V}_{\mathbf{x}}(\tilde{\mathbf{x}}, \mathbf{u}) \leq -\frac{\gamma_{\mathbf{x}3}}{2\gamma_{\mathbf{x}2}}V_{\mathbf{x}}(\tilde{\mathbf{x}}, \mathbf{u}) + \frac{1}{2\gamma_{\mathbf{x}3}}(\gamma_{\mathbf{x}5} + \gamma_{\mathbf{x}4}L_{\mathbf{X}})^2\|\dot{\mathbf{u}}\|^2. \tag{5.58}$$

From (5.58) and the comparison lemma (Khalil, 2002, Lemma 3.4), we obtain

$$\begin{aligned} V_{\mathbf{x}}(\tilde{\mathbf{x}}(t), \mathbf{u}(t)) \leq\ & V_{\mathbf{x}}(\tilde{\mathbf{x}}(t_0), \mathbf{u}(t_0))e^{-\frac{\gamma_{\mathbf{x}3}}{2\gamma_{\mathbf{x}2}}(t-t_0)} \\ & + \frac{1}{2\gamma_{\mathbf{x}3}}(\gamma_{\mathbf{x}5} + \gamma_{\mathbf{x}4}L_{\mathbf{X}})^2 \int_{t_0}^{t} e^{-\frac{\gamma_{\mathbf{x}3}}{2\gamma_{\mathbf{x}2}}(t-\tau)}\|\dot{\mathbf{u}}(\tau)\|^2 d\tau \end{aligned} \tag{5.59}$$

for all $t \geq t_0 \geq 0$. To find an upper bound for $\|\dot{\mathbf{u}}\|$, we note that it follows from (5.13) and (5.14) that

$$\dot{\mathbf{u}} = \dot{\hat{\mathbf{u}}} - g_{\alpha}\alpha_{\boldsymbol{\omega}}\boldsymbol{\omega} + \alpha_{\boldsymbol{\omega}}\dot{\boldsymbol{\omega}}. \tag{5.60}$$

From the definition of $\boldsymbol{\omega}$ in (5.11), it follows that there exist constants $L_{\boldsymbol{\omega}1}, L_{\boldsymbol{\omega}2} \in \mathbb{R}_{>0}$ such that

$$\|\boldsymbol{\omega}\| \leq L_{\boldsymbol{\omega}1}, \quad \|\dot{\boldsymbol{\omega}}\| \leq \eta_{\boldsymbol{\omega}}L_{\boldsymbol{\omega}2}. \tag{5.61}$$

Moreover, from (5.27), we have that $\|\dot{\hat{\mathbf{u}}}\| \leq \eta_{\mathbf{u}}$. Therefore, from (5.60), (5.61) and $\|\dot{\hat{\mathbf{u}}}\| \leq \eta_{\mathbf{u}}$, we obtain

$$\|\dot{\mathbf{u}}\| \leq \eta_{\mathbf{u}} + \alpha_{\boldsymbol{\omega}} g_\alpha L_{\boldsymbol{\omega}1} + \alpha_{\boldsymbol{\omega}} \eta_{\boldsymbol{\omega}} L_{\boldsymbol{\omega}2}. \tag{5.62}$$

Because $\alpha_{\boldsymbol{\omega}}$, $\eta_{\boldsymbol{\omega}}$ and $\eta_{\mathbf{u}}$ are nonincreasing (see (5.14) and (5.28)), from (5.30) in Theorem 5.7 and (5.62), it follows that

$$\|\dot{\mathbf{u}}(t)\| \leq \eta_{\mathbf{u}}(0) + \alpha_{\boldsymbol{\omega}}(0) c_g L_{\boldsymbol{\omega}1} + \alpha_{\boldsymbol{\omega}}(0)\eta_{\boldsymbol{\omega}}(0) L_{\boldsymbol{\omega}2} \tag{5.63}$$

for all $t \geq 0$. By substituting (5.62) in (5.59), we obtain

$$\begin{aligned} V_{\mathbf{x}}(\tilde{\mathbf{x}}(t), \mathbf{u}(t)) \leq V_{\mathbf{x}}(\tilde{\mathbf{x}}(0), \mathbf{u}(0)) + \frac{\gamma_{\mathbf{x}2}}{\gamma_{\mathbf{x}3}^2} \left(\gamma_{\mathbf{x}5} + \gamma_{\mathbf{x}4} L_{\mathbf{X}}\right)^2 \\ \times \left(\eta_{\mathbf{u}}(0) + \alpha_{\boldsymbol{\omega}}(0) c_g L_{\boldsymbol{\omega}1} + \alpha_{\boldsymbol{\omega}}(0)\eta_{\boldsymbol{\omega}}(0) L_{\boldsymbol{\omega}2}\right)^2 \end{aligned} \tag{5.64}$$

for all $t \geq 0$. From (5.32) in Theorem 5.7 and (5.62), it follows that

$$\|\dot{\mathbf{u}}(t)\| \leq \alpha_{\boldsymbol{\omega}}(t)\eta_{\boldsymbol{\omega}}(t)(\varepsilon_5\varepsilon_6 + \varepsilon_2\varepsilon_5 L_{\boldsymbol{\omega}1} + L_{\boldsymbol{\omega}2}) \tag{5.65}$$

for all $t \geq t_1$, all $g_\alpha \leq \eta_{\mathbf{m}}\varepsilon_2$, all $\eta_{\mathbf{m}} \leq \eta_{\boldsymbol{\omega}}\varepsilon_5$ and all $\eta_{\mathbf{u}} \leq \alpha_{\boldsymbol{\omega}}\eta_{\mathbf{m}}\varepsilon_6$. From (5.14), we have that

$$\alpha_{\boldsymbol{\omega}}(t) = \alpha_{\boldsymbol{\omega}}(\tau) e^{-\int_\tau^t g_\alpha(s)ds}, \qquad \eta_{\boldsymbol{\omega}}(t) = \eta_{\boldsymbol{\omega}}(\tau) e^{-\int_\tau^t g_{\boldsymbol{\omega}}(s)ds} \tag{5.66}$$

for any $t \geq \tau \geq 0$. Without loss of generality, we assume that ε_1 in Theorem 5.7 is sufficiently small such that it follows from (5.32) and (5.66) that

$$\alpha_{\boldsymbol{\omega}}(\tau)\eta_{\boldsymbol{\omega}}(\tau) = \alpha_{\boldsymbol{\omega}}(t)\eta_{\boldsymbol{\omega}}(t) e^{\int_\tau^t (g_\alpha(s) + g_{\boldsymbol{\omega}}(s))ds} \leq \alpha_{\boldsymbol{\omega}}(t)\eta_{\boldsymbol{\omega}}(t) e^{\frac{\gamma_{\mathbf{x}3}}{8\gamma_{\mathbf{x}2}}(t-\tau)}. \tag{5.67}$$

for all $t \geq \tau \geq t_1$ and all $g_\alpha + g_{\boldsymbol{\omega}} \leq \varepsilon_1$. From (5.65) and (5.67), we have

$$\int_{t_1}^t e^{-\frac{\gamma_{\mathbf{x}3}}{2\gamma_{\mathbf{x}2}}(t-\tau)} \|\dot{\mathbf{u}}(\tau)\|^2 d\tau \leq 4\alpha_{\boldsymbol{\omega}}^2(t)\eta_{\boldsymbol{\omega}}^2(t)\frac{\gamma_{\mathbf{x}2}}{\gamma_{\mathbf{x}3}}(\varepsilon_5\varepsilon_6 + \varepsilon_2\varepsilon_5 L_{\boldsymbol{\omega}1} + L_{\boldsymbol{\omega}2})^2 \tag{5.68}$$

for all $t \geq t_1$. Therefore, from (5.59) and (5.68), we obtain

$$\begin{aligned} V_{\mathbf{x}}(\tilde{\mathbf{x}}(t), \mathbf{u}(t)) \leq \max\Bigg\{ & 2V_{\mathbf{x}}(\tilde{\mathbf{x}}(t_1), \mathbf{u}(t_1)) e^{-\frac{\gamma_{\mathbf{x}3}}{2\gamma_{\mathbf{x}2}}(t-t_1)}, \\ & 4\alpha_{\boldsymbol{\omega}}^2(t)\eta_{\boldsymbol{\omega}}^2(t)\frac{\gamma_{\mathbf{x}2}}{\gamma_{\mathbf{x}3}^2}\left(\gamma_{\mathbf{x}5} + \gamma_{\mathbf{x}4} L_{\mathbf{X}}\right)^2 (\varepsilon_5\varepsilon_6 + \varepsilon_2\varepsilon_5 L_{\boldsymbol{\omega}1} + L_{\boldsymbol{\omega}2})^2 \Bigg\} \end{aligned} \tag{5.69}$$

for all $t \geq t_1$. From (5.53) in Lemma 5.15 and (5.64), it follows that the solutions $\tilde{\mathbf{x}}(t)$ are bounded for all $t \geq 0$ and all $\tilde{\mathbf{x}}(0) \in \mathbb{R}^{n_{\mathbf{x}}}$. The bound in (5.37) of Lemma 5.8 follows from (5.53) and (5.69).

5.7.2 Proof of Lemma 5.9

We note that $\tilde{\mathbf{Q}}$ in (5.34) is well defined if $\mathbf{Q}^{-1}$ exists. First we will show that the solution $\mathbf{Q}(t)$ of (5.25) is invertible for all $t \geq 0$ and all symmetric and positive-definite $\mathbf{Q}(0)$. Let $[0, t_{\mathbf{Q}})$ be the maximal interval of existence of $\mathbf{Q}^{-1}(t)$, with $t_{\mathbf{Q}} \in \mathbb{R}_{\geq 0} \cup \{\infty\}$. We note that $\mathbf{Q}^{-1}(t)$ is positive definite for all $t_{\mathbf{Q}} \in \mathbb{R}_{\geq 0} \cup \{\infty\}$ because $\mathbf{Q}(0)$ is positive definite. From (5.25), it follows that the time derivative of $\mathbf{Q}^{-1}$ is given by

$$\frac{d}{dt}\left(\mathbf{Q}^{-1}\right) = -\eta_{\mathbf{m}}\mathbf{Q}^{-1} + 2g_{\alpha}\mathbf{Q}^{-1} + \eta_{\mathbf{m}}\boldsymbol{\omega}\boldsymbol{\omega}^{T} \tag{5.70}$$

for all $t \in [0, t_{\mathbf{Q}})$, where we omitted the time index t for brevity. From (5.70), we obtain

$$-\eta_{\mathbf{m}}\mathbf{Q}^{-1} \preceq \frac{d}{dt}\left(\mathbf{Q}^{-1}\right) \preceq 2g_{\alpha}\mathbf{Q}^{-1} + \eta_{\mathbf{m}}\|\boldsymbol{\omega}\|^{2}\mathbf{I} \tag{5.71}$$

for all $t \in [0, t_{\mathbf{Q}})$. Because $\eta_{\mathbf{m}}$ is nonincreasing (see (5.26)), we have from (5.30) in Theorem 5.7, (5.61) in the proof of Lemma 5.8 and (5.71) that

$$-\eta_{\mathbf{m}}(0)\mathbf{Q}^{-1}(t) \preceq \frac{d}{dt}\left(\mathbf{Q}^{-1}(t)\right) \preceq 2c_{g}\mathbf{Q}^{-1}(t) + \eta_{\mathbf{m}}(0)L_{\boldsymbol{\omega}1}^{2}\mathbf{I} \tag{5.72}$$

for all $t \in [0, t_{\mathbf{Q}})$. Subsequently, from the comparison lemma (Khalil, 2002, Lemma 3.4), we obtain

$$\mathbf{Q}^{-1}(0)e^{-\eta_{\mathbf{m}}(0)t} \preceq \mathbf{Q}^{-1}(t) \preceq \mathbf{Q}^{-1}(0)e^{2c_{g}t} + \frac{\eta_{\mathbf{m}}(0)}{2c_{g}}L_{\boldsymbol{\omega}1}^{2}\mathbf{I} \tag{5.73}$$

for all $t \in [0, t_{\mathbf{Q}})$. From (5.73) and the continuity of the solutions of $\mathbf{Q}^{-1}$, it follows that $\mathbf{Q}^{-1}(t)$ is defined for all $t \geq 0$ and all positive definite $\mathbf{Q}(0)$. Hence, $t_{\mathbf{Q}} = \infty$. Moreover, from (5.73), we have that $\mathbf{Q}^{-1}(t)$ is positive definite for all $t \geq 0$ and all positive definite $\mathbf{Q}(0)$.

Now, from (5.26), (5.28), (5.34), (5.35) and (5.70), we obtain that the state equation for $\tilde{\mathbf{Q}}$ is given by

$$\dot{\tilde{\mathbf{Q}}} = -\eta_{\mathbf{m}}\tilde{\mathbf{Q}} + 2g_{\alpha}\tilde{\mathbf{Q}} + g_{\alpha}\mathbf{I} + \left(2g_{\alpha} + g_{\mathbf{m}} - g_{\boldsymbol{\omega}} - \eta_{\mathbf{m}}\right)\frac{\eta_{\mathbf{m}}}{\eta_{\boldsymbol{\omega}}}\mathbf{l}_{2}. \tag{5.74}$$

Because $\mathbf{Q}(0)$ is symmetric and $\mathbf{l}_2$ in (5.36) is a symmetric function, we obtain from (5.34) that $\tilde{\mathbf{Q}}(0)$ is symmetric as well. Subsequently, from (5.74), it follows that $\tilde{\mathbf{Q}}(t)$ remains symmetric for all $t \geq 0$. We define the following Lyapunov-function candidate for the $\tilde{\mathbf{Q}}$-dynamics:

$$V_{\mathbf{Q}}(\tilde{\mathbf{Q}}) = \operatorname{tr}\left(\tilde{\mathbf{Q}}^{2}\right). \tag{5.75}$$

From (5.74), it follows that the time derivative of $V_{\mathbf{Q}}$ can be written as

$$\begin{aligned}\dot{V}_{\mathbf{Q}}(\tilde{\mathbf{Q}}) = {} & -2\eta_{\mathbf{m}}\operatorname{tr}\left(\tilde{\mathbf{Q}}^{2}\right) + 4g_{\alpha}\operatorname{tr}\left(\tilde{\mathbf{Q}}^{2}\right) + 2g_{\alpha}\operatorname{tr}\left(\tilde{\mathbf{Q}}\right) \\ & + 2(2g_{\alpha} + g_{\mathbf{m}} - g_{\boldsymbol{\omega}} - \eta_{\mathbf{m}})\frac{\eta_{\mathbf{m}}}{\eta_{\boldsymbol{\omega}}}\operatorname{tr}\left(\tilde{\mathbf{Q}}\mathbf{l}_{2}\right).\end{aligned} \tag{5.76}$$

From Young's inequality, (5.75) and (5.76), we obtain

$$\begin{aligned}\dot{V}_{\mathbf{Q}}(\tilde{\mathbf{Q}}) \leq -\eta_{\mathbf{m}} V_{\mathbf{Q}}(\tilde{\mathbf{Q}}) + 4g_\alpha V_{\mathbf{Q}}(\tilde{\mathbf{Q}}) + \frac{2}{\eta_{\mathbf{m}}} g_\alpha^2 \operatorname{tr}(\mathbf{I}) \\ + \frac{2}{\eta_{\mathbf{m}}}(2g_\alpha + g_{\mathbf{m}} - g_{\boldsymbol{\omega}} - \eta_{\mathbf{m}})^2 \left(\frac{\eta_{\mathbf{m}}}{\eta_{\boldsymbol{\omega}}}\right)^2 \operatorname{tr}\left(\mathbf{l}_2^2\right).\end{aligned} \tag{5.77}$$

We note that $\operatorname{tr}(\mathbf{I}) = n_{\mathbf{u}}$. Moreover, from the definition of $\mathbf{l}_2$ in (5.35), it follows that there exists a constant $L_{\mathrm{l}2} \in \mathbb{R}_{>0}$ such that

$$\|\mathbf{l}_2\| \leq L_{\mathrm{l}2}, \tag{5.78}$$

which implies that $\operatorname{tr}(\mathbf{l}_2^2) \leq n_{\mathbf{u}} L_{\mathrm{l}2}^2$. We therefore obtain that

$$\begin{aligned}\dot{V}_{\mathbf{Q}}(\tilde{\mathbf{Q}}) \leq -\eta_{\mathbf{m}} V_{\mathbf{Q}}(\tilde{\mathbf{Q}}) + 4g_\alpha V_{\mathbf{Q}}(\tilde{\mathbf{Q}}) + \frac{2}{\eta_{\mathbf{m}}} g_\alpha^2 n_{\mathbf{u}} \\ + \frac{2}{\eta_{\mathbf{m}}}(2g_\alpha + |g_{\mathbf{m}} - g_{\boldsymbol{\omega}}| + \eta_{\mathbf{m}})^2 \left(\frac{\eta_{\mathbf{m}}}{\eta_{\boldsymbol{\omega}}}\right)^2 n_{\mathbf{u}} L_{\mathrm{l}2}^2.\end{aligned} \tag{5.79}$$

From (5.30) in Theorem 5.7, (5.14) and (5.26), it follows that

$$\eta_{\boldsymbol{\omega}}(0) e^{-c_g t} \leq \eta_{\boldsymbol{\omega}}(t), \qquad \eta_{\mathbf{m}}(0) e^{-c_g t} \leq \eta_{\mathbf{m}}(t) \tag{5.80}$$

for all $t \geq 0$. Because $\eta_{\mathbf{m}}$ is nonincreasing (see (5.26)), from (5.30) in Theorem 5.7, (5.79) and (5.80), we obtain that

$$\begin{aligned}\dot{V}_{\mathbf{Q}}(\tilde{\mathbf{Q}}(t)) \leq 4c_g V_{\mathbf{Q}}(\tilde{\mathbf{Q}}(t)) + \frac{2}{\eta_{\mathbf{m}}(0)} c_g^2 n_{\mathbf{u}} e^{c_g t} \\ + \frac{2}{\eta_{\mathbf{m}}(0)}(3c_g + \eta_{\mathbf{m}}(0))^2 \left(\frac{\eta_{\mathbf{m}}(0)}{\eta_{\boldsymbol{\omega}}(0)}\right)^2 n_{\mathbf{u}} L_{\mathrm{l}2}^2 e^{3c_g t}\end{aligned} \tag{5.81}$$

for all $t \geq 0$. Applying the comparison lemma (Khalil, 2002, Lemma 3.4) gives

$$\begin{aligned}V_{\mathbf{Q}}(\tilde{\mathbf{Q}}(t)) \leq V_{\mathbf{Q}}(\tilde{\mathbf{Q}}(0)) e^{4c_g t} + \frac{2}{3\eta_{\mathbf{m}}(0)} c_g n_{\mathbf{u}} e^{c_g t} \\ + \frac{2}{\eta_{\mathbf{m}}(0) c_g}(3c_g + \eta_{\mathbf{m}}(0))^2 \left(\frac{\eta_{\mathbf{m}}(0)}{\eta_{\boldsymbol{\omega}}(0)}\right)^2 n_{\mathbf{u}} L_{\mathrm{l}2}^2 e^{3c_g t}\end{aligned} \tag{5.82}$$

for all $t \geq 0$. Without loss of generality, we assume that ε_2, ε_3 and ε_5 in Theorem 5.7 are sufficiently small such that it follows from (5.32) and (5.79) that

$$\dot{V}_{\mathbf{Q}}(\tilde{\mathbf{Q}}) \leq -\frac{\eta_{\mathbf{m}}}{2} V_{\mathbf{Q}}(\tilde{\mathbf{Q}}) + \frac{\eta_{\mathbf{m}}}{256} \tag{5.83}$$

for all $t \geq t_1$, all $g_\alpha \leq \eta_{\mathbf{m}} \varepsilon_2$, all $|g_{\mathbf{m}} - g_{\boldsymbol{\omega}}| \leq \eta_{\mathbf{m}} \varepsilon_3$ and all $\eta_{\mathbf{m}} \leq \eta_{\boldsymbol{\omega}} \varepsilon_5$. Use of the comparison lemma (Khalil, 2002, Lemma 3.4) yields

$$V_{\mathbf{Q}}(\tilde{\mathbf{Q}}(t)) \leq \max\left\{2V_{\mathbf{Q}}(\tilde{\mathbf{Q}}(t_1)) e^{-\frac{1}{2}\int_{t_1}^{t} \eta_{\mathbf{m}}(\tau) d\tau}, \frac{1}{64}\right\} \tag{5.84}$$

for all $t \geq t_1$. We note that, from (5.75), it follows that

$$\|\tilde{\mathbf{Q}}\|^2 \leq V_{\mathbf{Q}}(\tilde{\mathbf{Q}}) \leq n_{\mathbf{u}}\|\tilde{\mathbf{Q}}\|^2. \tag{5.85}$$

The boundedness of the solutions $\tilde{\mathbf{Q}}(t)$ follows from (5.82) and (5.85) for $0 \leq t \leq t_1$ and from (5.84) and (5.85) for $t \geq t_1$. The bound in (5.38) of Lemma 5.9 follows from (5.84) and (5.85).

5.7.3 Proof of Lemma 5.10

From (5.23), (5.25), (5.34) and (5.35), we obtain that the state equations for $\tilde{m}_1$ and $\tilde{\mathbf{m}}_2$ are given by

$$\begin{aligned}\dot{\tilde{m}}_1 = &-\eta_{\mathbf{m}}\tilde{m}_1 - \frac{\dot{\hat{\mathbf{u}}}^T}{\alpha_{\boldsymbol{\omega}}}\mathbf{m}_2 + (g_{\mathbf{m}} - g_{\boldsymbol{\omega}} - \eta_{\mathbf{m}})\,\eta_{\mathbf{m}}k_1 \\ &+ (g_\alpha + g_{\mathbf{m}} - g_{\boldsymbol{\omega}} - \eta_{\mathbf{m}})\,\frac{\eta_{\mathbf{m}}}{\eta_{\boldsymbol{\omega}}}\mathbf{l}_1^T\mathbf{m}_2 - \alpha_{\boldsymbol{\omega}}^2\frac{\eta_{\mathbf{m}}}{\eta_{\boldsymbol{\omega}}}\mathbf{l}_1^T\mathbf{w} + \alpha_{\boldsymbol{\omega}}^2\eta_{\mathbf{m}}v + \eta_{\mathbf{m}}z\end{aligned} \tag{5.86}$$

and

$$\begin{aligned}\dot{\tilde{\mathbf{m}}}_2 = &-g_\alpha\tilde{\mathbf{m}}_2 - \eta_{\mathbf{m}}\mathbf{Q}\boldsymbol{\omega}\tilde{m}_1 - \eta_{\mathbf{m}}\mathbf{Q}\boldsymbol{\omega}\boldsymbol{\omega}^T\tilde{\mathbf{m}}_2 - \eta_{\mathbf{m}}\mathbf{Q}\boldsymbol{\omega}\eta_{\mathbf{m}}k_1 - \eta_{\mathbf{m}}\mathbf{Q}\boldsymbol{\omega}\frac{\eta_{\mathbf{m}}}{\eta_{\boldsymbol{\omega}}}\mathbf{l}_1^T\mathbf{m}_2 \\ &+ (g_\alpha + g_{\mathbf{m}} - g_{\boldsymbol{\omega}} - \eta_{\mathbf{m}})\,\eta_{\mathbf{m}}\mathbf{Q}\mathbf{k}_2 - \alpha_{\boldsymbol{\omega}}^2\mathbf{w} + \alpha_{\boldsymbol{\omega}}^2\eta_{\mathbf{m}}\mathbf{Q}\boldsymbol{\omega}v + \eta_{\mathbf{m}}\mathbf{Q}\boldsymbol{\omega}z \\ &+ \eta_{\mathbf{m}}\mathbf{Q}\mathbf{b}_{\boldsymbol{\omega}d}.\end{aligned} \tag{5.87}$$

We introduce the following Lyapunov-function candidate for the $\tilde{m}_1, \tilde{\mathbf{m}}_2$-dynamics:

$$V_{\mathbf{m}}(\tilde{m}_1, \tilde{\mathbf{m}}_2, \mathbf{Q}) = \tilde{m}_1^2 + \tilde{\mathbf{m}}_2^T\mathbf{Q}^{-1}\tilde{\mathbf{m}}_2. \tag{5.88}$$

We note that

$$\begin{aligned}\max\left\{|\tilde{m}_1|^2, \lambda_{\min}(\mathbf{Q}^{-1})\|\tilde{\mathbf{m}}_2\|^2\right\} &\leq V_{\mathbf{m}}(\tilde{m}_1, \tilde{\mathbf{m}}_2, \mathbf{Q}) \\ &\leq \max\left\{2|\tilde{m}_1|^2, 2\lambda_{\max}(\mathbf{Q}^{-1})\|\tilde{\mathbf{m}}_2\|^2\right\},\end{aligned} \tag{5.89}$$

where $\lambda_{\min}(\mathbf{Q}^{-1})$ and $\lambda_{\max}(\mathbf{Q}^{-1})$ are the smallest and largest eigenvalue of $\mathbf{Q}^{-1}$, respectively. From (5.25) (see also (5.70) in the proof of Lemma 5.9), (5.86) and (5.87), it follows that the time derivative of $V_{\mathbf{m}}$ can be written as

$$\begin{aligned}\dot{V}_{\mathbf{m}}(\tilde{m}_1, \tilde{\mathbf{m}}_2, \mathbf{Q}) = &-\eta_{\mathbf{m}}\tilde{m}_1^2 - \eta_{\mathbf{m}}\tilde{\mathbf{m}}_2^T\mathbf{Q}^{-1}\tilde{\mathbf{m}}_2 - \eta_{\mathbf{m}}(\tilde{m}_1 + \boldsymbol{\omega}^T\tilde{\mathbf{m}}_2)^2 \\ &- \frac{2}{\alpha_{\boldsymbol{\omega}}}\tilde{m}_1\dot{\hat{\mathbf{u}}}^T\mathbf{m}_2 + 2\,(g_{\mathbf{m}} - g_{\boldsymbol{\omega}})\,\eta_{\mathbf{m}}\tilde{m}_1k_1 - 2\eta_{\mathbf{m}}\eta_{\mathbf{m}}(\tilde{m}_1 + \boldsymbol{\omega}^T\tilde{\mathbf{m}}_2)k_1 \\ &+ 2\,(g_\alpha + g_{\mathbf{m}} - g_{\boldsymbol{\omega}})\,\frac{\eta_{\mathbf{m}}}{\eta_{\boldsymbol{\omega}}}\tilde{m}_1\mathbf{l}_1^T\mathbf{m}_2 - 2\eta_{\mathbf{m}}\frac{\eta_{\mathbf{m}}}{\eta_{\boldsymbol{\omega}}}(\tilde{m}_1 + \boldsymbol{\omega}^T\tilde{\mathbf{m}}_2)\mathbf{l}_1^T\mathbf{m}_2 \\ &+ 2\,(g_\alpha + g_{\mathbf{m}} - g_{\boldsymbol{\omega}} - \eta_{\mathbf{m}})\,\eta_{\mathbf{m}}\tilde{\mathbf{m}}_2^T\mathbf{k}_2 - 2\alpha_{\boldsymbol{\omega}}^2\frac{\eta_{\mathbf{m}}}{\eta_{\boldsymbol{\omega}}}\tilde{m}_1\mathbf{l}_1^T\mathbf{w} - 2\alpha_{\boldsymbol{\omega}}^2\tilde{\mathbf{m}}_2^T\mathbf{Q}^{-1}\mathbf{w} \\ &+ 2\eta_{\mathbf{m}}\tilde{\mathbf{m}}_2^T\mathbf{b}_{\boldsymbol{\omega}d} + 2\alpha_{\boldsymbol{\omega}}^2\eta_{\mathbf{m}}(\tilde{m}_1 + \boldsymbol{\omega}^T\tilde{\mathbf{m}}_2)v + 2\eta_{\mathbf{m}}(\tilde{m}_1 + \boldsymbol{\omega}^T\tilde{\mathbf{m}}_2)z.\end{aligned} \tag{5.90}$$

By applying Young's inequality and using (5.88), we obtain

$$\begin{aligned}\dot{V}_{\mathbf{m}}(\tilde{m}_1, \tilde{\mathbf{m}}_2, \mathbf{Q}) \leq & -\frac{\eta_{\mathbf{m}}}{2} V_{\mathbf{m}}(\tilde{m}_1, \tilde{\mathbf{m}}_2, \mathbf{Q}) + \frac{8}{\alpha_{\boldsymbol{\omega}}^2 \eta_{\mathbf{m}}} \|\dot{\hat{\mathbf{u}}}\|^2 \|\mathbf{m}_2\|^2 \\ & + 4\eta_{\mathbf{m}} \left(\frac{\eta_{\mathbf{m}}}{\eta_{\boldsymbol{\omega}}}\right)^2 \|\mathbf{l}_1\|^2 \|\mathbf{m}_2\|^2 + \frac{8}{\eta_{\mathbf{m}}} |g_{\mathbf{m}} - g_{\boldsymbol{\omega}}|^2 \eta_{\mathbf{m}}^2 |k_1|^2 + 4\eta_{\mathbf{m}} \eta_{\mathbf{m}}^2 |k_1|^2 \\ & + \frac{8}{\eta_{\mathbf{m}}} \left(g_\alpha + |g_{\mathbf{m}} - g_{\boldsymbol{\omega}}|\right)^2 \left(\frac{\eta_{\mathbf{m}}}{\eta_{\boldsymbol{\omega}}}\right)^2 \|\mathbf{l}_1\|^2 \|\mathbf{m}_2\|^2 + 6\eta_{\mathbf{m}} \|\mathbf{Q}\| \|\mathbf{b}_{\boldsymbol{\omega} d}\|^2 \\ & + \frac{6}{\eta_{\mathbf{m}}} \left(g_\alpha + |g_{\mathbf{m}} - g_{\boldsymbol{\omega}}| + \eta_{\mathbf{m}}\right)^2 \eta_{\mathbf{m}}^2 \|\mathbf{Q}\| \|\mathbf{k}_2\|^2 + 4\eta_{\mathbf{m}} |z|^2 \\ & + 8\frac{\alpha_{\boldsymbol{\omega}}^4}{\eta_{\mathbf{m}}} \left(\frac{\eta_{\mathbf{m}}}{\eta_{\boldsymbol{\omega}}}\right)^2 \|\mathbf{l}_1\|^2 \|\mathbf{w}\|^2 + 6\frac{\alpha_{\boldsymbol{\omega}}^4}{\eta_{\mathbf{m}}} \|\mathbf{Q}^{-1}\| \|\mathbf{w}\|^2 + 4\alpha_{\boldsymbol{\omega}}^4 \eta_{\mathbf{m}} |v|^2. \end{aligned} \tag{5.91}$$

From Assumption 5.3 and (5.20), we have

$$\|\mathbf{m}_2\| \leq \alpha_{\boldsymbol{\omega}} L_{F2} \|\tilde{\mathbf{u}}\|. \tag{5.92}$$

From Assumption 5.6 and (5.35), it follows that

$$|k_1| \leq q_d, \qquad \|\mathbf{k}_2\| \leq q_{\boldsymbol{\omega} d}. \tag{5.93}$$

From the definition of $\mathbf{l}_1$ in (5.35), it follows that there exists a constant $L_{\mathrm{l}1} \in \mathbb{R}_{>0}$ such that

$$\|\mathbf{l}_1\| \leq L_{\mathrm{l}1}. \tag{5.94}$$

From Assumption 5.3 and (5.24), we obtain

$$\|\mathbf{w}\| \leq \frac{1}{\alpha_{\boldsymbol{\omega}}} L_{F2} \|\dot{\hat{\mathbf{u}}}\|. \tag{5.95}$$

Similarly, from Assumption 5.3, (5.61) in the proof of Lemma 5.8 and (5.24), we obtain

$$|v| \leq \frac{1}{2} L_{F2} L_{\boldsymbol{\omega}1}^2. \tag{5.96}$$

Furthermore, to obtain a bound on $|z|$, from (5.24), we have

$$\begin{aligned} |z| \leq & \left| \int_0^1 \left(\frac{\partial h}{\partial \mathbf{x}}(\sigma \tilde{\mathbf{x}} + \mathbf{X}(\mathbf{u}), \mathbf{u}) - \frac{\partial h}{\partial \mathbf{x}}(\mathbf{X}(\mathbf{u}), \mathbf{u}) \right) d\sigma \tilde{\mathbf{x}} \right| \\ & + \left| \left(\frac{\partial h}{\partial \mathbf{x}}(\mathbf{X}(\mathbf{u}), \mathbf{u}) - \frac{\partial h}{\partial \mathbf{x}}(\mathbf{X}(\mathbf{u}^*), \mathbf{u}^*) \right) \tilde{\mathbf{x}} \right| + \left| \frac{\partial h}{\partial \mathbf{x}}(\mathbf{X}(\mathbf{u}^*), \mathbf{u}^*) \tilde{\mathbf{x}} \right| \end{aligned} \tag{5.97}$$

From Assumption 5.4, it follows that

$$\left\| \frac{\partial h}{\partial \mathbf{x}}(\mathbf{x}_1, \mathbf{u}_1) - \frac{\partial h}{\partial \mathbf{x}}(\mathbf{x}_2, \mathbf{u}_2) \right\| \leq L_{h\mathbf{x}} \|\mathbf{x}_1 - \mathbf{x}_2\| + L_{h\mathbf{u}} \|\mathbf{u}_1 - \mathbf{u}_2\| \tag{5.98}$$

for all $\mathbf{x}_1, \mathbf{x}_2 \in \mathbb{R}^{n_\mathbf{x}}$ and all $\mathbf{u}_1, \mathbf{u}_2 \in \mathbb{R}^{n_\mathbf{u}}$. By applying the bound in (5.98) to (5.97), we obtain

$$|z| \leq \frac{L_{h\mathbf{x}}}{2}\|\tilde{\mathbf{x}}\|^2 + L_{h\mathbf{x}}\|\mathbf{X}(\mathbf{u}) - \mathbf{X}(\mathbf{u}^*)\|\|\tilde{\mathbf{x}}\| + L_{h\mathbf{u}}\|\mathbf{u} - \mathbf{u}^*\|\|\tilde{\mathbf{x}}\| + L_{h*}\|\tilde{\mathbf{x}}\|, \tag{5.99}$$

with $L_{h*} = \|\frac{\partial h}{\partial \mathbf{x}}(\mathbf{X}(\mathbf{u}^*), \mathbf{u}^*)\|$. Subsequently, from Assumption 5.1, it follows that

$$|z| \leq \frac{L_{h\mathbf{x}}}{2}\|\tilde{\mathbf{x}}\|^2 + (L_{h\mathbf{x}}L_\mathbf{X} + L_{h\mathbf{u}})\|\mathbf{u} - \mathbf{u}^*\|\|\tilde{\mathbf{x}}\| + L_{h*}\|\tilde{\mathbf{x}}\|. \tag{5.100}$$

From (5.13), (5.34) and (5.61) in the proof of Lemma 5.8, we have

$$\|\mathbf{u} - \mathbf{u}^*\| \leq \|\tilde{\mathbf{u}}\| + \alpha_{\boldsymbol{\omega}} L_{\boldsymbol{\omega}1}. \tag{5.101}$$

By substituting (5.101) in (5.100), we obtain the following bound on $|z|$:

$$\begin{aligned} |z| \leq \frac{L_{h\mathbf{x}}}{2}\|\tilde{\mathbf{x}}\|^2 &+ (L_{h\mathbf{x}}L_\mathbf{X} + L_{h\mathbf{u}})\|\tilde{\mathbf{u}}\|\|\tilde{\mathbf{x}}\| \\ &+ \alpha_{\boldsymbol{\omega}}(L_{h\mathbf{x}}L_\mathbf{X} + L_{h\mathbf{u}})L_{\boldsymbol{\omega}1}\|\tilde{\mathbf{x}}\| + L_{h*}\|\tilde{\mathbf{x}}\|. \end{aligned} \tag{5.102}$$

From (5.27), it follows that $\|\dot{\hat{\mathbf{u}}}\| \leq \eta_\mathbf{u}$. By substituting $\|\dot{\hat{\mathbf{u}}}\| \leq \eta_\mathbf{u}$ and the bounds in (5.92)-(5.96) and (5.102) in (5.91), we obtain

$$\begin{aligned} \dot{V}_\mathbf{m}(\tilde{m}_1, \tilde{\mathbf{m}}_2, \mathbf{Q}) \leq\ & -\frac{\eta_\mathbf{m}}{2}V_\mathbf{m}(\tilde{m}_1, \tilde{\mathbf{m}}_2, \mathbf{Q}) + 8\frac{\eta_\mathbf{u}^2}{\eta_\mathbf{m}}L_{F2}^2\|\tilde{\mathbf{u}}\|^2 \\ &+ 4\alpha_{\boldsymbol{\omega}}^2\eta_\mathbf{m}\left(\frac{\eta_\mathbf{m}}{\eta_{\boldsymbol{\omega}}}\right)^2 L_{\mathrm{l}1}^2 L_{F2}^2\|\tilde{\mathbf{u}}\|^2 + \frac{8}{\eta_\mathbf{m}}|g_\mathbf{m} - g_{\boldsymbol{\omega}}|^2\eta_\mathbf{m}^2 q_d^2 + 4\eta_\mathbf{m}\eta_\mathbf{m}^2 q_d^2 \\ &+ 8\frac{\alpha_{\boldsymbol{\omega}}^2}{\eta_\mathbf{m}}\left(g_\alpha + |g_\mathbf{m} - g_{\boldsymbol{\omega}}|\right)^2\left(\frac{\eta_\mathbf{m}}{\eta_{\boldsymbol{\omega}}}\right)^2 L_{\mathrm{l}1}^2 L_{F2}^2\|\tilde{\mathbf{u}}\|^2 \\ &+ \frac{6}{\eta_\mathbf{m}}\left(g_\alpha + |g_\mathbf{m} - g_{\boldsymbol{\omega}}| + \eta_\mathbf{m}\right)^2\eta_\mathbf{m}^2\|\mathbf{Q}\|q_{\boldsymbol{\omega}d}^2 + 6\eta_\mathbf{m}\|\mathbf{Q}\|\|\mathbf{b}_{\boldsymbol{\omega}d}\|^2 \\ &+ 8\frac{\alpha_{\boldsymbol{\omega}}^2}{\eta_\mathbf{m}}\left(\frac{\eta_\mathbf{m}}{\eta_{\boldsymbol{\omega}}}\right)^2 L_{\mathrm{l}1}^2 L_{F2}^2\|\dot{\hat{\mathbf{u}}}\|^2 + 6\frac{\alpha_{\boldsymbol{\omega}}^2}{\eta_\mathbf{m}}\|\mathbf{Q}^{-1}\|L_{F2}^2\|\dot{\hat{\mathbf{u}}}\|^2 \\ &+ \alpha_{\boldsymbol{\omega}}^4\eta_\mathbf{m}L_{F2}^2L_{\boldsymbol{\omega}1}^4 + 4\eta_\mathbf{m}\Bigg((L_{h\mathbf{x}}L_\mathbf{X} + L_{h\mathbf{u}})\|\tilde{\mathbf{u}}\|\|\tilde{\mathbf{x}}\| \\ &+ \alpha_{\boldsymbol{\omega}}(L_{h\mathbf{x}}L_\mathbf{X} + L_{h\mathbf{u}})L_{\boldsymbol{\omega}1}\|\tilde{\mathbf{x}}\| + L_{h*}\|\tilde{\mathbf{x}}\| + \frac{L_{h\mathbf{x}}}{2}\|\tilde{\mathbf{x}}\|^2\Bigg)^2. \end{aligned} \tag{5.103}$$

We note that if the right-hand side of (5.103) is bounded and $\mathbf{Q}^{-1}$ is positive definite and bounded for all $0 \leq t \leq t_2$, where $t_2 \geq t_1$ is a finite time, then it follows from (5.89) and (5.103) that the solutions $\tilde{m}_1(t)$ and $\tilde{\mathbf{m}}_2(t)$ are bounded for all $0 \leq t \leq t_2$ using the same arguments as applied in the proofs of Lemmas 5.8 and 5.9. From (5.73) in the proof of Lemma 5.9, it follows that

$$\begin{aligned} &\lambda_{\min}(\mathbf{Q}^{-1}(0))e^{-\eta_\mathbf{m}(0)t} \leq \lambda_{\min}(\mathbf{Q}^{-1}(t)), \\ &\lambda_{\max}(\mathbf{Q}^{-1}(t)) \leq \lambda_{\max}(\mathbf{Q}^{-1}(0))e^{2c_g t} + \frac{\eta_\mathbf{m}(0)}{2c_g}L_{\boldsymbol{\omega}1}^2 \end{aligned} \tag{5.104}$$

for all $t \geq 0$, which implies that $\mathbf{Q}^{-1}$ is positive definite and bounded for all $0 \leq t \leq t_2$. The boundedness of the right-hand side of (5.103) for all $0 \leq t \leq t_2$ follows from the bounds on g_α, $g_{\boldsymbol{\omega}}$ and $g_{\mathbf{m}}$ in (5.30) of Theorem 5.7, from the lower bound on $\eta_{\boldsymbol{\omega}}$ and $\eta_{\mathbf{u}}$ in (5.80) in the proof of Lemma 5.9 and the fact that $\alpha_{\boldsymbol{\omega}}$, $\eta_{\mathbf{m}}$ and $\eta_{\mathbf{u}}$ are nonincreasing (see (5.14) and (5.28)), from the boundedness of $\tilde{\mathbf{x}}$ and $\tilde{\mathbf{u}}$ for $0 \leq t \leq t_2$ in Lemmas 5.8 and 5.11, respectively, from $\|\dot{\hat{\mathbf{u}}}\| \leq \eta_{\mathbf{u}}$ (see (5.27)) and from the bounds in (5.104), which imply that $\|\mathbf{Q}^{-1}(t)\| = \lambda_{\max}(\mathbf{Q}^{-1}(t))$ and $\|\mathbf{Q}(t)\| = \frac{1}{\lambda_{\min}(\mathbf{Q}^{-1}(t))}$ are bounded for all $0 \leq t \leq t_2$. Further details regarding the boundedness of the solutions $\tilde{m}_1(t)$ and $\tilde{\mathbf{m}}_2(t)$ for $0 \leq t \leq t_2$ are left to the reader.

Let us define $t_2 \geq t_1$ such that

$$\|\tilde{\mathbf{x}}(t)\| \leq \alpha_{\boldsymbol{\omega}}(t)\eta_{\boldsymbol{\omega}}(t)c_{\mathbf{x}2}, \qquad \|\tilde{\mathbf{Q}}(t)\| \leq \frac{1}{8} \tag{5.105}$$

for all $t \geq t_2$. The existence of a finite time $t_2 \geq t_1$ such that $\|\tilde{\mathbf{x}}(t)\| \leq \alpha_{\boldsymbol{\omega}}(t)\eta_{\boldsymbol{\omega}}(t)c_{\mathbf{x}2}$ for all $t \geq t_2$ follows from Lemma 5.8, where we assume without loss of generality that ε_1 in Theorem 5.7 is sufficiently small such that $g_\alpha(t)+g_{\boldsymbol{\omega}}(t) < \beta_{\mathbf{x}}$ for all $t \geq t_1$ and all $g_\alpha + g_{\boldsymbol{\omega}} \leq \varepsilon_1$. Similarly, the existence of a constant $t_2 \geq t_1$ such that $\|\tilde{\mathbf{Q}}(t)\| \leq \frac{1}{8}$ for all $t \geq t_2$ follows from Lemma 5.9 if $\int_{t_1}^{\infty} \eta_{\mathbf{m}}(t)dt = \infty$, which implies that first term in the right-hand side of (5.38) becomes smaller than $\frac{1}{8}$ as time goes to infinity. From (5.26) and the first equation in (5.29) of Theorem 5.7, we have

$$\begin{aligned}\int_{t_1}^{\infty} \eta_{\mathbf{m}}(t)dt &= \eta_{\mathbf{m}}(0)\int_{t_1}^{\infty} e^{-\int_0^t g_{\mathbf{m}}(\tau)d\tau}dt \\ &= \eta_{\mathbf{m}}(0)\left(\underbrace{\int_0^{\infty} e^{-\int_0^t g_{\mathbf{m}}(\tau)d\tau}dt}_{=\infty} - \underbrace{\int_0^{t_1} e^{-\int_0^t g_{\mathbf{m}}(\tau)d\tau}dt}_{\leq t_1}\right) = \infty\end{aligned} \tag{5.106}$$

for all $\eta_{\mathbf{m}}(0) \in \mathbb{R}_{>0}$. Hence, there exist a time $t_2 \geq t_1$ such that (5.105) holds for all $t \geq t_2$.

Now, from (5.34) and (5.78) in the proof of Lemma 5.9, it follows that

$$\left\|\mathbf{Q}^{-1} - \frac{1}{2}\mathbf{I}\right\| \leq \|\tilde{\mathbf{Q}}\| + \frac{\eta_{\mathbf{m}}}{\eta_{\boldsymbol{\omega}}}L_{\mathbf{l}2}. \tag{5.107}$$

Without loss of generality, we assume that ε_5 in Theorem 5.7 is sufficiently small such that it follows from (5.32), Lemma 5.9 and (5.105) that

$$\frac{1}{4}\mathbf{I} \preceq \mathbf{Q}^{-1} \preceq \frac{3}{4}\mathbf{I} \tag{5.108}$$

for all $t \geq t_2$ and all $\eta_{\mathbf{m}} \leq \eta_{\boldsymbol{\omega}}\varepsilon_5$. Subsequently, from (5.89) and (5.108), we obtain

$$\max\left\{|\tilde{m}_1|^2, \frac{1}{4}\|\tilde{\mathbf{m}}_2\|^2\right\} \leq V_{\mathbf{m}}(\tilde{m}_1, \tilde{\mathbf{m}}_2, \mathbf{Q}) \leq \max\left\{2|\tilde{m}_1|^2, \frac{3}{2}\|\tilde{\mathbf{m}}_2\|^2\right\} \tag{5.109}$$

for $t \geq t_2$. Moreover, from (5.108), it follows that

$$\|\mathbf{Q}^{-1}\| \leq \frac{3}{4}, \quad \|\mathbf{Q}\| \leq 4 \tag{5.110}$$

for all $t \geq t_2$. From (5.27) and (5.34), we have that

$$\|\dot{\hat{\mathbf{u}}}\| \leq \lambda_{\mathbf{u}} \|\hat{\mathbf{m}}_2\| \leq \lambda_{\mathbf{u}} \left(\|\tilde{\mathbf{m}}_2\| + \|\mathbf{m}_2\| + \eta_{\mathbf{m}} \|\mathbf{Q}\| \|\mathbf{k}_2\|\right). \tag{5.111}$$

Subsequently, from (5.92), (5.93) and (5.110), we obtain

$$\|\dot{\hat{\mathbf{u}}}\| \leq \lambda_{\mathbf{u}} \left(\|\tilde{\mathbf{m}}_2\| + \alpha_{\boldsymbol{\omega}} L_{F2} \|\tilde{\mathbf{u}}\| + 4\eta_{\mathbf{m}} q_{\boldsymbol{\omega} d}\right). \tag{5.112}$$

for all $t \geq t_2$. From (5.109) and (5.112), it follows that

$$\|\dot{\hat{\mathbf{u}}}\|^2 \leq 12\lambda_{\mathbf{u}}^2 V_{\mathbf{m}}(\tilde{m}_1, \tilde{\mathbf{m}}_2, \mathbf{Q}) + 3\alpha_{\boldsymbol{\omega}}^2 \lambda_{\mathbf{u}}^2 L_{F2}^2 \|\tilde{\mathbf{u}}\|^2 + 48\eta_{\mathbf{m}}^2 \lambda_{\mathbf{u}}^2 q_{\boldsymbol{\omega} d} \tag{5.113}$$

for all $t \geq t_2$. Without loss of generality, we assume that ε_2, ε_3, ε_4, ε_5 and ε_7 in Theorem 5.7 are sufficiently small such that we obtain from (5.32), (5.103), (5.105), (5.110) and (5.113) that

$$\begin{aligned}
\dot{V}_{\mathbf{m}}(\tilde{m}_1, \tilde{\mathbf{m}}_2, \mathbf{Q}) \leq{}& -\frac{\eta_{\mathbf{m}}}{4} V_{\mathbf{m}}(\tilde{m}_1, \tilde{\mathbf{m}}_2, \mathbf{Q}) + 2\alpha_{\boldsymbol{\omega}}^4 \eta_{\mathbf{m}} L_{F2}^2 L_{\boldsymbol{\omega}1}^4 + 16\alpha_{\boldsymbol{\omega}}^2 \eta_{\boldsymbol{\omega}}^2 \eta_{\mathbf{m}} c_{\mathbf{x}2}^2 L_{h*}^2 \\
&+ 16\alpha_{\boldsymbol{\omega}}^2 \eta_{\boldsymbol{\omega}}^2 \eta_{\mathbf{m}} c_{\mathbf{x}2}^2 (L_{h\mathbf{x}} L_{\mathbf{X}} + L_{h\mathbf{u}})^2 \|\tilde{\mathbf{u}}\|^2 + 8\frac{\alpha_{\boldsymbol{\omega}}^2 \eta_{\mathbf{m}}^3}{\eta_{\boldsymbol{\omega}}^2} L_{\mathrm{l}1}^2 L_{F2}^2 \|\tilde{\mathbf{u}}\|^2 \\
&+ 27\frac{\alpha_{\boldsymbol{\omega}}^4 \lambda_{\mathbf{u}}^2}{\eta_{\mathbf{m}}} L_{F2}^4 \|\tilde{\mathbf{u}}\|^2 + \frac{8\eta_{\mathbf{u}}^2}{\eta_{\mathbf{m}}} L_{F2}^2 \|\tilde{\mathbf{u}}\|^2 + 8\eta_{\mathbf{m}}^3 q_d^2 + 96\eta_{\mathbf{m}}^3 q_{\boldsymbol{\omega} d}^2 + 24\eta_{\mathbf{m}} \|\mathbf{b}_{\boldsymbol{\omega} d}\|^2
\end{aligned} \tag{5.114}$$

for all $t \geq t_2$, all $g_\alpha \leq \eta_{\mathbf{m}} \varepsilon_2$, all $|g_{\mathbf{m}} - g_{\boldsymbol{\omega}}| \leq \eta_{\mathbf{m}} \varepsilon_3$, all $\eta_{\boldsymbol{\omega}} \leq \varepsilon_4$, $\eta_{\mathbf{m}} \leq \eta_{\boldsymbol{\omega}} \varepsilon_5$ and all $\alpha_{\boldsymbol{\omega}} \lambda_{\mathbf{u}} \leq \eta_{\mathbf{m}} \varepsilon_7$. From this, it follows that

$$\dot{V}_{\mathbf{m}}(\tilde{m}_1, \tilde{\mathbf{m}}_2, \mathbf{Q}) \leq -\frac{\eta_{\mathbf{m}}}{8} V_{\mathbf{m}}(\tilde{m}_1, \tilde{\mathbf{m}}_2, \mathbf{Q}) \tag{5.115}$$

if

$$\begin{aligned}
V_{\mathbf{m}}(\tilde{m}_1, \tilde{\mathbf{m}}_2, \mathbf{Q}) \geq 72 \max\Big\{ & 2\alpha_{\boldsymbol{\omega}}^4 \eta_{\mathbf{m}} L_{F2}^2 L_{\boldsymbol{\omega}1}^4, 16\alpha_{\boldsymbol{\omega}}^2 \eta_{\boldsymbol{\omega}}^2 \eta_{\mathbf{m}} c_{\mathbf{x}2}^2 L_{h*}^2, \\
& 16\alpha_{\boldsymbol{\omega}}^2 \eta_{\boldsymbol{\omega}}^2 \eta_{\mathbf{m}} c_{\mathbf{x}2}^2 (L_{h\mathbf{x}} L_{\mathbf{X}} + L_{h\mathbf{u}})^2 \|\tilde{\mathbf{u}}\|^2, 8\frac{\alpha_{\boldsymbol{\omega}}^2 \eta_{\mathbf{m}}^3}{\eta_{\boldsymbol{\omega}}^2} L_{\mathrm{l}1}^2 L_{F2}^2 \|\tilde{\mathbf{u}}\|^2, 27\frac{\alpha_{\boldsymbol{\omega}}^4 \lambda_{\mathbf{u}}^2}{\eta_{\mathbf{m}}} L_{F2}^4 \|\tilde{\mathbf{u}}\|^2, \\
& \frac{8\eta_{\mathbf{u}}^2}{\eta_{\mathbf{m}}} L_{F2}^2 \|\tilde{\mathbf{u}}\|^2, 8\eta_{\mathbf{m}}^3 q_d^2, 96\eta_{\mathbf{m}}^3 q_{\boldsymbol{\omega} d}^2, 24\eta_{\mathbf{m}} \|\mathbf{b}_{\boldsymbol{\omega} d}\|^2 \Big\}
\end{aligned} \tag{5.116}$$

for all $t \geq t_2$. The bounds in (5.39), (5.40) and (5.41) of Lemma 5.10 follow from (5.109), (5.115) and (5.116), respectively.

5.7.4 Proof of Lemma 5.11

From (5.20), (5.27) and (5.34), we obtain that the state equation for $\tilde{\mathbf{u}}$ is given by

$$\dot{\tilde{\mathbf{u}}} = -\lambda_{\mathbf{u}} \frac{\eta_{\mathbf{u}} \left(\alpha_{\boldsymbol{\omega}} \frac{dF}{d\mathbf{u}^T}(\hat{\mathbf{u}}) + \tilde{\mathbf{m}}_2 + \eta_{\mathbf{m}} \mathbf{Q} \mathbf{k}_2 \right)}{\eta_{\mathbf{u}} + \lambda_{\mathbf{u}} \left\| \alpha_{\boldsymbol{\omega}} \frac{dF}{d\mathbf{u}^T}(\hat{\mathbf{u}}) + \tilde{\mathbf{m}}_2 + \eta_{\mathbf{m}} \mathbf{Q} \mathbf{k}_2 \right\|}. \tag{5.117}$$

From (5.117), it follows that $\|\dot{\tilde{\mathbf{u}}}\| \leq \eta_{\mathbf{u}}$, from which we obtain that

$$\|\tilde{\mathbf{u}}(t)\| \leq \|\tilde{\mathbf{u}}(0)\| + \eta_{\mathbf{u}}(0) t \tag{5.118}$$

for all $t \geq 0$. We define the following Lyapunov-function candidate for the $\tilde{\mathbf{u}}$-dynamics:

$$V_{\mathbf{u}}(\tilde{\mathbf{u}}) = \|\tilde{\mathbf{u}}\|^2. \tag{5.119}$$

From (5.117) and (5.119), it follows that the time derivative of $V_{\mathbf{u}}$ is given by

$$\dot{V}_{\mathbf{u}}(\tilde{\mathbf{u}}) = -2\lambda_{\mathbf{u}} \frac{\eta_{\mathbf{u}} \left(\alpha_{\boldsymbol{\omega}} \frac{dF}{d\mathbf{u}}(\hat{\mathbf{u}}) \tilde{\mathbf{u}} + \tilde{\mathbf{u}}^T \tilde{\mathbf{m}}_2 + \eta_{\mathbf{m}} \tilde{\mathbf{u}}^T \mathbf{Q} \mathbf{k}_2 \right)}{\eta_{\mathbf{u}} + \lambda_{\mathbf{u}} \left\| \alpha_{\boldsymbol{\omega}} \frac{dF}{d\mathbf{u}^T}(\hat{\mathbf{u}}) + \tilde{\mathbf{m}}_2 + \eta_{\mathbf{m}} \mathbf{Q} \mathbf{k}_2 \right\|}. \tag{5.120}$$

From Assumption 5.3, we subsequently obtain that

$$\begin{aligned} \dot{V}_{\mathbf{u}}(\tilde{\mathbf{u}}) \leq & -\frac{2\alpha_{\boldsymbol{\omega}} \lambda_{\mathbf{u}} \eta_{\mathbf{u}} L_{F1} \|\tilde{\mathbf{u}}\|^2}{\eta_{\mathbf{u}} + \lambda_{\mathbf{u}} \left\| \alpha_{\boldsymbol{\omega}} \frac{dF}{d\mathbf{u}^T}(\hat{\mathbf{u}}) + \tilde{\mathbf{m}}_2 + \eta_{\mathbf{m}} \mathbf{Q} \mathbf{k}_2 \right\|} \\ & + \frac{2\lambda_{\mathbf{u}} \eta_{\mathbf{u}} \|\tilde{\mathbf{u}}\| \left(\|\tilde{\mathbf{m}}_2\| + \eta_{\mathbf{m}} \|\mathbf{Q}\| \|\mathbf{k}_2\| \right)}{\eta_{\mathbf{u}} + \lambda_{\mathbf{u}} \left\| \alpha_{\boldsymbol{\omega}} \frac{dF}{d\mathbf{u}^T}(\hat{\mathbf{u}}) + \tilde{\mathbf{m}}_2 + \eta_{\mathbf{m}} \mathbf{Q} \mathbf{k}_2 \right\|}. \end{aligned} \tag{5.121}$$

By applying Young's inequality, it follows that

$$\begin{aligned} \dot{V}_{\mathbf{u}}(\tilde{\mathbf{u}}) \leq & -\frac{\alpha_{\boldsymbol{\omega}} \lambda_{\mathbf{u}} \eta_{\mathbf{u}} L_{F1} \|\tilde{\mathbf{u}}\|^2}{\eta_{\mathbf{u}} + \lambda_{\mathbf{u}} \left\| \alpha_{\boldsymbol{\omega}} \frac{dF}{d\mathbf{u}^T}(\hat{\mathbf{u}}) + \tilde{\mathbf{m}}_2 + \eta_{\mathbf{m}} \mathbf{Q} \mathbf{k}_2 \right\|} \\ & + \frac{4\lambda_{\mathbf{u}} \eta_{\mathbf{u}} \max \left\{ \|\tilde{\mathbf{m}}_2\|^2, \eta_{\mathbf{m}}^2 \|\mathbf{Q}\|^2 \|\mathbf{k}_2\|^2 \right\}}{\alpha_{\boldsymbol{\omega}} L_{F1} \left(\eta_{\mathbf{u}} + \lambda_{\mathbf{u}} \left\| \alpha_{\boldsymbol{\omega}} \frac{dF}{d\mathbf{u}^T}(\hat{\mathbf{u}}) + \tilde{\mathbf{m}}_2 + \eta_{\mathbf{m}} \mathbf{Q} \mathbf{k}_2 \right\| \right)}. \end{aligned} \tag{5.122}$$

If $V_{\mathbf{u}}(\tilde{\mathbf{u}}) \geq \frac{8}{\alpha_{\boldsymbol{\omega}}^2 L_{F1}^2} \max \left\{ \|\tilde{\mathbf{m}}_2\|^2, \eta_{\mathbf{m}}^2 \|\mathbf{Q}\|^2 \|\mathbf{k}_2\|^2 \right\}$, then from (5.119) and (5.122), it follows that

$$\dot{V}_{\mathbf{u}}(\tilde{\mathbf{u}}) \leq -\frac{\alpha_{\boldsymbol{\omega}} \lambda_{\mathbf{u}} \eta_{\mathbf{u}} L_{F1} \|\tilde{\mathbf{u}}\|^2}{2 \left(\eta_{\mathbf{u}} + \lambda_{\mathbf{u}} \left\| \alpha_{\boldsymbol{\omega}} \frac{dF}{d\mathbf{u}^T}(\hat{\mathbf{u}}) + \tilde{\mathbf{m}}_2 + \eta_{\mathbf{m}} \mathbf{Q} \mathbf{k}_2 \right\| \right)}. \tag{5.123}$$

From Assumption 5.3, (5.119) and (5.123), we obtain that

$$\dot{V}_{\mathbf{u}}(\tilde{\mathbf{u}}) \leq -\frac{\alpha_{\boldsymbol{\omega}} \lambda_{\mathbf{u}} \eta_{\mathbf{u}} L_{F1} V_{\mathbf{u}}(\tilde{\mathbf{u}})}{2 \left(\eta_{\mathbf{u}} + \alpha_{\boldsymbol{\omega}} \lambda_{\mathbf{u}} \left(L_{F2} + \frac{L_{F1}}{\sqrt{2}} \right) \sqrt{V_{\mathbf{u}}(\tilde{\mathbf{u}})} \right)}, \tag{5.124}$$

if $V_{\mathbf{u}}(\tilde{\mathbf{u}}) \geq \frac{8}{\alpha_{\boldsymbol{\omega}}^2 L_{F1}^2} \max\{\|\tilde{\mathbf{m}}_2\|^2, \eta_{\mathbf{m}}^2 \|\mathbf{Q}\|^2 \|\mathbf{k}_2\|^2\}$. From Assumption 5.6, from (5.93) and (5.110) in the proof of Lemma 5.10 and from (5.124), it follows that, for all $t \geq t_2$,

$$\dot{V}_{\mathbf{u}}(\tilde{\mathbf{u}}) \leq -\frac{1}{4} \min\left\{ \alpha_{\boldsymbol{\omega}} \lambda_{\mathbf{u}} L_{F1} V_{\mathbf{u}}(\tilde{\mathbf{u}}), \eta_{\mathbf{u}} \frac{\sqrt{2} L_{F1}}{\sqrt{2} L_{F2} + L_{F1}} \sqrt{V_{\mathbf{u}}(\tilde{\mathbf{u}})} \right\}, \tag{5.125}$$

if $V_{\mathbf{u}}(\tilde{\mathbf{u}}) \geq \frac{8}{\alpha_{\boldsymbol{\omega}}^2 L_{F1}^2} \max\{\|\tilde{\mathbf{m}}_2\|^2, 16 \eta_{\mathbf{m}}^2 q_{\boldsymbol{\omega} d}^2\}$. The boundedness of the solutions $\tilde{\mathbf{u}}(t)$ for all $0 \leq t \leq t_2$ follows from (5.118). The bounds in (5.42), (5.43) and (5.42) of Lemma 5.11 follow from $V_{\mathbf{u}}(\tilde{\mathbf{u}}) \geq \frac{8}{\alpha_{\boldsymbol{\omega}}^2 L_{F1}^2} \max\{\|\tilde{\mathbf{m}}_2\|^2, 16 \eta_{\mathbf{m}}^2 q_{\boldsymbol{\omega} d}^2\}$, (5.119) and (5.125), respectively.

5.7.5 Proof of Lemma 5.12

For notational convenience, we introduce the shorthand notation $W(t) = V(\tilde{m}_1(t), \tilde{\mathbf{m}}_2(t), \tilde{\mathbf{u}}(t), \mathbf{Q}(t), \alpha_{\boldsymbol{\omega}}(t))$. We note that the function V in (5.45) is not continuously differentiable with respect to time due to the use of the maximum function. Let the upper right-hand time derivative of V (see for example Khalil (2002)) be denoted by $D^+W(t)$ using the shorthand notation above. Let us consider the following three cases, similar to Jiang et al. (1996).

Case 1: $V_{\mathbf{u}}(\tilde{\mathbf{u}}) > \frac{1}{\alpha_{\boldsymbol{\omega}}^2} \frac{c_{\mathbf{u}1}}{\gamma_{\mathbf{m}2}} V_{\mathbf{m}}(\tilde{m}_1, \tilde{\mathbf{m}}_2, \mathbf{Q})$. We note that $W = V_{\mathbf{u}}(\tilde{\mathbf{u}})$ for Case 1. Therefore, we obtain from Lemma 5.11 that, for all $t \geq t_2$,

$$D^+W \leq -\min\left\{ \alpha_{\boldsymbol{\omega}} \lambda_{\mathbf{u}} \gamma_{\mathbf{u}3} W, \eta_{\mathbf{u}} \gamma_{\mathbf{u}4} \sqrt{W} \right\} \tag{5.126}$$

if

$$W \geq \max\left\{ \frac{1}{\alpha_{\boldsymbol{\omega}}^2} c_{\mathbf{u}1} \|\tilde{\mathbf{m}}_2\|^2, \frac{\eta_{\mathbf{m}}^2}{\alpha_{\boldsymbol{\omega}}^2} c_{\mathbf{u}2} q_{\boldsymbol{\omega} d}^2 \right\}. \tag{5.127}$$

It follows from Lemma 5.10 that

$$\frac{1}{\alpha_{\boldsymbol{\omega}}^2} \frac{c_{\mathbf{u}1}}{\gamma_{\mathbf{m}2}} V_{\mathbf{m}}(\tilde{m}_1, \tilde{\mathbf{m}}_2, \mathbf{Q}) \geq \frac{1}{\alpha_{\boldsymbol{\omega}}^2} c_{\mathbf{u}1} \|\tilde{\mathbf{m}}_2\|^2. \tag{5.128}$$

Because $W > \frac{1}{\alpha_{\boldsymbol{\omega}}^2} \frac{c_{\mathbf{u}1}}{\gamma_{\mathbf{m}2}} V_{\mathbf{m}}(\tilde{m}_1, \tilde{\mathbf{m}}_2, \mathbf{Q})$ for Case 1, we conclude from (5.127) and (5.128) that, for all $t \geq t_2$, (5.126) holds if

$$W \geq \frac{\eta_{\mathbf{m}}^2}{\alpha_{\boldsymbol{\omega}}^2} c_{\mathbf{u}2} q_{\boldsymbol{\omega} d}^2. \tag{5.129}$$

Case 2: $V_{\mathbf{u}}(\tilde{\mathbf{u}}) < \frac{1}{\alpha_{\boldsymbol{\omega}}^2} \frac{c_{\mathbf{u}1}}{\gamma_{\mathbf{m}2}} V_{\mathbf{m}}(\tilde{m}_1, \tilde{\mathbf{m}}_2, \mathbf{Q})$. We have $W = \frac{1}{\alpha_{\boldsymbol{\omega}}^2} \frac{c_{\mathbf{u}1}}{\gamma_{\mathbf{m}2}} V_{\mathbf{m}}(\tilde{m}_1, \tilde{\mathbf{m}}_2, \mathbf{Q})$ for Case 2. Therefore, it follows from (5.14) and Lemma 5.10 that, for all $t \geq t_2$,

$$D^+W \leq -(\eta_{\mathbf{m}} \gamma_{\mathbf{m}5} - 2 g_\alpha) W \tag{5.130}$$

if

$$W \geq \frac{c_{\mathbf{u}1}}{\gamma_{\mathbf{m}2}} \max\Bigg\{ \alpha_{\boldsymbol{\omega}}^2 c_{\mathbf{m}1}, \eta_{\boldsymbol{\omega}}^2 c_{\mathbf{m}2}, \eta_{\boldsymbol{\omega}}^2 c_{\mathbf{m}3} \|\tilde{\mathbf{u}}\|^2, \frac{\eta_{\mathbf{m}}^2}{\eta_{\boldsymbol{\omega}}^2} c_{\mathbf{m}4} \|\tilde{\mathbf{u}}\|^2, \frac{\alpha_{\boldsymbol{\omega}}^2 \lambda_{\mathbf{u}}^2}{\eta_{\mathbf{m}}} c_{\mathbf{m}5} \|\tilde{\mathbf{u}}\|^2, \\ \frac{\eta_{\mathbf{u}}^2}{\alpha_{\boldsymbol{\omega}}^2 \eta_{\mathbf{m}}^2} c_{\mathbf{m}6} \|\tilde{\mathbf{u}}\|^2, \frac{\eta_{\mathbf{m}}^2}{\alpha_{\boldsymbol{\omega}}^2} c_{\mathbf{m}7} q_d^2, \frac{\eta_{\mathbf{m}}^2}{\alpha_{\boldsymbol{\omega}}^2} c_{\mathbf{m}8} q_{\boldsymbol{\omega}d}^2, \frac{1}{\alpha_{\boldsymbol{\omega}}^2} c_{\mathbf{m}9} \|\mathbf{b}_{\boldsymbol{\omega}d}\|^2 \Bigg\}. \tag{5.131}$$

Without loss of generality, we assume that ε_2 in Theorem 5.7 is sufficiently small such that we obtain from (5.32) and (5.130) that

$$D^+ W \leq -\frac{\eta_{\mathbf{m}}}{2} \gamma_{\mathbf{m}5} W \tag{5.132}$$

for all $g_\alpha \leq \eta_{\mathbf{m}} \varepsilon_2$. Moreover, without loss of generality, we assume that ε_4, ε_5, ε_6 and ε_7 in Theorem 5.7 are sufficiently small such it follows from (5.32) and Lemma 5.11 that

$$V_{\mathbf{u}}(\tilde{\mathbf{u}}) \geq \frac{c_{\mathbf{u}1}}{\gamma_{\mathbf{m}2}} \max\Bigg\{ \eta_{\boldsymbol{\omega}}^2 c_{\mathbf{m}3} \|\tilde{\mathbf{u}}\|^2, \frac{\eta_{\mathbf{m}}^2}{\eta_{\boldsymbol{\omega}}^2} c_{\mathbf{m}4} \|\tilde{\mathbf{u}}\|^2, \frac{\alpha_{\boldsymbol{\omega}}^2 \lambda_{\mathbf{u}}^2}{\eta_{\mathbf{m}}} c_{\mathbf{m}5} \|\tilde{\mathbf{u}}\|^2, \frac{\eta_{\mathbf{u}}^2}{\alpha_{\boldsymbol{\omega}}^2 \eta_{\mathbf{m}}^2} c_{\mathbf{m}6} \|\tilde{\mathbf{u}}\|^2 \Bigg\} \tag{5.133}$$

for all $\eta_{\boldsymbol{\omega}} \leq \varepsilon_4$, $\eta_{\mathbf{m}} \leq \eta_{\boldsymbol{\omega}} \varepsilon_5$, $\eta_{\mathbf{u}} \leq \alpha_{\boldsymbol{\omega}} \eta_{\mathbf{m}} \varepsilon_6$ and $\alpha_{\boldsymbol{\omega}} \lambda_{\mathbf{u}} \leq \eta_{\mathbf{m}} \varepsilon_7$. Because $W > V_{\mathbf{u}}(\tilde{\mathbf{u}})$ for Case 2, we conclude from (5.131) and (5.133) that, for all $t \geq t_2$, (5.132) holds if

$$W \geq \max\Bigg\{ \alpha_{\boldsymbol{\omega}}^2 \frac{c_{\mathbf{u}1}}{\gamma_{\mathbf{m}2}} c_{\mathbf{m}1}, \eta_{\boldsymbol{\omega}}^2 \frac{c_{\mathbf{u}1}}{\gamma_{\mathbf{m}2}} c_{\mathbf{m}2}, \frac{\eta_{\mathbf{m}}^2}{\alpha_{\boldsymbol{\omega}}^2} \frac{c_{\mathbf{u}1}}{\gamma_{\mathbf{m}2}} c_{\mathbf{m}7} q_d^2, \\ \frac{\eta_{\mathbf{m}}^2}{\alpha_{\boldsymbol{\omega}}^2} \frac{c_{\mathbf{u}1}}{\gamma_{\mathbf{m}2}} c_{\mathbf{m}8} q_{\boldsymbol{\omega}d}^2, \frac{1}{\alpha_{\boldsymbol{\omega}}^2} \frac{c_{\mathbf{u}1}}{\gamma_{\mathbf{m}2}} c_{\mathbf{m}9} \|\mathbf{b}_{\boldsymbol{\omega}d}\|^2 \Bigg\}. \tag{5.134}$$

Case 3: $V_{\mathbf{u}}(\tilde{\mathbf{u}}) = \frac{1}{\alpha_{\boldsymbol{\omega}}^2} \frac{c_{\mathbf{u}1}}{\gamma_{\mathbf{m}2}} V_{\mathbf{m}}(\tilde{m}_1, \tilde{\mathbf{m}}_2, \mathbf{Q})$. We note that $W = V_{\mathbf{u}}(\tilde{\mathbf{u}}) = \frac{1}{\alpha_{\boldsymbol{\omega}}^2} \frac{c_{\mathbf{u}1}}{\gamma_{\mathbf{m}2}} V_{\mathbf{m}}(\tilde{m}_1, \tilde{\mathbf{m}}_2, \mathbf{Q})$ for Case 3. Therefore, we obtain from (5.14) and Lemmas 5.10 and 5.11 that, for all $t \geq t_2$,

$$D^+ W \leq -\min\Big\{ \alpha_{\boldsymbol{\omega}} \lambda_{\mathbf{u}} \gamma_{\mathbf{u}3} W, \eta_{\mathbf{u}} \gamma_{\mathbf{u}4} \sqrt{W}, (\eta_{\mathbf{m}} \gamma_{\mathbf{m}5} - 2 g_\alpha) W \Big\} \tag{5.135}$$

if

$$W \geq \max\Bigg\{ \frac{1}{\alpha_{\boldsymbol{\omega}}^2} c_{\mathbf{u}1} \|\tilde{\mathbf{m}}_2\|^2, \frac{\eta_{\mathbf{m}}^2}{\alpha_{\boldsymbol{\omega}}^2 \eta_{\boldsymbol{\omega}}^2} c_{\mathbf{u}2} q_{\boldsymbol{\omega}d}^2, \alpha_{\boldsymbol{\omega}}^2 \frac{c_{\mathbf{u}1}}{\gamma_{\mathbf{m}2}} c_{\mathbf{m}1}, \\ \eta_{\boldsymbol{\omega}}^2 \frac{c_{\mathbf{u}1}}{\gamma_{\mathbf{m}2}} c_{\mathbf{m}2}, \eta_{\boldsymbol{\omega}}^2 \frac{c_{\mathbf{u}1}}{\gamma_{\mathbf{m}2}} c_{\mathbf{m}3} \|\tilde{\mathbf{u}}\|^2, \frac{\eta_{\mathbf{m}}^2}{\eta_{\boldsymbol{\omega}}^2} \frac{c_{\mathbf{u}1}}{\gamma_{\mathbf{m}2}} c_{\mathbf{m}4} \|\tilde{\mathbf{u}}\|^2, \frac{\alpha_{\boldsymbol{\omega}}^2 \lambda_{\mathbf{u}}^2}{\eta_{\mathbf{m}}} \frac{c_{\mathbf{u}1}}{\gamma_{\mathbf{m}2}} c_{\mathbf{m}5} \|\tilde{\mathbf{u}}\|^2, \\ \frac{\eta_{\mathbf{u}}^2}{\alpha_{\boldsymbol{\omega}}^2 \eta_{\mathbf{m}}^2} \frac{c_{\mathbf{u}1}}{\gamma_{\mathbf{m}2}} c_{\mathbf{m}6} \|\tilde{\mathbf{u}}\|^2, \frac{\eta_{\mathbf{m}}^2}{\alpha_{\boldsymbol{\omega}}^2} \frac{c_{\mathbf{u}1}}{\gamma_{\mathbf{m}2}} c_{\mathbf{m}7} q_d^2, \frac{\eta_{\mathbf{m}}^2}{\alpha_{\boldsymbol{\omega}}^2} \frac{c_{\mathbf{u}1}}{\gamma_{\mathbf{m}2}} c_{\mathbf{m}8} q_{\boldsymbol{\omega}d}^2, \frac{1}{\alpha_{\boldsymbol{\omega}}^2} c_{\mathbf{m}9} \|\mathbf{b}_{\boldsymbol{\omega}d}\|^2 \Bigg\}. \tag{5.136}$$

By following the same steps as for Case 1 and Case 2, we obtain from (5.135) and (5.136) that, for all $t \geq t_2$,

$$D^+W \leq -\min\left\{\alpha_{\boldsymbol{\omega}}\lambda_{\mathbf{u}}\gamma_{\mathbf{u}3}W, \eta_{\mathbf{u}}\gamma_{\mathbf{u}4}\sqrt{W}, \frac{\eta_{\mathbf{m}}}{2}\gamma_{\mathbf{m}5}W\right\} \tag{5.137}$$

if

$$\begin{aligned} W \geq \max\Bigg\{ & \alpha_{\boldsymbol{\omega}}^2 \frac{c_{\mathbf{u}1}}{\gamma_{\mathbf{m}2}} c_{\mathbf{m}1}, \eta_{\boldsymbol{\omega}}^2 \frac{c_{\mathbf{u}1}}{\gamma_{\mathbf{m}2}} c_{\mathbf{m}2}, \frac{\eta_{\mathbf{m}}^2}{\alpha_{\boldsymbol{\omega}}^2} \frac{c_{\mathbf{u}1}}{\gamma_{\mathbf{m}2}} c_{\mathbf{m}7} q_d^2, \\ & \frac{\eta_{\mathbf{m}}^2}{\alpha_{\boldsymbol{\omega}}^2} \max\left\{c_{\mathbf{u}2}, \frac{c_{\mathbf{u}1}}{\gamma_{\mathbf{m}2}} c_{\mathbf{m}8}\right\} q_{\boldsymbol{\omega}d}^2, \frac{1}{\alpha_{\boldsymbol{\omega}}^2} c_{\mathbf{m}9} \|\mathbf{b}_{\boldsymbol{\omega}d}\|^2 \Bigg\}. \end{aligned} \tag{5.138}$$

We note that both (5.126) and (5.132) imply that (5.137) holds. Moreover, the inequalities in (5.129) and (5.134) are satisfied if (5.138) is satisfied. Hence, for all three cases and for all $t \geq t_2$, we have that the (5.137) holds if the inequality in (5.138) is satisfied. From (5.32) in Theorem 5.7 and (5.137), we obtain that, for all $t \geq t_2$ (with $t_2 \geq t_1$),

$$D^+W \leq -\min\left\{\alpha_{\boldsymbol{\omega}}\lambda_{\mathbf{u}}, \eta_{\mathbf{u}}\right\} \beta_V \min\left\{W, \sqrt{W}\right\} \tag{5.139}$$

for all $\alpha_{\boldsymbol{\omega}}\lambda_{\mathbf{u}} \leq \eta_{\mathbf{m}}\varepsilon_7$ if (5.138) holds, with $\beta_V = \min\left\{\gamma_{\mathbf{u}3}, \gamma_{\mathbf{u}4}, \frac{\gamma_{\mathbf{m}5}}{2\varepsilon_7}\right\}$. By applying the same reasoning as for (5.106) in the proof of Lemma 5.10, it follows from the second equation in (5.29) that

$$\int_{t_2}^{\infty} \min\left\{\alpha_{\boldsymbol{\omega}}(\tau)\lambda_{\mathbf{u}}(\tau), \eta_{\mathbf{u}}(\tau)\right\} d\tau = \infty. \tag{5.140}$$

Now, from (5.139), (5.140) and the comparison lemma (Khalil, 2002, Lemma 3.4), we obtain that the solutions $W(t)$ monotonically converge to zero as time goes to infinity for any initial condition $W(t_2) \geq 0$ if the right-hand side of (5.138) is zero. By using similar arguments as in the proof of (Khalil, 2002, Theorem 4.18), we obtain from (5.138), (5.139) and (5.140) that

$$\begin{aligned} \sup_{t\geq t_2} W(t) \leq \sup_{t\geq t_2} \max\Bigg\{ & W(t_2), \alpha_{\boldsymbol{\omega}}^2(t) \frac{c_{\mathbf{u}1}}{\gamma_{\mathbf{m}2}} c_{\mathbf{m}1}, \eta_{\boldsymbol{\omega}}^2(t) \frac{c_{\mathbf{u}1}}{\gamma_{\mathbf{m}2}} c_{\mathbf{m}2}, \frac{\eta_{\mathbf{m}}^2(t)}{\alpha_{\boldsymbol{\omega}}^2(t)} \frac{c_{\mathbf{u}1}}{\gamma_{\mathbf{m}2}} c_{\mathbf{m}7} q_d^2, \\ & \frac{\eta_{\mathbf{m}}^2(t)}{\alpha_{\boldsymbol{\omega}}^2(t)} \max\left\{c_{\mathbf{u}2}, \frac{c_{\mathbf{u}1}}{\gamma_{\mathbf{m}2}} c_{\mathbf{m}8}\right\} q_{\boldsymbol{\omega}d}^2, \frac{1}{\alpha_{\boldsymbol{\omega}}^2(t)} c_{\mathbf{m}9} \|\mathbf{b}_{\boldsymbol{\omega}d}\|^2 \Bigg\} \end{aligned} \tag{5.141}$$

and

$$\begin{aligned} \limsup_{t\to\infty} W(t) \leq \limsup_{t\to\infty} \max\Bigg\{ & \alpha_{\boldsymbol{\omega}}^2(t) \frac{c_{\mathbf{u}1}}{\gamma_{\mathbf{m}2}} c_{\mathbf{m}1}, \eta_{\boldsymbol{\omega}}^2(t) \frac{c_{\mathbf{u}1}}{\gamma_{\mathbf{m}2}} c_{\mathbf{m}2}, \frac{\eta_{\mathbf{m}}^2(t)}{\alpha_{\boldsymbol{\omega}}^2(t)} \frac{c_{\mathbf{u}1}}{\gamma_{\mathbf{m}2}} c_{\mathbf{m}7} q_d^2, \\ & \frac{\eta_{\mathbf{m}}^2(t)}{\alpha_{\boldsymbol{\omega}}^2(t)} \max\left\{c_{\mathbf{u}2}, \frac{c_{\mathbf{u}1}}{\gamma_{\mathbf{m}2}} c_{\mathbf{m}8}\right\} q_{\boldsymbol{\omega}d}^2, \frac{1}{\alpha_{\boldsymbol{\omega}}^2(t)} c_{\mathbf{m}9} \|\mathbf{b}_{\boldsymbol{\omega}d}\|^2 \Bigg\}, \end{aligned} \tag{5.142}$$

where we applied (Sontag and Wang, 1996, Lemma II.1) to obtain the limit superior in the right-hand side of (5.142). Because $\alpha_{\boldsymbol{\omega}}$ and $\eta_{\boldsymbol{\omega}}$ are nonincreasing (see (5.14)), it follows that the second and third term in the right-hand side of (5.141) are bounded. Moreover, from (5.31) in Theorem 5.7, we have that the fourth, fifth and sixth term in the right-hand side of (5.141) are bounded. Hence, we obtain from (5.141) that the solutions $W(t)$ are bounded for all $t \geq t_2$. From Lemmas 5.10 and 5.11 and from the definition of V in (5.45), we have that

$$\begin{aligned} \max \left\{ \frac{c_{\mathbf{u}1}}{\alpha_{\boldsymbol{\omega}}^2} \frac{\gamma_{\mathbf{m}1}}{\gamma_{\mathbf{m}_2}} |\tilde{m}_1|^2, \frac{c_{\mathbf{u}1}}{\alpha_{\boldsymbol{\omega}}^2} \|\tilde{\mathbf{m}}_2\|^2, \gamma_{\mathbf{u}1} \|\tilde{\mathbf{u}}\|^2 \right\} &\leq W \\ \leq \max \left\{ \frac{c_{\mathbf{u}1}}{\alpha_{\boldsymbol{\omega}}^2} \frac{\gamma_{\mathbf{m}3}}{\gamma_{\mathbf{m}_2}} |\tilde{m}_1|^2, \frac{c_{\mathbf{u}1}}{\alpha_{\boldsymbol{\omega}}^2} \frac{\gamma_{\mathbf{m}4}}{\gamma_{\mathbf{m}_2}} \|\tilde{\mathbf{m}}_2\|^2, \gamma_{\mathbf{u}2} \|\tilde{\mathbf{u}}\|^2 \right\} & \end{aligned} \tag{5.143}$$

for $t \geq t_2$, where we used the shorthand notation $W = V(\tilde{m}_1, \tilde{\mathbf{m}}_2, \tilde{\mathbf{u}}, \mathbf{Q}, \alpha_{\boldsymbol{\omega}})$. From (5.141) and (5.143), it follows that the solutions $\tilde{m}_2(t)$, $\tilde{\mathbf{m}}_2(t)$ and $\tilde{\mathbf{u}}(t)$ are bounded for all $t \geq t_2$, all $\tilde{m}_1(t_2) \in \mathbb{R}$, $\tilde{\mathbf{m}}_2(t_2) \in \mathbb{R}^{n_{\mathbf{u}}}$ and all $\tilde{\mathbf{u}}(t_2) \in \mathbb{R}^{n_{\mathbf{u}}}$. The bound in (5.46) of Lemma 5.12 follows from (5.142) and (5.143).

Chapter 6

An extremum-seeking control approach to harmonic mitigation in electrical grids

This chapter focuses on the minimization of the harmonic distortion in multi-bus electrical grids using a single active power filter. Active-power-filter control for local filtering has been studied extensively in the literature. The few works about system-wide harmonic mitigation using active power filters are based on an accurate grid model as well as multiple current measurements. The effort and expenses required to obtain an accurate grid model may be substantial, especially if the complexity and scale of the grid are large. In this chapter, we investigate the use of extremum-seeking control in order to optimize the injection current of an active power filter for system-wide harmonic mitigation. Because extremum-seeking control is often model free, it can be used without knowledge of the electrical grid. The price to pay is a slow convergence compared to model-based control methods. A case study of a two-bus electrical grid with distributed generators displays an improved performance of the used extremum-seeking control method compared to a local-filtering approach under constant load conditions of the electrical grid, while the performance with respect to a model-based system-wide filtering method is comparable. The case study also shows that the used extremum-seeking control method is slower to respond to changes in load conditions than the local and the model-based system-wide filtering methods. Extremum-seeking control can be implemented on top of existing approaches to combine the fast transient response of conventional harmonic-mitigation methods with the optimizing capabilities of extremum-seeking control.

6.1 Introduction

In this chapter, we apply extremum-seeking control to compute the injection current of an active power filter that minimizes the harmonic distortion in all nodes of an electrical grid. Harmonic distortion in alternating-current power grids is the presence of harmonic components in current and voltage signals other

than the fundamental frequency. Harmonic distortion is caused by nonlinear loads in the power grid. Although low levels of harmonic distortion are often tolerated, high levels of harmonic distortion can result in significant power losses and an increased wear of mechanical components in the grid. Severe harmonic distortion may even lead to overheating and failure of components. Several harmonic mitigation methods are discussed in Key and Lai (1998); Singh (2009); Akagi et al. (2007).

An active power filter injects a current to counteract the harmonic distortion generated by the nonlinear loads in the power grid. For local compensation of the harmonic distortion generated by a single nonlinear load, the optimal current injection by the active power filter has the same amplitude and the opposite phase of the load harmonics other than the fundamental frequency component. The control of active power filters for local filtering has been studied extensively in Akagi et al. (2007); El-Habrouk et al. (2000); Grady et al. (1990); Singh et al. (1999) and references therein. Computing the optimal current injection for simultaneously compensating harmonics in all nodes of a multi-bus system is more cumbersome as minimizing the harmonic distortion in one bus may increase the level of distortion in another. To find the optimal current injection of an active power filter for system-wide mitigation in a multi-bus electrical grid under constant load conditions, a cost function is introduced in Grady et al. (1991, 1992) to weigh the harmonic voltage distortion in the buses of the grid. The impedance matrix of the power grid is used to link the voltage distortion to the current of the active power filter. The optimal current injection is subsequently obtained by minimizing the cost function. In addition, this method can be applied to find the optimal location of the active power filter in the grid.

In Skjong et al. (2015a,b,c, 2016), a model-predictive control method is presented for system-wide harmonic mitigation in multi-bus electrical grids. The proposed method is applied to find the optimal current injection of the active power filter to mitigate the dominant harmonics in the electrical grid.

We note that the methods in Grady et al. (1991, 1992) and in Skjong et al. (2015a,b,c, 2016) require a reasonably accurate grid model to effectively mitigate the harmonic distortion in the electric grid. Accurately modeling the electrical grid may require the modeling of many components in the grid as well as their interconnections. The effort and expenses required to obtain an accurate grid model may be substantial, especially if the complexity and scale of the grid are large. Extremum-seeking control can be a valid alternative in this case, because a model of the grid is not required. The contributions of this chapter can be summarized as follows. First, we present a discrete-time extremum-seeking control method to find the injection current of the active power filter such that the harmonic distortions in all the nodes of the electrical grid are minimized. The presented extremum-seeking method is computationally cheap and can easily be implemented to an electrical grid with an arbitrary number of nodes since no grid model is required. Second, the extremum-seeking controller can be imple-

mented on top of existing approaches to combine the fast transient response of conventional harmonic-mitigation methods with the optimizing capabilities of extremum-seeking control. Third, we present a case study of a two-bus electrical grid with distributed generators. We compare harmonic-mitigation capabilities of the presented extremum-seeking control method in this chapter with those of a local-filtering method and of the model-predictive control method in Skjong et al. (2015a,b,c, 2016). We investigate the effects of static and dynamic load conditions, measurement noise and model mismatch on the harmonic mitigation for these three methods and for a combination of the extremum-seeking control method and the local-filtering method.

The organization of this chapter is as follows. We formulate the harmonic-mitigation problem in Section 6.2. The extremum-seeking control method is introduced in Section 6.3. The case study is presented in Section 6.4, followed by the conclusion of this chapter in Section 6.5.

6.2 Harmonic-mitigation problem formulation

Consider a three-phase three-wire multi-bus power grid with an active power filter. The active power filter is connected to one of the buses of the grid. Suppose we want to minimize the harmonic distortion in n buses of the electrical grid. Let these buses be numbered one to n. Moreover, let the three phases be denoted by a, b and c. Under constant load conditions, the voltage in bus j of phase p may be written as

$$V_{j,p}(t) = \sum_{h=1}^{\infty} V_{j,p}^{h} \sin\left(\frac{2\pi h t}{T_f} + \phi_{j,p}^{h}\right) \tag{6.1}$$

for $j = \{1, 2, \ldots, n\}$ and $p = \{a, b, c\}$, where $V_{j,p}^{h}$ and $\phi_{j,p}^{h}$ are the amplitude and the phase of the hth-order harmonic of $V_{i,j}(t)$ with time t, and where T_f is the period of the fundamental frequency. To balance the objective of minimizing the harmonic distortion in the n buses, we introduce the following cost function consisting of the sum of squared voltage amplitudes of the dominant distortion harmonics in the electrical grid, similar to Grady et al. (1991, 1992):

$$Z(V_{1,a}^{h_1}, \ldots, V_{n,c}^{h_m}) = \sum_{p\in\{a,b,c\}} \sum_{j=1}^{n} \sum_{h\in\mathcal{H}} \beta_{j,p}^{h} \left(V_{j,p}^{h}\right)^2, \tag{6.2}$$

where $\beta_{j,p}^{h}$ is a positive weighting constant for the voltage amplitude $V_{j,p}^{h}$, and where $\mathcal{H} = \{h_1, h_2, \ldots, h_m\}$ is a set consisting of the orders of m dominant harmonics in the electrical grid to be mitigated, where each element of $\mathcal{H}$ is unique and larger than one. As pointed out in Grady et al. (1992), the cost function in (6.2) is suited to incorporate several harmonic-distortion measures, including

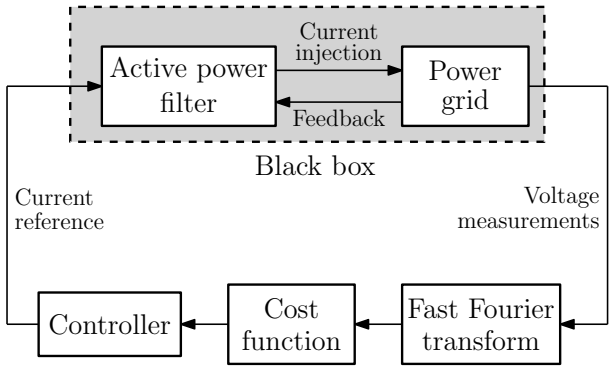

Figure 6.1: Harmonic-mitigation scheme.

the total harmonic distortion, the telephone influence factor and the motor-load loss function. Assuming the voltage signals $V_{j,p}(t)$ in (6.1) are measured, the amplitudes $V_{j,p}^h$ can be obtained by applying the fast Fourier transform to one period of the fundamental harmonic of the voltage signals.

To minimize the harmonic distortion in the buses, we provide the following current reference to the active power filter for the three phases a, b and c:

$$\begin{aligned} i_{AF,a}(t) &= \sum_{h\in\mathcal{H}} \left(u_{1,a}^h \sin\left(\frac{2\pi h t}{T_f}\right) + u_{2,a}^h \cos\left(\frac{2\pi h t}{T_f}\right)\right), \\ i_{AF,b}(t) &= \sum_{h\in\mathcal{H}} \left(u_{1,b}^h \sin\left(\frac{2\pi h t}{T_f} - \frac{2\pi}{3}h\right) + u_{2,b}^h \cos\left(\frac{2\pi h t}{T_f} - \frac{2\pi}{3}h\right)\right), \\ i_{AF,c}(t) &= \sum_{h\in\mathcal{H}} \left(u_{1,c}^h \sin\left(\frac{2\pi h t}{T_f} + \frac{2\pi}{3}h\right) + u_{2,c}^h \cos\left(\frac{2\pi h t}{T_f} + \frac{2\pi}{3}h\right)\right), \end{aligned} \tag{6.3}$$

with parameters $u_{1,p}^h, u_{2,p}^h$ for $p \in \{a,b,c\}$ and $h \in \mathcal{H}$. By feeding the references in (6.3) to the active power filter, the active power filter generates a current injection for the three phases with feedback from the power grid. In turn, the current injection to the grid influences the voltages in the buses. Hence, there is a relation between the parameters $u_{1,a}^{h_1}, u_{2,a}^{h_1}, \ldots, u_{2,c}^{h_m}$ of the current reference of the active power filter in (6.3) and the harmonics of the voltage signals in (6.1). Without detailed knowledge of the electrical grid, as we assume here, the relation between the parameters $u_{1,a}^{h_1}, u_{2,a}^{h_1}, \ldots, u_{2,c}^{h_m}$ and voltage signals is unknown. The active power filter and the power grid can be regarded as one black box with the current reference in (6.3) as input and the measured voltage signals in (6.1) as output; see Figure 6.1.

Nonetheless, for constant values of the parameters $u_{1,a}^{h_1}, u_{2,a}^{h_1}, \ldots, u_{2,c}^{h_m}$, we assume that the relation between the parameters and the amplitudes of the harmonics of the voltage signals that are part of the cost function in (6.2) are static

under constant load conditions. With this, we mean that there exist unknown static functions $g^h_{j,p}$ such that

$$V^h_{j,p} = g^h_{j,p}(u^{h_1}_{1,a}, u^{h_1}_{2,a}, \ldots, u^{h_m}_{2,c}) \tag{6.4}$$

for all $j \in \{1, 2, \ldots, n\}$, all $p \in \{a, b, c\}$ and all $h \in \mathcal{H}$. The same assumption is implicitly made in Grady et al. (1991, 1992) by linking the injection current of the active power filter to the amplitudes of the voltages in the buses via the impedance matrix of the power grid. The main difference with this work is that the impedance matrix in Grady et al. (1991, 1992) is assumed to be known while the static functions $g^h_{j,p}$ in this work are unknown.

By combining (6.4) and the cost function in (6.2), we obtain that the output of the cost function can be expressed as a function of the parameters $u^{h_1}_{1,a}, u^{h_1}_{2,a}, \ldots, u^{h_m}_{2,c}$:

$$\begin{aligned} F(u^{h_1}_{1,a}, u^{h_1}_{2,a}, \ldots, u^{h_m}_{2,c}) &= Z(g^{h_1}_{1,a}(u^{h_1}_{1,a}, \ldots, u^{h_m}_{2,c}), \ldots, g^{h_m}_{n,c}(u^{h_1}_{1,a}, \ldots, u^{h_m}_{2,c})) \\ &= \sum_{p\in\{a,b,c\}} \sum_{j=1}^{n} \sum_{h\in\mathcal{H}} \beta^h_{j,p} \left(g^h_{j,p}(u^{h_1}_{1,a}, \ldots, u^{h_m}_{2,c})\right)^2 . \end{aligned} \tag{6.5}$$

We refer to the function F as the objective function. To minimize the cost function in (6.2) under constant steady-state conditions of the power grid, we aim to find the values of the parameters $u^{h_1}_{1,a}, u^{h_1}_{2,a}, \ldots, u^{h_m}_{2,c}$ for which the value of the objective function is minimal. We note however that the objective function is unknown because the functions $g^h_{j,p}$ are unknown. An extremum-seeking controller may be defined to tune the parameters $u^{h_1}_{1,a}, u^{h_1}_{2,a}, \ldots, u^{h_m}_{2,c}$ such that the objective function is minimal using the output of the cost function as feedback; see Figure 6.1.

Note that the number of parameters is $6m$. The convergence speed of extremum-seeking control methods is inversely dependent on the number of parameters. Hence, a slow convergence is obtained if the number of harmonics to be mitigated (that is, m) is large. We make the following design assumptions to reduce the number of parameters:

- the electrical grid is balanced;
- the harmonics in the grid are isolated.

A balanced electrical grid implies that the phases of the harmonics in the buses have the same amplitude and are shifted 120° with respect to each other. Therefore, the same parameters can be chosen for the three phases of the current reference in (6.3), that is,

$$u^h_1 = u^h_{1,a} = u^h_{1,b} = u^h_{1,c}, \qquad u^h_2 = u^h_{2,a} = u^h_{2,b} = u^h_{2,c} \tag{6.6}$$

for all $h \in \mathcal{H}$. With this assumptions, the number of parameters is reduced to $2m$. The design assumption of a balanced grid is common in many text books about harmonic mitigation; see for example Akagi et al. (2007).

In addition, we assume that the harmonics in the grid are isolated. By isolated harmonics, we mean that the current reference for a given harmonic does not influence different-order harmonics in the voltages of the buses, that is

$$V_{j,p}^h = \tilde{g}_{j,p}^h(u_{1,a}^h, u_{2,a}^h, \dots, u_{2,c}^h) \tag{6.7}$$

for all $j \in \{1, 2, \dots, n\}$, all $p \in \{a, b, c\}$, all $h \in \mathcal{H}$ and some unknown functions $\tilde{g}_{j,p}^h$. We note that the output of the function $g_{j,p}^h$ in (6.4) depends on parameters of all harmonics in $\mathcal{H}$, while the output of the function $\tilde{g}_{j,p}^h$ in (6.7) only depends on parameters of the harmonic h. From (6.6) and (6.7), it follows that the objective function in (6.5) can be written as

$$F(u_{1,a}^{h_1}, u_{2,a}^{h_1}, \dots, u_{2,c}^{h_m}) = \sum_{h \in \mathcal{H}} F^h(u_1^h, u_2^h), \tag{6.8}$$

with

$$F^h(u_1^h, u_2^h) = \sum_{p \in \{a,b,c\}} \sum_{j=1}^{n} \beta_{j,p}^h \left(\tilde{g}_{j,p}^h(u_1^h, u_2^h, \dots, u_1^h, u_2^h)\right)^2. \tag{6.9}$$

Because the parameters $u_1^{h_r}, u_2^{h_r}$ do not affect the output of the function F^{h_q} for each $r, q \in \{1, 2, \dots, m\}$, $r \neq q$, the minima of the functions F^h can be computed in parallel for $h \in \mathcal{H}$. The functions F^h are unknown because the functions $\tilde{g}_{j,p}^h$ are unknown. For balanced grids with isolated harmonics, m extremum-seeking controllers can be used in parallel to generate the reference current of the active filter, where each controller generates the reference for one harmonic; see Figure 6.2. We note that each controller is required to tune only two parameters. The corresponding cost function for each $h \in \mathcal{H}$ is given by

$$Z^h(V_{1,a}^h, \dots, V_{n,c}^h) = \sum_{p \in \{a,b,c\}} \sum_{j=1}^{n} \beta_{j,p}^h \left(V_{j,p}^h\right)^2. \tag{6.10}$$

Similarly to having a balanced grid, the isolation of harmonics is a standard assumption for the design of harmonic-mitigation devices Akagi et al. (2007).

We note that any unbalance in the grid and any coupling between harmonics will deteriorate the obtainable performance of the extremum-seeking controllers. However, even in the presence of unbalance and coupling between harmonics, it may be beneficial to make the simplifications in (6.6) and (6.7) because of the significantly faster optimization response that can be achieved due to the reduction in parameters and the parallelization of the extremum-seeking control method.

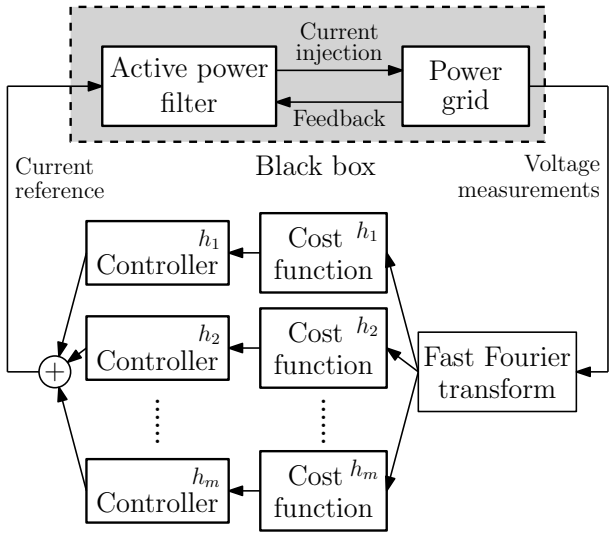

Figure 6.2: Harmonic-mitigation scheme for isolated harmonics.

6.3 Extremum-seeking control method

For each $h \in \mathcal{H}$, we introduce a discrete-time extremum-seeking controller to find the values of the parameters u_1^h and u_2^h for which the objective function F^h in (6.9) exhibits a minimum. The controller in this chapter is a modified version of the extremum-seeking controller in Chapter 3. Let the sampling time of the extremum-seeking controller be denoted by the positive constant T_s. At each sampling instance $t = kT_s$, the extremum-seeking controller computes an update for the parameter values $u_{1,k}^h$ and $u_{2,k}^h$, denoted by $u_{1,k+1}^h$ and $u_{2,k+1}^h$ respectively, such that $u_1^h(t) = u_{1,k+1}^h$ and $u_2^h(t) = u_{2,k+1}^h$ for all $t \in (kT_s, (k+1)T_s]$ and all integers k. Here, we assume that the computation time is small compared to the sampling time. Note that $t = (k+1)T_s$ is the last (and not the first) time instance that $u_1^h(t) = u_{1,k+1}^h$ and $u_2^h(t) = u_{2,k+1}^h$.

We define

$$u_{1,k}^h = \hat{u}_{1,k}^h + \alpha_{\boldsymbol{\omega}}^h \omega_{1,k}^h, \qquad u_{2,k}^h = \hat{u}_{2,k}^h + \alpha_{\boldsymbol{\omega}}^h \omega_{2,k}^h, \tag{6.11}$$

where $\omega_{1,k}^h$ and $\omega_{2,k}^h$ are perturbations with amplitude $\alpha_{\boldsymbol{\omega}}^h > 0$. The amplitude $\alpha_{\boldsymbol{\omega}}^h$ can be regarded as a tuning parameter and is commonly chosen to be small. The perturbations $\omega_{1,k}^h$ and $\omega_{2,k}^h$ are given by

$$\omega_{1,k}^h = \sin\left(\frac{2\pi k}{N_{\boldsymbol{\omega}}^h}\right), \qquad \omega_{2,k}^h = \cos\left(\frac{2\pi k}{N_{\boldsymbol{\omega}}^h}\right), \tag{6.12}$$

where the tuning parameter $N_{\boldsymbol{\omega}}^h > 0$ is a sufficiently large integer. The nominal values $\hat{u}_{1,k}^h$ and $\hat{u}_{2,k}^h$ can be regarded as an estimate of the parameter values

that minimize the objective function F^h. The extremum-seeking controller uses an estimate of the gradient of the objective function F^h to regulate the nominal parameters $\hat{u}^h_{1,k}$ and $\hat{u}^h_{2,k}$ to the minimum of the objective function using a gradient-descent approach.

To estimate the gradient of the objective function F^h, we derive a general dynamic model for the relation between the parameters $u^h_{1,k}$, $u^h_{2,k}$ and the output of the cost function Z^h in (6.10). Let y^h_k denote the output of the cost function Z^h, where the input $V^h_{1,a}, \ldots, V^h_{n,c}$ of the cost function Z^h is obtained by taking the fast Fourier transform of the measured voltage signals in (6.1) for the time interval $(kT_s - T_f, kT_s]$. From (6.7), (6.9) and (6.10), we obtain that $y_k \approx F^h(u^h_{1,k}, u^h_{2,k})$ for constant parameter values $u^h_{1,k} = u^h_1$ and $u^h_{2,k} = u^h_2$ under constant load conditions of the electrical grid. Due to the use of the fast Fourier transform, a distributed time delay is introduced between the parameter values $u^h_{1,k}$, $u^h_{2,k}$ and the output y^h_k. This delay is especially large if $T_f \gg T_s$. Bounded time delays in extremum-seeking schemes can be handled by making the extremum-seeking controller sufficiently slow; see for example Yu and Ozguner (2002); Haring et al. (2013). Here, we will compensate for the time delay to be able to obtain a faster convergence of the extremum-seeking controller. We model the output for time-varying parameters $u^h_{1,k}$ and $u^h_{2,k}$ as

$$y^h_k \approx \frac{1}{N} \sum_{r=0}^{N-1} F^h(u^h_{1,k-r}, u^h_{2,k-r}), \tag{6.13}$$

where we assume that $N = \frac{T_f}{T_s}$ is a positive integer. Linear interpolation can be applied to obtain a similar expression if $\frac{T_f}{T_s}$ is not a positive integer. From (6.11) and Taylor's theorem, we have that

$$\begin{aligned} F^h(u^h_{1,k}, u^h_{2,k}) \approx F^h(\hat{u}^h_{1,k}, \hat{u}^h_{2,k}) + \alpha^h_{\boldsymbol{\omega}} \frac{\partial F^h}{\partial u^h_1}(\hat{u}^h_{1,k}, \hat{u}^h_{2,k})\omega^h_{1,k} \\ + \alpha^h_{\boldsymbol{\omega}} \frac{\partial F^h}{\partial u^h_2}(\hat{u}^h_{1,k}, \hat{u}^h_{2,k})\omega^h_{2,k} \end{aligned} \tag{6.14}$$

for sufficiently small values of $\alpha^h_{\boldsymbol{\omega}} > 0$. Similarly, from Taylor's theorem, it follows that

$$\begin{aligned} F^h(\hat{u}^h_{1,k+1}, \hat{u}^h_{2,k+1}) \approx F^h(\hat{u}^h_{1,k}, \hat{u}^h_{2,k}) + \alpha^h_{\boldsymbol{\omega}} \frac{\partial F^h}{\partial u^h_1}(\hat{u}^h_{1,k}, \hat{u}^h_{2,k}) \frac{\Delta \hat{u}^h_{1,k}}{\alpha^h_{\boldsymbol{\omega}}} \\ + \alpha^h_{\boldsymbol{\omega}} \frac{\partial F^h}{\partial u^h_2}(\hat{u}^h_{1,k}, \hat{u}^h_{2,k}) \frac{\Delta \hat{u}^h_{2,k}}{\alpha^h_{\boldsymbol{\omega}}}, \end{aligned} \tag{6.15}$$

$$\frac{\partial F^h}{\partial u^h_1}(\hat{u}^h_{1,k+1}, \hat{u}^h_{2,k+1}) \approx \frac{\partial F^h}{\partial u^h_1}(\hat{u}^h_{1,k}, \hat{u}^h_{2,k}) \tag{6.16}$$

and

$$\frac{\partial F^h}{\partial u_2^h}(\hat{u}_{1,k+1}^h, \hat{u}_{2,k+1}^h) \approx \frac{\partial F^h}{\partial u_2^h}(\hat{u}_{1,k}^h, \hat{u}_{2,k}^h), \tag{6.17}$$

with

$$\Delta\hat{u}_{1,k}^h = \hat{u}_{1,k+1}^h - \hat{u}_{1,k}^h, \qquad \Delta\hat{u}_{2,k}^h = \hat{u}_{2,k+1}^h - \hat{u}_{2,k}^h, \tag{6.18}$$

for sufficiently small values of $\alpha_{\boldsymbol{\omega}}^h > 0$, where we assume that $\Delta\hat{u}_{1,k}^h = \mathcal{O}(\alpha_{\boldsymbol{\omega}}^h)$ and $\Delta\hat{u}_{2,k}^h = \mathcal{O}(\alpha_{\boldsymbol{\omega}}^h)$ as $\alpha_{\boldsymbol{\omega}}^h \to 0$, where $\mathcal{O}$ denotes the big-O notation. By combining (6.11) and (6.13)-(6.18), we obtain

$$\begin{aligned} y_k^h \approx F^h(\hat{u}_{1,k}^h, \hat{u}_{2,k}^h) &+ \alpha_{\boldsymbol{\omega}}^h \frac{\partial F^h}{\partial u_1^h}(\hat{u}_{1,k}^h, \hat{u}_{2,k}^h) \frac{\frac{1}{N}\sum_{r=0}^{N-1} u_{1,k-r}^h - \hat{u}_{1,k}^h}{\alpha_{\boldsymbol{\omega}}^h} \\ &+ \alpha_{\boldsymbol{\omega}}^h \frac{\partial F^h}{\partial u_2^h}(\hat{u}_{1,k}^h, \hat{u}_{2,k}^h) \frac{\frac{1}{N}\sum_{r=0}^{N-1} u_{2,k-r}^h - \hat{u}_{2,k}^h}{\alpha_{\boldsymbol{\omega}}^h}. \end{aligned} \tag{6.19}$$

Now, let us define the following state vector of the model:

$$\mathbf{m}_k^h = \begin{bmatrix} F^h(\hat{u}_{1,k}^h, \hat{u}_{2,k}^h) \\ \alpha_{\boldsymbol{\omega}}^h \frac{\partial F^h}{\partial u_1^h}(\hat{u}_{1,k}^h, \hat{u}_{2,k}^h) \\ \alpha_{\boldsymbol{\omega}}^h \frac{\partial F^h}{\partial u_2^h}(\hat{u}_{1,k}^h, \hat{u}_{2,k}^h) \end{bmatrix}. \tag{6.20}$$

From (6.15)-(6.20), it follows that the relation between the parameters $u_{1,k}^h$, $u_{2,k}^h$ and the output y_k^h can be approximated by the following dynamic model:

$$\begin{aligned} \mathbf{m}_{k+1}^h &= \mathbf{A}_k^h \mathbf{m}_k^h \\ y_k^h &= \mathbf{C}_k^h \mathbf{m}_k^h, \end{aligned} \tag{6.21}$$

with

$$\mathbf{A}_k^h = \begin{bmatrix} 1 & \frac{\Delta\hat{u}_{1,k}^h}{\alpha_{\boldsymbol{\omega}}^h} & \frac{\Delta\hat{u}_{2,k}^h}{\alpha_{\boldsymbol{\omega}}^h} \\ 0 & 1 & 0 \\ 0 & 0 & 1 \end{bmatrix} \tag{6.22}$$

and

$$\mathbf{C}_k^h = \begin{bmatrix} 1 & \frac{\frac{1}{N}\sum_{r=0}^{N-1} u_{1,k-r}^h - \hat{u}_{1,k}^h}{\alpha_{\boldsymbol{\omega}}^h} & \frac{\frac{1}{N}\sum_{r=0}^{N-1} u_{2,k-r}^h - \hat{u}_{2,k}^h}{\alpha_{\boldsymbol{\omega}}^h} \end{bmatrix}. \tag{6.23}$$

We note the last two elements of the state vector $\mathbf{m}_k^h$ in (6.20) are equal to the gradient of the objective function F^h scaled by the tuning parameter $\alpha_{\boldsymbol{\omega}}^h$. Therefore, an estimate of the gradient of the objective function can be obtained by estimating the state vector $\mathbf{m}_k^h$.

We introduce the following three-step observer to estimate the state vector $\mathbf{m}_k^h$, as in Chapter 3:

Step $1 \rightarrow 2$ (correction step):

$$\begin{aligned}\hat{\mathbf{m}}_{k|2}^h &= \hat{\mathbf{m}}_{k|1}^h + \mathbf{L}_{k|1}^h \left(y_k^h - \mathbf{C}_k^h \hat{\mathbf{m}}_{k|1}^h\right), \\ \mathbf{Q}_{k|2}^h &= \left(\mathbf{I} - \mathbf{L}_{k|1}^h \mathbf{C}_k^h\right) \mathbf{Q}_{k|1}^h \left(\mathbf{I} - \mathbf{L}_{k|1}^h \mathbf{C}_k^h\right)^T + \frac{1}{1-\lambda_{\mathbf{m}}^h} \mathbf{L}_{k|1}^h \left(\mathbf{L}_{k|1}^h\right)^T,\end{aligned} \tag{6.24}$$

Step $2 \rightarrow 3$ (regularization step):

$$\begin{aligned}\hat{\mathbf{m}}_{k|3}^h &= \hat{\mathbf{m}}_{k|2}^h - \mathbf{L}_{k|2}^h \mathbf{D} \hat{\mathbf{m}}_{k|2}^h, \\ \mathbf{Q}_{k|3}^h &= \left(\mathbf{I} - \mathbf{L}_{k|2}^h \mathbf{D}\right) \mathbf{Q}_{k|2}^h \left(\mathbf{I} - \mathbf{L}_{k|2}^h \mathbf{D}\right)^T + \frac{1}{\sigma_r^h (1-\lambda_{\mathbf{m}}^h)} \mathbf{L}_{k|2}^h \left(\mathbf{L}_{k|2}^h\right)^T,\end{aligned} \tag{6.25}$$

Step $3 \rightarrow 1$ (prediction step):

$$\begin{aligned}\hat{\mathbf{m}}_{k+1|1}^h &= \mathbf{A}_k^h \hat{\mathbf{m}}_{k|3}^h, \\ \mathbf{Q}_{k+1|1}^h &= \frac{1}{\lambda_{\mathbf{m}}^h} \mathbf{A}_k^h \mathbf{Q}_{k|3}^h \left(\mathbf{A}_k^h\right)^T,\end{aligned} \tag{6.26}$$

with

$$\begin{aligned}\mathbf{L}_{k|1}^h &= \mathbf{Q}_{k|1}^h \left(\mathbf{C}_k^h\right)^T \left(\frac{1}{1-\lambda_{\mathbf{m}}^h} + \mathbf{C}_k^h \mathbf{Q}_{k|1}^h \left(\mathbf{C}_k^h\right)^T\right)^{-1}, \\ \mathbf{L}_{k|2}^h &= \mathbf{Q}_{k|2}^h \mathbf{D}^T \left(\frac{1}{\sigma_r^h (1-\lambda_{\mathbf{m}}^h)} \mathbf{I} + \mathbf{D} \mathbf{Q}_{k|2}^h \mathbf{D}^T\right)^{-1}\end{aligned} \tag{6.27}$$

and

$$\mathbf{D} = \begin{bmatrix} 0 & 1 & 0 \\ 0 & 0 & 1 \end{bmatrix}. \tag{6.28}$$

Here, $\hat{\mathbf{m}}_{k|3}^h$ is an estimate of the state vector $\mathbf{m}_k^h$, and $\hat{\mathbf{m}}_{k|1}^h$ and $\hat{\mathbf{m}}_{k|2}^h$ are intermediate variables. The matrix $\mathbf{Q}_{k|3}^h$ and the intermediate variables $\mathbf{Q}_{k|1}^h$ and $\mathbf{Q}_{k|2}^h$ are positive definite. The tuning parameter $\lambda_{\mathbf{m}}^h \in (0,1)$ is sometimes referred to as the forgetting factor Johnstone and Anderson (1982). Its value is often chosen to be close to one. The tuning parameter $\sigma_r^h > 0$ is a regularization constant. Because regularization deteriorates the estimate of the state vector $\mathbf{m}_k^h$, its value is commonly chosen to be small. The correction step in (6.24) updates the estimate of the state vector with the output y_k of the cost function as feedback. The regularization step in (6.25) prevents the elements of the matrix $\mathbf{Q}_{k|3}^h$ from becoming excessively large if the parameter signals $u_{1,k}^h$ and $u_{2,k}^h$ are (momentarily) not sufficiently rich to accurately estimate the state vector $\mathbf{m}_k^h$. The prediction step in (6.26) predicts the state vector at the next sampling instance using the same update equation as the model in (6.21).

Noting that $\hat{\mathbf{m}}_{k|3}^h$ is an estimate of the state vector $\mathbf{m}_k^h$, we obtain that $\mathbf{D}\hat{\mathbf{m}}_{k|3}^h$

is an estimate of the gradient of the objective function F^h scaled by the tuning parameter $\alpha^h_{\boldsymbol{\omega}}$. Similarly, $\mathbf{D}_1\hat{\mathbf{m}}^h_{k|3}$ and $\mathbf{D}_2\hat{\mathbf{m}}^h_{k|3}$ are estimates of the scaled partial derivatives of F^h with respect to u^h_1 and u^h_2, respectively, with

$$\mathbf{D}_1 = \begin{bmatrix} 0 & 1 & 0 \end{bmatrix}, \qquad \mathbf{D}_2 = \begin{bmatrix} 0 & 0 & 1 \end{bmatrix}. \tag{6.29}$$

With this in mind, we define the following gradient-descent optimizers for the parameters $u^h_{1,k}$ and $u^h_{2,k}$:

$$\begin{aligned} u^h_{1,k+1} &= u^h_{1,k} - \lambda^h_{\mathbf{u}} \frac{\eta^h_{\mathbf{u}} \mathbf{D}_1 \hat{\mathbf{m}}^h_{k|3}}{\eta^h_{\mathbf{u}} + \lambda^h_{\mathbf{u}} \|\mathbf{D}\hat{\mathbf{m}}^h_{k|3}\|}, \\ u^h_{2,k+1} &= u^h_{2,k} - \lambda^h_{\mathbf{u}} \frac{\eta^h_{\mathbf{u}} \mathbf{D}_2 \hat{\mathbf{m}}^h_{k|3}}{\eta^h_{\mathbf{u}} + \lambda^h_{\mathbf{u}} \|\mathbf{D}\hat{\mathbf{m}}^h_{k|3}\|}. \end{aligned} \tag{6.30}$$

The tuning parameter $\lambda^h_{\mathbf{u}}$ can be regarded as the linear part of the gains of the optimizers since $|\Delta u^h_{1,k}| \leq \lambda^h_{\mathbf{u}} |\mathbf{D}_1 \hat{\mathbf{m}}^h_{k|3}|$ and $|\Delta u^h_{2,k}| \leq \lambda^h_{\mathbf{u}} |\mathbf{D}_2 \hat{\mathbf{m}}^h_{k|3}|$. The gains of the optimizers are normalized. The tuning parameter $\eta^h_{\mathbf{u}} > 0$ can be regarded as the normalization gain. We note that $|\Delta u^h_{1,k}| \leq \eta^h_{\mathbf{u}}$ and $|\Delta u^h_{2,k}| \leq \eta^h_{\mathbf{u}}$ so that the model in (6.21) is accurate for sufficiently small values of $\alpha^h_{\boldsymbol{\omega}} > 0$ and $\eta^h_{\mathbf{u}} > 0$ under constant load conditions of the electrical grid.

The extremum-seeking controller for each $h \in \mathcal{H}$ is obtained by combining the observer in (6.24)-(6.26) and the optimizers in (6.30). We note the average parameter values $\frac{1}{N}\sum_{r=0}^{N-1} u^h_{1,k-r}$ and $\frac{1}{N}\sum_{r=0}^{N-1} u^h_{2,k-r}$ of the matrix $\mathbf{C}^h_k$ in (6.23) can be obtained by using moving-average filters as illustrated in Figure 6.3.

6.4 Case study: two-bus electrical grid with distributed generators

We consider the two-bus electrical grid with distributed generators in Figure 6.4. The electrical grid portrays a simplified shipboard power system. It consists of two generators, two buses with propulsion loads, an active power filter, an LCL filter and RC shunts. The two buses represent switchboards that connect each generator to its respective load. The effective impedance of the main bus connection (that is, the connection between the two buses) is described by the resistor R_{MB} and the inductor L_{MB}. The propulsion loads are modeled as variable-speed drives with 12-pulse rectifiers. The LCL filter is used to suppress the switching noise of the active power filter. The RC shunts represent the shunt capacitance of bus bars and cables. The parameters of the model are presented in Table 6.1. The per-unit model is given relative to the generator power rating. The current that can be produced by the active filter is limited. To avoid unwanted effects due to saturation of the filter current (that is, current clipping), the current

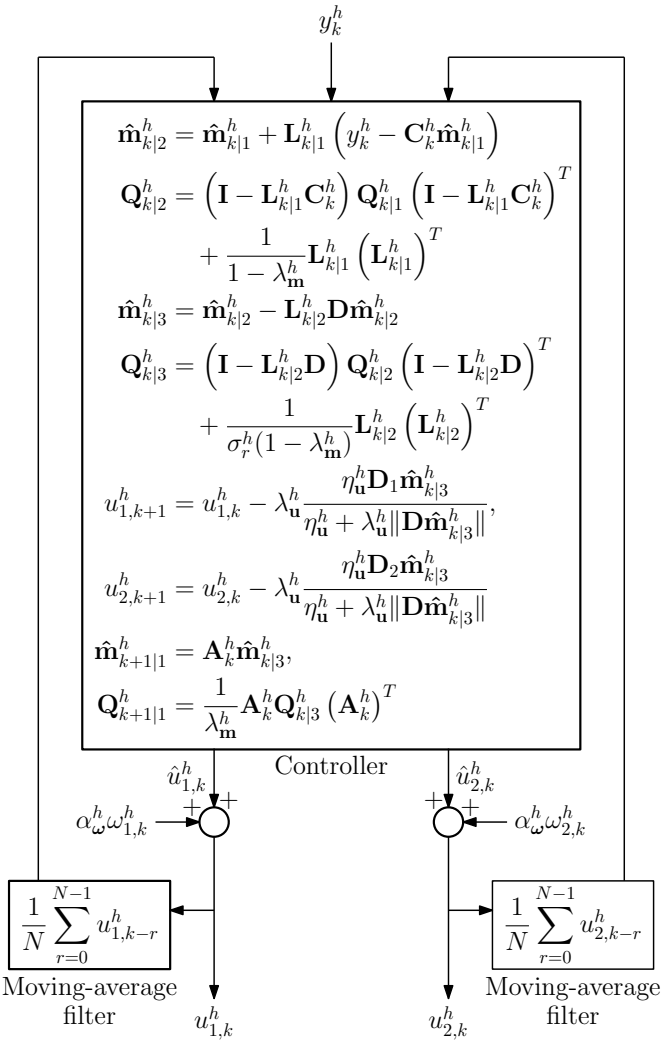

Figure 6.3: Extremum-seeking controller for $h \in \mathcal{H}$.

Table 6.1: Parameters of the electrical grid (with angular frequency $\omega_f = \frac{2\pi}{T_f}$).

Parameter	Value	Unit
Nominal voltage	690	V
Fundamental frequency $\left(\frac{1}{T_f}\right)$	50	Hz
Generator power rating	1	MVA
L_{G1}, L_{G2}	0.2	pu
R_{G1}	$0.1 \cdot L_{G1} \cdot \omega_f$	pu
R_{G2}	$0.1 \cdot L_{G2} \cdot \omega_f$	pu
L_{MB}	0.04	pu
R_{MB}	$0.1 \cdot L_{MB} \cdot \omega_f$	pu
C_{S1}, C_{S2}	2	µF
R_{S1}, R_{S2}	2	Ω
L_{L1}, L_{L2}	0.3	mH
R_{L1}, R_{L2}	0.03	Ω
C_C	30	µF
R_C	10	Ω
R_D	160	Ω

references given to the active power filter are cut off if they exceed the maximal allowable current that the active power filter can produce. More information about the model can be found in Skjong et al. (2016).

Many harmonics are eliminated due to the use of 12-pulse rectifiers. The dominating harmonics that remain are of the orders $12r \pm 1$ for positive integer values of r. This is due to the phase-shifting transformer that connects the two parallelled 6-pulse rectifiers to the main grid. We use the extremum-seeking control method in Section 6.3 to compute the optimal parameters u_1^h and u_2^h of the current reference (6.3) of the active power filter for the harmonics $h \in \{11, 13, 23, 25\}$. The sampling time of the extremum-seeking controller is given by $T_s = 10^{-3}$ s. The tuning parameters are set to $\alpha_{\boldsymbol{\omega}}^h = 0.01$ pu, $N_{\boldsymbol{\omega}}^h = 80$, $\lambda_{\mathbf{m}}^h = 0.985$, $\lambda_{\mathbf{u}}^{11} = \lambda_{\mathbf{u}}^{13} = 5$ pu, $\lambda_{\mathbf{u}}^{23} = \lambda_{\mathbf{u}}^{25} = 2$ pu, $\eta_{\mathbf{u}}^h = 5 \times 10^{-4}$ and $\sigma_r^h = 10^{-3}$ for all $h \in \{11, 13, 23, 25\}$. The parameters of the cost functions in (6.10) are set to $\beta_{j,p}^h = 1$ for all $j \in \{1, 2\}$, all $p \in \{a, b, c\}$ and all $h \in \{11, 13, 23, 25\}$.

To illustrate the difference between local and system-wide harmonic mitigation, we compare our results with those of a local-filtering method. The local-filtering method extracts the 11th, 13th, 23rd and 25th harmonic from current measurements of the local load (that is, Load 2 in Figure 6.4) using a fast Fourier transform and provides the same harmonics with an opposite phase to the ac-

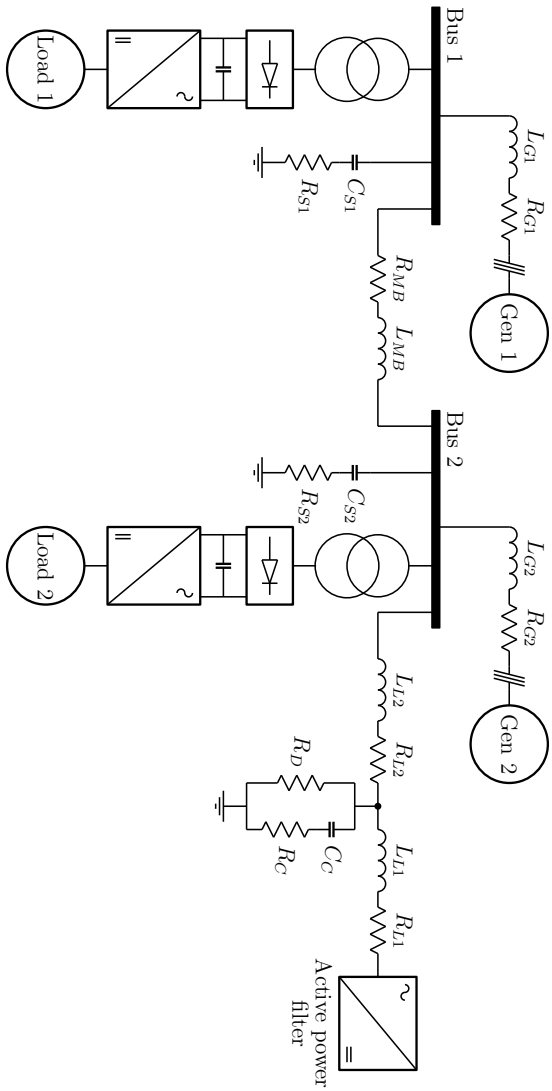

Figure 6.4: Model of two-bus shipboard power system.

tive power filter as current reference, similar to Williams and Hoft (1991). The extremum-seeking control method can easily be combined with other methods. To demonstrate this, we additionally present results for a combination of the extremum-seeking method and the local-filtering method. For this combined method, the current reference that is supplied to the active power filter is the sum of the current references of the extremum-seeking control method and the local-filtering method.

Moreover, we also compare our result with those of the model-predictive control method in Skjong et al. (2015a,b,c, 2016) that uses current measurements of the generators and the loads to mitigate the same harmonics. The model-predictive control method uses a simplified model of the grid to generate the current reference to the active power filter. In this simplified grid model, the active power filter is modeled as perfect current sources, the generators are considered to be perfect voltage sources, the variable-speed drives with 12-rectifiers are modeled as perfect current sources, the RC shunts are replaced by shunt capacitors, and the LCL filter is omitted. More details about the model-predictive control method are discussed in Skjong et al. (2016).

6.4.1 Harmonic mitigation under constant load conditions

We use the total harmonic distortion (THD) as a measure for the mitigation performance. Table 6.2 presents the total harmonic distortion of the voltage in the buses under different constant load conditions, where the power of Load 1 and Load 2 is denoted by P_1 and P_2, respectively. From Table 6.2, we obtain the total harmonic distortion of the model-predictive control (MPC) method and the extremum-seeking control (ESC) method are comparable. Compared to these two system-wide harmonic-mitigation methods, the local-filtering method (Local) performs significantly worse. Combining the extremum-seeking control method and the local-filtering method (Local + ESC) gives a harmonic-mitigation performance that is similar to those of the model-predictive control method and the extremum-seeking control method. We note that the values of the total harmonic distortion of the voltages in the buses mildly oscillate if the extremum-seeking controller is applied due to the use of perturbations. The values in Table 6.2 are the time-averaged values of the total harmonic distortion.

As mentioned before, the current references are constrained in order not to exceed the maximal allowable current of the active power filter. In Figure 6.5, the constrained current references for phase a for the load condition $P_1 = P_2 = 1.0$ pu are presented. We observe that the current references of the model-predictive control method, the extremum-seeking control method and the combined extremum-seeking control and local-filtering method are cut off to stay within the allowable current range of $[-1, 1]$ pu. Moreover, we note that the current references for all methods apart from the local-filtering method are very similar, which explains the numbers in Table 6.2. The corresponding current injection produced by the

active power filter is shown in Figure 6.6. We observe that the current-injection signals are more noisy compared to the current-reference signals in Figure 6.5 due to the switching of the active power filter.

6.4.2 Harmonic mitigation under dynamic load conditions

In Figures 6.7 and 6.8, the THD dynamic responses to a step in the power of the loads are displayed; the power of both loads is increased from 0.3 pu to 1.0 pu at time zero. Compared to the model-predictive control and the local-filtering method, it takes the extremum-seeking control method much longer to adapt to the new power levels of the loads. The converge is faster for the combined extremum-seeking control and local-filtering method, but not as fast as for the model-predictive control and the local-filtering methods. We note that convergence rate of the extremum-seeking control method and the combined method can be increased under a different tuning of the extremum-seeking controllers. However, this will deteriorate the steady-state performance of the extremum-seeking method due to the tuning trade-off discussed in Tan et al. (2006).

6.4.3 Measurement noise

To investigate the effect of measurement noise on the performance of the harmonic-mitigation methods, we add additive Gaussian white noise to all measurement signals such that the corresponding signal-to-noise ratios (SNR) are equal to ten. All four methods are based on measurements and are therefore influenced by measurement noise. The measurement noise is transmitted to the electrical grid via the generated current references and the active power filter. We observe in Figures 6.9 and 6.10 that the voltage signals in Bus 2, which is connected to the active power filter, are most affected by measurement noise: the differences in total harmonic distortion over time can be as large as one percent for all methods. Other than a minor increase in the values of the total harmonic distortion for the model-predictive control method, no significant difference in noise sensitivity between the methods is observed, also for other noise levels.

6.4.4 Model mismatch

Of the four methods presented in this section, model-predictive control is the only method that relies on a model to mitigate the harmonic distortion in the voltage and current signals of the electrical grid. The model-predictive control method uses a simplified version of the model in Figure 6.4 to compute the current references of the active power filter; see Skjong et al. (2016). For the above simulations, the parameters of the simplified model have the same values as in Table 6.1. In real-life applications, the parameters for the model of the model-predictive control method have to be measured or estimated. Six sets

Table 6.2: Percentage of time-averaged voltage THD in the buses for various constant load conditions.

	MPC	Local	ESC	Local + ESC	P_1 [pu]	P_2 [pu]
Bus 1	3.92	6.44	4.07	4.11	1.0	1.0
Bus 2	4.06	5.57	4.20	4.27		
Bus 1	1.80	3.21	1.95	1.96	0.3	0.3
Bus 2	2.00	2.76	1.93	1.96		
Bus 1	2.45	6.06	2.65	2.67	1.0	0.3
Bus 2	2.43	5.11	2.35	2.37		
Bus 1	2.07	3.98	2.17	2.19	0.3	1.0
Bus 2	2.35	4.02	2.31	2.34		

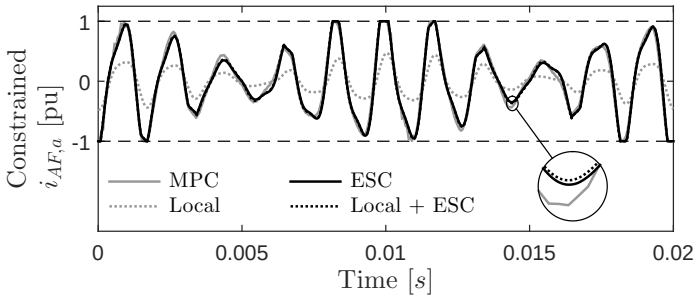

Figure 6.5: Constrained current reference for phase a as a function of time for $P_1 = P_2 = 1.0$ pu.

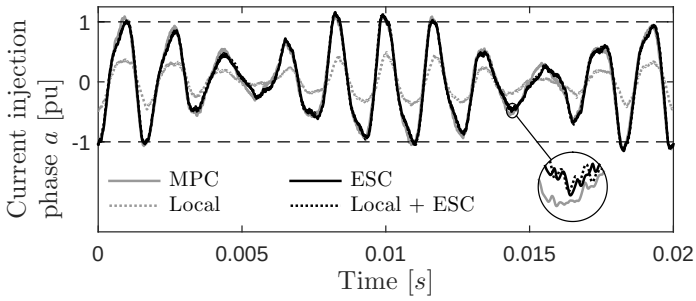

Figure 6.6: Current injection for phase a generated by the active power filter as a function of time for $P_1 = P_2 = 1.0$ pu.

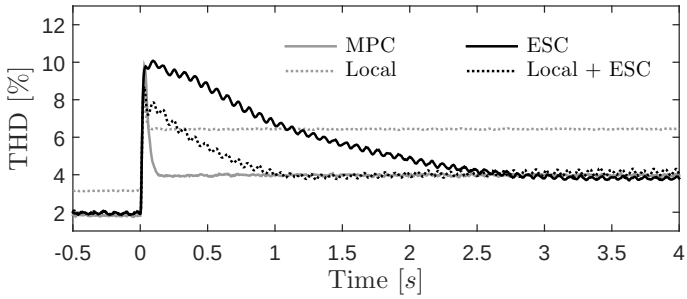

Figure 6.7: Percentage of voltage THD in Bus 1 as a function of time as the values of P_1 and P_2 jump from 0.3 pu to 1.0 pu at time zero.

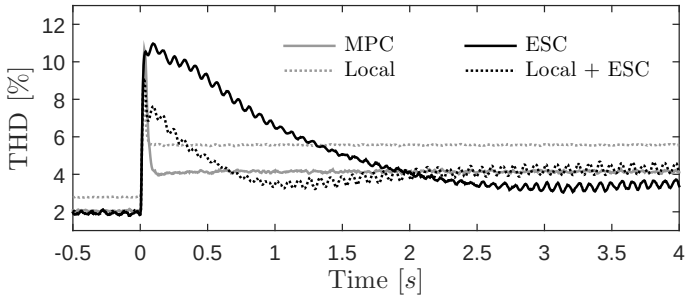

Figure 6.8: Percentage of voltage THD in Bus 2 as a function of time as the values of P_1 and P_2 jump from 0.3 pu to 1.0 pu at time zero.

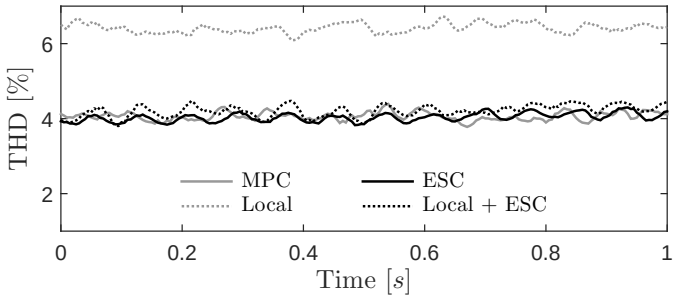

Figure 6.9: Percentage of voltage THD in Bus 1 as a function of time for $P_1 = P_2 = 1.0$ pu.

of model parameters are presented in Table 6.3 to simulate the case of model mismatch. The corresponding total harmonic distortion of the voltages in the buses are given in Table 6.4.

From Table 6.4, we obtain that total harmonic distortion for the first five parameter sets is comparable to the total harmonic distortion for the exact parameters in Table 6.2. We note that the total harmonic distortion for the first and second parameter set is slightly lower than for the exact parameters. Overall, the model-predictive control method is not very sensitive to model mismatch for parameters moderately close to their exact values. Set 6 appears to be an exception to the rule.

6.5 Conclusion

In this chapter, we have presented an extremum-seeking control method that optimizes the injection current of an active power filter for the minimization of harmonic distortion in electrical grids. The method relies on measurements of the voltages at all nodes in the grid. The main advantage of the presented method compared to other methods is that no grid model is required. The presented method is computationally cheap, can easily be applied to an electrical grid with an arbitrary number of nodes, and can be implemented on top of existing methods. A case study of a two-bus electrical grid with distributed generators is presented, where we compare the performance of the extremum-seeking control method with the performances of harmonic-mitigation method based on local measurements and a model-predictive control method. The case study displays that the performance of the presented extremum-seeking control method is significantly better than that of the local-filtering method and comparable to that of the model-predictive control method under constant steady-state conditions of the grid. The convergence of the extremum-seeking control method is slower than for the other methods. The convergence rate can be increased by combining the extremum-seeking control method and the local-filtering method.

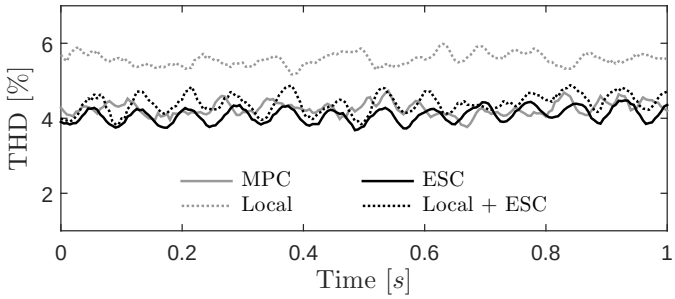

Figure 6.10: Percentage of voltage THD in Bus 2 as a function of time for $P_1 = P_2 = 1.0$ pu with SNR = 10.

Table 6.3: Parameter sets for the model of the MPC. Percentages are with respect to the values in Table 6.1.

	Set 1	Set 2	Set 3	Set 4	Set 5	Set 6
L_{G1}, L_{G2}	110%	95%	120%	90%	95%	90%
R_{G1}, R_{G2}	110%	95%	120%	90%	95%	90%
L_{MB}, R_{MB}	110%	110%	120%	90%	105%	120%
C_{S1}, C_{S2}	110%	110%	120%	90%	105%	120%

Table 6.4: Percentage of voltage THD in the buses for $P_1 = P_2 = 1.0$ pu for the MPC method, with the parameter sets for the model of the MPC in Table 6.3.

	Set 1	Set 2	Set 3	Set 4	Set 5	Set 6
Bus 1	3.79	3.88	3.94	3.97	3.99	4.67
Bus 2	3.86	3.97	4.10	4.12	4.13	4.32

Chapter 7

Concluding remarks

7.1 Conclusions regarding the objectives of the thesis

Black-box extremum-seeking control methods have been studied in this work, with a main focus on perturbation-based methods. The first objective of this work has been to develop a black-box extremum-seeking control method with an increased convergence rate compared to classical extremum-seeking control methods that uses small-amplitude low-frequency perturbations.

- Classical perturbation-based extremum-seeking control methods use an estimate of the gradient of the objective function to optimize the steady-state performance of a plant. In Chapter 2, we have pointed out that the convergence speed of classical perturbation-based extremum-seeking control methods is dependent on the accuracy of the gradient estimate. For classical methods, the gradient estimate is based on the perturbation-related content in the plant-parameter signals and the corresponding plant-performance signal. Because the perturbation-related content in the plant-parameter signals is low if small-amplitude low-frequency perturbations are used, an improved accuracy of the gradient estimate and a faster convergence may be achieved if the entire plant-parameters signals (and not only the perturbation-related content) are used to estimate the gradient of the objective function. An extremum-seeking controller with a least-squares observer has been introduced in Chapter 2. The least-squares observer uses the entire plant-parameter signals to obtain a gradient estimate. Moreover, curvature information of the objective function can be utilized to further enhance the gradient estimate. In addition, the observer provides inherent filtering of plant dynamics and noise. To test the overall performance, the convergence rate of the extremum-seeking controller has been compared with the convergence rate of three other extremum-seeking controllers in the literature for several examples. The comparison reveals that the maximal obtained convergence rate of the presented controller is comparable or higher than those of the other three controllers. An extensive simulation example displays that a faster convergence is obtained for small-amplitude low-frequency perturbations with the two observer-based

controllers that use the entire plant-parameter signals to estimate the gradient of the objective function than with the classical extremum-seeking controller and the phasor extremum-seeking controller that do not utilize the entire plant-parameter signals for their gradient estimation. In addition, it shows that incorporating curvature information of the objective function can significantly improve the convergence rate for sufficiently low perturbation frequencies.

- Although many extremum-seeking control methods assume that the measurements of the performance indicators and the update of the plant parameters are continuous in time, the performance-indicator measurements are often sampled and the plant parameters are updated in a discrete-time fashion in many practical applications. In Chapter 3, a discrete-time version of the continuous-time extremum-seeking controller in Chapter 2 has been presented to optimize the steady-state plant performance in a sampled-data setting. The discrete-time controller in Chapter 3 reduces to the continuous-time controller in Chapter 2 for the limit as the sampling time approaches zero.

- In Chapter 6, an application of the discrete-time extremum-seeking controller in Chapter 3 has been developed in the form of active-power-filter control for system-wide harmonic-mitigation in electrical grids. A case study of a two-bus electrical grid with distributed generators displays an improved performance of the used extremum-seeking control method compared to a local-filtering approach under constant load conditions of the electrical grid, while a comparable performance with respect to a model-based system-wide filtering method is observed. The case study also shows that the used extremum-seeking control method is slower to respond to changes in load conditions than the local and the model-based system-wide filtering methods. The extremum-seeking control method can be implemented on top of existing approaches to combine the fast transient response of conventional harmonic-mitigation methods with the optimizing capabilities of extremum-seeking control.

The second objective of this thesis has been to develop a black-box extremum-seeking method for general nonlinear dynamical plants that ensures global asymptotic stability of the resulting closed-loop system of plant and controller with respect to the optimal steady-state performance of the plant.

- In Chapter 4, we have presented a self-driving extremum-seeking controller that optimizes the steady-state performance of a class of nonlinear dynamical plants. The stability analysis in Chapter 4 shows that exponential convergence to the optimal steady-state performance can be guaranteed under suitable initial conditions and tuning conditions. To the best of the authors' knowledge, the stability proof in Chapter 4 is the first rigorous

stability proof for self-driving extremum-seeking schemes with dynamical plants.

- Local convergence to the optimum has been proved for a certain class of nonlinear dynamical plants with the self-driving extremum-seeking controller in Chapter 4. To obtain global asymptotic convergence for general nonlinear dynamical plants, we have introduced a perturbation-based extremum-seeking controller in Chapter 5. We have shown that global asymptotic stability of the closed-loop system of plant and controller with respect to the optimal steady-state plant performance can be obtained for any plant that satisfies the assumptions in Chapter 5. The key to this result is that the tuning parameters of the controller are time varying and asymptotically decay to zero as time goes to infinity. Global asymptotic stability can even be obtained if the plant is subjected to a time-varying disturbance under the assumption that the perturbations of the controller and the zero-mean component of the disturbance are uncorrelated. Moreover, the time-varying tuning parameters can be chosen such that global asymptotic stability is achieved for all plants that satisfy the assumptions.

7.2 Recommendations for future work

The following recommendations for future work are based on the findings in this thesis:

- In Chapter 2, we have illustrated with a simulation example that a faster convergence may be obtained with an extremum-seeking controller that uses the entire plant-parameter signals to estimate the gradient of the objective function than with a classical extremum-seeking controller if small-amplitude low-frequency perturbations are used. To be able to make a more general assessment of performance, the convergence speed could be compared for many more plants. Ideally, the improvements in convergence speed should be proved mathematically.

- It has been shown in Chapter 3 that the discrete-time extremum-seeking controller in Chapter 3 reduces to the continuous-time extremum-seeking controller in Chapter 2 for the limit as the sampling time goes to zero. Moreover, it has been proved in Chapter 2 that the closed-loop scheme of plant and continuous-time extremum-seeking controller is stable under certain assumptions. A stability proof could be added to Chapter 3 to show that also the stability of the closed-loop system of plant and discrete-time extremum-seeking controller can be guaranteed under similar assumptions.

- The self-driving extremum-seeking controller in Chapter 4 can only be applied to single-parameter plants. The extension to multi-parameter

plants is not straightforward. Additional research is required to develop a self-driving extremum-seeking controller that can be applied to multi-parameter plants.

Additionally, the following recommendations are given:

- There are often many different extremum-seeking control methods that can be applied to optimize the steady-state performance of a plant. Some extremum-seeking control method possess properties that uniquely distinguish them from others, such as the convergence to a global optimum in the presence of local optima (Khong et al., 2013a,b; Nešić et al., 2013b) or the stabilization of unstable plants (Moase and Manzie, 2012b; Scheinker and Krstić, 2013; Zhang et al., 2007b). For many other extremum-seeking control methods, it is much harder to distinguish when it is appropriate to apply them and when other methods form a better alternative. Users of extremum-seeking control may end up with several methods that appear to be equally suitable at first sight. A clear overview of the advantages and drawbacks of different extremum-seeking control methods would be most helpful and is still something that is missing at the moment.

- Perturbation are frequently added to extremum-seeking control schemes to ensure that that the plant-parameter signals are sufficiently rich to obtain the information required to optimize the steady-state performance of a plant. The optimal level of added excitation is dependent on the plant, disturbances and noise, and changes as the plant parameters converge to their performance-optimizing values. Several extremum-seeking controllers have been proposed in the literature to regulate the level of excitation by changing the amplitude of the perturbations (Moase et al., 2010; Moura and Chang, 2013; Wang et al., 2016). What the optimal level of excitation is remains a mystery however. Adding perturbations to increase the level of excitation may not be required, as we have seen in Chapter 4. How much excitation is desirable and how the desired level of excitation can be achieved are interesting research questions. Most probably, the answers of these questions involve solving a dual-control problem, as discussed in Section 1.1.1. Although solving a dual-control problem can be a challenging task, knowing how much excitation to apply and how to do this would be a great help in developing more efficient extremum-seeking control methods.

Bibliography

V. Adetola and M. Guay. Adaptive output feedback extremum seeking receding horizon control of linear systems. *Journal of Process Control*, 16(5):521–533, 2006.

V. Adetola and M. Guay. Parameter convergence in adaptive extremum-seeking control. *Automatica*, 43(1):105–110, 2011.

V. Adetola, D. DeHaan, and M. Guay. Adaptive model predictive control for constrained nonlinear systems. *Systems & Control Letters*, 58(5):320–326, 2009.

H. Akagi, E. H. Watanabe, and M. Aredes. *Instantaneous power theory and applications to power conditioning*. John Wiley & Sons, Hoboken, New Jersey, 2007.

V. Alstad and S. Skogestad. Null space method for selecting optimal measurement combinations as controlled variables. *Industrial & Engineering Chemistry Research*, 46(3):846–853, 2007.

V. Alstad, S. Skogestad, and E. S. Hori. Optimal measurement combinations as controlled variables. *Journal of Process Control*, 19(1):138–148, 2009.

R. Antonello, R. Oboe, L. Prandi, and F. Biganzoli. Automatic mode matching in MEMS vibrating gyroscopes using extremum-seeking control. *IEEE Transactions on Industrial Electronics*, 56(10):3880–3891, 2009.

K. B. Ariyur and M. Krstić. *Real-time optimization by extremum-seeking control*. Wiley-Interscience, Hoboken, NJ, 2003.

K. T. Atta, A. Johansson, and T. Gustafsson. Extremum seeking control based on phasor estimation. *Systems & Control Letters*, 85:37–45, 2015.

W. Bamberger and R. Isermann. Adaptive on-line steady-state optimization of slow dynamic processes. *Automatica*, 14(3):223–230, 1978.

G. Bastin, D. Nešić, Y. Tan, and I. Mareels. On extremum seeking in bioprocesses with multivalued cost functions. *Biotechnology Progress*, 25(3):683–689, 2009.

J. F. Beaudoin, O. Cadot, J. L. Aider, and J. E. Wesfreid. Bluff-body drag reduction by extremum-seeking control. *Journal of Fluids and Structures*, 22(6-7):973–978, 2006.

R. Becker, R. King, R. Petz, and W. Nitsche. Adaptive closed-loop separation control on a high-lift configuration using extremum seeking. *AIAA Journal*, 45(6):1382–1392, 2007.

R. Bellman, J. Bentsman, and S. M. Meerkov. Vibrational control of nonlinear systems: vibrational stabilizability. *IEEE Transactions on Automatic Control*, 31(8):710–716, 1986.

D. Bertsimas, D. B. Brown, and C. Caramanis. Theory and applications of robust optimization. *SIAM Review*, 53(3):464–501, 2011.

H.-G. Beyer and B. Sendhoff. Robust optimization - a comprehensive survey. *Computer Methods in Applied Mechanics and Engineering*, 196(33-34):3190–3218, 2007.

N. Bizon. On tracking robustness in adaptive extremum seeking control of the fuel cell power plants. *Applied Energy*, 87(10):3115–3130, 2010.

P. F. Blackman. Extremum-seeking regulators. In J. H. Westcott, editor, *An Exposition of Adaptive Control*, pages 36–50. Pergamon Press, Oxford, 1962.

P. Borg, T. Moen, and J. Aalbu. Adaptive control of alumina reduction ccell with point feeders. *Modeling, Identification and Control*, 7(1):45–56, 1986.

S. P. Boyd and L. Vandenberghe. *Convex optimization*. Cambridge University Press, Cambridge, U.K., 2004.

A. Bratcu, I. Munteanu, S. Bacha, and B. Raison. Maximum power point tracking of grid-connected photovoltaic arrays by using extremum seeking control. *Journal of Control Engineering and Applied Informatics*, 10(4):3–12, 2008.

S. L. Brunton, C. W. Rowley, S. R. Kulkarni, and C. Clarkson. Maximum power point tracking for photovoltaic optimization using ripple-based extremum seeking control. *IEEE Transactions on Power Electronics*, 25(10):2531–2540, 2010.

F. Bullo. Averaging and vibrational control of mechanical systems. *SIAM Journal on Control and Optimization*, 41(2):542–562, 2002.

D. Carnevale, A. Astolfi, C. Centioli, S. Podda, V. Vitale, and L. Zaccarian. A new extremum seeking technique and its application to maximize RF heating on FTU. *Fusion Engineering and Design*, 84(2-6):554–558, 2009.

C. Centioli, F. Iannone, G. Mazza, M. Panella, L. Pangione, S. Podda, A. Tuccilo, V. Vitale, and L. Zaccarian. Maximization of the lower hybrid power coupling in the Frascati Tokamak Upgrade via extremum seeking. *Control Engineering Practice*, 16(12):1468–1478, 2008.

B. Chachuat, B. Srinivasan, and D. Bonvin. Adaptation strategies for real-time optimization. *Computers & Chemical Engineering*, 33(10):1557–1567, 2009.

J.-Y. Choi, M. Krstić, K. B. Ariyur, and J. S. Lee. Extremum seeking control for discrete-time systems. *IEEE Transactions on Automatic Control*, 47(2):318–323, 2002.

D. W. Clarke and K. R. Godfrey. Simultaneous estimation of first and second derivatives of a cost function. *Electronics Letters*, 2(9):338–339, 1966.

D. W. Clarke and K. R. Godfrey. Simulation study of a two-derivative hill climber. *Electronics Letters*, 3(6):261–263, 1967.

J. Cochran and M. Krstić. Nonholonomic source seeking with tuning of angular velocity. *IEEE Transactions on Automatic Control*, 54(4):717–731, 2009.

J. Cochran, E. Kanso, S. D. Kelly, H. Xiong, and M. Krstić. Source seeking for two nonholonomic models of fish locomotion. *IEEE Transactions on Robotics*, 25(5): 1166–1176, 2009.

A. R. Conn, K. Scheinberg, and P. L. Toint. Recent progress in unconstrained nonlinear optimization witwith derivatives. *Mathematical Programming*, 79(1):397–414, 1997.

A. R. Conn, K. Scheinberg, and L. N. Vicente. *Introduction to derivative-free optimization*. MPS/SIAM Series on Optimization. Society for Industrial and Applied Mathematics and Mathematical Programming Society, Philadelphia, 2009.

P. Cougnon, D. Dochain, M. Guay, and M. Perrier. On-line optimization of fedbatch bioreactors by adaptive extremum seeking control. *Journal of Process Control*, 21 (10):1526–1532, 2011.

J. Creaby, Y. Li, and J. E. Seem. Maximizing wind turbine energy capture using multivariable extremum seeking control. *Wind Engineering*, 33(4):361–388, 2009.

A. Dalvi and M. Guay. Control and real-time optimization of an automotive hybrid fuel cell power system. *Control Engineering Practice*, 17(8):924–938, 2009.

S. Dashkovskiy, B. S. Rüffer, and F. R. Wirth. An ISS small gain theorem for general networks. *Mathematics of Control, Signals and Systems*, 19(2):93–122, 2007.

S. N. Dashkovskiy, B. S. Rüffer, and F. R. Wirth. Small gain theorems for large scale systems and construction of ISS Lyapunov functions. *SIAM Journal on Control and Optimization*, 48(6):4089–4118, 2010.

G. De Souza, D. Odloak, and A. C. Zanin. Real time optimization (RTO) with model predictive control (MPC). *Computers & Chemical Engineering*, 34(12):1999–2006, 2010.

D. DeHaan and M. Guay. Extremum-seeking control of state-constrained nonlinear systems. *Automatica*, 41(9):1567–1574, 2005.

M. Diehl, H. G. Bock, J. Schlöder, R. Findeisen, Z. Nagy, and F. Allgöwer. Real-time optimization and nonlinear model predictive control of processes governed by differential-algebraic equations. *Journal of Process Control*, 12(4):577–585, 2002.

E. Dinçmen, B. A. Güvenc, and T. Acarman. Extremum-seeking control of ABS braking in road vvehicle with lateral force improvement. *IEEE Transactions on Control Systems Technology*, 22(1):230–237, 2014.

C. Dixon and E. Frew. Maintaining optimal communication chains in robotic sensor networks using mobility control. *Mobile Networks and Applications*, 14(3):281–291, 2009.

C. Dixon and E. W. Frew. *Advances in Cooperative Control and Optimization*, chapter Decentralized extremum-seeking control of nonholonomic vehicles to form a communication chain, pages 311–322. Springer-Verlag, Berlin/Heidelberg, 2007.

D. Dochain, M. Perrier, and M. Guay. Extremum seeking control and its application to process and reaction systems: A survey. *Mathematics and Computers in Simulation*, 82(3):369–380, 2011.

S. Drakunov, U. Özgüner, P. Dix, and B. Ashrafi. ABS control using optimum search via sliding modes. *IEEE Transactions on Control Systems Technology*, 3(1):79–85, 1995.

C. S. Draper and Y. T. Li. Principles of optimoptimal control systems and an application to the internal combustion engine. In R. Oldenburger, editor, *Optimal and selfoptimizing control*. M.I.T. Press, Boston, MA, 1951.

H.-B. Dürr, M. S. Stanković, C. Ebenbauer, and K. H. Johansson. Lie bracket approximation of extremum seeking systems. *Automatica*, 49(6):1538–1552, 2013.

H.-B. Dürr, M. Krstić, A. Scheinker, and C. Ebenbauer. Singularly perturbed Lie bracket approximation. *IEEE Transactions on Automatic Control*, 60(12):3287–3292, 2015.

M. El-Habrouk, M. K. Darwish, and P. Mehta. Active power filters: a review. *IEE Proceedings - Electric Power Applications*, 147(5):403–413, 2000.

F. Esmaeilzadeh Azar, M. Perrier, and B. Srinivasan. A global optimization method based on multi-unit extremum-seeking for scalar nonlinear systems. *Computers & Chemical Engineering*, 35(3):456–463, 2011.

V. W. Eveleigh. *Adaptive control and optimization techniques*. McGraw-Hill, London, 1967.

S. G. Fabri, B. Wittenmark, and M. K. Bugeja. Dual adaptive extremum control of Hammerstein systems. *International Journal of Control*, 88(6):1271–1286, 2015.

A. A. Feldbaum. Dual control theory i. *Automation and Remote Control*, 21:874–880, 1960a.

A. A. Feldbaum. Dual control theory ii. *Automation and Remote Control*, 21:1033–1039, 1960b.

A. A. Feldbaum. Dual control theory iii. *Automation and Remote Control*, 22:1–12, 1961a.

A. A. Feldbaum. Dual control theory iv. *Automation and Remote Control*, 22:109–121, 1961b.

N. M. Filatov and H. Unbehauen. Survey of adaptive dual control methods. *IEE Proceedings - Control Theory and Applications*, 147(1):118–128, 2000.

N. M. Filatov and H. Unbehauen. *Adaptive dual control: theory and applications*. Springer-Verlag, Berlin, Heidelberg, 2004.

W. Findeisen, F. N. Bailey, M. Brdyś, K. Malinowski, P. Tatjewski, and A. Woźniak. *Control and coordination in hierarchical systems*. John Wiley & Sons, Chichester, UK, 1980.

O. Flärdh, K. H. Johansson, and M. Johansson. A new feedback control mechanism for error correction in packet-switched networks. In *Proceedings of the 44th IEEE Conference on Decision and Control, and the European Control Conference 2005*, pages 488–493, Seville, Spain, December 12-15, 2005.

J. S. Frait and D. P. Eckman. Optimizing control of single input extremum systems. *Journal of Fluids Engineering*, 84(1):85–90, 1962.

G. François, B. Srinivasan, and D. Bonvin. Use of measurements for enforcing the necessary conditions of optimality in the presence of constraints and uncertainty. *Journal of Process Control*, 15(6):701–712, 2005.

A. L. Frey, W. B. Deem, and R. J. Altpeter. Stability and optimal gain in extremum-seeking adaptive control of a gas furnace. In G. D. S. McLeillan, editor, *Proceedings of the 3rd IFAC world congress*, 48A, London, UK, June 20-25, 1966.

P. Frihauf, M. Krstić, and T. Başar. Nash equilibrium seeking in noncooperative games. *IEEE Transactions on Automatic Control*, 57(5):1192–1207, 2012.

P. Frihauf, M. Krstić, and T. Başar. Finite-horizon LQ control for unknown discrete-time linear systems via extremum seeking. *European Journal of Control*, 19(5): 399–407, 2013.

L. Fu and U. Özgüner. Extremum seeking with sliding mode gradient estimation and asymptotic regulation for a class of nonlinear systems. *Automatica*, 47(12): 2595–2603, 2011.

G. Gelbert, J. P. Moeck, O. Paschereit, and R. King. Advanced algorithms for gradient estimation in one- and two-parameter extremum seeking controllers. *Journal of Process Control*, 22(4):700–709, 2012.

A. Ghaffari, M. Krstić, and D. Nešić. Multivariable Newton-based extremum seeking. *Automatica*, 48(8):1759–1767, 2012.

A. Ghaffari, M. Krstić, and S. Seshagiri. Power optimization and control in wind energy conversion systems using extremum seeking. *IEEE Transactions on Control Systems Technology*, 22(5):1684–1695, 2014.

A. Ghaffari, S. Seshagiri, and M. Krstić. Multivariable maximum power point tracking for photovoltaic micro-converters using extremum seeking. *Control Engineering Practice*, 35:83–91, 2015.

M. P. Golden and B. E. Ydstie. Adaptive extremum control using approximate process models. *AIChE Journal*, 35(7):1157–1169, 1989.

W. M. Grady, M. J. Samotyj, and A. H. Noyola. Survey of active power line conditioning methodologies. *IEEE Transactions on Power Delivery*, 5(3):1536–1542, 1990.

W. M. Grady, M. J. Samotyj, and A. H. Noyola. Minimizing network harmonic voltage distortion with an active power line conditioner. *IEEE Transactions on Power Delivery*, 6(4):1690–1697, 1991.

W. M. Grady, M. J. Samotyj, and A. H. Noyola. The application of network objective functions for acactive minimizing the impact of voltage harmonic in power systems. *IEEE Transactions on Power Delivery*, 7(3):1379–1386, 1992.

M. Guay. A time-varying extremum-seeking control approach for discrete-time systems. *Journal of Process Control*, 24(3):98–112, 2014.

M. Guay and D. Dochain. A time-varying extremum-seeking control approach. *Automatica*, 51:356–363, 2015.

M. Guay and T. Zhang. Adaptive extremum seeking control of nonlinear dynamic systems with parametric uncertainties. *Automatica*, 39(7):1283–1293, 2003.

M. Guay, D. Dochain, and M. Perrier. Adaptive extremum seeking control of continuous stirred tank bioreactors with unknown growth kinetics. *Automatica*, 40(5): 881–888, 2004.

M. Guay, D. Dochain, M. Perrier, and N. Hudon. Flatness-based extremum-seeking control over periodic orbits. *IEEE Transactions on Automatic Control*, 52(10): 2005–2012, 2007.

M. Guay, E. Moshksar, and D. Dochain. A constrained extremum-seeking control approach. *International Journal of Robust and Nonlinear Control*, 25(16):3132–3153, 2015.

H. Hammouri and J. de Leon Morales. Observer synthesis for state-affine systems. In *Proceedings of the 29th IEEE Conference on Decision and Control*, pages 784–785, Honolulu, HI, December 1990.

M. Hamza. Extremum control of continuous systems. *IEEE Transactions on Automatic Control*, 11(2):182–189, 1966.

M. Haring and T. A. Johansen. Extremum-seeking control for nonlinear plants by least-squares gradient estimation. *Automatica*, 2015. Manuscript submitted for publication.

M. Haring and T. A. Johansen. Asymptotic stability of perturbation-based extremum-seeking control for nonlinear plants. *IEEE Transactions on Automatic Control*, 2016. Manuscript submitted for publication.

M. Haring, N. van de Wouw, and D. Nešić. Extremum-seeking control for nonlinear systems with periodic steady-state outputs. *Automatica*, 49(6):1883–1891, 2013.

M. Haring, B. Hunnekens, T. A. Johansen, and N. van de Wouw. Self-driving extremum-seeking control for nonlinear dynamic plants. *Automatica*, 2016a. Manuscript submitted for publication.

M. Haring, E. Skjong, T. A. Johansen, and M. Molinas. An extremum-seeking control approach to harmonic mitigation in electrical grids. *IEEE Transactions on Control Systems Technology*, 2016b. Manuscript submitted for publication.

I. Haskara, U. Özgüner, and J. Winkelman. Extremum control for optimal operating point determination and set point optimization via sliding modes. *Journal of Dynamic Systems, Measurement, and Control*, 122(4):719–724, 2000.

T. A. N. Heirung, B. Foss, and B. E. Ydstie. MPC-based dual control with online experiment design. *Journal of Process Control*, 32:64–76, 2015a.

T. A. N. Heirung, B. E. Ydstie, and B. Foss. Dual MPC for FIR systems: information anticipation. In *Proceedings of the 9th IFAC Symposium on Advanced Control of Chemical Processes*, pages 1033–1038, Whistler, Canada, June 7-10, 2015b.

E. Hellström, D. Lee, L. Jiang, A. G. Stefanopoulou, and H. Yilmaz. On-board calibration of spark timing by extremum seeking for flex-fuel engines. *IEEE Transactions on Control Systems Technology*, 21(6):2272–2279, 2013.

K. Höffner, N. Hudon, and M. Guay. On-line feedback control for optimal periodic control problems. *The Canadian Journal of Chemical Engineering*, 85(4):479–489, 2007.

R. Horst and P. M. Pardalos, editors. *Handbook of global optimization*. Kluwer, Dordrecht, 1994.

B. Hunnekens, A. Di Dino, N. van de Wouw, and N. van Dijk. Extremum-seeking control for the adaptive design of variable gain controllers. *IEEE Transactions on Control Systems Technology*, 23(3):1041–1051, 2015.

B. G. B. Hunnekens, M. A. M. Haring, N. van de Wouw, and H. Nijmeijer. Steady-state performance optimization for variable-gain motion control using extremum seeking. In *Proceedings of the 51st IEEE Conference on Decision and Control*, pages 3796–3801, Maui, Hawaii, USA, December 10-13, 2012.

B. G. B. Hunnekens, M. A. M. Haring, N. van de Wouw, and H. Nijmeijer. A dither-free extremum-seeking control approach using 1st-order least-squares fits for gradient estimation. In *Proceedings of the 53rd IEEE Conference on Decision and Control*, pages 2679–2684, Los Angeles, California, December 15-17, 2014.

P. A. Ioannou and J. Sun. *Robust adaptive control*. Prentice Hall, Upper Saddle River, NJ, 1996.

O. L. R. Jacobs and G. C. Shering. Design of a single-input sinusoidal-perturbation extremum-control system. *Proceedings of the Institution of Electrical Engineers*, 115 (1):212–217, 1968.

O. L. R. Jacobs and W. M. Wonham. Extremum control in the presence of noise. *Journal of Electronics and Control*, 11(3):193–211, 1961.

J. Jäschke and S. Skogestad. NCO tracking and self-optimizing control in the context of real-time optimization. *Journal of Process Control*, 21(10):1407–1416, 2011.

Z.-P. Jiang, I. M. Y. Mareels, and Y. Wang. A Lyapunov formulation of the nonlinear small-gain theorem for interconnected ISS systems. *Automatica*, 32(8):1211–1215, 1996.

K. E. Johnson and G. Fritsch. Assessment of extremum seeking control for wind farm energy production. *Wind Engineering*, 36(6):701–716, 2012.

R. M. Johnstone and B. D. O. Anderson. Exponential convergence of recursive least squares with exponential forgetting factor. *Systems & Control Letters*, 2(2), 1982.

V. Kariwala, Y. Cao, and S. Janardhanan. Local self-optimizing control with average loss minimization. *Industrial & Engineering Chemistry Research*, 47(4):1150–1158, 2008.

V. V. Kazakevich. *On extremum seeking.* PhD thesis, Moscow High Technical University, 1944.

V. V. Kazakevich. Extremum control of objects with inertia and on unstable objects. *Soviet Physics - Doklady*, 5(4):658–661, 1961.

V. V. Kazakevich and I. A. Mochalov. Statistical study of some algorithm for the control of inertial objects of optimization in the presence of drift. *Automation and Remote Control*, 35(11):1747–1753, 1975.

V. V. Kazakevich and I. A. Mochalov. Joint identification and accelerated optimization of plants with lag. *Automation and Remote Control*, 45(9):1152–1162, 1984.

L. Keviczky and R. Haber. Adaptive dual extremum control of Hammerstein models. In *Proceedings of the IFAC Symposium on Stochastic Control*, pages 333–341, Budapest, Hungary, 1974.

T. Key and J.-S. Lai. Analysis of harmonic mitigation methods for building wiring systems. *IEEE Transactions on Power Systems*, 13(3):890–897, 1998.

H. K. Khalil. *Nonlinear systems, 3rd edition.* Prentice Hall, Upper Saddle River, NJ, 2002.

S. Z. Khong, D. Nešić, C. Manzie, and Y. Tan. Multidimensional global extremum seeking via the DIRECT optimisation algorithm. *Automatica*, 49(7):1970–1978, 2013a.

S. Z. Khong, D. Nešić, Y. Tan, and C. Manzie. Unified frameworks for sampled-data extremum seeking control: global optimisation and multi-unit systems. *Automatica*, 49(9):2720–2733, 2013b.

S. Z. Khong, D. Nešić, and M. Krstić. Iterative learning control based on extremum seeking. *Automatica*, 66:238–245, 2016.

N. J. Killingsworth and M. Krstić. PID tuning using extremum seeking. *IEEE Control Systems Magazine*, 26(1):70–79, 2006.

N. J. Killingsworth, S. M. Aceves, D. L. Flowers, F. Espinosa-Loza, and M. Krstić. HCCI engine combustion-timing control: optimizing ggain and fuel consumption via extremum seeking. *IEEE Transactions on Control Systems Technology*, 17(6): 1350–1361, 2009.

K. Kim, C. Kasnakoglu, A. Serrani, and M. Samimy. Extremum-seeking control of subsonic cavity flow. *AIAA Journal*, 47(1):195–205, 2009.

A. J. Kisiel and D. W. T. Rippin. Adaptive optimisation of a water-gas shift reactor. In *Proceedings of the Second IFAC Symposium on the Theory of Self-Adaptive Control Systems*, pages 335–346, Teddington, England, September 14-17, 1965.

M. Krstić. Performance improvement and limitations in extremum seeking control. *Systems & Control Letters*, 39(5):313–326, 2000.

M. Krstić and H.-H. Wang. Stability of extremum seeking feedback for general nonlinear dynamic systems. *Automatica*, 36(4):595–601, 2000.

S. Larsson and I. Andersson. Self-optimising control of an SI-engine using a torque sensor. *Control Engineering Practice*, 14(5):505–514, 2008.

M. Leblanc. Sur l'électrification deschemins de fer au moyen de courants alternatifs de fréquence élevé. *Revue Générale de l' Electricité*, 1922.

R. Leyva, C. Alonso, I. Queinnec, A. Cid-Pastor, D. Lagrange, and L. Martínez-Salamero. MPPT of photovoltaic systems using extremum-seeking control. *IEEE Transactions on Aerospace and Electronic Systems*, 42(1):249–258, 2006.

S.-J. Liu and M. Krstić. Stochastic source seeking for nonholonomic unicycle. *Automatica*, 46(9):1443–1453, 2010.

T. Liu, D. J. Hill, and Z.-P. Jiang. Lyapunov formulation of ISS cyclic-small-gain in continuous-time dynamical networks. *Automatica*, 47(9):2088–2093, 2011.

G. Marafioti, R. R. Bitmead, and M. Hovd. Persistently exciting model predictive control. *International Journal of Adaptive Control and Signal Processing*, 28(6): 536–552, 2014.

A. S. Matveev, H. Teimoori, and A. V. Savkin. Navigation of a unicycle-like mobile robot for environmental extremum seeking. *Automatica*, 47(1):85–91, 2011.

S. M. Meerkov. Asymptotic methods for investigating quasistationary states in continuous systems of automatic optimization. *Automation and Remote Control*, 28 (11):1725–1743, 1967a.

S. M. Meerkov. Asymptotic methods for investigating a class of forced states in extremal systems. *Automation and Remote Control*, 28(12):1916–1920, 1967b.

S. M. Meerkov. Asymptotic methods for investigating stability of continuous systems of automatic optimization subjected to disturbance action. *Automation and Remote Control*, 29(12):1903–1919, 1968.

S. M. Meerkov. Principle of vibrational control: theory and applications. *IEEE Transactions on Automatic Control*, 25(4):755–762, 1980.

S. Michalowsky and C. Ebenbauer. Model-based extremum seeking for a class of nonlinear systems. In *Proceedings of the American Control Conference*, pages 2026–2031, Chicago, IL, July 1-3, 2015.

G. Mills and M. Krstić. Constrained extremum seeking in 1 dimension. In *Proceedings of the 53rd Conference on Decision and Control*, pages 2654–2659, Los Angeles, California, USA, December 15-17, 2014.

W. H. Moase and C. Manzie. Fast extremum-seeking on Hammerstein plants. In *Proceedings of the 18th IFAC World Congress*, pages 108–113, Milano, Italy, August 28-September 2, 2011.

W. H. Moase and C. Manzie. Semi-global stability analysis of observer-based extremum-seeking for Hammerstein plants. *IEEE Transactions on Automatic Control*, 57(7): 1685–1695, 2012a.

W. H. Moase and C. Manzie. Fast extremum-seeking for Wiener-Hammerstein plants. *Automatica*, 48(10):2433–2443, 2012b.

W. H. Moase, C. Manzie, and M. J. Brear. Newton-like extremum-seeking for the control of thermoacoustic instability. *IEEE Transactions on Automatic Control*, 55 (9):2094–2105, 2010.

A. Mohammadi, C. Manzie, and D. Nešić. Online optimization of spark advance in alternative fueled engines using extremum seeking control. *Control Engineering Practice*, 29:201–211, 2014.

I. S. Morosanov. Methods of extremum control. *Automation and Remote Control*, 18 (11):1077–1092, 1957.

S. J. Moura and Y. A. Chang. Lyapunov-based switched extremum seeking for photovoltaic power maximization. *Control Engineering Practice*, 21(7):971–980, 2013.

D. Nešić, Y. Tan, W. H. Moase, and C. Manzie. A unifiying approach to extremum seeking: adaptive schemes based on estimation of derivatives. In *Proceedings of the 49th IEEE Conference on Decision and Control*, pages 4625–4630, Atlanta, GA, USA, December 15-17, 2010.

D. Nešić, Y. Tan, C. Manzie, A. Mohammadi, and W. Moase. A unifying framework for analysis and design of extremum seeking controllers. In *Proceedings of the 24th Chinese Control and Decision Conference*, Taiyuan, May 23-25, 2012.

D. Nešić, A. Mohammadi, and C. Manzie. A framework for extremum seeking control of systems with parameter uncertainties. *IEEE Transactions on Automatic Control*, 58(2):435–448, 2013a.

D. Nešić, T. Nguyen, Y. Tan, and C. Manzie. A non-gradient approach to global extremum seeking: An adaptation of the Shubert algorithm. *Automatica*, 49(3): 809–815, 2013b.

J. Nocedal and S. J. Wright. *Numerical optimization*. Springer-Verlag, New York, 1999.

T. O. Olsen, H. Berstad, and S. Danielsen. Automatic control of continuous autogenous grinding. In *Proceedings of the second IFAC Symposium on Automation in Mining Minerals and Metal Processing*, pages 225–234, Johannesburg, Republic of South Africa, 1976.

I. I. Ostrovskii. Extremum regulation. *Automation and Remote Control*, 18(9):900–907, 1957.

Y. Ou, C. Xu, E. Schuster, T. C. Luce, J. R. Ferron, M. L. Walker, and D. A. Humphreys. Design and simulation of extremum-seeking open-loop optimal control of current profile in the DII-D tokamak. *Plasma Physics and Controlled Fusion*, 50 (11):1–24, 2008.

Y. Pan, U. Özgüner, and T. Acarman. Stability and performance improvement of extremum seeking control with sliding mode. *International Journal of Control*, 76 (9/10):968–985, 2003.

M. Pastoor, L. Henning, B. R. Noack, R. King, and G. Tadmor. Feedback shear layer control for bluff body drag reduction. *Journal of Fluid Mechanics*, 608:161–196, 2008.

I. I. Perelman. Statistical investigation of extremal control extrapolation systems with object parabolic characteristic. *Automation and Remote Control*, 22(11):1453–1465, 1961.

A. A. Pervozvanskii. Continuous extremum control systems in the presence of random noise. *Automatic & Remote Control*, 21(7):673–677, 1960.

K. S. Peterson and A. G. Stefanopoulou. Extremum seeking control for soft landing of an electromechanical valve actuator. *Automatica*, 40(6):1063–1069, 2004.

D. Popović, M. Janković, S. Magner, and A. Teel. Extremum seeking methods for optimization of variable cam timing engine operation. In *Proceedings of the American Control Conference*, pages 3136–3141, Denver, Colorado, June 4-6, 2003.

M. J. D. Powell. UOBYQA: unconstrained optimzation by quadratic approximation. *Mathematical Programming*, 92(3):555–582, 2002.

J. D. Roberts. Extremum or hill-climbing regulation: a statistical theory involving lags, disturbances and noise. *Proceedings of the Institute of Electrical Engineers*, 112(1):137–150, 1965.

J. J. Ryan and J. L. Speyer. Peak-seeking control using gradient and Hessian estimates. In *Proceedings of the 2010 American Control Conference*, Baltimore, MD, USA, June 30-July 2, 2010.

A. Scheinker and M. Krstić. Minimum-seeking for CLFs: universal semiglobally stabilizing feedback under unknown control directions. *IEEE Transactions on Automatic Control*, 58(5):1107–1122, 2013.

A. Scheinker and M. Krstić. Extremum seeking with bounded update rates. *Systems & Control Letters*, 63:25–31, 2014.

S. Serdengecti. Optimalizing control in the presence of noise interference. *Journal of Jet Propulsion*, 26(6):465–473, 1956.

J. Sharafi, W. H. Moase, and C. Manzie. Fast extremum seeking on Hammerstein plants: a model-based approach. *Automatica*, 59:171–181, 2015.

R. C. Shekhar, W. H. Moase, and C. Manzie. Discrete-time extremum-seeking for Wiener-Hammerstein plants. *Automatica*, 50(12):2998–3008, 2014.

M. S. Shouche, H. Genceli, V. Premkiran, and M. Nikolaou. Simultaneous constrained model predictive control and identification of DARX processes. *Automatica*, 34(12): 1521–1530, 1998.

M. S. Shouche, H. Genceli, and M. Nikolaou. Effect of on-line optimization techniques on model predictive control and identification (MPCI). *Computers & Chemical Engineering*, 26(9):1241–1252, 2002.

B. Singh, K. Al-Haddad, and A. Chandra. A review of active filters for power quality improvement. *IEEE Transactions on Industrial Electronics*, 46(5):960–971, 1999.

G. K. Singh. Power system harmonics research: a survey. *European Transactions on Electrical Power*, 19(2):151–172, 2009.

E. Skjong, M. Molinas, and T. A. Johansen. Optimized current reference generation for system-level harmonic mitigation in a diesel-electric ship using non-linear model predictive control. In *Proceedings of the IEEE International Conference on Industrial Technology*, pages 2314–2321, Seville, March 17-19, 2015a.

E. Skjong, M. Molinas, T. A. Johansen, and R. Volden. Shaping the current waveform of an active filter for optimization system level harmonic conditioning. In *Proceedings of the International Conference on Vehicle Technology and Intelligent Transport Systems*, pages 98–106, Lisbon, Portugal, May 20-22, 2015b.

E. Skjong, M. Ochoa-Gimenez, M. Molinas, and T. A. Johansen. Management of harmonic propagation in a marine vessel by use of optimization. In *Proceedings of the IEEE Transportation Electrification Conference and Expo*, pages 1–8, Dearborn, MI, June 14-17, 2015c.

E. Skjong, J. A. Suul, A. Rygg, M. Molinas, and T. A. Johansen. System-wide harmonic mitigation in a diesel electric ship by model predictive control. *IEEE Transactions on Industrial Electronics*, 2016. Manuscript accepted for publication.

S. Skogestad. Plantwide control: the search for the self-optimizing control structure. *Journal of Process Control*, 10(5):487–507, 2000.

S. Skogestad. Control structure design for complete chemical plants. *Computers & Chemical Engineering*, 28(1-2):219–234, 2004.

E. D. Sontag and Y. Wang. New characterizations of input-to-state stability. *IEEE Transactions on Automatic Control*, 41(9):1283–1294, 1996.

B. Srinivasan. Real-time optimization of dynamic systems using multiple units. *International Journal of Robust and Nonlinear Control*, 17(13):1183–1193, 2007.

B. Srinivasan, L. T. Biegler, and D. Bonvin. Tracking the necessary conditions of optimality with changing set of active constraints using a barrier-penalty function. *Computers & Chemical Engineering*, 32(3):572–579, 2008.

M. S. Stanković and D. M. Stipanović. Extremum seeking under stochastic noise and applications to mobile sensors. *Automatica*, 46(8):1243–1251, 2010.

J. Sternby. Extremum control systems: An area for adaptive control? In *Proceedings of the 20th Joint Automatic Control Conference*, WA2-A, San Francisco, CA, USA, August 13-15, 1980.

Y. Tan, D. Nešić, and I. M. Y. Mareels. On non-local stability properties of extremum seeking control. *Automatica*, 42(6):889–903, 2006.

Y. Tan, D. Nešić, I. M. Y. Mareels, and A. Astolfi. On global extremum seeking in the presence of local extrema. *Automatica*, 45(1):245–251, 2009.

Y. Tan, W. H. Moase, C. Manzie, D. Nešić, and I. M. Y. Mareels. Extremum seeking from 1922 to 2010. In *Proceedings of the 29th Chinese Control Conference*, pages 14–26, Beijing, China, July 29-31, 2010.

Y. Tan, Y. Li, and I. M. Y. Mareels. Extremum seeking for constrained inputs. *IEEE Transactions on Automatic Control*, 58(9):2405–2410, 2013.

A. R. Teel and D. Popović. Solving smooth and nonsmooth multivariable extremum seeking problems by the methods of nonlinear programming. In *Proceedings of the American Control Conference*, pages 2394–2399, Arlington, VA, June 25-27, 2001.

H. S. Tsien and S. Serdengecti. Analysis of peak-holding optimalizing control. *Journal of the Aeronautical Sciences*, 22(8):561–570, 1955.

N. van de Wouw, M. Haring, and D. Nešić. Extremum-seeking control for periodic steady-state response optimization. In *Proceedings of the 51st IEEE Conference on Decision and Control*, pages 1603–1608, Maui, Hawaii, USA, December 10-13, 2012.

S. van der Meulen, B. de Jager, F. Veldpaus, E. van der Noll, F. vand der Sluis, and M. Steinbuch. Improving continuously variable transmission efficiency with extremum seeking control. *IEEE Transactions on Control Systems Technology*, 20 (5):1376–1383, 2012.

S. van der Meulen, B. de Jager, F. Veldpaus, and M. Steinbuch. Combining extremum seeking control and tracking control for high-performance CVT operation. *Control Engineering Practice*, 29:86–102, 2014.

H.-H. Wang and M. Krstić. Extremum seeking for limit cycle minimization. *IEEE Transactions on Automatic Control*, 45(12):2432–2437, 2000.

H.-H. Wang, M. Krstić, and G. Bastin. Optimizing bioreactors by extremum seeking. *International Journal of Adaptive Control and Signal Processing*, 13(8):651–669, 1999.

L. Wang, S. Chen, and K. Ma. On stability and application of extremum seeking control without steady-state oscillation. *Automatica*, 68:18–26, 2016.

S. M. Williams and R. G. Hoft. Adaptive frequency domain control of PWM switched power line conditioner. *IEEE Transactions on Power Electronics*, 6(4):665–670, 1991.

B. Wittenmark. Adaptive control of a stochastic non-linear system: an example. *International Journal of Adaptive Control and Signal Processing*, 7(5):327–337, 1993.

B. Wittenmark. Adaptive dual control methods: an overview. In *Proceedings of the 5th IFAC Symposium on Adaptive Systems in Control and Signal Processing*, pages 67–72, Budapest, Hungary, 1995.

B. Wittenmark and R. J. Evans. Extremal control of Wiener model processes. In *Proceedings of the 41st IEEE Conference on Decision and Control*, pages 4637–4642, Las Vegas, Nevada, USA, December 10-13, 2002.

B. Wittenmark and A. Urquhart. Adaptive extremal control. In *Proceedings of the 34th IEEE Conference on Decision and Control*, pages 1639–1644, New Orleans, LA, December 13-15, 1995.

M. Ye and G. Hu. Extremum seeking under input constraint for systems with a time-varying extremum. In *Proceedings of the 52nd IEEE Conference on Decision and Control*, pages 1708–1713, Florence, Italy, December 10-13, 2013.

H. Yu and U. Ozguner. Extremum-seeking control strategy for ABS system with time delay. In *Proceedings of the American Control Conference*, Anchorage, AK, May 8-10, 2002.

C. Zhang and R. Ordóñez. Numerical optimization-based extremum seeking control with application to ABS design. *IEEE Transactions on Automatic Control*, 52(3): 454–467, 2007.

C. Zhang and R. Ordóñez. *Advances in industrial control, Extremum-seeking control and applications: a numerical optimization-based approach.* Springer, 2012.

C. Zhang, D. Arnold, N. Ghods, A. Siranosian, and M. Krstić. Source seeking with non-holonomic unicycle without position measurement and with tuning of forward velocity. *Systems & Control Letters*, 56(3):245–252, 2007a.

C. Zhang, A. Siranosian, and M. Krstić. Extremum seeking for moderately unstable systems and for autonomous vehicle target tracking witwith position measurements. *Automatica*, 43(10):1832–1839, 2007b.

Z. Zhong, H. Huo, X. Zhu, G. Cao, and Y. Ren. Adaptive maximum power point tracking control of fuel cell power plants. *Journal of Power Sources*, 176(1):259–269, 2008.